DOCTORAL THESIS IN AUTOMATIC CONTROL
STOCKHOLM, SWEDEN 2014

Fuel-Efficient Heavy-Duty Vehicle Platooning

ASSAD ALAM

KTH ROYAL INSTITUTE OF TECHNOLOGY
SCHOOL OF ELECTRICAL ENGINEERING

KTH Electrical Engineering

Fuel-Efficient Heavy-Duty Vehicle Platooning

ASSAD ALAM

Doctoral Thesis
Stockholm, Sweden 2014

KTH School of Electrical Engineering
Automatic Control Lab
SE-100 44 Stockholm
SWEDEN

TRITA-EE 2014:027
ISSN 1653-5146
ISBN 978-91-7595-194-2

Akademisk avhandling som med tillstånd av Kungliga Tekniska högskolan framlägges till offentlig granskning för avläggande av teknologie doktorsexamen i Reglerteknik fredagen den 13:e juni 2014 klockan 14.00 i sal F3 Kungliga Tekniska högskolan, Lindstedtsvägen 26, Stockholm.

Tryck: Universitetsservice US AB

Abstract

The freight transport industry faces big challenges as the demand for transport and fuel prices are steadily increasing, whereas the environmental impact needs to be significantly reduced. Heavy-duty vehicle (HDV) platooning is a promising technology for a sustainable transportation system. By semi-autonomously governing each platooning vehicle at small inter-vehicle spacing, we can effectively reduce fuel consumption, emissions, and congestion, and relieve driver tension. Yet, it is not evident how to synthesize such a platoon control system and how constraints imposed by the road topography affect the safety or fuel-saving potential in practice.

This thesis presents contributions to a framework for the design, implementation, and evaluation of HDV platooning. The focus lies mainly on establishing fuel-efficient platooning control and evaluating the fuel-saving potential in practice. A vehicle platoon model is developed together with a system architecture that divides the control problem into manageable subsystems. Presented results show that a significant fuel reduction potential exists for HDV platooning and it is favorable to operate the vehicles at a small inter-vehicle spacing. We address the problem of finding the minimum distance between HDVs in a platoon without compromising safety, by setting up the problem in a game theoretical framework. Thereby, we determine criteria for which collisions can be avoided in a worst-case scenario and establish the minimum safe distance to a vehicle ahead. A systematic design methodology for decentralized inter-vehicle distance control based on linear quadratic regulators is presented. It takes dynamic coupling and engine response delays into consideration, and the structure of the controller feedback matrix can be tailored to the locally available state information. The results show that a decentralized controller gives good tracking performance and attenuates disturbances downstream in the platoon for dynamic scenarios that commonly occur on highways. We also consider the problem of finding a fuel-efficient controller for HDV platooning based on road grade preview information under road and vehicle parameter uncertainties. We present two model predictive control policies and derive their fuel-saving potential. The thesis finally evaluates the fuel savings in practice. Experimental results show that a fuel reduction of 3.9–6.5 % can be obtained on average for a heterogenous platoon of HDVs on a Swedish highway. It is demonstrated how the savings depend on the vehicle position in the platoon, the behavior of the preceding vehicles, and the road topography. With the results obtained in this thesis, it is argued that a significant fuel reduction potential exists for HDV platooning.

To my family.

Acknowledgements

There are many who have contributed to the work presented in this thesis. First of all, I would like to thank my main advisor Karl Henrik Johansson at KTH. Your guidance, eye for details, and truly inspiring enthusiasm have been invaluable. I have learned a lot from you. Then, I would like to thank Tony Sandberg at Scania for giving me the opportunity to pursue a Ph.D and for his never-ending support. Many thanks to Magnus Adolfson, my supervisor at Scania, for his support and guidance in all matters. My current and previous co-advisors Jonas Mårtensson and Ather Gattami, respectively, at KTH deserve many thanks for their insights and enthusiasm. Henrik Petterson, my advisor at Scania, deserves a lot gratitude for his unbelievable effort and dedication throughout this work. Thank you for all the knowledge and support that you have given me during the toughest hours. A heartfelt thanks goes to Per Sahlholm for his mentoring and the fruitful discussions throughout the first part of my Ph.D. Many thanks to Kuo-Yun Liang, who has been an ally both as a Master's student and a fellow Ph.D. candidate at Scania and at the Control department, KTH. I have greatly enjoyed our travels together along with a varied range of discussions. My gratitude goes to Claire J. Tomlin for her constructive feedback and interest in my research. I am also grateful for the valuable insights and advice from Roy Smith after my Licentiate defense.

I am extremely grateful to my colleagues Farhad Farokhi, Bart Besselink, and Chithrupa Ramesh for proofreading parts of my thesis and providing valuable comments. Naturally, you are now to blame for any mistakes in the thesis! Thanks to all my Master's students for all the nice discussions and inspiring ideas.

I am grateful for all the support and help from my colleagues at Scania. In particular, I would like to extend my gratitude to the senior engineers Jan Dellrud and Samuel Wickström, at Scania CV AB, for assisting with the experimental results provided in this thesis. Thank you Tom Nyström, Jon Andersson, Anders Johansson, Carl Svärd, Pär Degerman, Joseph Ah-King, and Jonny Andersson for all the help and nice discussions that we have had. Thanks to the additional members in my steering group, Helene Sjöblom and Fredrik Stensson, for keeping this project on a straight path. I am also appreciative for the valuable input given by my reference group. A special thanks goes out to the late Rickard Lyberger for providing a lot of technical insight into this project. He will be greatly missed.

All my present and former colleagues at KTH deserve thanks for providing such an inspiring and positive work environment. Specially, I would like to thank Burak

Demirel, Farhad Farokhi, Euhanna Ghadimi, Chithrupa Ramesh, Arda Aytekin, Valerio Turri, Christian Larsson, Bart Besselink, Demia Della Penda, PG Di Marco, Iman Shames, Themistoklis Charalambous, Jana Tumova, Pablo Soldati, Ubaldo Tiberi, Torbjörn Nordling, Alireza Ahmadi, José Araujo, and André Teixeira who have been my brothers and sisters in arms and also become good friends during my time as a Ph.D. student. It has been a great pleasure to work, discuss, and spend time with all of you. Conversations with Erik Henriksson, Oscar Flärdh, Tao Yang, Afrooz Ebadat, Hamid Reza Feyzmahdavian, Per Hägg, and Mariette Annergren were always welcome breaks. I would also like to thank Henrik Sandberg for providing valuable assistance in certain subject matters in this thesis. Many thanks to Karin, Anneli, Kristina, and Hanna for their great spirit and assistance with any issue I've had.

The research presented in this thesis has been financed by Vinnova (FFI), and by Scania CV AB. Thank you for your faith and bestowing upon me this great opportunity.

Last, but definitely not the least, I would specially like to thank my family. First, I would like to thank my most beloved Ma and my brother Abbas for their patience, love and endless all-around support. Also, gratitude to my choto Ma Chobi for your great affection, encouragement, and inspiration. Mejokhala, Shejokhala, Bachubhaia, and Butkiapa, thanks for all your heartfelt dowas in everything.

Assad Alam
Stockholm, May 2014.

Contents

Chapter 1

Introduction

> "*I have been impressed with the urgency of doing. Knowing is not enough; we must apply. Being willing is not enough; we must do.*"
>
> Leonardo da Vinci

The traffic intensity is escalating in most part of the world, making traffic congestion a growing issue. In parallel, to facilitate the continuously advancing needs for goods, the demand for transportation services is increasing. In 2010, 58 thousand heavy-duty vehicles (HDVs) were in use in Sweden and 1.8 million HDVs in the EU-15 countries, with a corresponding growth rate of 2.8 % and 0.5 %, respectively, from the previous year (ACEA, 2012). Congruently, the International Transport Forum (ITF), which is a strategic think tank for the transport sector, predicts that the surface freight transport in OECD countries will increase up to 125 % by the year 2050, based on measured levels in 2010 (OECD/ITF, 2013). In line with this prediction, 2.3 billion tonne[1]-kilometers of inland freight was transported in 2010, of which 76.4 % was transported over roads (Eurostat, 2011).

The cost of EU infrastructure development to match the demand for transport has been estimated at over € 1.5 trillion for 2010–2030 (European Commission, 2011). This does not include investment in vehicles, equipment and charging infrastructure which may require an additional trillion to achieve the emission reduction goals for the transport system. Hence, the vast costs clearly indicates that the future solutions cannot solely be based on improving aging infrastructure, but cheaper innovative solutions must be established for sustainability. One such solution is an integrated goods transport system based on HDV platooning, as illustrated in Figure 1.1.

1.1 Necessity for Future Fuel-Efficient Freight Transports

The transport industry faces great challenges. Freight transport demand has escalated and will continue to do so as economies grow. An increase in traffic naturally

[1] 1 tonne [t]= 1000 kg

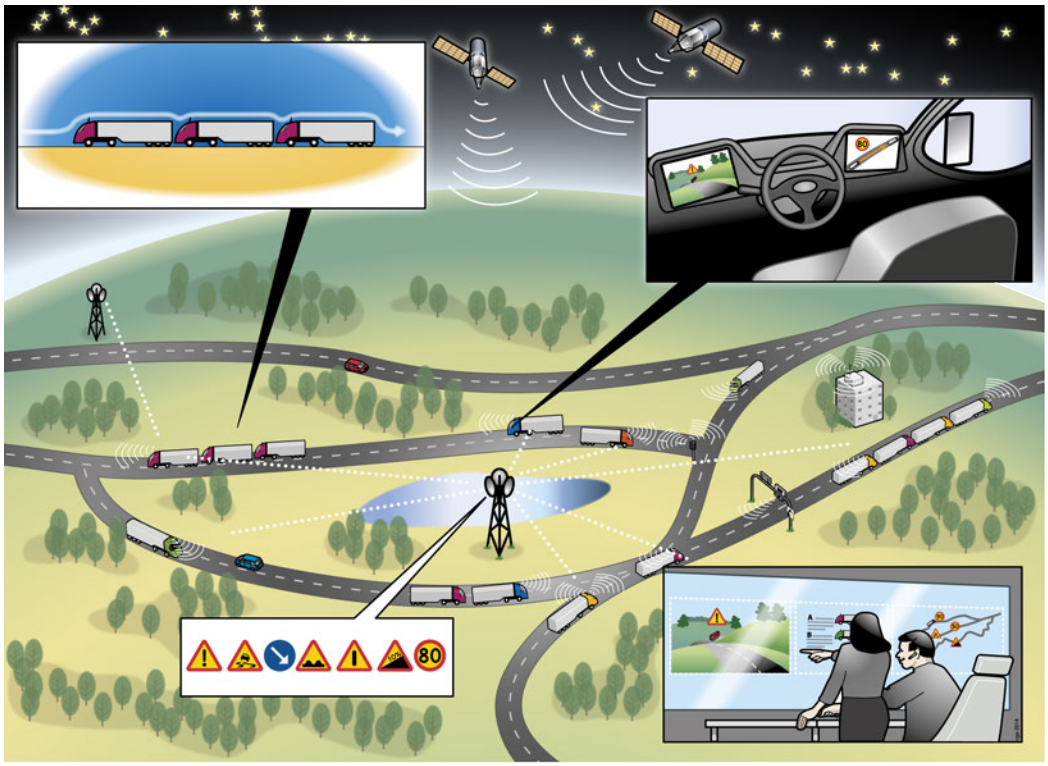

Figure 1.1: Future intelligent road transportation systems, where goods transport is integrated with platooning. Commercial vehicles are governed semi-autonomously at small inter-vehicle spacings and thereby effectively improve fuel consumption, reduce emissions, reduce congestion, and relieve driver tension without compromising safety. Each vehicle is able to serve as an information node through wireless communication; enabling a cooperative networked transportation system. Instructions, for example, regarding the possibility to platoon with vehicles further ahead and how to merge to an appropriate platoon position for fuel-optimality can be displayed on advanced human to machine interfaces. Furthermore, the infrastructure aids the vehicle platoons by providing information regarding the upcoming road incidents, traffic signals, road construction, road tolls, etc. A central office, such as a fleet management system, monitors each vehicle on the road and systematically coordinate scattered vehicles on the road network to form platoons in order to maximize the benefits of platooning. (Illustration provided courtesy of the Smart Mobility Lab, KTH Royal Institute of Technology.)

corresponds to higher fossil fuel usage and inherently a higher emission of harmful exhaust gas as well as more complex traffic situations. The drivers of today are already faced with several challenging scenarios each time they venture out on the road—challenges that will become harsher with increasing traffic intensity. Hence, governments, non-governmental agencies, the private sector, and individuals around the world are trying to find ways to reduce the emissions and design systems to aid the driver in handling difficult situations. In line with these goals, the road transport

sector has been targeted as a main policy area where further environmental and overall efficiency improvements are critical for a sustainable future of European transport (European Commission, 2014). Furthermore, complex traffic scenarios can have a devastating impact: more than 1.3 million people die every year in road accidents. If nothing is done, this number might rise to 1.9 million deaths per year according to ITF (2011). Urban transport is responsible for 69 % of accidents that occur in cities (European Commission, 2011). In parallel, the growing traffic intensity have led to that almost every weekday morning and evening, the main roads saturate throughout the major cities in the world.

In addition, harmful emissions have proved to result in severe long term consequences. Hence, industrialized countries have agreed to reduce greenhouse gas emissions under the Kyoto protocol. Working toward the development of a low-carbon economy is vital for averting climate change. Combating climate change and rooting out its main causes, a problem due to increase in greenhouse gases, are among the top priorities in Europe. Road transport constitute the dominant mode of transportation, as illustrated in Figure 1.2, and contribute to 72 % of the greenhouse gas emissions (European Commission, 2013). Overall green house gas emissions were recorded to be reduced by 17 % between 1990 and 2009 (Eurostat, 2011). While emissions from other sectors are falling, those from the transport sector have increased by 21 %. The road sector emissions dominate transport emissions globally. Road transport alone contributes about 20 % of the EU's total emissions of CO_2, the main greenhouse gas, from fossil fuel combustion. Similar results were presented by the Community Research and Development Service (CORDIS), which is part of the European Commission. They reported that road freight accounts for approximately 35 % of transport CO_2 emissions, 75 % of the particulate emissions, and 60 % of nitrogen oxides (NO_X) emissions. Thus, the European Union have set the goal to reduce emissions by 80–95 % by 2050 with respect to the levels measured in 1990, which implies a 60 % reduction in green house gas emissions from the transport sector. Considering the high emission of greenhouse gases from fossil fuel combustion, especially in freight transports, legislation and policies have been set. Thus, vehicle manufacturers are facing increasingly difficult emission challenges.

Along with challenges regarding safety and emission policies, the vehicle manufacturers also experience an increase in fuel prices. The oil price is expected to increase by 60 % by 2050, compared to the prices in 2010 (OECD/ITF, 2013). Transportation constitutes the main part of the increase in oil consumption during the last three decades and the growth is expected to continue. As the fuel price increases, the strain on operating costs grows for an HDV fleet provider. This issue has a major impact within the transport industry. Road transport serves as the backbone of the economy in many countries. With the rise in fuel prices, road transportation becomes less economically viable. Figure 1.3 shows the main operational costs for an HDV in Europe. Fuel cost constitutes approximately one third of the total life cycle cost in European long haulage HDVs. An HDV fleet provider generally owns many vehicles that travel over 200 000 km per year. With an average fuel consumption of 0.3 liter/km and the current diesel fuel price in Sweden being 14.42 kr/liter, only the

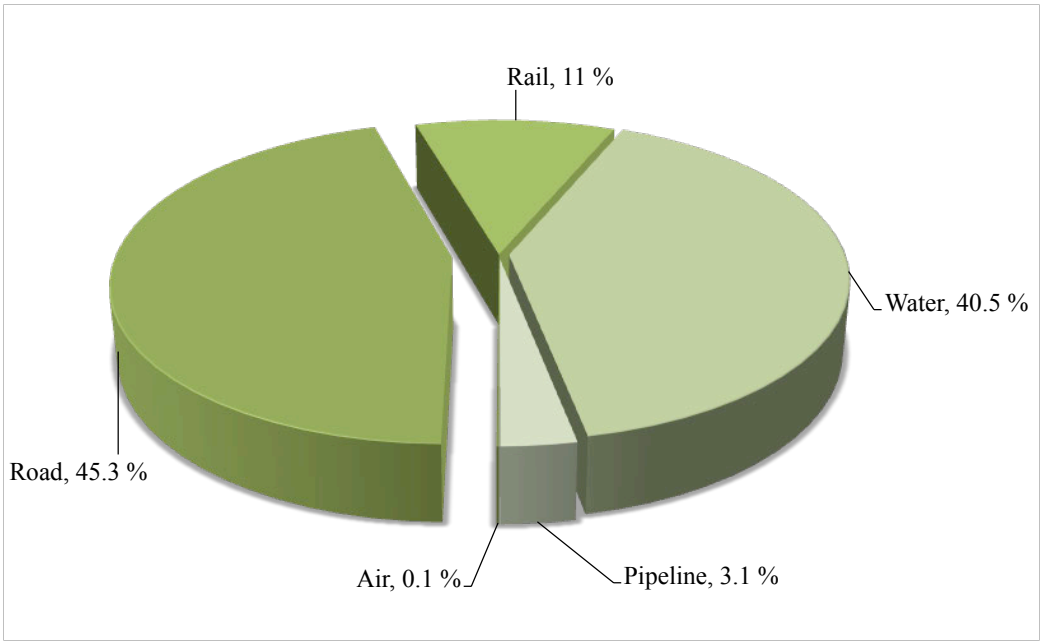

Figure 1.2: Freight transport in % based on tonne-kilometers. Adapted from European Commission (2013).

fuel cost amounts to over 0.86 million Swedish kronor, which is equivalent to € 95 thousand, per year for a single HDV. Hence, the HDV fleet industry is extremely fuel price sensitive and reducing only a few percent in fuel consumption has a substantial impact for the HDV customer and inherently for HDV manufacturers. The White Paper on Transport 2011 of the European Commission states that transport has become more energy efficient, but EU transport still depends on oil and oil products for 96 % of its energy needs (European Commission, 2011). Thus, there is still a strong need for fuel-efficient freight transports solution.

Vehicle manufacturers' responses to the emission challenges and the life cycle cost issues have mainly been technical. Vast research efforts have been dedicated to combustion engines to the extent that it is difficult to improve them further. Aftertreatment systems have been developed as a natural next step. As an example, exhaust gas recirculation has been used to reduce NO_X formation. However, there is a trade-off between NO_X emission and fuel efficiency, as most methods to suppress NO_X formation reduce the engine's thermal efficiency. An alternative approach for diminishing greenhouse gases by car manufacturers is to reduce the weight of the vehicle and thereby lower the fuel consumption. So far, development has mostly been focused on making the powertrain more energy efficient. Attention spent on reducing greenhouse gases and fuel-efficiency have to a vast extent been focused on electric cars, hybrid vehicles, fuel-efficient tires, and alternative fuels such as hydrogen, solar cells, etc. An overview of such existing technologies is given in AEA Technology (2011). Most of these approaches demand a reconstruction of the powertrain, which

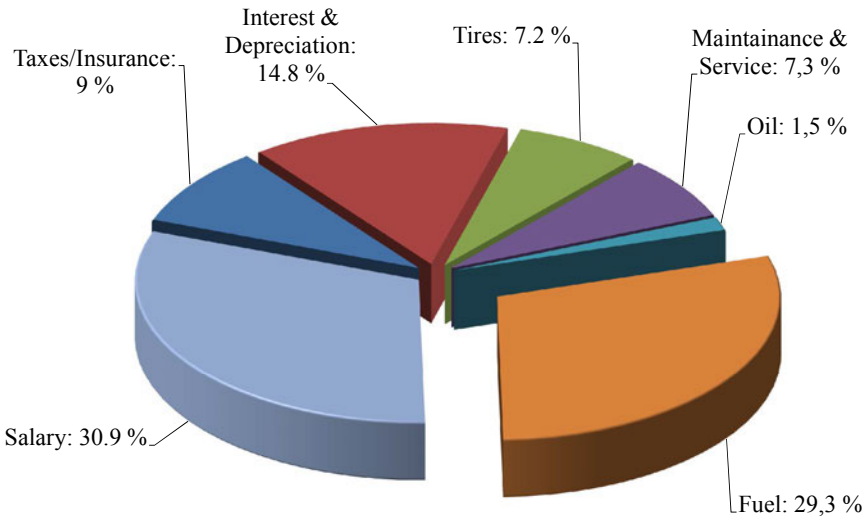

Figure 1.3: Life cycle costs of class 8 HDVs in Europe over a 4 year period (Schittler, 2003). The fuel cost ratio is similar for a Scania HDV (Scania CV AB, 2010).

is costly and still does not improve the global issues of traffic congestion and safety.

To ensure the sustainability and global acceptance of commercial transportation, new systems that reduce the dependence on oil and minimize the emission of greenhouse gases need to be developed. HDV platooning serves as a possible solution to reduce fuel consumption and exhaust gas emissions. The concept of platooning for congestion and energy reduction is not new. Many experienced HDV drivers have for a long time noticed that when driving at a short relative distance to a vehicle ahead results in a lower required throttle action to propel the vehicle forward. This fact have also been observed in terms of lowered effort in professional bicycling and high velocity race driving. It is due to a lowered air drag that occurs when operating in such a formation, as illustrated in Figure 1.4. Hence, vehicle platoons (Figure 1.5), operating as a cooperative system, have become an important research area, which addresses the issues of safety, traffic congestion, fuel consumption and harmful exhaust emissions. By packing HDVs close to each other, the total road capacity can be increased and emissions can be reduced. Additionally, governing vehicle platoons by an automated control strategy, the overall traffic flow is expected to improve.

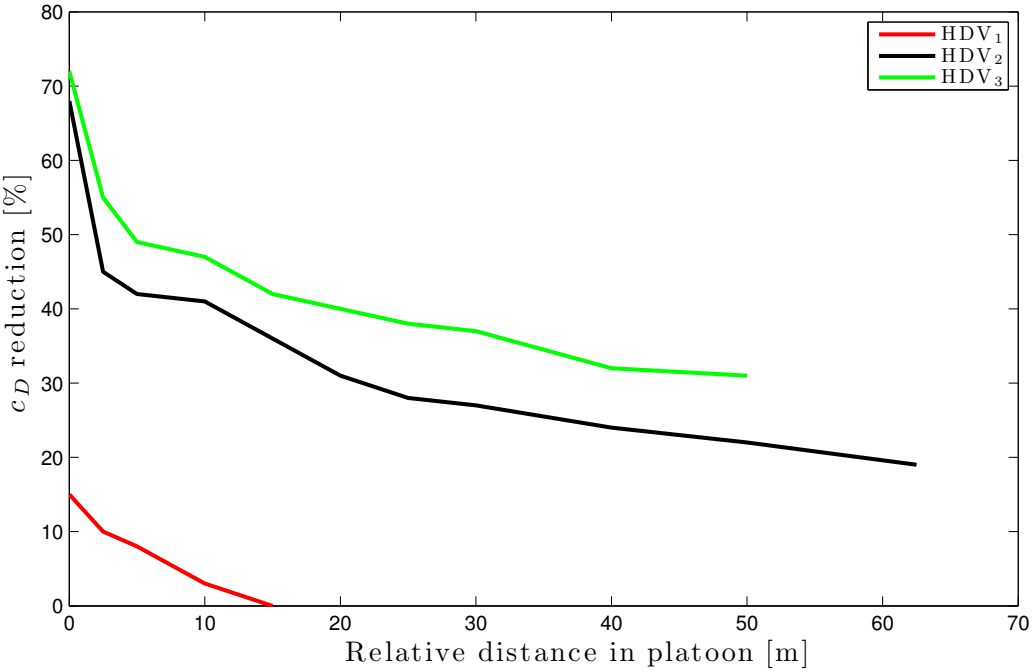

Figure 1.4: Change in air drag coefficient c_D with respect to distance between the vehicles in a platoon. The top curve shows the air drag reduction for the last vehicle, denoted as HDV_3 in a three-HDV platoon. The middle curve shows the air drag reduction for the second vehicle HDV_2 in a two-HDV platoon. The lead vehicle HDV_1, also experiences a lowered air drag from having a follower vehicle, as shown by the bottom curve. Adapted from Wolf-Heinrich and Ahmed (1998). Similar findings have been established by the fluid dynamics department at Scania CV AB and in Bonnet and Fritz (2000).

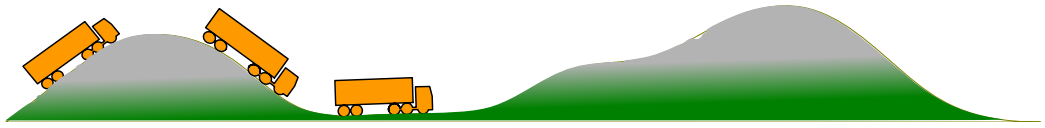

Figure 1.5: HDVs traveling in a platoon can achieve significant fuel reduction. It is fuel-efficient for the lead vehicle to utilize the gravitational force and coast along the downhill. However, the second vehicle, still traveling along the downhill, might have to apply its brakes in order not to collide with the third vehicle, which is not fuel-efficient. The relative distance and the air drag will increase if the third vehicle is not able to maintain or increase its speed when facing an uphill. Alternatively, the third vehicle must produce a higher control effort to maintain the relative distance, which might not be possible since its engine power is limited. Hence, a cooperative control strategy is advantageous for all vehicles traveling in a platoon.

1.2 Enabling Platooning Technologies

Vehicle platooning has been widely recognized as a means to reduce energy consumption. However, with increasing traffic density and traffic network complexity, more pressure is put on the driver performance. Driving a vehicle at a close inter-vehicle spacing is a very strenuous task for the driver. The driver has to be alert at all times, constantly adjusting the velocity and relative distance according to the behavior of the vehicle ahead. The response time of human drivers are insufficient to navigate the vehicle under such conditions with respect to safety and fuel efficiency. Often the driver fails to react in time causing unnecessary harsh braking and acceleration or at times even an accident. Due to recent advances in technology, systems as depicted in Figure 1.6 can be developed to aid the driver in platooning applications.

Electronic control systems and sensors within vehicles have been increasing rapidly in numbers over the last decades. They enable additional functionality in terms of software and smart control logic. Thereby, advanced driver assistance systems (ADAS), described in more detail in Section 2.4, have been developed to aid the driver and relieving certain driving tasks. For instance, the lane departure warning system is such a functionality that issues a warning if it detects that the driver is drifting off the lane. It utilizes a camera often mounted in the front window to determine the vehicle position with respect to the lane markings. Another system, specially designed for HDVs, is commonly referred to as the downhill speed control (DHSC) for maintaining a maximum desired speed over downhill segments. The commercially available adaptive cruise control (ACC) has been considered as a means to enable vehicle platooning in Hedrick et al. (1991) and Rajamani and Zhu (1999). It generally acts as an extension to the CC, with the addition of actuating the vehicle with the brake system. By utilizing the relative distance and velocity to a preceding vehicle, provided by radar or lidar technology, control strategies can be established with respect to a single vehicle ahead.

Road topography has a significant effect on the behavior of an HDV. An HDV will accelerate without any propulsion force from the engine when going down one hill and drop in speed when climbing the next one, even though maximum engine torque is applied. Thus, a fuel-efficient system known as look-ahead cruise control (LAC) is now commercially available, which is based on road map data (Hellström, 2010). By using the road grade preview information, suitable control action commands can be sent to the engine and gearbox control systems. Thereby, the instantaneous power demand, that is mandated in the upcoming hilly road segment, can be obtained while keeping fuel consumption and environmental impact as low as possible. For example, by lowering the speed before un upcoming downhill segment, unnecessary braking actions can be avoided and the total fuel-consumption can be reduced significantly. Map providers can currently only deliver road grade information over a limited region. However, vehicle manufacturers themselves have the possibility to obtain road grade information by using on-board sensors and a global positioning system (GPS) (Sahlholm, 2011).

Key enabling technology for platooning such as vehicle-to-vehicle (V2V) and

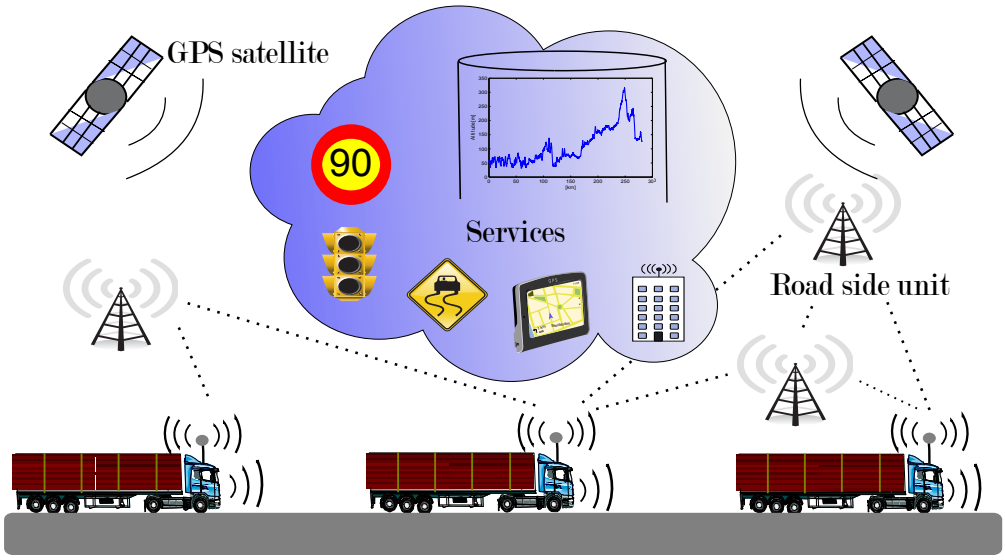

Figure 1.6: The figure depicts some of the available technology to enable HDV platooning. It shows several information attributes. The vehicles obtain local information limited to the vehicle ahead through radar communication. The local information is extended to the immediate environment through V2V communication amongst the vehicles. The information is extended further through V2I communication with road side units in range. The road side units are wireless transmitters, providing the vehicles with relevant road traffic information. Additionally, the infrastructure can provide several services that can be utilized in platooning control applications, such as dynamic road speed, road topography databases, smart lights, traffic congestion reports, shock waves information, and optimal routing.

vehicle-to-infrastructure (V2I) have matured. To enable V2V and V2I (V2X) communication a communication protocol, IEEE 802.11p, has been approved as an amendment to the IEEE 802.11 standard to add wireless access in vehicular environments (WAVE). In the beginning, IEEE 802.11p was considered for dedicated short-range communication. It was mainly considered for use cases in vehicle-based communication networks, particularly for applications such as toll collection, vehicle safety services, and commerce transactions via cars. In 2008 the European Commission licensed part of the 5.9 GHz band (5.85–5.925 GHz) for priority road safety applications and inter-vehicle, infrastructure communications. Required enhancements to the 802.11 standard have been defined to support data exchange between high-speed vehicles and between the vehicles and the roadside infrastructure. The Car 2 Car communication consortium (C2C, 2002) have been tasked to develop an open standard for V2X communication. The European Commission have also issued an invitation to key actors for preparing a coherent set of standards, specifications and guidelines to support a wide implementation and deployment of cooperative intelligent transportation systems (European Commission, 2009). Hence, the stan-

Figure 1.7: An HDV platoon traveling with a given initial set speed and relative distance. Several external forces such as air drag, road friction and gravity along with internal forces affect a vehicle in motion. (Photo provided courtesy of Scania CV AB.)

dard is currently under development. V2X information can also be conveyed over the mobile broadband network as presented in the European CoCar project (Dietz, 2009). However, applications are mainly considered for infotainment and apps, as latency issues must first be resolved for real-time vehicle control applications.

The wireless communication can provide a rich information range that allows for improvement in the control strategy with respect to fuel consumption and emission. In addition, V2X communication can provide the driver or system with local information and global information, such as dynamic behavior of the vehicles within the platoon, optimal traffic routing, safety issues, etc. – enabling strategies based upon events occurring over a large horizon. Hence, several technologies exist and can be fused to enable and enhance the performance for platooning. However, economical feasibility, standardization, and safety aspects are still unresolved issues. Thus, implementing new enabling technologies requires careful consideration and design to facilitate a wide range implementation.

1.3 Problem Formulation

The problem that is studied in this thesis is the fuel reduction potential for a platoon of N long haulage HDVs, illustrated in Figure 1.7, traveling on a road with a given

initial set speed and relative distance.

Each HDV in the platoon can be modeled based upon the road grade α, the internal forces produced by the powertrain and the main external forces acting upon the vehicle. A longitudinal dynamics model can be derived for each vehicle in the platoon based upon their individual vehicle properties. Dynamics of the relative distance between the vehicles is modeled as the change in velocity between two vehicles in the platoon. The HDV platoon model is

$$\begin{aligned}
\dot{s}_1 &= v_1, \\
\dot{v}_1 &= f_1(v_1, s_1 - s_2, \alpha(s_1), u_1), \\
\dot{s}_2 &= v_2, \\
\dot{v}_2 &= f_2(v_2, s_1 - s_2, s_2 - s_3, \alpha(s_2), u_2), \\
&\vdots \\
\dot{s}_{N-1} &= v_{N-1}, \\
\dot{v}_{N-1} &= f_{N-1}(v_{N-1}, s_{N-2} - s_{N-1}, s_{N-1} - s_N, \alpha(s_{N-1}), u_{N-1}), \\
\dot{s}_N &= v_N, \\
\dot{v}_N &= f_N(v_N, s_{N-1} - s_N, \alpha(s_N), u_N),
\end{aligned} \tag{1.1}$$

where s_i denotes the absolute traveled distance for the ith HDV from a reference point common to all vehicles in the platoon, v_i is the velocity for vehicle i, u_i denotes the control input to the vehicle and $i = 1, \ldots, N$ denotes the vehicle position index in the platoon. The maps f_i are the longitudinal dynamics. For convenience, let us introduce $d_{i-1,i} = s_{i-1} - s_i$ as the relative distance between ith vehicle its preceding vehicle.

A coupling is induced by the variation in aerodynamics between HDVs operating at a close distance. This is essential in the analysis of fuel reduction potential for HDV platooning. The aerodynamic drag decreases as the gap between the vehicles are reduced. However, as the relative distance decreases, it becomes more costly to maintain the relative distance due to safety aspects. Moreover, additional constraints are induced due to physical limitation on the control inputs. An HDV can generally produce a maximum engine torque of 2000–3000 Nm depending on the specific diesel engine. Thus, due to its extensive mass, an HDV might not be able to maintain a constant velocity when traversing steep uphill segments. The maximum braking torque depends on the vehicle configuration but can be approximated by 60 000 Nm/axle. Hence, the physical constraints for an HDV has an influence on the minimum achievable safe relative distance. Also, fuel-optimal control for a single vehicle on a flat road is to maintain a constant velocity, under the presumption that the traveling time is fixed. Any deviations in the form of acceleration and deceleration result in an increased fuel consumption. An HDV platoon control strategy generally receives information regarding the relative velocity and distance to the vehicles in the platoon and thereby maintains the relative distance by adjusting its speed

accordingly. The increased control effort that the strategy creates, in the sense of additional transient engine actions and brake events, produces an increased fuel consumption.

Hence, the problem that we consider is finding the fuel reduction potential for an HDV platoon consisting of N vehicles, traveling without any surrounding traffic, subject to the HDV vehicle dynamics, the safety constraints, road grade influence, and the physical constraints on the control inputs imposed by the vehicle configuration.

1.4 Thesis Outline and Contributions

In this section, we outline the contents of the thesis and the main contributions. In Chapter 2, we describe the background for vehicle platooning. A brief description intelligent transportation systems is presented along with a short survey on the current technology development for vehicle platooning. A review of the existing literature on automated vehicle platooning is given, followed by a description of current ADAS that can already be used for vehicle platooning or serve as inspiration for future possible use cases. In Chapter 3, several models are presented, which are utilized to address certain aspects of vehicle platooning. We present an advanced simulation model that serves as a basis for evaluation and verification throughout this thesis. Furthermore, a model for a platoon system architecture is presented that divides the large and complex system into smaller manageable subsystems. In Chapter 4, the fuel reduction potential of HDV platooning for a commercial controller is evaluated on a measured highway in Sweden. In Chapter 5 we address the problem of finding the minimum safety distance between two HDVs traveling on a road without compromising safety, where an experimental setup for evaluating the derived safe sets is given together with experimental evaluations. A methodology to produce a systematic decentralized LQR control design for HDV platooning is presented in Chapter 6, where simulation and experiment results are given to determine and evaluate the performance of the proposed controller in practice. In Chapter 7, we consider the problem of finding a suitable fuel-efficient controller for HDV platooning under road and vehicle parameter uncertainties, where we propose two novel model predictive control strategies based on road grade preview information. The fuel-saving potential is studied for a three-vehicle platoon in Chapter 8, where the follower vehicles are governed by our proposed decentralized cooperative controllers over a varying topography. Chapter 9 provides concluding remarks and future outlook for HDV platooning. In the following, we discuss the details of the contributions.

System Modeling

In Chapter 3, we consider the longitudinal dynamics for a single vehicle and form models that serve as a basis for the analysis and control design presented in the following chapters. We present the main components that influence the considered

dynamics for a single HDV, which is then extended to a linearized platoon model. However, the analytical model does not capture the dynamics that arise from gear changes, effects of switching between the embedded systems, brake blending, etc., that come into play in practice. A more complex simulation model is thus necessary to evaluate the fuel reduction potential of the implemented control strategy and platoon behavior. Hence, we present an advanced simulation model that has been tested and verified to mimic real life behavior for a single vehicle. The simulation model serves as a basis for evaluation and validation throughout this thesis. It also facilitates reproducible data and serves as a necessary precaution measure before evaluating safety critical operations in practice. Furthermore, there are several technologies and systems that are involved in the process of automated HDV platooning. Analyzing the entire system is not manageable due to the system complexity. There are no available tools to handle all the aspects of such a large control system. Thus, we propose a suitable system architecture for dividing the complex problem into manageable subsystems for optimal control. The material presented in this chapter is in part based on the work presented in

A. Alam. *Optimally Fuel Efficient Speed Adaptation.* Master's thesis, Royal Institute of Technology, Automatic Control (2008)

Part of the proposed architecture in this thesis is based on the journal paper in

A. Alam, J. Mårtensson, and K. H. Johansson. Experimental evaluation of decentralized cooperative cruise control for heavy-duty vehicle platooning (2014*c*). Submitted for journal publication.

Preliminary work, in line with the interests of this chapter, were also conducted as a supervised Master's thesis project in

H. J. Tehrani. *Study of Disturbance Models for Heavy-duty Vehicle Platooning.* Master's thesis, Royal Institute of Technology (KTH) (2010)

D. Norrby. *A CFD study of the aerodynamic effects of platooning trucks.* Master's thesis, Royal Institute of Technology (2014)

Fuel-Saving Potential of Platooning

In Chapter 4, we investigate the fuel reduction potential of heavy-duty vehicle platooning, solely with respect to a commercial control strategy. The aim is not to investigate the specifics of the control strategy, but rather the translation from the lowered air drag to the fuel reduction potential in HDV platooning based on simulations and experimental studies. Fuel-optimal control for a single vehicle on a flat road is to maintain a constant velocity, under the presumption that the traveling time is fixed. Any deviations in the form of acceleration and deceleration result in an increased fuel consumption. The ACC generally receives information regarding the relative velocity and distance to the vehicle ahead and thereby maintains the

relative distance by adjusting its speed accordingly. The increased control effort that the ACC creates, in the sense of additional transient engine actions and brake events, produces an overall increased fuel consumption. Thus, it is interesting to determine whether the increased control effort produced by the ACC possibly cancels the reduction in fuel consumption achieved by decreasing the air drag. Furthermore, we show that it is beneficial to reduce the inter-vehicle spacing between each vehicle in the platoon and that the conventional control strategy can be improved with respect to fuel consumption. However, safety becomes an issue when reducing the relative distance. The material presented in this chapter is based on the conference publication in

A. Alam, A. Gattami, and K. H. Johansson. An experimental study on the fuel reduction potential of heavy duty vehicle platooning. In *13th International IEEE Conference on Intelligent Transportation Systems*. Madeira, Portugal (2010)

Safety Constraints

In Chapter 5, we investigate the minimum possible relative distance between platooning HDVs that can be maintained without compromising safety. We primarily establish safe sets, which can serve as a reference for HDV platooning in collision avoidance. We propose a novel approach by setting up a relative coordinate framework and thereby computing so called reachable sets to develop safety criteria for HDV platooning. A differential game formulation of the problem enables the safe set derivation by capturing the event when the lead vehicle blunders in the worst possible manner. A collision can occur if the unsafe set is entered. Computing safe sets is an efficient method to capture the behavior of entire sets of trajectories simultaneously. We establish empiric results for validation of the analytical framework and numerical safe set computation for collision avoidance in HDV platooning scenarios. We propose an automated and reproducible method to derive empiric results for validation of safe sets. We show how the method has been evaluated experimentally using real HDVs provided by Scania CV AB on a test site near Stockholm. Based on the theoretic and empiric results, we determine criteria for which collisions can be avoided in a worst-case scenario and thereby establish the minimum possible safe distance in practice between vehicles in a platoon. We show that the minimum relative distance with respect to safety depends on the nonlinear behavior of the brake system and delays in information propagation along with the implemented control actions. By introducing V2V communication, the relative distance between the HDVs can be reduced significantly compared to what is utilized in current ACCs. The material presented in this chapter is based on the conference publication and journal paper in

A. Alam, A. Gattami, K. H. Johansson, and C. J. Tomlin. Establishing safety for heavy duty vehicle platooning: A game theoretical approach. In *18th IFAC World Congress*. Milan, Italy (2011*b*)

A. Alam, A. Gattami, K. H. Johansson, and C. J. Tomlin. Guaranteeing safety for heavy duty vehicle platooning: Safe set computations and experimental evaluations. *Control Engineering Practice*, 24: 33 – 41 (2014*a*)

Decentralized Cooperative Control for HDV Platooning

In Chapter 6, we derive a decentralized controller for HDV platooning and establish empiric performance results for the presented control design. Several studies on vehicle platooning have been based on simplified theoretical models. However, as shown in this chapter, delay and nonlinear dynamics can have a significant influence on the closed-loop system. We present a method for designing suboptimal decentralized feedback controllers, with low computational complexity, that takes dynamic coupling and engine response delays into consideration. The controller performance is evaluated through implementation on commercial HDVs. The design method is scalable in the sense that an additional vehicle can be added at the tail of the platoon without mandating a change in the controllers of the already platooning vehicles. Our proposed vehicle system architecture in Section 3.3.3 is shown to be robust to packet losses or short outages in V2V communication. As modern HDVs in general have two separate low-level control systems for governing the longitudinal propulsion and deceleration of the vehicle, the engine management system (EMS) and the brake management system (BMS), we present a simple bumpless transfer scheme to switch between these systems. The proposed platooning controller can be easily implemented on modern HDVs, without requiring any changes in the already existing vehicle architecture. We show that the controller behaves well even when performing outside the linear region of operation. We also show that the proposed controller attenuates the effect of disturbances downstream in the platoon, when studying scenarios that commonly occur on highways with dynamic operating conditions and physical constraints. Experimental results are given to qualitatively validate the proposed control system behavior. The results show that the controller performance is improved with increasing position index in the platoon, by utilizing additional information from preceding vehicles. However, the effects of unmodeled nonlinearities, such as gear changes, brake blending, and engine dynamics, can cause undesirable behavior in some cases. The experiments were conducted on a test site south of Stockholm, using HDVs provided by Scania CV AB. The material presented in this chapter is based on the conference publications and journal paper in

A. Alam, A. Gattami, and K. H. Johansson. Suboptimal decentralized controller design for chain structures: Applications to vehicle formations. In *50th IEEE Conference on Decision and Control and European Control Conference*. Orlando, FL, USA (2011*a*)

A. Alam, J. Mårtensson, and K. H. Johansson. Experimental evaluation of decentralized cooperative cruise control for heavy-duty vehicle platooning (2014*c*). Submitted for journal publication.

K.-Y. Liang, A. Alam, and A. Gattami. The impact of heterogeneity and order in heavy duty vehicle platooning networks. In *3rd IEEE Vehicular Networking Conference*. Amsterdam, Netherlands (2011)

O. Khorsand, A. Alam, and A. Gattami. Optimal distributed controller synthesis for chain structures: Applications to vehicle formations. In *9th International Conference on Informatics in Control, Automation and Robotics*. Rome, Italy (2012)

Preliminary work for this chapter were also conducted as a supervised Master's thesis projects in

G. Hammar and V. Ovtchinnikov. *Structural Intelligent Platooning by a Systematic LQR Algorithm*. Master's thesis, Royal Institute of Technology, Automatic Control (2010)

K.-Y. Liang. *Linear Quadratic Control for Heavy Duty Vehicle Platooning*. Master's thesis, Royal Institue of Technology, Osquldas väg 10, 100 44 Stockholm, Sweden (2011)

J. Kemppainen. *Model Predictive Control for Heavy Duty Vehicle Platooning*. Master's thesis, Linköping University, Automatic Control (2012)

Look-Ahead Control for HDV Platooning

In Chapter 7, we propose two novel fuel-efficient controllers based on road grade preview information for HDV platooning and determine guidelines for handling system uncertainties to maintain the fuel reduction benefits. The instantaneous fuel consumption can increase by a factor of four over a steep uphill segment when the engine is operating at maximum torque. Hence, the air drag reduction has a lower effect on the total resistive forces that are exerted on an HDV in motion over steep hills. We focus on establishing fuel-efficient controllers with low computational complexity, since it is generally not possible to implement complex control algorithms due to the limited computational power in the on-board electronic control units. The first proposed controller adapts its velocity solely based on the look-ahead velocity profile of the vehicle ahead. A more fuel-efficient strategy is established with the second proposed controller, which cooperatively forms a common look-ahead control strategy for all platooning vehicles with respect to the most restricted vehicle in the platoon. The main idea for this control strategy is to initiate the control actions in a platoon based on a point in the road rather than simultaneously implementing each HDV's control action to maintain a fixed spacing. The results for a heterogeneous HDV platoon of nine HDVs traveling over a 2 km road segment show that a fuel reduction of 12 % or 19 % can be achieved with the cooperative look-ahead controller when traversing a typical steep uphill or downhill segment of 240 m, respectively. Thus, the findings show that the fuel-saving potential can be improved significantly by considering the road grade preview information in control for HDV platooning.

We also study commercially available controllers that could be utilized for platooning. It is shown that the commercially available ACC is not fuel-efficient for a varying topography and that the LAC for a single HDV is not practical in HDV platooning. Furthermore, we investigate whether it is better to split up or maintain a platoon over steep hills and show that it is most fuel-efficient to maintain a platoon when traversing a hill, as opposed to split the platoon and resume it during or after the hill. We study what effect a varying road topography and the system uncertainties have on the fuel consumption for HDV platooning. It is shown that the fuel reduction potential with the proposed controller can degrade depending on the magnitude of the inherent errors. Hence, guidelines are determined for handling common system uncertainties that occur in practice, to maintain the fuel-saving potential. The material in this chapter is based on the conference publication and journal paper in

A. Alam, J. Mårtensson, and K. H. Johansson. Look-ahead cruise control for heavy duty vehicle platooning. In *16th International IEEE Conference on Intelligent Transportation Systems*, 928–935. Hague, The Netherlands (2013*a*)

A. Alam, J. Mårtensson, and K. H. Johansson. Cooperative control with preview topography information under system uncertainties for heavy-duty vehicle platooning (2014*b*). Submitted for journal publication.

Preliminary work, in line with the interests of this chapter, were also conducted as a supervised Master's thesis projects in

G. J. Babu. *Look-Ahead Platooning through Guided Dynamic Programming.* Master's thesis, Royal Institute of Technology, Automatic Control (2013)

L. Bühler. *Fuel-Efficient Platooning of Heavy Duty Vehicles through Road Topography Preview Information.* Master's thesis, Royal Institute of Technology, Automatic Control (2013)

Experimental Evaluation for HDV Platooning

In Chapter 8, we study the possible issues that might arise when governing an HDV platoon in practice with a cooperative adaptive cruise control (CACC) that is based on simplified linear models. We present an experimental evaluation of the fuel reduction possibilities for a heterogeneous three-vehicle platoon in practice, where results are presented based on data recorded over 2700 km per vehicle. The effects of unmodeled nonlinearities, such as gear changes, brake blending between the various brake systems in an HDV, and engine dynamics, can have unforeseen consequences. Thus, it is important to understand the issues with implementing a CACC based on linear models. Hence, we derive empirical results for our proposed CACC through experiments conducted over a Swedish highway with varying topography. It can be inferred from the obtained results that linear controllers, which does not account for road topography constraints, can reduce the fuel-saving potential significantly.

However, the results also show that the fuel-saving potential can be lost due to unmodeled engine dynamics for uphill segments and excessive braking over downhill segments. Nevertheless, a vast fuel savings can be obtained over relatively flat road segments. Furthermore, the shape and behavior of the preceding vehicles also have an impact of the fuel-saving potential. This chapter is to be submitted as a journal paper. Preliminary work for some of the material in this chapter is based on the journal publication in

J. Mårtensson, A. Alam, S. Behere, M. Khan, J. Kjellberg, K.-Y. Liang, H. Pettersson, and D. Sundman. The development of a cooperative heavy-duty vehicle for the GCDC 2011: Team Scoop. *IEEE Transactions on Intelligent Transportation Systems*, 13(3): 1033–1049 (2012)

and the supervised Master's thesis projects in

H. Pettersson. *Estimation and Pre-Processing of Sensor Data in Heavy Duty Vehicle Platooning*. Master's thesis, Linköping University, Automatic Control (2012)

S. Nilsson. *Sensor Fusion for Heavy Duty Vehicle Platooning*. Master's thesis, Linköping University, Automatic Control (2012)

Other Academic Publications

The following publications are not covered in this thesis but they inspired some of the contents.

H. Feyzmahdavian, A. Alam, and A. Gattami. Optimal distributed controller design with communication delays: Application to vehicle formations. In *IEEE 51st Annual Conference on Decision and Control*, 2232–2237. Maui, HI, USA (2012)

M. Larsson, J. Lindberg, J. Lycke, K. Hansson, E. R. A. Khakulov, F. Svensson, I. Tjernberg, A. Alam, J. Araujo, F. Farokhi, E. Ghadimi, A. Teixeira, D. V. Dimarogonas, and K. H. Johansson. Towards an indoor testbed for mobile networked control systems. In *Proceedings of the 1st Workshop on Research, Development, and Education on Unmanned Aerial Systems*, 51–60 (2011)

Contributions by the Author

The order of the authors' names reflect the work load of the paper, where the main contribution is attributed to the first author. An exception with the journal publication in Mårtensson et al. (2012), where the first author was the corresponding author. All other authors' names are given in alphabetical order and the workload is divided into their respective fields. Several Master's thesis projects have also been conducted in parallel with this thesis work. Each thesis project have been

supervised by the author of this thesis, where the author participated actively through discussions and derivations of the theories.

Patents

Along with academic publications, two Swedish and nine international patent applications have been published during the course of this work. Two, out of the nine international patent applications, have been granted as Swedish patents.

A. Alam, J. Andersson, and P. Sahlholm. *A Vehicle Speed Control Method.* International patent application number: PCT/SE09/050030 (filed 2009*a*)

A. Alam, J. Andersson, and P. Sahlholm. *Determination of acceleration behavior.* International patent application number: PCT/SE09/051299 (filed 2009*b*)

A. Alam, K.-Y. Liang, and A. Gattami. *Metod i samband med fordonståg, och ett fordon som använder metoden [A method in connection to vehicle trains and a vehicle that uses that method].* Swedish patent application number: 1150579-9 (filed 2011*c*)

A. Alam, H. Pettersson, T. Sandberg, and J. Dellrud. *Method and management unit pertaining to vehicle trains.* International patent application number: PCT/SE12/050066 (filed 2011*d*)

A. Alam, J. Andersson, H. Gustafsson, H. Pettersson, P. Sahlholm, and H. Schauman. *Metod i samband med trafikövervakning, och ett trafikövervakningssystem [Method in connection with traffic monitoring and a traffic monitoring system].* Swedish patent application number: 1150073-3 (filed 2011*b*)

A. Alam, J. Andersson, H. Gustafsson, H. Pettersson, P. Sahlholm, and H. Schauman. *Method and system for speed verification.* European patent application number: 11193590.4 (filed 2011*a*)

A. Alam, S. Nilsson, J. Kemppainen, H. Pettersson, and H. Pettersson. *System and method for assisting a vehicle when overtaking a vehicle train.* International patent application number: PCT/SE13/050674 (filed 2012*b*)

A. Alam, S. Nilsson, J. Kemppainen, H. Pettersson, and H. Pettersson. *System och metod för att assistera ett fordon vid omkörning av fordonståg [System and method for assisting a vehicle when overtaking a vehicle train].* Swedish patent number: 1250627-5 (Granted 2014*a*)

A. Alam, S. Nilsson, J. Kemppainen, H. Pettersson, and H. Pettersson. *System and method for regulating of vehicle pertaining to a vehicle train.* International patent application number: PCT/SE13/050673 (filed 2012*c*)

A. Alam, S. Nilsson, J. Kemppainen, H. Pettersson, and H. Pettersson. *System och metod för reglering av fordon i ett fordonståg [System and method for regulating of vehicle pertaining to a vehicle train].* Swedish patent number: 1250628-3 (Granted 2014*b*)

A. Alam, S. Nilsson, J. Kemppainen, H. Pettersson, and H. Pettersson. *System and method for regulation of vehicles in vehicle trains.* International patent application number: PCT/SE13/050672 (filed 2012*d*)

A. Alam, S. Nilsson, J. Kemppainen, H. Pettersson, and H. Pettersson. *System and method pertaining to vehicle trains.* International patent application number: PCT/SE13/050687 (filed 2012*e*)

A. Alam, A. Johansson, R. Lyberger, and H. Pettersson. *Method and system for spacing adjustment in a moving vehicle train.* International patent application number: PCT/SE13/050317 (filed 2012*a*)

In addition, thirteen international patent applications have been filed and are currently under examination. Due to the confidential nature of the patents, the filing numbers are only given as follows:

PCT/SE14/050241, PCT/SE14/050243, 1351125-8, 1351126-6, 1351127-4, 1351128-2, 1351129-0, 1351130-8, 1351131-6, PCT/SE13/051382, 1351132-4, 1350891-6, 1350266-1.

Chapter 2

Background

"*Learn from yesterday, live for today, hope for tomorrow.*"

Albert Einstein

Information and communication technology (ICT) is paving its path into transportation systems. Many governments spend a countless amount of money on the infrastructure in restoration and expansion of the road network. However, the future improvement lies not in increasingly stringent road taxation policies to change incentives or only in improving aging infrastructure, but also increasing the utilization of information technology and thereby introducing intelligence to road traffic networks. The rapid development in ICT presents an excellent opportunity to tackle transport issues through novel integrated intelligent transportation systems (ITS) solutions.

In this chapter, we first list a few ITS applications in Section 2.1. Then, in Section 2.2, we present the contemporary technology premise for heavy-duty vehicle (HDV) platooning. Afterward, we give an overview of the related work on vehicle platooning in Section 2.3. The literature on control of platoons is quite extensive. Therefore, we have not attempted a thorough review of all the proposed control schemes here, but rather give a review of the general concepts and issues in vehicle platooning that is addressed in the literature. We then, in Section 2.4, give a brief overview of commercial advanced driver assistant systems (ADAS) that can be used, or integrated in the future, for control of HDV platoons. In particular, a detailed description of the adaptive cruise control (ACC) is given, since it serves as a first stepping stone to practical implementation of HDV platooning. A brief overview on collision avoidance and safety in vehicle applications is given in Section 2.5. The chapter is concluded with a short summary in Section 2.6.

2.1 Intelligent Transportation Systems

Transportation systems can be perceived as large mobile networks. By introducing decision making based on suitable and accurate ICT, intelligence is induced in the network. ITS, illustrated in Figure 2.1, empower actors in the system with information based actions. The European Road Transport Telematics Implementation Co-ordination Organisation (ERTICO) - ITS Europe is the network of intelligent transport systems and services stakeholders in Europe. It was founded at the initiative of leading members of the European Commission, Ministries of Transport and the European industry. ERTICO's official definition of ITS "is the integration of ICT with transport infrastructure, vehicles, and users. By sharing vital information, ITS allow people to get more from transport networks, in greater safety and with less impact on the environment" (ERTICO, 2014). ITS have received a great deal of attention in the transportation community as well as in governments over the last decade. The initial efforts were referred to as intelligent vehicle highway systems (IVHS). However, due to the increasingly intermodal focus, the scope was broadened to include modes beyond highways. There are numerous agencies working with ITS throughout the world, such as ITS America (ITSA, 2014) and ITS Japan (ITSJP, 2014) amongst others.

ITS include several applications and can be grouped within five main categories (Ezell, 2010):

- Advanced Public Transportation Systems include systems that for example allow trains, buses, and boats to report their position so passengers can be informed of their real-time arrival status and departure information.
- Advanced Traveler Information Systems provide travelers with real-time navigation routes, traffic lights, weather conditions, traffic construction, delays and congestion. Accident reports can also be provided.
- Advanced Transportation Management Systems include systems that monitors traffic flow and provide decision support based upon traffic control devices, such as traffic signals, variable message signs, and traffic operations centers.
- ITS-Enabled Transportation Pricing Systems provide services such as electronic toll collection and congestion pricing.
- Automated Transportation Systems include supporting and replacing human functions in various driving processes. The focus in this category lies on efforts for developing vehicles with automated components. Here, vehicle-to-vehicle and/or infrastructure (V2X) communication serves as a basis to provide information and enable communication between all the actors.

Through these categories, ITS aim at enhancing safety, operational performance, mobility, environmental benefits, and productivity by expanding economic and employment growth. ITS encompass the full scope of information technologies

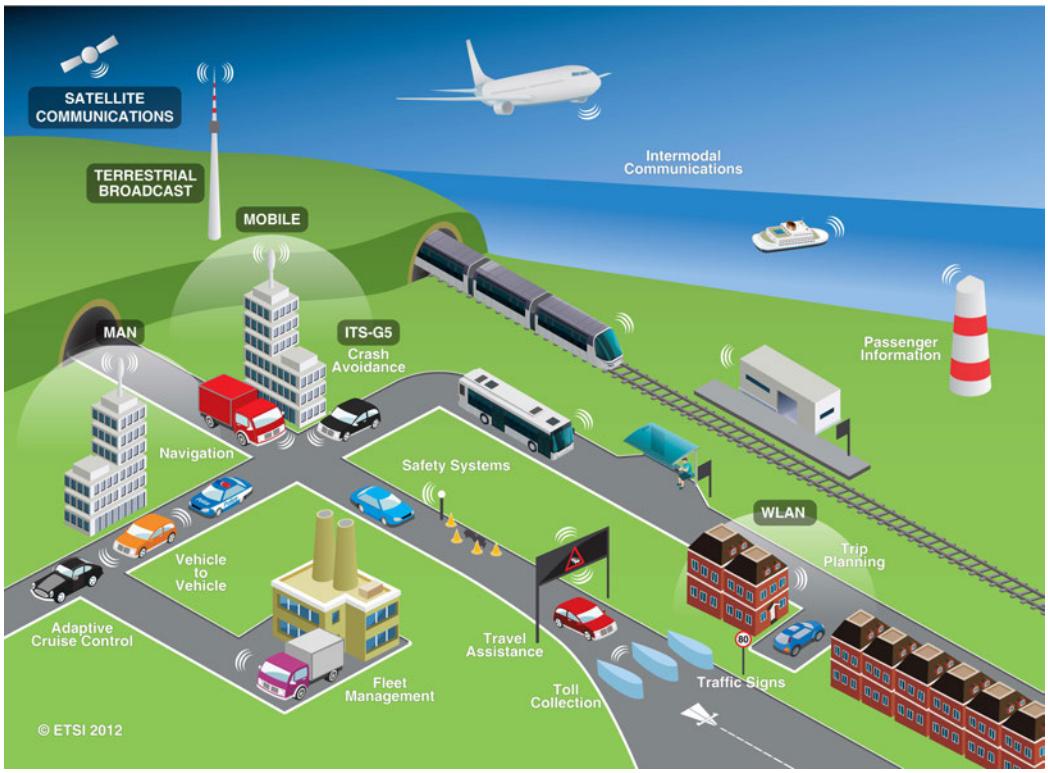

Figure 2.1: An illustration of ITS. ITS include all types of communications in and between vehicles along with communication between vehicles and infrastructure. Note that ITS are not restricted to road transport as they also include the use of information and communication technologies for rail, pipes, water and air transport, including navigation systems. (Illustration provided courtesy of ETSI (2014).)

used in transportation, including control with dynamic feedback, computation and communication, as well as the algorithms, databases, models and human interfaces. The emergence of these technologies as a new pathway for transportation is relatively new. Hence, research that adds to the scientific understanding of the impacts that ITS can have on accessibility, congestion, pollution, safety, and security is an active area.

HDV platooning is one important component of ITS. Research within intelligent vehicle platooning, in particular HDV platooning, addresses several ITS target issues. Under high traffic conditions vehicles typically maintain a small inter-vehicle spacing, effectively forming a vehicle platoon. Without the aid of intelligent systems, drivers must only rely on sounds and line of sight to gain information, which limits their capacity to make fuel-efficient decisions. Consequently, they use harsh accelerations and braking actions to maintain a short relative distance. Such transient control actions contribute to an increase in pollution in the form of emissions and road particles, as well as an increase in congestion and a decrease in accessibility. Automated vehicle platooning includes systems that allow agents within the platoon

to report their position and velocity in addition to systems that provide navigation routes, information from traffic control devices, road construction and congestion. With the aid of V2X communication devices, a cooperative system is formed for supporting and replacing human functions in various driving processes to enhance operational performance, mobility, environmental benefits, safety, and economic growth.

In line with the interests of this thesis, the challenges and benefits of HDV platooning in practice have been studied within several ITS research projects throughout the world. In the projects PROMOTE-CHAUFFEUR I & II, needs of intermediate and end users, along with safety and operational requirements, were investigated (Harker, 2001). In KONVOI, experimentally analyzing the use of electronically regulated truck convoys on the road with five vehicles was one of the main focuses (Deutschle et al., 2010). The acceptance of automated platoons in mixed traffic was studied, where it was observed that operating at an inter-vehicle spacing of 10 m seemed to be insignificant for passing vehicle, in comparison to a spacing of 50 m. It was inferred that road users expect automated platoons to behave cooperatively by, for example, open up a gap or change lanes if needed. California Partners for Advanced Transportation Technology (PATH), established in 1986, is a vast research project that addresses many traffic related research aspects (Bu et al., 2010). Results in this project have shown that the highway throughput can be increased three times through platooning by utilizing services provided by the automated transportation systems. Another research project, Strategic Platform for Intelligent Traffic Systems (SPITS), shows in addition that potential shock waves arising in traffic congestions can be removed through automated platooning (SPITS, 2014). Focus has lately been directed towards studying HDV platooning, mainly due to the fuel and congestion reduction potential. The recently concluded ENERGY ITS project, evaluated energy-efficiency for automated HDV platooning and methods for effectiveness of ITS on energy saving (Tsugawa, 2013). The results obtained in the project showed an average fuel-saving potential of 9–16 % for a three-vehicle platoon on a flat test track. In the Safe Road Trains for the Environment (SARTRE) project, the focused lied on mixed traffic in highway situations, where fuel-efficiency, safety, and comfort was evaluated, (Robinson et al., 2010). Findings within this project showed that a 20 % emission reduction, a 10 % reduction in fatalities, and a smoother traffic flow with potential increase in traffic flow can be obtained through automated vehicle platoons. The findings are based on that a lead vehicle with a professional driver will take responsibility and guide the vehicle platoon. Vehicles will join the platoon and enter an autonomous control mode that will allow the automated system to fully govern the vehicle while the driver can withdraw his attention from the road. In addition, experiments conducted on a flat test track in this project showed fuel saving results between 2–16 % depending on the vehicle type and inter-vehicle spacing. The aim of the Grand Cooperative Driving Challenge (GCDC) project was to accelerate the deployment of cooperative driving systems (van Nunen et al., 2012). Several, issues, such as communication constraints and erroneous information, were revealed in this project that needs to be solved before platooning can presented

commercially. Finally, in the recent project COMPANION (Adolfson, 2014) a wider perspective is undertaken, where the actual creation, coordination, and operation of platoons is studied. The goal is to identify means of applying the platooning concept in practice for daily transport operations.

2.2 Technology for HDV Platooning

The demand for enhancing vehicle performance has paved the way for several technological developments. On-board sensors have increased in number and accuracy. This has led to the development of on-board networks to share and convey information between electronic control units (ECUs). Faster and cheaper vehicle computer technology has been developed to process the growing amount of available information. With increasing reliability and computational performance, in parallel with decreasing size and price, new sensors have been implemented to further enhance the operational performance. However, currently we see a transition, which is not necessarily induced by the vehicle industry. Technology that was initially developed and intended for entirely different markets is now finding its use and presenting a new scope for enhancing vehicle applications and enabling vehicle platooning. Thus, automated HDV platooning could not be considered in practice until now and the understanding of the potential benefits is growing rapidly. In this section, we describe some of the key components that contribute to and enable HDV platooning, where we use Figure 2.2 to guide our discussion. We begin with the inner most ring and proceed outwards.

A wide range of vehicle specific information is provided through on-board sensors and ECUs. Traditionally vehicular research focus has been on improving the vehicle performance. During the last decades on-board sensors have been developed and implemented to facilitate the overall HDV operational efficiency. Initially, sensor technology was introduced to enhance the engine operational performance with respect to fuel efficiency and exhaust gasses. Crank-angle, RPM, pressure, and temperature sensors were implemented to enable better engine control. With the passage of time, additional sensors were implemented, for example rotational wheel sensors and gear box sensors, to further increase the operational performance. ECUs process the information and in some cases fuse it to create virtual sensors. Today, 30 to 80 ECUs are integrated in an average car, whereas 6 to 17 ECUs are integrated in an HDV. This substantial difference in ECUs is mainly due to that a passenger vehicle and an HDV operate under different premises. An HDV commonly travels under more strenuous conditions. Introducing more ECUs opens up the possibility for more system errors, which is less acceptable in the HDV market. Furthermore, underdeveloped countries demand less ECUs due to manageability and price sensitivity. Implementing electronic sensors has become a relatively cheap and efficient way to enable new functionality.

In 1985 Bosch developed the controller area network (CAN) for in-vehicle networks (Johansson et al., 2005). Thereby, dedicated wiring was replaced by a

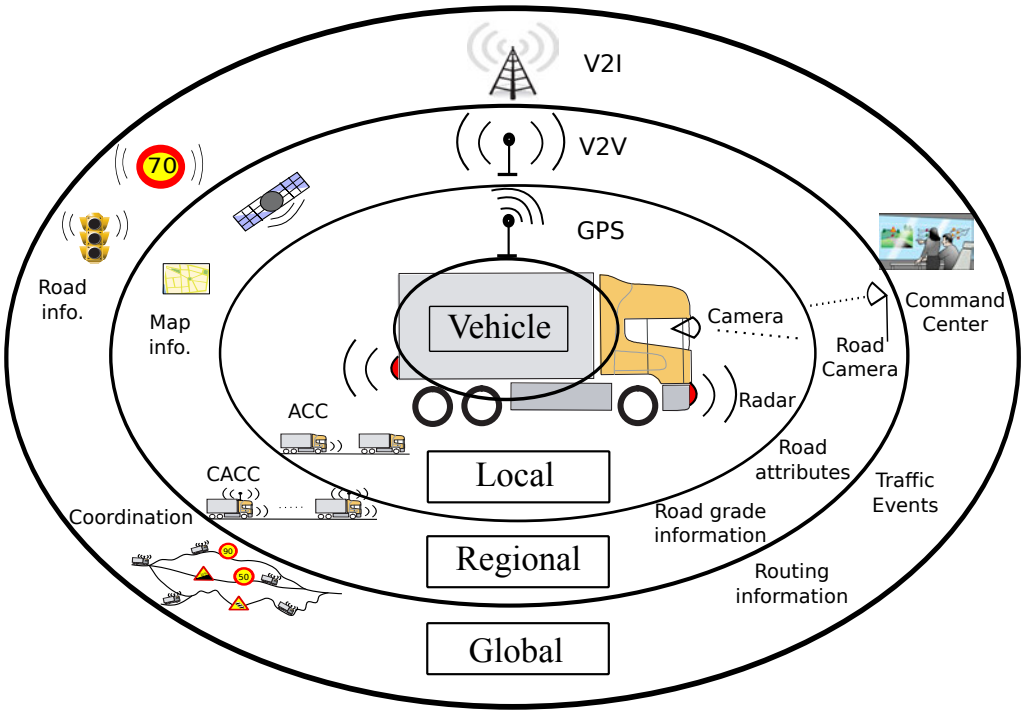

Figure 2.2: An overlay of the technological premise for HDV platooning. The top half shows the available technology for HDV platooning and the bottom half shows some enabled functionalities. Each ring represents a specific sensor group with respect to perception range. The inner ring, labeled vehicle, represents on-board sensors and ECUs that provide internal vehicle specific information and control systems. The next ring, labeled local, extends the perception range 50-100 m outside the vehicle through camera and radar sensors. With the introduction of maps, satellites and vehicle-to-vehicle (V2V) technology the perceived range is extended regionally. Wide area networks is enabled through vehicle-to-infrastructure (V2I) technology, in the final ring labeled global, which represents technology that facilitates HDV platooning by providing interaction between vehicles and the surrounding infrastructure over a whole country or even a continent.

communication bus, which reduced complexity, wiring cost, and weight. This was a revolutionary step, since monitoring and control of the entire electromechanical system could be achieved. Each ECU was now able to communicate internally, enabling more advanced functions, such as anti-lock braking system (ABS), electronic stability program (ESP), or the airbag, which relied on several sensors. With time, the sensors increased in reliability, accuracy and quality while the size and cost decreased. In parallel, the HDV ECUs memory and processing power have improved significantly. In the 1970s a standard ECU contained 1 kbyte of RAM, 8 kbyte of ROM, and 1 MHz clock speed, whereas today it can contain up to 4 MB flash memory, 256 kbyte RAM, and 264 MHz clock speed (Freescale, 2014). Thus, faster

and more computational complex functionalities have been developed over time.

A local environment awareness is obtained by monitoring the nearest vicinity. With the development of vehicle internal sensors for improving operational and safety performance, the next step in sensor development was to monitor the nearest vicinity. Initially the local environment sensors were costly, large, and therefore not yet suitable for the commercial market. To date, the technology has improved and is becoming fairly inexpensive. Radar or lidar sensors, to detect and monitor objects moving in the neighborhood of the subject vehicle, have matured to the extent of being commercially viable. The cost and hardware size have reduced significantly over the years. Low cost monolithic microwave integrated circuit based millimeter-wave front end modules, entailing down to a $1\,\mathrm{mm}^2$ chip, for automotive radar applications are now available (Walden and Garrod, 2003). In-vehicle camera monitoring devices is another local environment sensor technology that has matured. Initially the size of the cameras and the image processing unit were too large to mount in the front window. With the emerging improvement in camera lens technology and signal processing capabilities of microprocessors, most vehicle manufacturers are starting to implement camera based monitoring systems. Commonly, such systems involve lane departure warning or steering. More advanced systems involving traffic sign detection, driver attention, and pedestrian detection are now also being developed and offered by some vehicle manufacturers. Furthermore, fused with radar data, a three dimensional environment can be formed, which can be utilized in future arising safety and navigation systems. Hence, the small hardware size and the computation power for performing advanced calculations within milliseconds, have recently extended the range for the on-board vehicle sensors and their possible use cases.

The regional environment awareness is provided by information from global positioning system (GPS) technology, map data, and V2V communication devices. Due to recent advancements in improved map data and GPS accuracy, GPS technology can now deliver centimeter accuracy with the aid of real time kinematic base stations or differential GPS (Kaplan and Hegarthy, 2006). Alternatively, the relative position estimates in each vehicle can cooperatively be fused together with the estimates of neighboring vehicles that are obtained through V2V communication. Thereby, relative positioning can be made with higher accuracy and precision in comparison to the differential GPS (Alam et al., 2013*b*). Map providers, such as NAVTEQ, are developing methods for acquiring road grade information to obtain a three dimensional topography map and are currently able to deliver such maps over a limited region. Hence, in Sahlholm and Johansson (2010) a road grade estimation algorithm is presented, based on Kalman filter fusion of vehicle sensor data and GPS positioning information. Road grade estimation is a vast research area. It is typically estimated at the vehicle position, but it can also be estimated over segments. In Bae et al. (2001) one for road grade estimation method based on a GPS receiver with 3D velocity output and one using a two-antenna GPS were presented. A recursive least squares method with forgetting for online applications was presented in Vahidi et al. (2005). Another recursive least squares method and survey of online road

grade estimation without GPS, based on accelerometers and on-board sensors, can be found in Fathy et al. (2008). Moreover, GPS devices are becoming increasingly common among all traffic agents. Omnipresent mobile phone devices can deliver positioning, heading and velocity for pedestrians, mopeds, motorcycles and bicycles. Thus, ECUs might now not only be able to monitor and intelligently govern the internal vehicle systems, but also gather external information regarding the surrounding traffic and topography. Hence, an HDV will be able to react based upon the internal and external environment influences.

For effective and safe platooning additional information is necessary in addition to what is provided by radars and cameras. If vehicles interact through wireless communication, an HDV can adjust the velocity and relative distance based upon events occurring further ahead in the platoon. Thus, safety, fuel efficiency, road capacity and emissions can be improved significantly by enabling a reduced inter-vehicle spacing through preview information. The interaction through V2V communication can improve safety by setting for example a deceleration limit for the HDVs in the platoon or setting a safe distance based upon the vehicle characteristics. Smoother control can also be implemented through prediction based upon information on events occurring upstream. Hence, V2V communication enables cooperative driving and automated platooning systems. Several different wireless technologies are currently under consideration for V2V communication. These technologies include conventional IEEE 802.11 wireless local area network (LAN), dedicated short range communication, and GPRS/UMTS, amongst others. However, the IEEE 802.11 technology family is most likely to be used as the prevailing communication standard for future V2V communication, due to its success in the area of data communication. In particular, the recent wireless communication protocol IEEE 802.11p (802.11p, 2014) has opened up an entire new set of applications for vehicular systems. The purpose of this standard is to provide the minimum set of specifications required to ensure interoperability between wireless devices. The access layer technology for the European protocol stack has been given the name ITS-G5, even though it is purely based on IEEE standards with the addition of decentralized congestion control. For ITS-G5 in Europe this standard is given in ETSI EN 302 571 (2014). It is meant for devices attempting to communicate in rapidly changing communications environments and in situations where transactions must be completed in time frames much shorter than what is set for ad hoc 802.11 networks. This is obtained by splitting the high-rate data stream into a number of lower-rate data streams transmitted simultaneously over a number of subcarriers, where each subcarrier is narrow banded. The medium access control (MAC) in ITS-G5/802.11, is based on carrier sense multiple access with collision avoidance (CSMA/CA). The user can define own message types in the transport layer. However, two standardized message types must be generated, which are called cooperative awareness message (CAM) and decentralized environmental notification message (DENM), see the documents ETSI EN 302 637-2 (2014) and ETSI EN 302 637-3 (2014) for details. The DENMs consist of event-driven hazard warnings. CAMs are sent periodically, but not with a fixed frequency. The minimum time between two CAMs are 100 ms

and the maximum time is 1 s. The content of the CAM is divided in a number of containers, with different frequencies. There are currently no general purpose fields defined in any of the containers above, but there are possibilities to extend the number of choices in many places.

Vehicular ad hoc networks (VANETs) impose a new set of requirements on the communication systems. For example, vehicle communication cannot tolerate long delays and the moving vehicles form a dynamic ad hoc communication network. Numerous studies and evaluations have been performed on the standard, for example in Jiang and Delgrossi (2008); Ferreira et al. (2008); Barradi et al. (2010). Scalability and safety are challenging issues, since IEEE 802.11 is designed for data communication where reliability is more important than delay (Bilstrup et al., 2010). In dense and high load scenarios the throughput decreases and the delay increases significantly. Hence, even though wireless LAN is promising for the exchanging messages between vehicles in an ad hoc manner, it might not be able to provide the quality or time constraints for large vehicle networks (Gupta and Kumar, 2000). Furthermore, aspects like efficient message dissemination and information security mechanisms are still ongoing research areas for VANETs (Eichler et al., 2006). These issues must be resolved before full implementation of VANETs. Nevertheless, V2V communication enables a wide range of information to the vicinity. Previously most information has been gathered by direct visual observation and in response to sounds. Now, vehicles traveling in a platoon will be able to act faster with interaction, intents and events produced by several vehicles in the surrounding environment.

A global awareness is enabled by V2I information. Thereby, for example, coordinating and routing vehicles to form platoons for improved fuel-efficiency is achieved. In combination with GPS-technology, the position and movement of every connected vehicle are known to the fleet manager. If coordinated departures are not feasible, HDVs are typically scattered over the road network (Liang, 2014). Through V2I, a command center or a fleet manager can monitor the vehicles in traffic. For every transport assignment the fleet manager can pre-plan the routes and departures through optimization schemes, such that platoons are formed for maximized fuel-efficiency and fill rate in each vehicle. In addition, offline route optimization can be formed at the command center for every vehicle that is already out on the road. Thereby, directives are sent through V2I, instructing a vehicle to either increase its speed to catch up with an HDV further ahead, or slow down such that another HDV might catch up to form a platoon. Obstructing traffic situations that are reported to a traffic management center is also relayed to vehicles that plan to travel on that route. Hence, smart routing is formed by finding an alternative path to ensure that the transport assignment is on time.

Even though there is an apparent strong need for automated HDV platooning systems, they have only recently become a possibility. Each traffic agent will soon be able to serve as an information node through wireless communication; enabling other agents to interact, as opposed to simply react, to internal and external influences. Thereby, vehicles will be able to travel at small inter-vehicle spacings, effectively reducing congestion, relieving driver tension, improving fuel consumption

and emissions without compromising safety. There are however many challenges, such as safety, reliability, standards, etc., that must be addressed before HDV platooning can become commercially feasible. With respect to longitudinal control of the vehicles, the question of whether to implement a centralized or decentralized control arises. As depicted in Figure 2.2, there are several technologies and systems involved in the process of HDV platooning. Analyzing the entire system is not manageable due to the system complexity. There are no available tools to handle all the aspects of such a large control system. Thus, an important challenge is to establish a suitable system architecture, which is decomposable into manageable subsystems. In this thesis we present such a system architecture in Chapter 3. Chapter 6 presents a decentralized controller suitable for that architecture.

2.3 Cooperative Vehicle Platooning

The concept of partial automation of highway traffic is not a new idea. At the 1939 World's Fair in New York, General Motors presented a vision of automatically controlled vehicles on highways, aiming at guaranteeing safety for increased speed (General Motors, 1939). Even before the automatic control of vehicles was considered, studies on the dynamics of a collection of vehicles following each other in a single lane have been performed since the 1950s. By assuming a simple model of driver behavior, Pipes (1953) and Chandler et al. (1958) give early results on the dynamic response of follower vehicles to the behavior of the leading vehicle, where the latter reference includes experiments using real vehicles.

The first investigations into control for heavy vehicle platooning was in the early 1960s (Rothery et al., 1964). Vehicle platooning can be described as a chain of vehicles traveling at a given velocity and inter-vehicle spacings. The primary objective for each vehicle with respect to safety is to maintain its distance to the preceding vehicle in the platoon. Even under normal operating conditions there will be deviations from the desired velocities and desired relative distances. A vehicle platoon is most commonly modeled in the literature as a set of moving masses

$$\ddot{x}_i + k_i \dot{x}_i = u_i, \quad i = 1, \ldots, N \tag{2.1}$$

where x_i represents the position of the i:th vehicle, $k_i \geq 0$ denotes a system damping coefficient, sometimes referred to as the linearized drag coefficient per unit mass, and u_i is the applied control force. Control of vehicular platoons was early studied by Levine and Athans (1966) and Melzer and Kuo (1971a). Their work considered centralized control design for vehicle platoons, indirectly assuming that computational complexity and V2V communication hardware constraints would not be an issue. A linear quadratic regulator (LQR) control strategy was developed that regulates the position and velocity of every vehicle in a densely packed string of high-speed moving vehicles. The presented control methodology involved full state information of each vehicle in the platoon.

An early hope for high-speed vehicle platoons was that centralized automatic control could encompass very large platoons. Thus, control strategies were derived based upon a countably infinite number of vehicles in order to understand the fundamentals of the problem (Melzer and Kuo, 1971*b*). A new structural analysis was introduced, allowing for a bilateral Z-transform to convert the problem into a family of finite-dimensional systems. It was found that coupling between the vehicles decreases as the platoon index distance between them increases. It has been hypothesized that the controller gain will decrease with increasing index distance, concluding that vehicles far away in a platoon has less controller impact on performance. However, even though infinite platoons capture the essence of large platoons, the LQR problem formulation lacks observability and stabilizability in the infinite case and is therefore ill-posed (Jovanović and Bamieh, 2004).

Governing vehicle platoons by an automated control strategy, the overall traffic flow is expected to be improved (Ioannou and Chien, 1993). Through short relative distances down to 2 m, the road capacity is significantly increased. In De Schutter et al. (1999), it is shown that the total road capacity can be increased two to three times compared to roads with manually operated vehicles and emissions can be reduced through an automated controller for platooning. Traffic flow has been considered as a key performance index in vehicle platooning. In Varaiya (1993) it was shown that by forming platoons, the throughput of a highway can be increased from 2000 vehicles per lane per hour to more than 6000 vehicles per lane per hour. The findings were based on an average platoon size of 15 vehicles, with intra-platoon distances of 2 m, inter-platoon distances of 60 m, vehicle length of 5 m, and speed of 20 m/s. However, it was argued that only full automation can achieve significant capacity increases on highways and thereby reduce the occurrences of traffic congestion. In Wang and Rajamani (2004*b*) the effects of having a varying spacing policy on the traffic flow is studied. The research areas coordinating and forming platoons have grown recently. In Farokhi and Johansson (2013), a game-theoretic approach is undertaken for evaluating platoon incentives. Local controllers throughout the road network are introduced in Larson et al. (2013) to facilitate platoon formations with minimal information. The paper by Meisen et al. (2008) attempts to increase platooning throughout a network by using data-mining techniques to identify common routes where platoons can be formed. In Liang et al. (2013), the fuel-efficiency of increasing the speed to catch-up to a vehicle further ahead on the road is studied. Thereby, distance boundaries are given for when it is beneficial to form a platoon by increasing the speed temporarily.

Communication constraints is an important issue that can dictate the defining feature of the problem (Gupta et al., 2004). It is not realistic to assume that an agent in the platoon would know the state of all the other agents in the formation at any given time and be able to use it to calculate the control input due to physical constraints in the information flow. Hence, we argue in Chapter 6 that the problem at hand is a decentralized control problem with arbitrary information flow patterns. In general, this is a much harder to solve than the traditional optimal control problem.

The problem of decentralized control has a long history and much effort has been put in the research area. Decision team problems were introduced in Marshak (1955), where each team member is trying to optimize a common cost function through limited information concerning the global state of nature. Witsenhausen showed that, in general, a linear controller is not optimal for a quadratic performance criterion with a linear time-invariant system subject to Gaussian noise under the distributed information constraint and that the cost function is not necessarily convex in the controller variables (Witsenhausen, 1968). In Blondel and Tsitsiklis (2000); Papadimitriou and Tsitsiklis (1986) it was established that the discrete-time version of the Witsenhausen counter-example is NP-complete. There have been some efforts also to identify the cases in which a linear solution is optimal. For instance, Witsenhausen identified some cases where the resulting optimal controllers are linear (Witsenhausen, 1971). In Ho and Chu (1972) it was shown that under a partially nested information pattern the optimal controller is a linear controller. It was shown in Sandell and Athans (1974) that the optimal controller is linear if each subcontroller has access to all the previously implemented control values and observations made by any other subsystem in the system before the current time and its own observations including the current time. Decentralized control was studied through a sequential manner by closing one loop at a time in Mayne (1979). In Bamieh et al. (2002); D'Andrea (1998) it was studied under the assumption of spatial invariance. Decentralized controllers, using only relative distance measurements with respect to nearest neighbors, were first given by Chu (1974) and Peppard (1974). Control for chain structures in the context of platoons has been studied through various perspectives, for example in Dunbar and Murray (2006); Bamieh et al. (2008); Barooah et al. (2009), where it was studied based on following a predecessor in the first paper, under certain network topologies in the second paper, and based on bidirectional schemes in the third paper. A survey on platooning and inter-vehicle control can be found in Tsugawa (1999) and more recently in Kavathekar and Chen (2011). It has been shown that control strategies may vary depending on the available information within the platoon. Initially the ACC, not being cooperative in the sense of sharing information with other agents, simply reacted with respect to the behavior of the preceding vehicle. With the introduction of V2X communication, the question arises of what information is relevant, necessary, or critical for platooning applications. Furthermore, it is of interest to determine which agents should serve as the local information sources. A natural extension to the commercially available ACC is to implement a symmetric bidirectional control architecture, where each vehicle bases its control action on the error feedback from its predecessor and follower (Barooah and Hespanha, 2005). In Sudin and Cook (2004) a two-vehicle look-ahead information structure is proposed, where each vehicle bases its control strategy only on information regarding relative velocity and relative distance from two vehicles ahead. A more general approach can be found in Gupta et al. (2004), where the information flow is dictated by the constraints of a pre-specified topology. In recent work (Kianfar et al., 2014), a design procedure is proposed that matches a model predictive control (MPC), enforcing constraints satisfaction, with a linear controller

designed to guarantee string stability.

Maintaining a suitable relative distance, stability and robustness of the platoon have been identified to be amongst the main criteria to be considered. Control design for platooning applications is still an open problem, despite substantial academic work. In Levine and Athans (1966); Stanković et al. (2000); Dunbar and Murray (2006), optimized procedures were presented to give a systematic approach to the design. However, the vehicle coupling was only introduced through the cost function. To our knowledge, no control algorithm has yet considered decentralized optimal control based upon systems with interconnected dynamics. In HDV platooning applications the coupling is induced by the variation in aerodynamics, which is essential in the analysis of fuel reduction potential. Such a consideration is presented in Chapter 6.

For vehicle platooning it is essential to use realistic models (Sahlholm and Johansson, 2010; Guzzella and Sciarretta, 2007) and not just identical low-order coupled linear models, as has often been the case in the literature. In HDV platooning mass and road slope has a significant effect on the system dynamics. Research into more implementation-relevant aspects is only recently emerging. For example, in Naus et al. (2009) a setup is presented for the cooperative adaptive cruise control (CACC), where feasibility of the actual implementation is one of the main objectives. Several practical issues such as constrained communication, heterogeneous traffic and graceful degradation to standard ACC if communication fails, are taken into consideration. In Shaw and Hedrick (2007) heterogeneous vehicle strings under simple decentralized control laws with a constant spacing control policy are analyzed. The considered vehicles do not need to have the same dynamics or the same controllers and can be arranged in any order. It is further argued that centralized formation control is impractical due to the large amount of information that needs to be communicated. Another design approach for a practical CACC was presented in Bu et al. (2010). In Milanes et al. (2014), a control system is designed, which is evaluated on four production passenger cars and the performance is evaluated in comparison with the ACC. Experiments for a platoon of six passenger cars under longitudinal control is presented in Ploeg et al. (2011). Considering nonlinearities and powertrain actuator uncertainties in HDVs, a method for calculating worst-case spacing bounds is given in Rödönyi et al. (2013). In Geiger et al. (2012); Lidström et al. (2012); Mårtensson et al. (2012), system architectures, wireless communication, and control for platooning applications were studied and evaluated through experiments in mixed traffic on a highway. Fuel reduction potentials of 5–20 % was demonstrated in experiments by Alam et al. (2010); Robinson et al. (2010); Tsugawa (2013). These results indicate that HDV platooning is an attractive concept.

2.4 ADAS for HDV Platooning

One area that shows promise for energy-efficiency and improved safety is advanced driver assistant systems (ADAS). The increasing number of on-board sensors and

ECUs in modern HDVs facilitate systems that aid the driver in addressing challenging tasks on the road. Hence, commercially available systems have been developed such as the cruise control (CC) for maintaing a constant speed. The conventional CC (Shaout and Jarrah, 1997) uses feedback information from the on-board vehicle sensors to maintain a constant speed and offers three services: maintained vehicle speed, improved fuel economy, and driver comfort over long distances. However, HDVs typically accelerate over a downhill segments when coasting. Hence, the downhill speed control (DHSC) (Fancher et al., 1981; Lingman, 2005) has been developed specially for HDVs as an automatic brake system that prohibits the vehicle from exceeding a certain offset when using the CC. When a highway contains steep road grade segments such that the HDV cannot maintain its speed in the uphill or has to brake in the downhill in order not to overspeed, a possibility arises for reducing the fuel consumption and still maintain the travel time in comparison with the standard CC. By using the road grade preview information, suitable control action commands can be sent to the engine and gearbox control systems. Thereby, the instantaneous power demand, which is mandated in the upcoming hilly road segment, can be obtained while keeping fuel consumption and environmental impact as low as possible. For example, by lowering the speed before an upcoming downhill segment, unnecessary braking actions can be avoided and the total fuel-consumption can be reduced significantly. Early work on utilizing road grade information in vehicle speed control can be found in Schwarzkopf and Leipnik (1977), where a minimum-fuel problem for a nonlinear vehicle model is formulated and explicit solutions for constant road slopes are obtained by aid of the Pontryagin maximum principle. More recent work on fuel-optimal control for a single HDV based on preview information of the road topography, referred to as look-ahead cruise control (LAC), has been studied in Hellström (2010) and Fröberg (2008). They showed that the fuel consumption can be reduced by adjusting the velocity prior to an uphill or a downhill segment based on the vehicle parameters and the nonlinear dynamics of the HDV. However, it is fuel-optimal to maintain a constant speed if possible (Chang and Morlok, 2005). Explicit fuel-optimal speed profiles for HDVs for certain road profiles are given in Fröberg et al. (2006). In Ivarsson et al. (2011) the focus was turned to the connection between the engine nonlinearities and the characteristics of the LAC solution.

The ACC has been considered as a means to enable vehicle platooning in Hedrick et al. (1991) and Rajamani and Zhu (1999). Introduced in the late 1990s in luxury passenger vehicles, the ACC has become increasingly common in passenger vehicles and HDVs. As illustrated in Figure 2.3, the objective of the CC is to maintain a reference velocity by solely governing the throttle, whereas the ACC adapts the reference velocity with respect to the behavior of the immediate preceding vehicle by throttle and braking actions. Information regarding the relative distance and velocity of a preceding vehicle is generally provided through a radar or lidar. Hence, the ACC is solely based on sensor information from on-board sensors and makes no use of GPS or V2X. The relative distance is tracked by letting the driver set a desired spacing policy. Either a constant spacing is used (Swaroop et al., 1994)

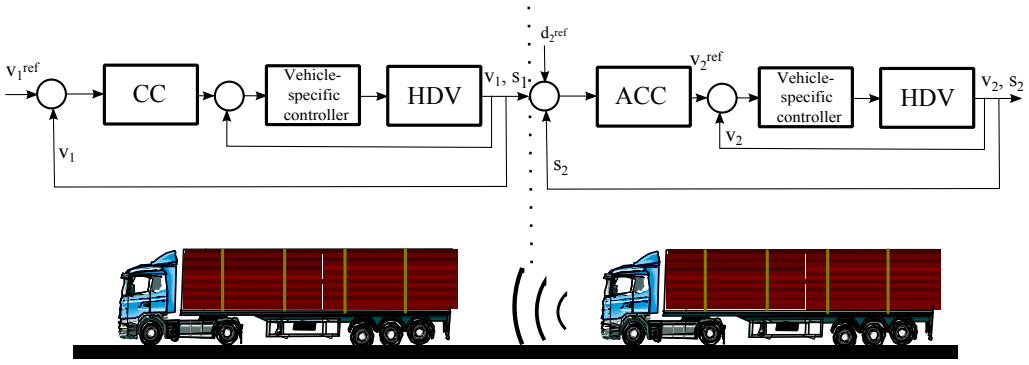

Figure 2.3: The flowchart shows the main blocks involved in CC and ACC. d_2^{ref} the reference relative distance, v_i denotes the velocity, and s_i the vehicle position with $i = 1, 2$. The controller computes a suitable velocity based upon its available inputs. The vehicle-specific controller, consisting of the engine management control and brake management control, ensures tracking of the given control demands.

a time headway gap (Wang and Rajamani, 2004*b*) or a nonlinear spacing policy (Yanakiev and Kanellakopoulos, 2008). In Omae et al. (2014), it is shown that a time headway policy results in a more energy efficient control, since constant spacing policy requires a higher acceleration variability for handling disturbances. The disadvantage with having a constant time headway is that it results in larger steady-state spacing, which increases the platoon length and thereby decreases the benefits from the air drag reduction along with the traffic throughput. Thus, two nonlinear policies was introduced in Yanakiev and Kanellakopoulos (2008), where the first policy is a variable time headway that varies linearly with the relative velocity error and the second policy is a nonlinear function of the separation error. It is concluded that the policies need to be evaluated in practice, since they add to the computational complexity and result in a trade-off between platoon performance, control smoothness, and robustness. The ACC is commonly designed based on predecessor following. However, in Barooah et al. (2009) a more elaborate approach based on bidirectional schemes is studied, where closed-loop stability with increasing number of vehicles is under scrutiny.

A commercial ACC generally acts as an extension to the CC, with the addition of actuating the vehicle with the brake system. Thus, the complexity of the control design increases. It can be described as a finite state machine, as illustrated in Figure 2.4. The commercial ACC is typically tuned to maintain the desired relative distance in a comfortable manner by sending appropriate requests to the engine and the various brake systems. Safety and fuel-efficiency are also sometimes considered as constraints. In Corona and De Schutter (2008) and Naus (2010) a systematic MPC approach was presented to account for the constraints of safety and comfort. However, safety, comfort, and fuel-efficiency constitute conflicting constraints. To implement control actions with respect to safety, quick and harsh behavior is

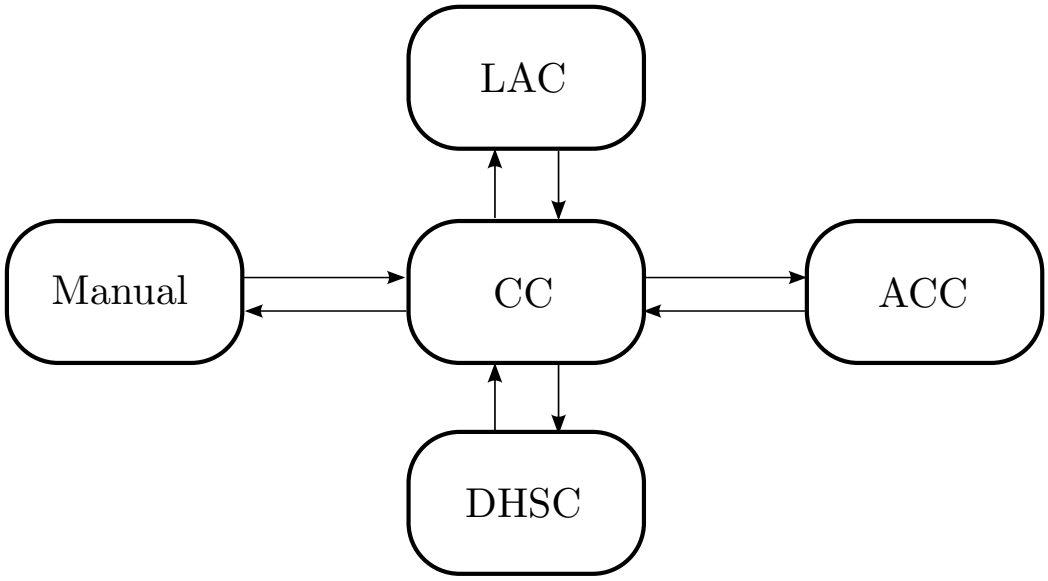

Figure 2.4: Illustration of a finite state machine for the commercially available speed control systems under consideration. If there is no vehicle in front of the subject vehicle, the ACC acts as an CC or LAC, depending on the driver setting. If the speed is exceeded with a given offset the DHSC will be activated automatically. The speed active control strategy is deactivated by pushing the brake pedal or manually switching off the system.

required, which in turn mandates a high acceleration or deceleration. Such behavior is neither comfortable nor fuel-efficient. The ACC accounts for switching between different modes, which induces a nonlinear behavior. The switching is generally based on logic rules and specific tuning parameters for each mode (Moon et al., 2009). Furthermore, it is desirable for the ACC to mimic reasonable human behavior for driver acceptance. The requirement of the ACC to mimic driver behavior for acceptance was investigated to some extent in Driel et al. (2007). Studies have shown that the ACC is most commonly utilized in highway situations. Hence, the impact of the speed controller on the traffic flow is of interest (Wang and Rajamani, 2004*a*). The ACC works reasonably well in a two-vehicle platoon. However, a delay arises from measuring the behavior of the preceding vehicle with the radar to producing the actual brake torque at the wheels. Thus, overshoots commonly occur when facing a velocity disturbance. In addition, the follower vehicle might not be able to reduce its speed in time if the preceding vehicle performs an emergency brake. Therefore, it is not suitable for longer vehicle platoons to operate at a short spacing due to safety issues. To further understand practical implementation issues and constraints, we consider the ACC in Chapter 4 and thereby investigate the fuel reduction potential of HDV platooning, with respect to a commercial control strategy.

2.5 Safety in Vehicle Platooning

Safety is of utmost importance in vehicle platooning. It is desirable to reduce the inter-vehicle spacing in an automated platoon to lower the air drag and, thereby, obtain a higher fuel reduction. However, the actions of one vehicle may in turn affect all vehicles in the linked chain, which makes ensuring safety an issue.

String stability addresses the property that a disturbance from the lead vehicle should not be amplified along the platoon (Swaroop and Hedrick, 1996; Shaw and Hedrick, 2007). It is related to the ability to suppress a disturbance in position, velocity, or acceleration, as it propagates along the platoon, which in turn might lead to a collision. Focusing on preventing collisions, the errors in spacing between the vehicles in the platoon is often considered. In Pipes (1953) dynamics of a line traffic with N vehicles were studied, where a wave phenomena was noticed when vehicles resumed the road speed after a traffic light turned green. This observation was later introduced as string stability by Peppard (1974). It is also known as the bullwhip effect in economic theory (Lee et al., 2004). In Swaroop (1994) and Swaroop and Hedrick (1996) a mathematical definition of string stability, in particular l_p-string stability, is presented. A more recent overview is given in Ploeg et al. (2014). The property of l_∞-string stability implies that there exists a bounded set of initial conditions such that the peaks of the spacings errors remain uniformly bounded along the string of vehicles. A weaker condition is l_2-string stability, which is more commonly used as a performance measure. l_2-string stability implies that the energy of the spacing errors are not amplified downstream in the platoon. It is not possible to achieve longitudinal string stability with a constant spacing policy for a homogeneous string of vehicles with feedback control based on nearest neighbor communications (Sheikholeslam and Desoer, 1993). In Seiler et al. (2004) it was shown that this limitation occurs due to a complementary sensitivity integral constraint, which can be solved by using a time headway policy. Hence, it is preferable to use a time headway policy both with respect to string stability and energy efficiency. Control difficulties for infinite vehicle platoons were studied in Bamieh and Jovanović (2005). In Middleton and Braslavsky (2010), communication constraints are considered in a chain of linear time-invariant autonomous vehicles with sufficient conditions for string stability are given. String stability is shown over a ring topology in Rogge and Aeyels (2005), where control design for identical vehicles is studied. In Rajamani and Zhu (2002) practical systems with ACC were considered, where both manually driven and automated cars can coexist. It was shown that the inter-vehicle spacing can be reduced while maintaining string stability through wireless communication. Numerical methods for analyzing robust peak-to-peak performance of heterogeneous vehicle platoons were presented and evaluated in practice on real HDVs in Rödönyi et al. (2014). String stability can also be obtained in some cases through an ordering strategy with respect to vehicle mass (Liang et al., 2011). In Kianfar et al. (2013) string stability is studied in a lateral direction and in Knorn and Middleton (2013), it is studied in both longitudinal and lateral directions. Note that ensuring string stability does not imply that safety is guaranteed. String stability only guarantees

that a disturbance is is not amplified along the platoon. Thus, if a collision occurs, for example, due to a harsh braking that causes a disturbance such that the error in spacing becomes equal to the relative distance between two neighboring vehicles, then additional collisions might still occur downstream. Hence, a more rigorous approach is needed for ensuring safety in vehicle platoons.

A collision avoidance system is designed to enhance safety by providing warnings to the driver or, in some cases, automating maneuvering procedures. Collision avoidance has been studied in many areas of engineering such as maritime transportation, unmanned aerial vehicles (UAV), see Ryan et al. (2004), mobile robotics, see Siegwart and Nourbakhsh (2004), and automotive engineering. The literature on safety strategies for HDVs is scarce, even though collision avoidance for cars is a vast area. In the car industry, ACC systems with collision avoidance have been studied extensively and are now commercially available. A review can be found in Vahidi and Eskandarian (2003). In Seiler et al. (1998) longitudinal collision avoidance algorithms by Mazda and Honda were reviewed and human factors were considered. Critical distances for a collision avoidance system are derived as a function of velocity and relative velocity. In Chapter 5, we consider a similar reference framework, but for HDVs. Additionally, we use a dynamical game formulation to capture the worst possible behavior by a preceding vehicle. In Gustafsson (2009), automotive safety systems were reviewed. Conditions on safe platooning for passenger vehicles under normal-mode of operation are investigated in Alvarez and Horowitz (1997). More recent work on collision avoidance for cars can be found in the thesis by Ali (2012), where reachability analysis tools were utilized for threat assessment and a novel automotive safety function was proposed, based on vehicle state and road preview information. Zonotopes, a special case of polytopes, is an approach for computing reachable sets by abstracting to differential inclusions of simpler dynamics (Girard, 2005). An approach to verify maneuvers of an automated car was presented in Althoff and Dolan (2012). Makhlouf and Kowalewski (2012) considered safety verification of a platoon of vehicles under a varying communication network using zonotopes.

Vehicle platooning can facilitate an improved safety through higher interactivity. We propose a novel approach in Chapter 5, through a game theoretical approach for HDV platooning. The approach is an extension of the work presented in Bayen et al. (2003), where collision avoidance was analyzed with a differential game formulation of an alerting logic for conflicts in high altitude air traffic. V2X communication enables new possibilities and naturally new challenges for safety applications. Safety is increased through automated functions and close coordination. Through interaction each agent in the platoon will be able to take precautionary measures, in the sense of adjusting its speed and relative distance, based upon several incidents ahead. However, uncertainties with respect to mixed traffic, communication failure and delays must be resolved.

2.6 Summary

A brief introduction has been given on ITS. ITS aim at enhancing safety, operational performance, mobility, environmental benefits, and productivity by expanding economic and employment growth. It covers a broad range of services and focuses on topics that adds understanding of accessibility, congestion, pollution, safety and security in transportation. We have discussed the technology premise for HDV platooning. On-board sensor technology and ECU functionality have improved and become increasingly present during the last decades. Sensors and ECUs have increased in numbers. ECUs have developed in memory and processing speed. Radar and camera technology have developed to extend the information range to a local environment. GPS technology can provide up to centimeter accuracy and map providers are focusing on delivering three-dimensional road topography. With the introduction of wireless communication to vehicle networks, which is the key technology that enables HDV platooning by providing interaction between vehicles and the surrounding infrastructure, a cooperative control system can be produced to improve fuel efficiency, safety and congestion. Several commercially available ADAS functionalities, such as the ACC, have been mentioned that can already be used for vehicle platooning or serve as inspiration for future possible use cases. A brief overview of the related work within platooning have been presented. String stability, collision avoidance and several control approaches have been mentioned. Despite the substantial academic work, control design for platooning in practice is still an open problem. Research into more implementation relevant aspects is only recently emerging.

Chapter 3

Modeling

"*A mathematical model does not have to be exact; it just has to be close enough to provide better results than can be obtained by common sense.*"
Herbert A. Simon

In this chapter we present models that serve as a basis for the analysis and control design presented in the following chapters. First, a general description of the internal and external forces affecting a vehicle in motion is given in Section 3.1, resulting in an analytical model. Then, a more detailed simulation model is presented in Section 3.2. Finally, the system architectures, to facilitate the control applications for heavy-duty vehicle (HDV) platooning developed in this work, are given in Section 3.3. A summary of the presented models and the benefits of the proposed architecture in Section 3.4 concludes this chapter.

3.1 Vehicle Models

Several forces are imposed on a moving vehicle. The main forces are depicted in Figure 3.1 with the arrows indicating the corresponding sign convention, where F_{a}, F_{r}, and F_{g} denote the external air drag, rolling resistance, and gravitational forces acting upon the vehicle, respectively. The road grade is denoted by α, F_{b} denotes the negative longitudinal force obtained if the brakes are applied and F_{p} denotes the positive longitudinal driving force from the powertrain, which is produced by the engine through fuel combustion. However, during coasting, i.e. when the fuel injection is cut-off, the engine exerts a constant braking force as it is propelled by the accumulated kinetic energy or potential energy and not by fuel. In our model this effect is accounted for in inertial force produced by the engine. Therefore, the sign convention indicated by Figure 3.1 is maintained. In this section, we discuss each force of interest and then combine them at the end to provide a complete vehicle dynamics model.

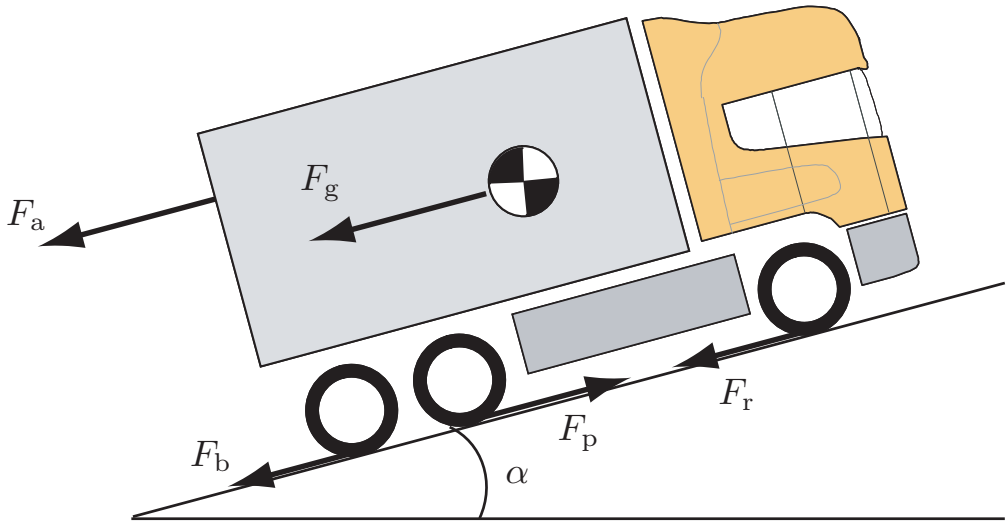

Figure 3.1: The longitudinal forces inflicted upon an HDV in motion.

3.1.1 Nonlinear Vehicle Model

The main propelling parts of an HDV consist of the engine, clutch, transmission shafts and wheels. A combination of all these parts forms the powertrain (driveline), which can be modeled in various ways depending on the specific purpose and use of the model. The main interest is first to create a continuous-time model of the powertrain, based upon the simple model depicted in Figure 3.2.

Powertrain

General powertrain modeling can be found in Kiencke and Nielsen (2003). Our main objective is to model the power transfer from the engine to the road surface. Each part of interest is described briefly and then combined at the end to provide the complete powertrain model for each HDV. Note that we skip the index i to indicate the individual vehicle i in the platoon. The notation for torques and angles used in the model is given in Figure 3.3.

Engine: The engine we consider produces a torque through combustion of diesel mixed with a surplus of air in a very high pressurized chamber. The highly explosive combustion drives the crank shafts, which in turn are connected to the clutch. In this model, we do not consider the internal dynamics that are characterized by the torque resulting from the combustion, the internal friction from the chamber walls, pumping losses, temperature variations, etc. for simplicity. Thus, given the engine inertia, using dot notation to indicate derivatives with respect to time, Newton's second law gives

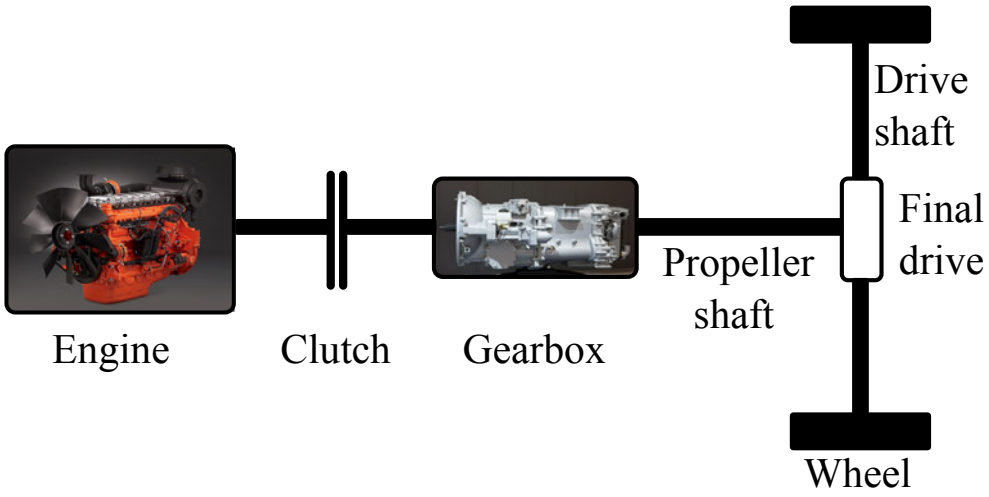

Figure 3.2: A basic model of the powertrain. (The picture of the engine and the gearbox is provided through the courtesy of Scania CV AB.)

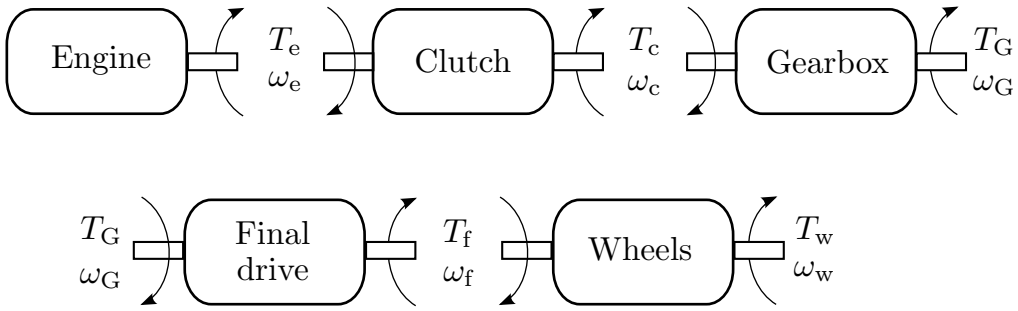

Figure 3.3: Subsystems of the powertrain with notation for torques and angular velocities used in the powertrain model.

$$J_e\dot{\omega}_e = T_e(\omega_e, \delta) - T_c, \tag{3.1}$$

where $T_e(\omega_e, \delta)$ is the net engine torque generated after the internal losses and the external load from the clutch T_c, J_e is the moment of inertia of the engine including the flywheel, and δ is the injected fuel amount, which is given in grams of fuel per engine cycle and cylinder.

A standard HDV diesel engine operates at 500 – 2500 RPM with the most efficient operating range between 950 – 1500 RPM. The net engine torque can be obtained empirically through a Torque–RPM–Fuel graphical model for each specific engine.

Clutch: The clutch involves two frictional discs, which are pressed together and connect the flywheel of the engine to the gearbox's input shaft. Such clutches are

commonly found in vehicles equipped with manual gearbox[1]. The purpose of the clutch is to decouple the engine from the drivetrain to enable gear shifts. When the clutch is engaged, negligible losses arise at the connection point. Thus, the connection between the gearbox and the clutch is considered to be stiff. Hence, it can be modeled as

$$\begin{aligned} T_{\mathrm{G}} &= T_{\mathrm{c}}, \\ \omega_{\mathrm{G}} &= \omega_{\mathrm{c}}, \end{aligned} \tag{3.2}$$

where T_{G} denotes the torque output from the gearbox, ω_{G} the output angular speed from the gearbox, T_{c} the torque output from the clutch and ω_{c} the output angular speed from the clutch.

Gearbox: The gearbox is the connection between the clutch and the propeller shaft. It consists of a set of cogwheels (gears) which are connected such that the output torque from the clutch is transformed depending on which gear is engaged. The transformation is modeled in this case as a conversion ratio γ_{G}, which varies according to the specific gearbox transmission characteristics. The gear shifts are assumed to be instantaneous, maintaining the RPM within operating range.

Typically a slight drop in power transfer occurs in the gear box due to frictional losses. This characteristic of the gearbox is modeled as an efficiency η_{G}. Hence, assuming an immediate change of conversion ratio and efficiency, the connection between the gearbox and the final drive is given as

$$\begin{aligned} T_{\mathrm{f}} &= \gamma_{\mathrm{G}} \eta_{\mathrm{G}} T_{\mathrm{G}}, \\ \gamma_{\mathrm{G}} \omega_{\mathrm{f}} &= \omega_{\mathrm{G}}, \end{aligned} \tag{3.3}$$

where T_{f} denotes the torque output and ω_{f} the output angular speed at the final drive.

Final Drive: The final drive is connected to the gearbox through the propeller shaft. The frictional losses in the propeller shaft are negligible and the connection is considered to be stiff. Like the gearbox, the final drive is characterised by a conversion ratio γ_{f} and an efficiency η_{f}. The value for the ratio and the efficiency depend on the final drive design. A small final drive implies that the vehicle will run faster for a fixed RPM and a large final drive implies that vehicle can output a larger propulsion torque at the same RPM. Neglecting inertia, the following relation can be established between the wheels and the final drive torque and angular velocity:

$$\begin{aligned} T_{\mathrm{w}} &= \gamma_{\mathrm{f}} \eta_{\mathrm{f}} T_{\mathrm{f}}, \\ \gamma_{\mathrm{f}} \omega_{\mathrm{w}} &= \omega_{\mathrm{f}}, \end{aligned} \tag{3.4}$$

[1] In this work we consider a manual transmission and an automatically operated clutch.

where T_{w} denotes the torque output and ω_{w} the output angular speed at the wheels.

Wheels: The wheels are connected to the final drive through the drive shafts. In this simplified model it is assumed that the wheel speed is the same for both wheels. In reality, the wheel speed differs when the vehicle enters a curve. However, it is negligible compared to other simplifications within the model. The connection between the road and the wheels is assumed to have no slip, hence

$$\begin{aligned} J_{\mathrm{w}}\dot{\omega}_{\mathrm{w}} &= T_{\mathrm{w}} - T_{\mathrm{b}} - r_{\mathrm{w}}F_{\mathrm{p}}, \\ v = r_{\mathrm{w}}\omega_{\mathrm{w}} &= \frac{r_{\mathrm{w}}}{\gamma_{\mathrm{G}}\gamma_{\mathrm{f}}}\omega_{\mathrm{e}}, \end{aligned} \tag{3.5}$$

where r_{w} denotes the wheel radius, J_{w} is the moment of inertia of the wheels, F_{p} is the resulting vehicle propulsion force, and v denotes the vehicle velocity. The equation for the velocity v, as a function of the angular velocity of the engine is obtained by combining (3.1)–(3.5). The braking torque T_{b} is often difficult to model, since the characteristics varies significantly with respect to vehicle configuration and brake control logic.

To conclude the first part of the nonlinear vehicle model, combining (3.1)–(3.5) the longitudinal driving force produced in the powertrain is given as

$$F_{\mathrm{p}} + F_{\mathrm{b}} = \frac{\gamma_{\mathrm{G}}\gamma_f\eta_{\mathrm{G}}\eta_{\mathrm{f}}}{r_{\mathrm{w}}}T_{\mathrm{e}}(\omega_{\mathrm{e}}, \delta) - \frac{J_{\mathrm{w}} + \gamma_{\mathrm{G}}^2\gamma_{\mathrm{f}}^2\eta_{\mathrm{G}}\eta_{\mathrm{f}}J_{\mathrm{e}}}{{r_{\mathrm{w}}}^2}\dot{v}, \tag{3.6}$$

where the first term denotes the vehicle propulsion force produced by the engine and the second term is the internal inertial force. Note that F_{b} is separated, since it is governed by a different actuator.

External Longitudinal Forces

The external forces are described briefly in the discussion below and then combined with the presented powertrain model to provide the complete vehicle dynamics.

Air Drag: The aerodynamic drag has a strong impact on an HDV and can amount up to 50 % of the total resistive forces at full speed. Studies have shown that the wind resistance can be reduced significantly by arranging trucks in a platoon formation as depicted in Figure 3.4. The air drag is partly reduced due by having a follower drive at a close relative distance, which increases the pressure at the back. The main part of the air drag reduction occurs for a follower vehicle that experiences a significant reduction of air drag due to a relatively large reduced pressure at the front. Hence, the total air drag is reduced, which in turn lowers the fuel consumption. Studies based on computational fluid dynamics (CFD) have been conducted to determine how much the air drag coefficient varies as a function of inter-vehicle spacing, see Yamazaki et al. (2009); Davila et al. (2013); Norrby (2014).

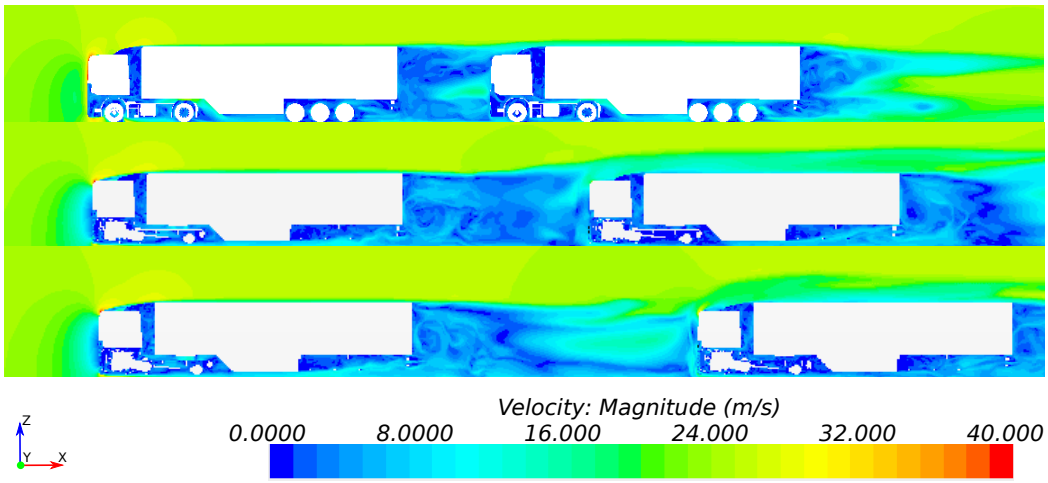

Figure 3.4: CFD results for a platoon of two HDVs with varying inter-vehicle spacings. An HDV experiences an increased wind speed at the front, which results in an increased pressure. The wind speed drops behind the vehicle and hence the pressure is also lowered at the back. The combination of these to occurrences is what is referred to as the air drag. If two HDVs travel at a small inter-vehicle spacing, the pressure at the back of the lead vehicle is increased and the pressure at the front of the follower vehicle is reduced, which will create an overall reduced air drag. An increased spacing, raises the air drag (Picture is provided through the courtesy of Norrby (2014)).

However, the results vary considerably based on the type of model used to describe the vehicles, the computation method, and the mesh quality.

Experimental results obtained from wind tunnel experiments for two van-shaped vehicles can be found in Zabat et al. (1994) and Browand (2005). The results show that the drag coefficient decreases with increasing order in the platoon. Hence, the aerodynamic effects may be transferred from vehicle-to-vehicle in an N-vehicle platoon. Hence, the air drag is reduced further with increasing vehicle position index in a long and structured platoon. The presented results also show that a small vehicle following a large vehicle will obtain a greater benefit. For the purposes of this work, the reduction in the air drag coefficient is modeled based on empirical results, as presented in Figure 3.5. The empirical results are derived through measurements in a wind tunnel with commercial buses. The bottom (green) curve shows the air drag ratio for the last vehicle, denoted as HDV_3 in a three-HDV platoon. The middle (black) curve shows the air drag ratio for the second vehicle HDV_2 in a two-HDV platoon. The lead vehicle HDV_1, also experiences a lowered air drag from having a follower vehicle, as shown by the top (red) curve. Similar findings have been confirmed by the fluid dynamics department at Scania CV AB and in Bonnet and Fritz (2000).

Let $\Phi(d)$ denote the nonlinear air drag ratio, which is given by a graphical model, as shown in Figure 3.5. The total aerodynamic drag force is then given by

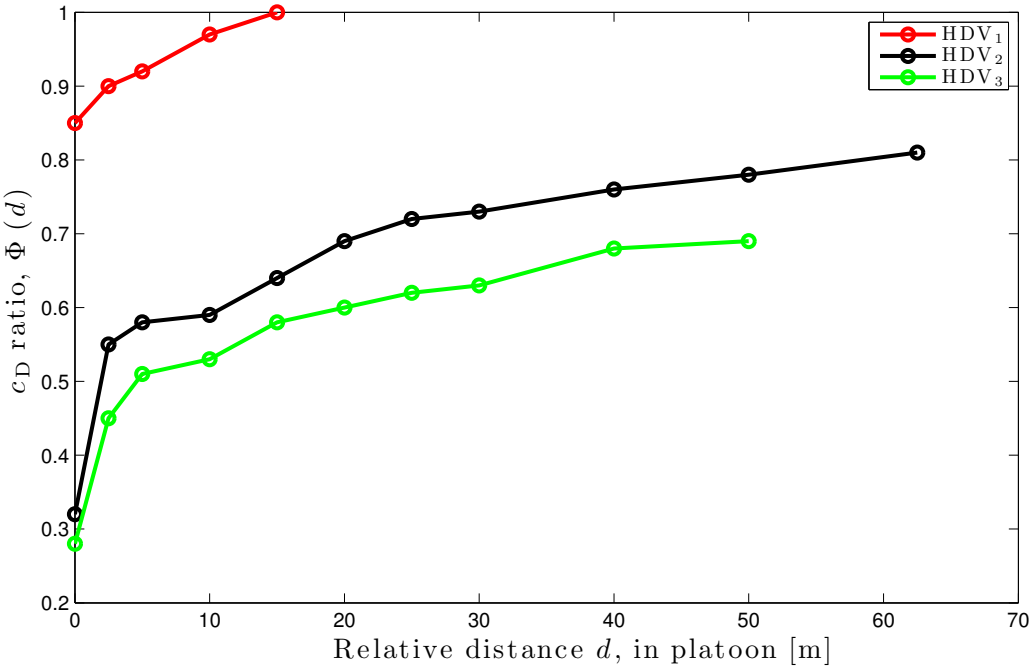

Figure 3.5: Mapping of the empirical air drag coefficient (c_D) ratio with respect to the distance d, between the vehicles. Adapted from Wolf-Heinrich and Ahmed (1998). The circles indicate each measurement point in the wind tunnel experiments.

$$F_a = \frac{1}{2} c_D A_a \rho_a \Phi(d)(v + v_{\text{wind}})^2, \tag{3.7}$$

where c_D denotes the airdrag coefficient, d the relative distance between vehicles, A_a the maximum cross-sectional area of the vehicle, ρ_a the air density, and v_{wind} denotes the velocity of the wind. The velocity of the wind is typically unknown and is therefore neglected in this work.

Rolling Resistance: The rolling resistance occurs due to the resistive frictional force that occurs between the road surface and the wheels. It is given by

$$F_r = c_r m g \cos(\alpha), \tag{3.8}$$

where c_r denotes the roll resistance coefficient, g the gravitational constant, and m the vehicle mass. Recall that α denotes the road grade.

Gravitational Force: As an HDV travels along an incline, the gravitational force has a strong influence. In contrast to a passenger vehicle, an HDV weighing 40 t is typically not able to produce a sufficient driving torque to maintain the velocity when traveling along an uphill with a slope greater than 2.9 % at 80 km/h. Similarly, when facing a downhill the vehicle will typically experience a speed increase, even

though no fuel is injected, if the slope is less than -0.9 %. Hence, the induced gravitational force can act as a positive or negative longitudinal force depending on the incline of the road. It is given by

$$F_{\mathrm{g}} = mg\sin(\alpha). \tag{3.9}$$

Vehicle Model Composition

Applying Newton's second law of motion along with all the external forces described above, a nonlinear continuous mathematical vehicle model is derived as

$$\begin{aligned}
\frac{\mathrm{d}s}{\mathrm{dt}} =& v \\
m_{\mathrm{t}}(G)\frac{\mathrm{d}v}{\mathrm{dt}} =& F_{\mathrm{e}} - F_{\mathrm{b}} - F_{\mathrm{a}}(v,d) - F_{\mathrm{r}}(\alpha(s)) - F_{\mathrm{g}}(\alpha(s)), \\
=& \frac{\gamma_{\mathrm{G}}\gamma_{\mathrm{f}}\eta_{\mathrm{G}}\eta_{\mathrm{f}}}{r_{\mathrm{w}}} T(\omega_{\mathrm{e}},\delta) - F_{\mathrm{b}} - \frac{1}{2}c_{\mathrm{D}}A_{\mathrm{a}}\rho_{\mathrm{a}}\Phi(d)v^2 \\
& - c_{\mathrm{r}}mg\cos(\alpha(s)) - mg\sin(\alpha(s)), \\
=& k_{\mathrm{e}}T(\omega_{\mathrm{e}},\delta) - F_{\mathrm{b}} - k_{\mathrm{d}}v^2 - k_{\mathrm{r}}\cos(\alpha(s)) - k_{\mathrm{g}}\sin(\alpha(s))
\end{aligned} \tag{3.10}$$

where

$$m_{\mathrm{t}}(G) = \frac{J_{\mathrm{w}}}{r_{\mathrm{w}}^2} + m + \frac{{\gamma_{\mathrm{G}}}^2{\gamma_{\mathrm{f}}}^2\eta_{\mathrm{G}}\eta_{\mathrm{f}}J_{\mathrm{e}}}{r_{\mathrm{w}}^2} \tag{3.11}$$

is the total inertial mass, G denotes the active gear number, and s is the absolute traveled distance from a known point of origin. Note that γ_{G} and η_{G} varies with the active gear number G. We omit to express G explicitly in (3.11) in some chapters, unless gear changes are considered in the control design. The model parameters used in this thesis, unless otherwise stated, are given in Table 3.1.

Model Uncertainties

The vehicle model is based upon perfect knowledge of the vehicle parameters. In practice, only the gearbox ratio and the final gear ratio is known to be static. The inertias and efficiencies vary based upon the temperature and quality of the corresponding lubricating oil. The wheel radius also varies based upon the current air pressure and the friction between the road surface and tire is not static. The rolling resistance varies nonlinearly with tire temperature and velocity. However, the dominant uncertainty in (3.10) is the vehicle mass. During a freight transport assignment the cargo is often unloaded at several points, since it generally encompasses different contractors. Each time part of the cargo is unloaded there is seldom a measuring device to obtain new accurate mass measurements. The mass is generally several magnitudes larger than the other parameters. We adopt the common approach that all the parameter uncertainties can be aggregated as an uncertainty in mass.

Table 3.1: Nominal vehicle model parameters.

Parameter	Symbol	Value	Unit
Rolling resistance coefficient	c_r	1.5×10^{-3}	-
Air drag coefficient	c_D	0.56	-
Engine inertia	J_e	3.5	kg m^2
Wheel inertia	J_w	32.9	kg m^2
Vehicle mass	m	40 000	kg
Frontal area	A_a	10.26	m^2
Wheel radius	r_w	0.5	m
Final drive ratio	γ_f	3.08	-
Final gear efficiency	η_e	0.97	-
Air density	ρ_a	1.29	kg m^{-3}

An accurate model of the powertrain would mandate flexible shafts, where energy is stored when the shafts are twisted. However, the effects of such dynamics come into play when there are quickly varying changes in the engine torque, which might cause oscillations in the powertrain or backlash (Lagerberg and Egart, 2007). These dynamics mainly impact driveability and not the fuel consumption (Sandberg, 2001). The platooning scenarios we consider does not involve such behavior, since the objective is fuel efficiency, which requires only smooth control actions. Therefore, dynamics for backlash and oscillations in the vehicular powertrain are neglected for the purposes of this model.

3.1.2 Linearized Vehicle Model

When studying the behavior of vehicles within a platoon, the velocities are controlled and should not deviate significantly from the lead vehicles velocity trajectory. Thus, a linearized model, used for control design in this thesis, might satisfactorily describe vehicle behavior. The nonlinear model (3.10) can be linearized with respect to a set reference velocity v^ref, a fixed gear number G_0, an engine torque which maintains the velocity T_0, a fixed time headway setting τ, and a constant slope α_0. The equilibria are denoted

$$\begin{aligned} v_0 &= v^\mathrm{ref} \\ \alpha_0 &= \alpha^\mathrm{ref} \\ d_0 &= v_0 \tau \\ T_0 &= \frac{c_\mathrm{d}(d_0){v_0}^2 + c_\mathrm{r}\cos(\alpha_0) + c_\mathrm{g}\sin(\alpha_0)}{c_\mathrm{e}} \end{aligned} \tag{3.12}$$

where d_0 is the equilibrium inter-vehicle spacing for a time headway setting and

$$c_{\mathrm{e}} = \frac{r_{\mathrm{w}}\gamma_{\mathrm{G}}\gamma_{\mathrm{f}}\eta_{\mathrm{G}}\eta_{\mathrm{f}}}{J_{\mathrm{w}} + mr_{\mathrm{w}}^2 + \gamma_{\mathrm{G}}^2\gamma_{\mathrm{f}}^2\eta_{\mathrm{G}}\eta_{\mathrm{f}}J_{\mathrm{e}}}, \qquad c_{\mathrm{d}}(d_0) = \frac{\frac{1}{2}r_{\mathrm{w}}^2 c_{\mathrm{D}} A_{\mathrm{a}}\rho_{\mathrm{a}}}{J_{\mathrm{w}} + mr_{\mathrm{w}}^2 + \gamma_{\mathrm{G}}^2\gamma_{\mathrm{f}}^2\eta_{\mathrm{G}}\eta_{\mathrm{f}}J_{\mathrm{e}}}\Phi(d_0),$$
$$c_{\mathrm{r}} = \frac{c_{\mathrm{r}} r_{\mathrm{w}}^2 mg}{J_{\mathrm{w}} + mr_{\mathrm{w}}^2 + \gamma_{\mathrm{G}}^2\gamma_{\mathrm{f}}^2\eta_{\mathrm{G}}\eta_{\mathrm{f}}J_{\mathrm{e}}}, \qquad c_g = \frac{r_{\mathrm{w}}^2 mg}{J_{\mathrm{w}} + mr_{\mathrm{w}}^2 + \gamma_{\mathrm{G}}^2\gamma_{\mathrm{f}}^2\eta_{\mathrm{G}}\eta_{\mathrm{f}}J_{\mathrm{e}}}. \tag{3.13}$$

To account for the aerodynamics, we approximate the nonlinear air drag function $\Phi(d)$ with a least square approximation. Hence, the approximated affine air drag reduction is given as

$$\varphi(d) = a_{\mathrm{lsq}}d + b_{\mathrm{lsq}},$$

where $\varphi(d) \in [0, 1]$. The parameters a_{lsq} and b_{lsq} are determined with respect to the relevant operating range.

Let $F(v, T, \alpha, d)$ denote the function for the nonlinear vehicle dynamics model in (3.10). Applying a first order Taylor approximation to (3.10) around the equilibrium points v_0, T_0, α_0, d_0, the linearized model for a single vehicle is given by

$$\begin{aligned}\frac{dv}{dt} &\approx F(v_0, T_0, \alpha_0, d_0) + \frac{\partial}{\partial v}F(v_0, T_0, \alpha_0, d_0)\Delta v \\ &\qquad + \frac{\partial}{\partial d}F(v_0, T_0, \alpha_0, d_0)\Delta d + \frac{\partial}{\partial T}F(v_0, T_0, \alpha_0, d_0)\Delta T \\ &= c_{\mathrm{e}}\Delta T - 2c_{\mathrm{d}}(d_0)v_0\Delta v - \frac{\frac{1}{2}a_{\mathrm{lsq}}r_{\mathrm{w}}^2 A_{\mathrm{a}}\rho_{\mathrm{a}}v_0^2}{J_{\mathrm{w}} + mr_{\mathrm{w}}^2 + \gamma_{\mathrm{G}}^2\gamma_{\mathrm{f}}^2\eta_{\mathrm{G}}\eta_{\mathrm{f}}J_{\mathrm{e}}}\Delta d,\end{aligned} \tag{3.14}$$

where c_{e} and $c_{\mathrm{d}}(d_0)$ is given in (3.13). Approximately we have

$$\dot{v} = c_{\mathrm{e}}T + \Theta v + \beta d, \tag{3.15}$$

where, with abuse of notation, T and v denote the deviation in control input and the vehicle velocity from the equilibrium point, respectively. The characteristic coefficients Θ and β are given by

$$\begin{aligned}\Theta &= -2c_{\mathrm{d}}(d_0)v_0, \\ \beta &= -\frac{\frac{1}{2}a_{\mathrm{lsq}}r_{\mathrm{w}}^2 A_{\mathrm{a}}\rho_{\mathrm{a}}v_0^2}{J_{\mathrm{w}} + mr_{\mathrm{w}}^2 + \gamma_{\mathrm{G}}^2\gamma_{\mathrm{f}}^2\eta_{\mathrm{G}}\eta_{\mathrm{f}}J_{\mathrm{e}}}.\end{aligned} \tag{3.16}$$

Note that for the lead vehicle we get

$$\dot{v} = c_{\mathrm{e}}T - \frac{r_{\mathrm{w}}^2 c_{\mathrm{D}} A_{\mathrm{a}}\rho_{\mathrm{a}}v_0}{J_{\mathrm{w}} + mr_{\mathrm{w}}^2 + \gamma_{\mathrm{G}}^2\gamma_{\mathrm{f}}^2\eta_{\mathrm{G}}\eta_{\mathrm{f}}J_{\mathrm{e}}}v,$$

since the air drag reduction obtained due to a following vehicle is minor and therefore not considered.

3.2 Simulation Model

An analytical model can serve as a basis for controller design. However, in practice the vehicle and its interaction with the environment is highly complex. The analytical model describes the dynamic behavior of vehicles in the platoon. Yet, the presented model does not directly account for fuel consumption and is not sufficiently detailed for real life evaluation. In reality, for example, dynamics such as internal engine friction and internal brake friction have an impact on the behavior and fuel consumption. In addition, power train oscillations in the flexible shafts, if excited, have an impact on the vehicle dynamics and drivability. Moreover, an HDV, as opposed to a passenger vehicle, has additional braking systems in parallel with the service brakes (wheel brakes). Due to the extensive mass of an HDV, there is lots of wear on the service brakes and the brake power can fade if they overheat. Therefore, an exhaust brake is implemented. In addition, there is a retarder brake, which effectively is a hydraulic brake system. Furthermore, the engine does not only drive the vehicle forward, but also propels auxiliary systems such as the alternator, servo steering, the air condition system, etc., which have an impact on the fuel consumption. Energy losses in the bearings also influence the fuel consumption. An analytical model does not capture the behavior of the embedded systems that come into play. Thus, a more complex simulation model is necessary to evaluate the fuel reduction potential of the implemented control strategy and platoon behavior. A validated simulation model that mimics real life behavior also serves as a necessary precaution measure before evaluating safety critical operations in practice. In addition, a simulation model facilitates reproducible data. In experimental HDV studies it is very difficult to obtain repeatable environment conditions during field experiments because the ambient variables temperature, wind, humidity and traffic conditions are constantly changing.

The model was constructed in Dymola (Dynasim, 2007). Dymola is an modeling environment that enables bidirectional data flow, which in turn makes it possible to model and simulate acceleration as well as coasting. In the process of acceleration, the force produced by the engine flows towards the road surface, whereas it is reversed during coasting. To create a simulation model, which produces reliable results and mirrors real-life behavior, an advanced model for coupled HDVs traveling in a platoon is developed as an extension to the nonlinear Dymola model for a single vehicle created in Sandberg (2001). Figure 3.6 illustrates the individual parts in the powertrain, such as engine, gearbox, clutch, auxiliary systems, bearing losses, etc., which are modeled in detail. The model consists of 3313 variables, 1058 equations, and 626 states for a single HDV. It incorporates the full braking system, including the nonlinear behavior and a complex model for rolling resistance. The gearbox model and hydraulic retarder brake are controlled by software utilized in real life HDVs. The model also includes the dynamic behavior of the tires and relates rolling resistance to tire temperature and vehicle speed, which along with the rolling radius is significant for accurate fuel consumption simulations. A controller area network (CAN) system is also modeled to describe the interaction between the electronic

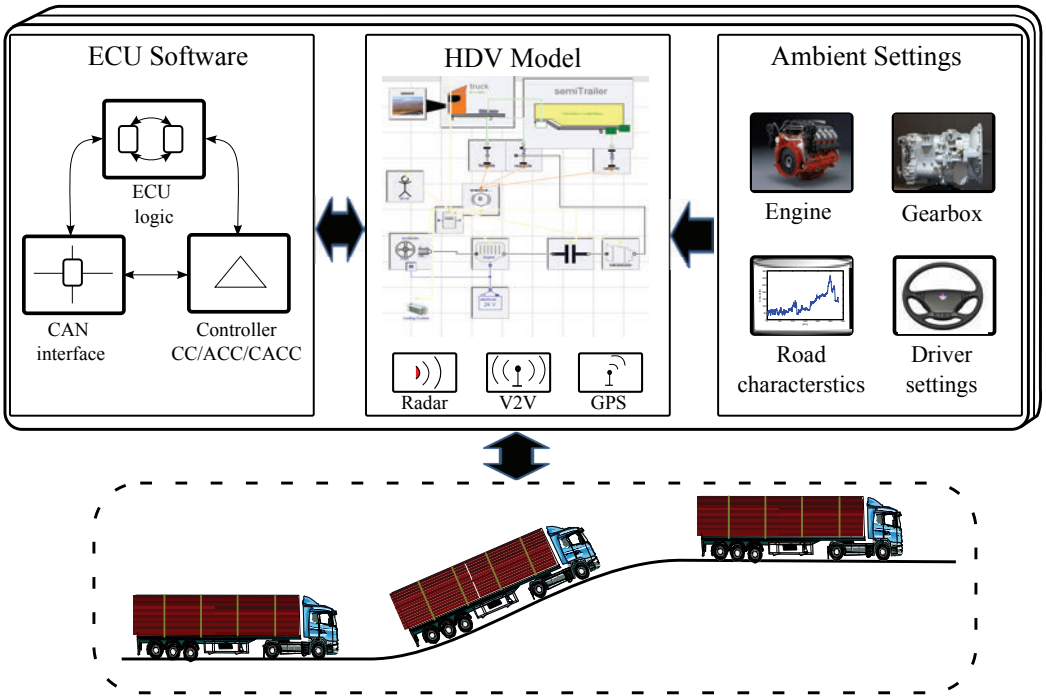

Figure 3.6: Schematic overlay of the simulation model. The ambient settings contains user input parameters, which consists of road topography, engine, gearbox, set speed and distance. The acausal HDV model created in Dymola communicates with the controller logic through the CAN system. The controller logic consists of production CC-, DHSC-, and ACC-logic to govern the trucks. The complete model is extended to several HDVs and includes simple models of wireless communication and radar information.

control units (ECUs), actuators and physical properties of the HDV.

The single HDV model in Sandberg (2001) is modified to handle additional control inputs consisting of external speed request and external brake request. It is modified to handle more advanced controller logic and extended to several vehicles by integrating the Dymola model with Simulink (Matlab). Cruise control (CC)-, downhill speed control (DHSC)- and adaptive cruise control (ACC)-logic to govern the trucks are implemented by utilizing the current software implemented in Scania CV AB's trucks in production. The ECU software is modeled in Simulink and communicates with the HDV model through the internal CAN system. Exchangeable data sets are utilized to allow for the whole production range of gearboxes, engine types and recorded road profiles throughout Europe. The overall behavior of the entire simulation model is tested and verified to mimic real-life behavior for a single vehicle. It serves as a basis for the evaluation of fuel reduction possibilities in HDV platooning that we consider in Chapter 4. In Chapter 5 safety regions with respect to collision avoidance for HDV platooning are derived. The simulation model then serves as a precautionary validation tool before the practical evaluation. In

Chapter 6, we provide experimental results to qualitatively verify the dynamical behavior of the simulation model for a three-vehicle platoon.

3.3 Systems Architecture

In this section, we present a three-layered system architecture for future transport systems, which aims to decompose the overall transport control problem into manageable subsystems. Control architectures for vehicle platoons have been studied, for example, in Varaiya (1993); Horowitz and Varaiya (2000); Alam (2011). We first give a general description of the transport system, where each layer is discussed separately. Then, in line with the main focus of this thesis, we propose two additional architectures, namely: the platoon system architecture and the vehicle system architecture. The systems architecture provides a modularized implementable solution, while also giving a better understanding of the main underlying systems and components that are involved in control for a vehicle in a platoon.

3.3.1 Transport System Architecture

Mission Planner

Starting from the top in Figure 3.7, the main tasks in the mission planner layer are distributing and assigning the required flow of goods over the available HDVs that are provided by one or several fleets, determining fuel-efficient routes, and coordinating transport assignments such that platoons can be formed for further fuel-efficiency. Thus, three closely related tasks are handled by the mission planning layer, namely: transport planning, routing, and vehicle coordination. The objective of the transport planning task is to maximize the utilization of the available vehicles and cargo capacity of individual HDVs by grouping similar transport assignments. Thereby, goods that need to be transported along the same route are combined into one or several HDVs. Deadlines and physical attributes of the goods such as weight, size, etc., have to be taken into account. They serve as underlying constraints when optimizing the assignment of goods transport with the objective of minimizing pollution and fuel consumption. By maximizing the fill rate for each HDV, the total number of vehicles or required trips might be reduced.

The objective of the routing task is to find the most fuel-efficient path by considering the constraints set by the road topography. For example, a flat long road might be more fuel-efficient compared to a shorter hilly road. The state of the traffic, infrastructure, and environment (e.g., weather), as well as driver's resting times are taken into account in the route calculation to obtain reliable assignment plans. One particularly important aspect towards fuel-optimal routing is that routes will be coordinated between a large number of HDVs, such that groups of vehicles can benefit from platooning on overlapping sections of their assigned paths. Consequently, a route for a single vehicle will not only contain the desired path, but also destinations and timing constraints are set to rendezvous with other

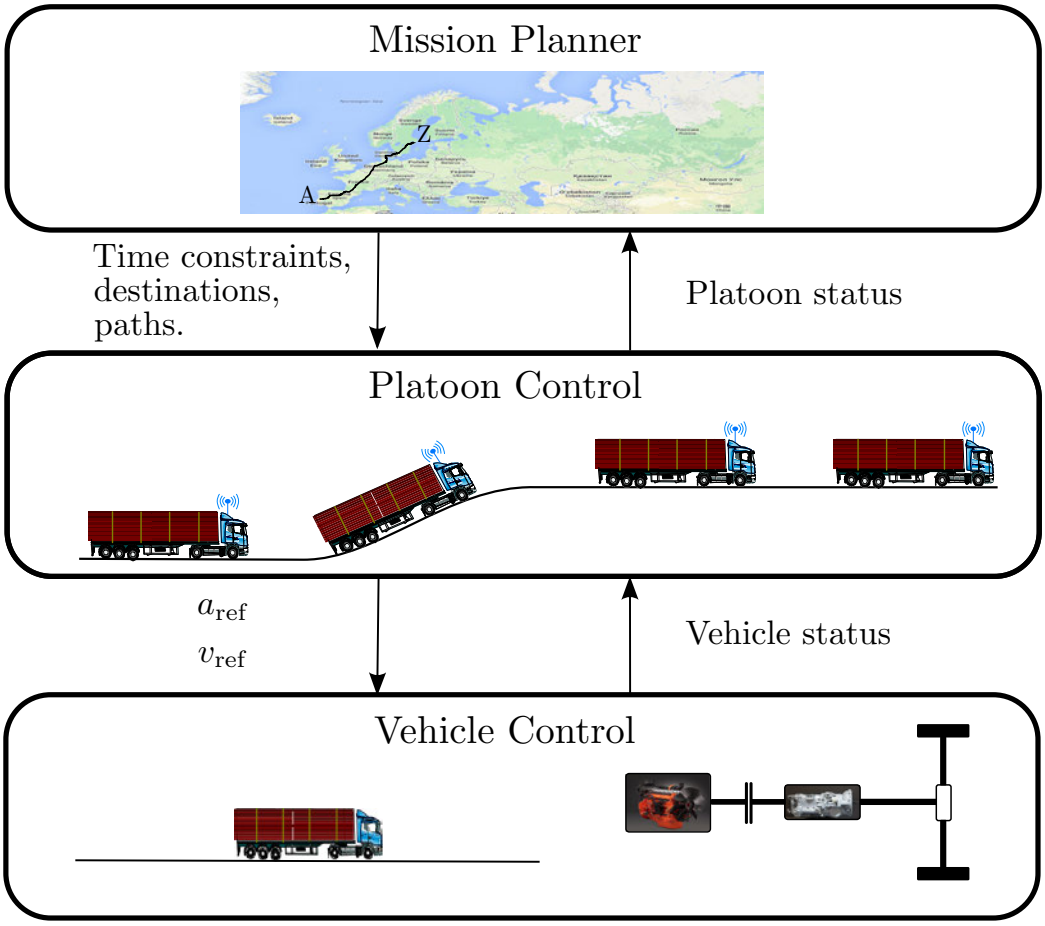

Figure 3.7: The three-layered system architecture for goods transport.

vehicles in order to form platoons when possible. Naturally, platoons can be formed from the starting destination if several vehicles depart at the same time and they have a common path assignment.

The large-scale transportation system will typically amount to a computationally complex optimization problem that is most likely solved and computed in a back-office. The optimization required in this layer will be continuously updated with the arrival of new transport assignments or heavy-duty vehicles deviating from earlier plans.

Platoon Control

In the platoon control layer, given in the middle of Figure 3.7, the main task is to form a fuel-optimal control based on vehicle-to-vehicle (V2V) communication and road topography preview information, without compromising safety. The challenges in this layer lie in maintaining a desired small inter-vehicle spacing policy without increasing the risk of a collision, adjust the speed suitably to merge with other

vehicles or platoons, and forming fuel-optimal policies in the presence of uncertainties in vehicle parameters, sensor information, and map data. It is fuel-efficient to drive the vehicles at a small inter-vehicle spacing to achieve a large reduction in air drag, but, as the number of vehicles in a platoon and the traffic intensity grows, the complexity of the coupled traffic dynamics increases. The actions of one vehicle may in turn affect all vehicles in a linked chain, where a disturbance in the first vehicle might propagate and amplify throughout the chain; causing an increased control effort to handle the disturbances or even a collision. V2V communication is introduced such that interaction is enabled between vehicles within spatial range of their wireless transceiver. Thereby, fuel-efficiency and safety are improved by making cooperative control decisions that takes the behavior of surrounding vehicles into account. Hence, suitable decentralized controllers are established in this layer for fuel-efficient and safe control. We consider a decentralized controller, mainly due to the communication constraints that occur in practice[2]. Furthermore, the fuel consumption of heavy-duty vehicles is strongly dependent on the road grade due to their extensive mass. However, when the topography of the road ahead is known through map data, this information can be used to optimize a velocity profile, for all the platooning vehicles, that minimizes the fuel consumption with respect to a fixed travel time[3].

The constraints provided by the top layer are translated into a reference velocity profile for each HDV, consisting of average velocities over upcoming road segments that need to be maintained in order to merge platoons or to meet the specified time constraints. A platoon status is transmitted suitably often to the top layer, reporting if the constraints can be satisfied. If the constraints are violated for some reason, for example, due to a disturbance in traffic, the mission planning layer is requested to provide a new set of feasible directions. The platoon control layer also includes tasks such as the merging of several HDVs, or platoons, or the splitting and reordering of platoons, where fuel-optimal trajectories are derived for every HDV.

Vehicle Control

The main task of the vehicle control layer, shown in the bottom of Figure 3.7, is to ensure tracking of the desired velocities and acceleration requests. In addition, fuel-efficient control strategies are executed based on on-board sensor information and the powertrain is optimized for energy efficiency. A vehicle status is continuously provided to the platoon layer, notifying if the desired velocities and acceleration requests are not feasible or if a system failure has occurred. Recall that the parts of the powertrain are elastic, hence velocities and torque differ along the powertrain. As a result, resonances may occur. The handling of such resonances for functionality, drivability, and noise reduction are challenges that are addressed in this layer.

[2] A more detailed motivation for why decentralized controllers are considered in this thesis is given in Chapter 6.

[3] A more detailed discussion regarding how to use road grade preview information in control for HDV platooning is given in Chapter 7.

Tracking of the desired velocities and acceleration requests is obtained through the vehicle's engine management system (EMS), brake management system (BMS), and gear management system (GMS). Hence, fuel-injection, brake blending, and gear shift strategies are also formed to optimize the response performance in this layer. Recall that the brake discs are susceptible to brake fade when used over longer periods, which can degrade the brake performance. Thus, an HDV is typically comprised of additional brake systems, such the exhaust brake and the retarder. Hence, the combination and coordination of the various braking systems to avoid brake performance loss are also handled in this layer. HDVs might drop drastically in speed during a gear change, for example, over an uphill segment. Therefore, the total driving resistance is estimated in this layer to determine whether a one or two step change in gear is required. To reduce the drop in velocity, the gear change must be quickly executed.

Several vehicle specific control tasks for a single vehicle that is traveling alone and catching up to form a platoon are also handled in this layer for fuel-efficient vehicle propulsion. Fuel-efficient control strategies such as the economical cruise control is formed by predicting if a hill crest is reached. If so, the torque can be reduced and the speed is then resumed slightly after the crest is passed for fuel-efficiency. If map data are available, road grade preview data are utilized to establish predictive controllers, for a single vehicle, that are typically implemented in a receding horizon fashion, see Hellström (2010). The conventional CC can also be optimized for fuel-efficiency, by handling disturbances that are induced by external forces in a suitable manner (Shaout and Jarrah, 1997).

3.3.2 Platoon System Architecture

The platoon system architecture that we consider is illustrated in Figure 3.8, which corresponds to the two lower layers of Figure 3.7. The control systems rely on the underlying information and their structure will vary with a varying range of inputs, which must be considered. Thus, an understanding of both the control architecture and the underlying sensor and communication systems is important.

The arrows indicate the direction of information flow in the system. Vehicle information is obtained through on-board sensors, which is used in feedback control, as illustrated by the arrow from a vehicle to its controllers. The arrow between a preceding vehicle and the ACC shows the information that is obtained through the radar. Here, state information is provided with respect to the preceding vehicle. The arrows between each cooperative adaptive cruise control (CACC) and the wireless communication network, show the two-way communication between the platooning vehicles. It includes the system state information and vehicle parameter information.

We propose a layered control system architecture, as illustrated in Figure 3.8. Starting from the bottom, the conventional CC offers three advantages: maintained vehicle speed, improved fuel economy, and driver comfort over long distances. It typically uses velocity feedback information and acts as a PI- or PID-controller to determine the required change in velocity, which is then sent as an input to the

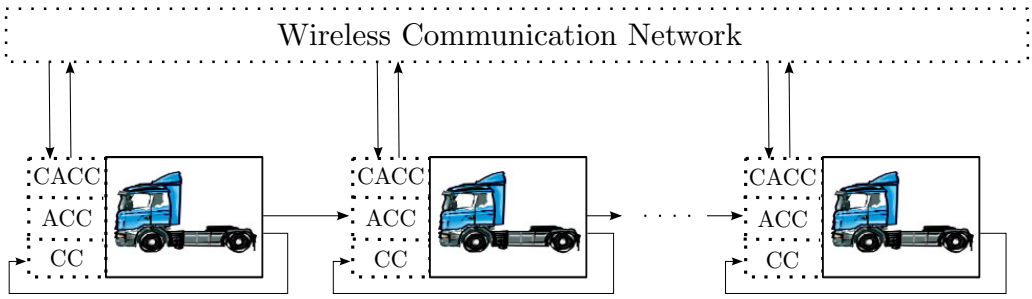

Figure 3.8: Platoon system architecture for an N vehicle platoon. The lead vehicle, with index $i = 1$, is to the left and the last vehicle is to the right. The control architecture for vehicle speed control is shown in front of each vehicle. The information flow in the system is given by the arrows.

low-level controllers. In case of system failure, the driver is instructed to take full control of the vehicle.

The ACC, in the layer above, aims to maintain a desired spacing policy by utilizing relative distance and velocity information based on the preceding vehicle. It determines the control input with respect to fuel-efficiency and driver comfort. Fuzzy logic controllers are also typically implemented for HDVs, where the fuel-efficiency is improved, for example, by allowing for a reduced spacing during downhills such that unnecessary braking actions are avoided. Safety is improved since, as opposed to the CC, the ACC is allowed to actuate the brakes and can react faster than a driver. In case of system failure, the driver is warned and the control actions are degraded to the CC layer.

The CACC, in the top layer, is a cooperative adaptive cruise controller, which forms optimal decentralized decisions based on vehicles within spatial range of its wireless transceiver. The cost function in the design of the decentralized optimal controllers for HDV platooning includes the behavior of the surrounding vehicles, hence control actions are based on self-interest as well as the interests of all other vehicles in the platoon. Thus, the aim is to maintain a suitable inter-vehicle distance to several preceding vehicles with respect to fuel-efficiency, robustness, and safety of HDVs within radio range. By displaying a cooperative and synchronous behavior the relative distance can be reduced, thereby lowering the fuel consumption. Safety is improved by forming control actions based on the behavior of several vehicles ahead in the platoon. Safety, comfort, and fuel-efficiency can be improved further by agreeing upon constraints with respect to maximum acceleration and deceleration in the platoon. By ensuring that the preceding vehicles does not brake harder than what is achievable by the follower vehicles, the inter-vehicle spacing can be reduced. Similarly, the inter-vehicle spacing is maintained by ensuring that the preceding vehicles do not accelerate faster compared to what is achievable by the follower vehicles. In the occurrence of a system failure in this layer, the control actions are degraded to the ACC layer.

There are several challenges in this architecture. The low-level controllers handle some of the nonlinearities in the vehicle and inherently linearize the vehicle behavior to some extent. However, a drawback is that the model uncertainty increases within certain dynamic range of operation, since the behavior of the nonlinear low-level controllers might vary in behavior depending on its current state. For example, step responses in velocity of the same magnitude might vary depending on the current gear, if the engine was idling or active, or if the BMS was active just before the step is requested. Furthermore, radar information can be lost, for example over road bends, when the preceding vehicle is not directly in front. Delays in wireless communication or in processing of radar information can occur, which must be handled by the active controller.

3.3.3 Vehicle System Architecture

Many on-board systems are involved in control of a platooning vehicle. An understanding of the main underlying systems for data processing and control is important for implementation purposes. Each HDV that we consider has the system architecture shown in Figure 3.9. Several control units are connected to the controller area network (CAN). The wireless sensor unit (WSU), global positioning system (GPS), and radar act as sensor units, providing information about the surrounding environment. Even though a wide range of information is available from wireless communication, ECUs, and on-board sensors, it is often noisy and must be processed before it can be used as input to the controllers. In the data processing block, the noisy data from all the transmitting vehicles in the established platoon are processed through a Kalman filter and GPS information from the preceding vehicle is fused together with the state information from the radar. In the event of packet losses or short outages, the Kalman filter acts as a state predictor. Each received message from other platooning vehicles contains GPS information. Based on the position and heading of each surrounding vehicles, the platooning vehicles are mapped to a local coordinate system. Filtered information, along with vehicle specific parameters, controller gains, and the current mode of operation for the platooning vehicles, is forwarded to the high-level controllers block. The active controller sends out the reference signal on CAN, which is then carried out by the low-level controllers shown to the right in Figure 3.9.

The low-level control systems consists of the EMS, BMS, and GMS. The EMS controller receives a velocity request as an input. It then calculates the required fueling amount for obtaining the necessary torque to obtain the requested velocity. The EMS also assures that no oscillations arise in the powertrain. It monitors the turbo pressure and limits the fueling in case a sufficient amount of air is not available for the combustion process. Hence, the achievable torque might be limited. There are several brake systems in a modern HDV, ranging from the weaker exhaust brake to the strong brake discs. The BMS receives a deceleration request and typically blends the brake power from the different systems depending on the magnitude of the requested signal. It also assures that no system overheats. Therefore, the achieved

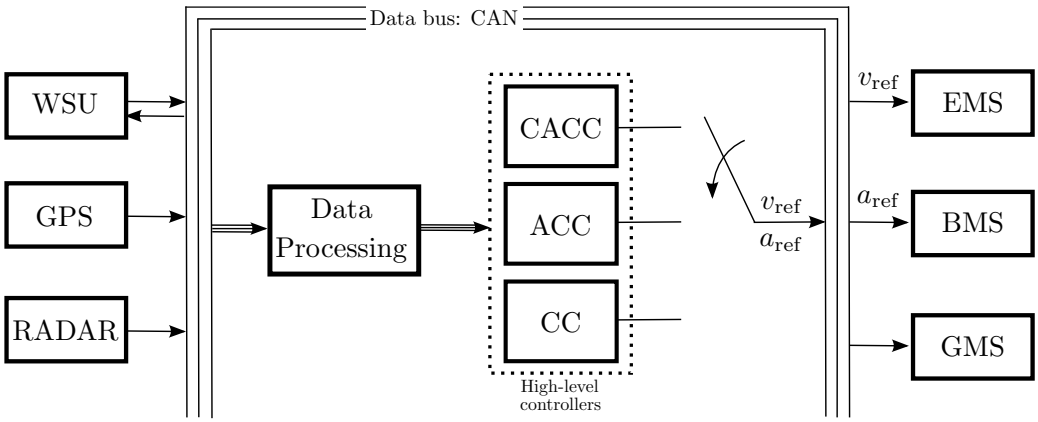

Figure 3.9: Vehicle system architecture for the data processing and control. The arrows indicate the information flow that is shared through can. The driver choses what controller to activate, which is indicated by the switch. If a failure occurs in the CACC when active, the system will automatically switch to the ACC and then to the CC if a failure in the ACC occurs.

braking force varies with respect to the current state of the system. The GMS is an automated gear changing system that enables the driver to devote more attention to handling the vehicle and to traffic. Monitoring the RPM and the engine torque request, it is designed to change the gear quickly and comfortably in a fuel-efficient manner. Note, however, that a delay typically arises when disengaging and engaging a new gear.

3.4 Summary

Several models for the analysis and synthesis of HDV platoons have been derived. A nonlinear model, obtained by modeling the powertrain along with the external forces affecting an HDV, serves as the basis for the analysis and control of the vehicles in the platoon. Additionally, the nonlinear air drag occurring between neighboring vehicles is modeled, which is essential in the fuel reduction analysis of HDV platooning presented in this thesis. A linearized model has been presented that captures the normal operating mode behavior to a certain extent. Even though the analytical models serve as a basis for control design, the controller performance must be evaluated and verified on a more advanced model before practical implementation. Thus, an advanced simulation model has been presented to serve as a evaluation platform. Last, we presented a three-layered transport system architecture, which decomposes the overall transport control problem into manageable subsystems. We also presented a platoon system architecture and a vehicle system architecture to provide a modularized implementable solution and a better understanding of the main systems that are involved in control for HDV platoons.

Chapter 4

Fuel-Saving Potential of Platooning

"*Every great advance in science has issued from a new audacity of imagination.*"

John Dewey

Vehicle platooning is important for the automotive industry. The focus lies on the environmental benefits and safety issues but it is of equal importance to also investigate the economical prospective and feasibility of platooning for commercial purposes. Recall that the road transport industry is very fuel price sensitive, since fuel cost constitutes approximately one third of the total operational cost in European long haulage heavy-duty vehicles (HDVs). Fuel saving potentials of 5–20 %, was demonstrated for HDV platooning in experiments on flat test tracks by Bonnet and Fritz (2000); Davila et al. (2013); Tsugawa (2013). The saving varies with set speed, inter-vehicle spacing, and vehicle mass. However, conclusive results remain unclear for the fuel-saving potential of platooning on roads with varying topography. The focus in this chapter is the fuel reduction that HDV platooning enables over a varying topography and the analysis with respect to the influence of a commercial adaptive cruise control (ACC) has on the fuel consumption. We consider a platoon consisting of N HDVs. The main forces affecting a vehicle in motion is given by

$$\begin{aligned} m_t \frac{dv}{dt} =& F_{\mathrm{e}}(\omega_{\mathrm{e}}, \delta) - F_{\mathrm{b}} - F_{\mathrm{a}}(v, d) - F_{\mathrm{r}}(\alpha) - F_{\mathrm{g}}(\alpha) \\ =& \frac{\gamma_{\mathrm{G}}\gamma_{\mathrm{f}}\eta_{\mathrm{G}}\eta_{\mathrm{f}}}{r_{\mathrm{w}}} T_{\mathrm{e}}(\omega_{\mathrm{e}}, \delta) - F_{\mathrm{b}} - \frac{1}{2} c_{\mathrm{D}} A_{\mathrm{a}} \rho_{\mathrm{a}} \Phi(d) v^2 - c_{\mathrm{r}} m g \cos\alpha - m g \sin\alpha, \end{aligned}$$

where $F_{\mathrm{e}} \geq 0$ denotes the force produced by the engine through fuel injection, $F_{\mathrm{b}} \geq 0$ denotes the braking force, α denotes the slope of the road, c_{D} and c_{r} are characteristic coefficients, g denotes the gravitational force, ρ_{a} the air density, r_{w} the wheel radius, and γ_{G}, γ_{f}, η_{G}, η_{f} are transmission and gear specific constants. Moreover, F^{a}, F^{r}, and F^{g} denote the external air drag, rolling resistance, and

gravitational forces acting upon the vehicle, respectively, and $\Phi(d)$ denotes the empirically derived nonlinear air drag reduction due a short relative distance d to a preceding vehicle. The control input T_{e} is the net engine torque, which is a function of the engine angular velocity ω_{e} and the injected fuel amount δ. The accelerated mass of the truck $m_{\mathrm{t}}(m, J_{\mathrm{w}}, J_{\mathrm{e}}, \gamma_{\mathrm{G}}, \gamma_{\mathrm{f}}, \eta_{\mathrm{G}}, \eta_{\mathrm{f}})$ varies with the active gear number and depends on the gross mass m, wheel inertia J_{w}, engine inertia J_{e}, gearbox ratio and efficiency $\gamma_{\mathrm{G}}, \eta_{\mathrm{G}}$ aswell as the final drive ratio and efficiency $\gamma_{\mathrm{f}}, \eta_{\mathrm{f}}$.

The aim of this study is to determine the fuel reduction possibilities for a platoon of N HDVs traveling on a road with a given set speed and relative distance. The fuel saving potential is studied for various settings of time headway τ. The objective is to separate the fuel saving obtained through the reduction in air drag and the fuel consumption produced by the commercial ACC effort. The reduction in the air drag coefficient is modeled by the empirical model presented in Section 3.2.

The main contribution of this chapter is to investigate the fuel reduction potential of HDV platooning for various time headway settings, solely with respect to a commercial control strategy. The aim is not to investigate the specifics of the control strategy, but rather establish its effect on the fuel consumption. Fuel-optimal control for a single vehicle on a flat road is to maintain a constant velocity, under the presumption that the traveling time is fixed (Hellström et al., 2008). Any deviations in the form of acceleration and deceleration result in an increased fuel consumption. The ACC generally receives information regarding the relative velocity and distance to the vehicle ahead and thereby maintains the relative distance by adjusting its speed accordingly. The increased control effort that the ACC creates, in the sense of additional transient engine actions and brake events, produces an overall increased fuel consumption. Thus, it is still unclear whether the increased control effort, produced by varying road topography, possibly cancels the reduction in fuel consumption achieved by decreasing the air drag. Hence, the aim is to determine the fuel reduction possibilities for a platoon of HDVs traveling on a road with varying topography, a given set speed and time headway setting.

The outline of this chapter is as follows. First the fuel reduction potential of a commercial ACC is evaluated for two identical HDVs with respect to different time headway settings in Section 4.1. In Section 4.2 a method is derived to isolate the ACC's influence on the fuel consumption. Several case studies are presented in Section 4.3 to deduce the consequences of provoking the ACC behavior by having two vehicles of different mass. In Section 4.4 empirical fuel consumption data obtained through field tests are presented and utilized as a basis for verification of the simulation model presented in Section 3.2. Finally, a brief summary of the presented results concludes this chapter in Section 4.5.

4.1 Fuel Consumption for Identical HDVs

It is known (Wolf-Heinrich and Ahmed, 1998; Bonnet and Fritz, 2000) that the air drag can be reduced significantly by arranging trucks in a platoon formation,

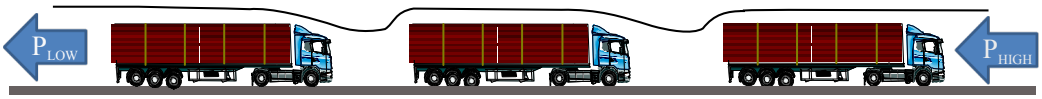

Figure 4.1: The air drag is reduced for all the vehicles in the platoon due to a lowered overall pressure experienced by each HDV.

as depicted in Figure 4.1. The reduction occurs partly due to the drag produced behind the lead vehicle will be lowered when allowing a follower vehicle to lie close behind. The follower vehicle will experience a significant reduction of air drag due to a relatively large reduced pressure at the front. Hence, the total air drag is reduced, which in turn lowers the fuel consumption. It is difficult to make an accurate deduction merely based on empirical results due to the varying external disturbances. For example, weather conditions might vary and traffic conditions might change, producing incomparable and inconclusive empirical results with respect to the fuel consumption. Note also that the behavior of an HDV differs significantly from a light vehicle. Physical constraints typically have a larger impact on the vehicle dynamics due to the higher mass and inertia. The advanced simulation model presented in Section 3.2 is evaluated on a 300 km long road to determine the fuel reduction possibilities for HDV platooning under practical circumstances. It is interesting to evaluate the implication a varying topography and air drag reduction have on the fuel consumption. Additional transient control actions are required to maintain the relative distance over a varying road topography. Hence, it is not obvious how the fuel consumption for the follower vehicle is affected under such conditions.

Results in this section were obtained by simulating a truck with a 620 hp engine and a 12 speed gear box on a measured road with a given set speed as an input. The vehicle configuration was 6×2 and the gross mass of the truck was chosen to be 40 t, which is the maximum allowed weight for long-haulage HDVs in most European countries. Both vehicles start at an initial velocity of 20 km/h, an initial relative distance of 20 m, and then accelerates to the set reference velocity. ACC- and cruise control (CC)-logic to govern the trucks was implemented by utilizing the current software implemented in Scania CV AB's HDVs in production.

To obtain results based upon conditions that represent real-life scenarios, a fairly hilly road was selected as a simulation basis. The Swedish road between Södertälje and Jönköping, depicted in Figure 4.2, is considered to characterize a varied range of road conditions. The set speed for the lead vehicle's CC is 70 km/h, as depicted in Figure 4.3, which is a common road speed for narrow Swedish highways. The set speed for the follower truck with ACC is set to 80 km/h in order to inhibit a possible loss of the leading vehicle due to factors in the topography. Hence, the normalized fuel consumption results from simulating two identical trucks on the aforementioned road are stated in Table 4.1 for various time headway settings.

The results show that a reduction of 4.7–7.7% in fuel consumption is attainable with an ACC compared to a truck with a conventional CC. Furthermore, the

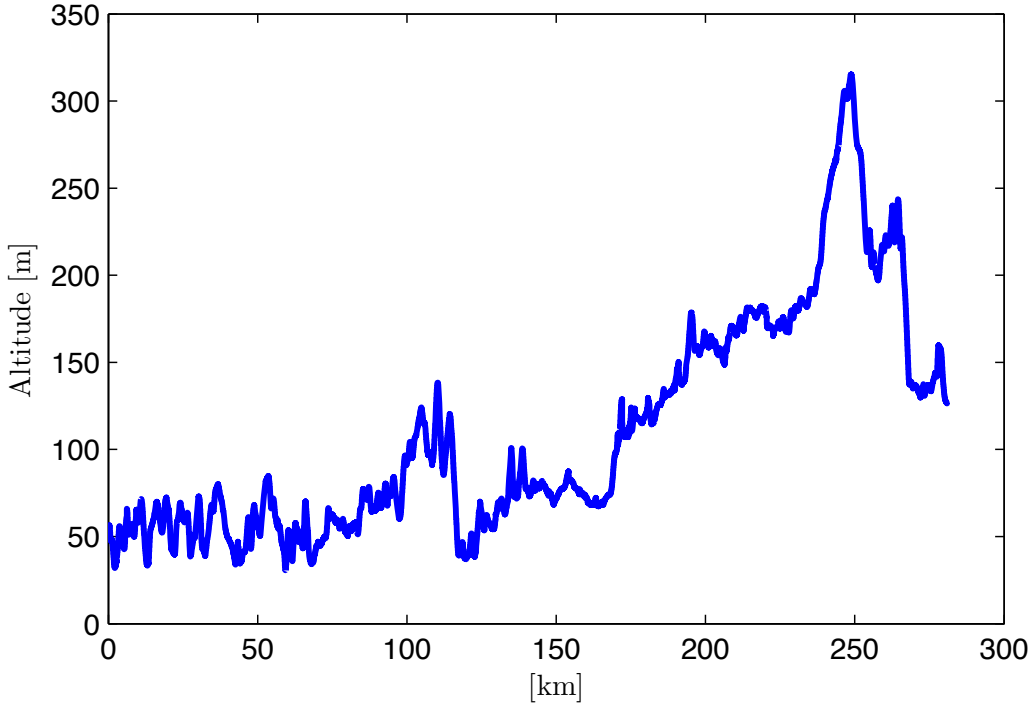

Figure 4.2: Topography for the road Södertälje - Jönköping, Sweden

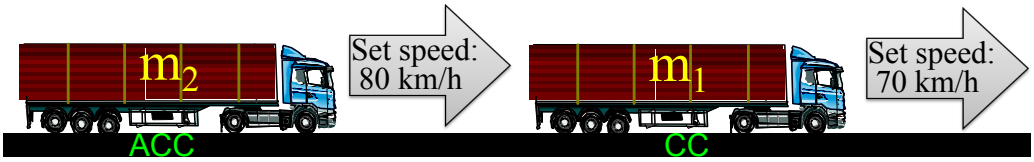

Figure 4.3: Simulation scenario.

fuel reduction is obtained without reducing the average velocity. Therefore, the traveling time is unaffected, which is considered to be a crucial factor for many HDV fleet operators as they are commonly commissioned based on delivery time and punctuality. The transport assignments are often very time sensitive, since a delay can in many cases result in a significant increase in cost as they might in turn lose their slot for unloading the goods.

4.2 Isolating the Influence from the ACC

It has now been shown that an overall fuel reduction can be obtained when driving two trucks in a platoon. Hence, the control effort produced by the ACC to maintain the inter-vehicle spacing between the vehicles over a varying road topography does not cancel the total fuel reduction possibilities obtained through the reduced air

Table 4.1: Normalized results from simulation with identical trucks for various time headway settings.

	Fuel consumption [%]	Average velocity [km/h]
Lead HDV	100	69.89
$\tau = 1\,\mathrm{s}$	92.3	69.90
$\tau = 2\,\mathrm{s}$	93.6	69.90
$\tau = 3\,\mathrm{s}$	95.3	69.89

Table 4.2: Normalized results from simulation with identical air drag and trucks for various time headway settings.

	Fuel consumption [%]	Average velocity [km/h]
Lead HDV	100	69.89
$\tau = 1\,\mathrm{s}$	98.8	69.90
$\tau = 2\,\mathrm{s}$	98.9	69.89
$\tau = 3\,\mathrm{s}$	99.1	69.89

drag. However, it is unclear whether the ACC effort produces an increase or decrease of fuel consumption and if it can be improved further.

To separate and determine the effect of the control effort on the fuel consumption, all other factors must be kept constant. Hence, the truck parameters, i.e. engine, gear box, weight, rolling resistance, etc., are set equal for both vehicles—eliminating any possibilities for the fuel consumption to differ due to different physical properties between the trucks. Furthermore, to facilitate a correct deduction, the ambient variables, i.e. ambient temperature, humidity, traffic conditions, etc., and the air drag, are also set equal for both vehicles, effectively isolating the effect of the control strategy on the fuel consumption within the simulation model in Section 3.2.

The simulation results for different time headway settings, over the road between Södertälje and Jönköping, presented in Table 4.2 show that the overall control effort actually reduces the fuel consumption. Maximum reduction in fuel consumption solely with respect to the control strategy is obtained for time headway setting $\tau = 1\,\mathrm{s}$. There is a slight but insignificant change in fuel consumption for $\tau = 5\,\mathrm{s}$.
A possible explanation for this discovery is derived by studying a segment of the road depicted in Figure 4.4, which shows the vehicle behavior for both of the trucks controlled with CC and ACC. The top plot shows the actual vehicle velocity trajectory of the two trucks, with implied speed requests. When traveling along a downhill, the ACC-logic allows the subject vehicle to increase its speed and thereby decrease the inter-vehicle spacing. When exiting the downhill the ACC deters the preservation of the set speed, thus effectively increasing the relative distance. The lead vehicle on the other hand, at the 6040m marker, exceeds its maximum set speed

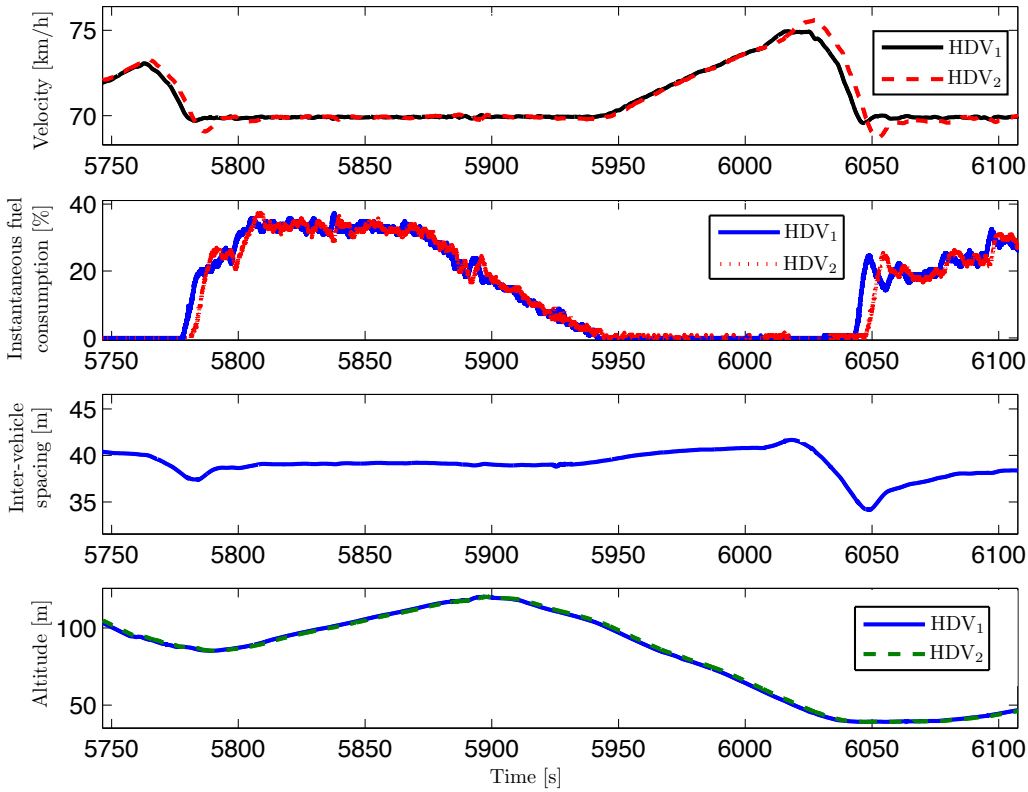

Figure 4.4: Simulation results: Top plot: Velocity trajectory for the lead vehicle controlled by CC, denoted by HDV_1 (black, solid line), and the follower vehicle governed by ACC, denoted by HDV_2 (red dashed line). Second plot from the top: Instantaneous fuel consumption for lead HDV (blue, solid line) and the follower HDV (red, dashed line). Third plot from the top: Relative distance between the vehicles (solid line). Bottom plot: Experienced topography for the lead HDV (blue, solid line) and the follower HDV (green, dashed line).

limit threshold of 75 km/h in this case and therefore the downhill speed control (DHSC) is activated. Hence, stored energy is lost through the braking action whereas it is maintained for the follower vehicle. Thus, it becomes evident by studying the instantaneous fuel consumption, shown in the second plot from the top in Figure 4.4, at the 6040m marker that the ACC strategy reduces the fuel consumption in this case, since the overall braking action is reduced through preview information from the lead vehicle. The area between the curves at the aforementioned markers represent the saved fuel. Studies in economical cruise control (ECC) strategy (Hellström et al., 2006), have also proven that utilizing the gravitational force obtained in a downhill to increase the velocity and utilizing the provided energy to deter control actions until mandated, reduces fuel consumption. Therefore the observed behavior can be characterized as enabling classical ECC behavior through preview information of

the road characteristics ahead from the lead vehicle, which undoubtedly reduces the fuel consumption.

The noted result could also have been a consequence of finding a more fuel-efficient Fuel–Torque–RPM point for the specific engine due to a small difference in actual speed between the two trucks. However, an identical simulation with different engine characteristics resulted in equivalent results concluded from Table 4.2.

4.3 Mass Variations

The aforementioned results indicate that platooning with two identical trucks reduces the fuel consumption due to both air drag reduction and control strategy. However, two HDVs with different masses could induce a different ACC behavior. In some cases when following a lighter truck over an uphill segment, the lead vehicle will be able to maintain its velocity, while the follower vehicle will drop in speed, even though maximum engine torque is applied, due to its extensive mass. Similarly when following a lighter vehicle, the follower vehicle will have to brake in a downhill segment to maintain the inter-vehicle spacing when the lead vehicle is coasting. Hence, a difference in mass between the two trucks will inflict constraints on the ACC and alter the controller behavior in comparison with the case of two identical trucks. Thus, it is of interest to study the effects of provoking the ACC strategy in such a manner.

Two scenarios are investigated. In the first scenario, the mass of the lead vehicle is set to $m_1 = 30\,\mathrm{t}$, whereas the truck governed by ACC is maintained at $m_2 = 40\,\mathrm{t}$, as illustrated in Figure 4.3. In the second scenario, the leading vehicle's mass is set to $m_1 = 50\,\mathrm{t}$. All other conditions are identical and the simulation is carried out on the same road as before.

The results displayed in Figure 4.5 were derived by comparing the fuel consumption of the follower vehicle, with the fuel consumption of a lead vehicle with the same mass to avoid ambiguity. The results show that a fuel saving of 3.8–7.4% can be obtained when following a lighter lead vehicle and a reduction in fuel consumption of 4.3–6.9% when following a heavier lead vehicle. Hence, a significant fuel reduction can still be obtained for various considered time headway settings. However, a noticeable difference in fuel consumption is detected due to the physically induced change in control. For time headway setting $\tau = 1\,\mathrm{s}$, a 0.5% higher fuel reduction can be obtained with a lighter lead vehicle in comparison with a heavier lead vehicle. It is probably due to the fact that the vehicle governed by ACC acts as a low pass filter when it is heavier, making it less sensitive to small fluctuations in the lead vehicle's velocity. Thus, a lower variance in control effort is required for the vehicle, resulting in lower fuel consumption. However, $\tau = 3\,\mathrm{s}$ a lighter lead vehicle produces an increase of 0.5% in fuel consumption compared to the results from a heavier lead vehicle. A lighter lead vehicle has a lower acceleration when coasting over steep downhill segments. Thus, the heavier vehicle governed by the ACC has to brake in those cases in order to maintain the relative distance. Hence, energy produced from

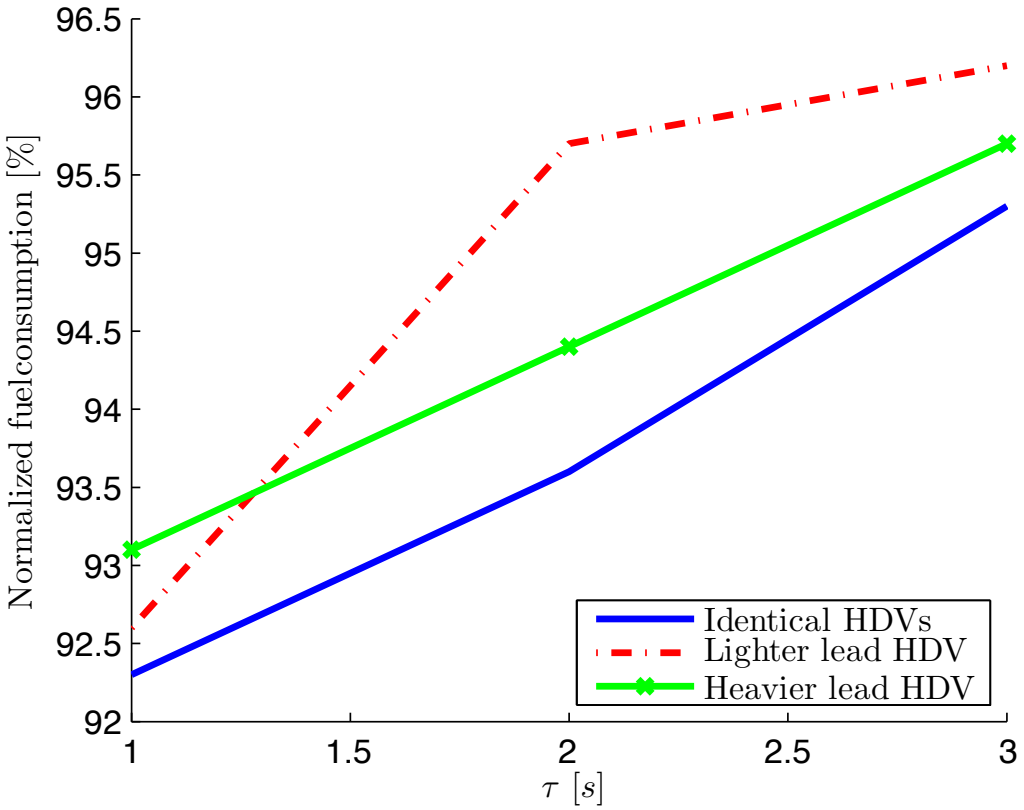

Figure 4.5: The figure illustrates the results of simulating platooing with two HDVs of different mass and identical mass.

fuel combustion is wasted through frictional heat losses in the brake discs.

4.4 Experiments

The main difficulty lies in producing an environment where reproducible results can be obtained. In this section, we present a method to obtain data empirically for $N = 2$ HDVs, to be utilized as a basis for verification of the simulation model presented in Section 3.2.

4.4.1 Setup

Experiments were conducted upon a Swedish highway with two identical trucks as illustrated in Figure 4.6. The masses of the HDVs was measured to be 39.3 t and 39.2 t. Both of them were equipped with a Scania 620 hp engine. The fuel consumption was measured and recorded through each vehicles' CAN-devices. It can be measured for two trucks traveling on the road, but to facilitate a correct deduction, the ambient variables, e.g., wind, ambient temperature, humidity, etc.,

Figure 4.6: Two HDVs traveling at close relative distance on a measured Swedish highway. (The picture is provided at the courtesy of Scania CV AB.)

must be equal during every measurement instance (test-run) to create reproducible results. Small variations in these disturbances can produce a significant difference in measured fuel consumption. An additional reference truck was therefore used as a calibration device to reduce the error due to the varying environment factors. All the vehicles were traveling with a set speed of 90 km/h.

4.4.2 Results

Several runs were conducted for which the accumulated results are presented in Table 4.3, where the accumulated fuel consumption data are provided for several test-runs with varying time headway settings. Simulated fuel consumption is given together with experimental fuel consumption. The lead vehicle was governed by a CC.

The results in Table 4.3 verify that a significant fuel reduction can be obtained through platooning and the simulated values correspond very well to the empirical results. The findings presented in Figure 3.5 were, however, derived from experiments conducted on buses in a wind tunnel. Hence no effects from additional aerodynamics, e.g., lateral winds, were taken into consideration. Driving in a platoon does not reduce the resistance from such winds. Thus, only 80% of the suggested values were utilized and assumed to give a good estimate of reasonable air drag reduction within platooning applications. The slightly lower values in fuel reduction are most likely

Table 4.3: Fuel reduction for a two vehicle platoon.

	Simul. Fuel consump. [%]	Exper. Fuel consump. [%]
Lead HDV	100	100
$\tau = 1\,\mathrm{s}$	93.2	92.9
$\tau = 2\,\mathrm{s}$	94.9	-
$\tau = 3\,\mathrm{s}$	98.8	98.7

a result of the aforementioned assumption. Therefore it can be deduced that the results produced by the simulation are most certainly reliable and mirrors real truck behavior quite accurately.

4.5 Summary

A maximum fuel saving of 4.7–7.7% depending on the time headway setting, at set speed equal to 70 km/h, can be obtained with two identical HDVs. If the lead vehicle is 10 t lighter a corresponding 3.8–7.4% fuel reduction can be obtained depending on the time headway setting. Similarly if the lead vehicle is 10 t heavier a 4.3–6.9% fuel reduction can be obtained. This indicates that HDVs in a platoon should be ordered based on mass and the time headway setting for fuel efficiency. The fuel consumption in a $N > 2$ HDV platoon could possibly be lowered further due to an additional reduction in air drag for additional vehicles. All results indicate that a maximum fuel reduction will be achieved with the smallest time headway setting of $\tau = 1\,\mathrm{s}$, due to both reduction in air drag and the control strategy.

The ACC-strategy does not increase the fuel consumption according to the results obtained in this study. By mirroring ECC behavior through preview information from the vehicle ahead, the current ACC becomes a fuel-efficient control strategy by reducing the overall braking actions over steep road segments. Approximately 1% fuel reduction was obtained solely based upon the ACC actions. Surprisingly, the additional transient control actions with the smallest time headway setting does not increase the overall fuel consumption. The results clearly show that no significant difference in fuel reduction occurs between time headway settings with respect to control effort. However, a vast reduction of air drag can be obtained by reducing the inter-vehicle spacing. Hence, it is favorable to drive the vehicles at a small inter-vehicle spacing to achieve a large reduction in air drag. However issues such as feedback delay and communication delay for safety and driver comfort arises. Thus a need for further investigation within the subject matter arises.

The ACC-strategy produces different fuel saving results when following an HDV of different mass. Hence, the results in this study shows that improvements can be made to the ACC-logic by designing it based upon fuel-optimal criteria. Furthermore,

the isolated strategies within this chapter have shown significant fuel reduction possibilities in HDV platooning at relatively large inter-vehicle spacings. The fuel saving can most likely be improved further by reducing the inter-vehicle spacing. However, driver comfort should be taken into consideration for widespread of the platooning system concept. Safety cannot be compromised, hence the impact of the automated vehicle control on the safety must be established and verified.

Chapter 5

Platooning under Safety Constraints

"*The most exciting phrase to hear in science, the one that heralds new discoveries, is not 'Eureka!' but 'That's funny...'*"

Isaac Asimov

It is fuel-efficient to drive at a small inter-vehicle spacing to achieve a high reduction in air drag, but, as traffic intensity grows, the complexity of the coupled traffic dynamics increases. The actions of one vehicle may in turn affect all vehicles in a linked chain. Through improved sensor technology, wireless communication, GPS devices, and digital maps, advanced driver assistance systems are being developed to aid the driver. Key enabling technologies, such as vehicle-to-vehicle (V2V) and vehicle-to-infrastructure (V2I) communication, have matured. However, they impose constraints in terms of accuracy, reliability, and delays. Therefore, safety constraints with respect to how close we can drive to the vehicle ahead without increasing the risk of a collision are a challenge to satisfy. A question arises of how close the automated vehicles can operate without compromising safety.

Commercially available systems, such as the adaptive cruise control (ACC), in a collision avoidance scenario currently use radar measurements of the relative distance and velocity to a preceding vehicle and adjust the velocity automatically. A delay arises from measuring the behavior of the preceding vehicle to producing the actual brake torque at the wheels, since it takes time in determining whether the preceding vehicle is braking and then creating the necessary pressure in the brake cylinders. As an alternative to radar measurements, wireless communication of the breaking signal may be utilized. However, delays are still imposed due to data processing, retransmissions, etc. Thus, the impact of the vehicle control on the safety must be established and verified. Rigorous guarantees cannot only be obtained through extensive simulations, but mathematical tools that are verified by experiments need to be developed.

In this chapter, we consider a heavy-duty vehicle (HDV) platooning scenario with two vehicles where the follower vehicle receives information regarding the

relative position and velocity of the vehicle ahead.[1] The objective is to determine the minimum relative distance between the vehicles that can be maintained without compromising safety. The aim is to find the largest set of initial states, irrespective of how the lead vehicle behaves, for which there exists a controller that manages to keep all executions inside a safe subset of the state space.

The main contribution of this chapter is to primarily establish safe sets, which can serve as a reference for HDV platooning in collision avoidance. The aim is to establish empirical results for validation of the analytical framework and numerical safe set computation for collision avoidance in HDV platooning scenarios. We propose an automated and reproducible method to derive empirical results for validation of safe sets. We show how the method has been evaluated experimentally using real HDVs provided by Scania CV AB on a test site near Stockholm. A differential game formulation of the problem enables the safe set derivation by capturing the event when the lead vehicle blunders in the worst possible manner. We model the game as the follower vehicle (player u_2) is trying its best to avoid a collision while the lead vehicle (player u_1) is trying its best to create a collision. Based on the theoretical and empirical results, we determine criteria for which collisions can be avoided for the worst-case scenario and thereby, establish the minimum possible safe distance in practice between vehicles in a platoon. We show that the minimum relative distance with respect to safety depends on the nonlinear behavior of the brake system, the delays in information propagation, and the constraints on the implemented control actions.

The differential game approach based on optimization (Basar and Olsder, 1995, Chapter 5.3), adopted in this chapter has previously been applied to air traffic management, e.g. Bayen et al. (2003). The computational challenges for our system are similar, but the implementation aspects are quite different. For example, the delays imposed by inter-vehicle communication and sensor processing are important for platoon safety. Moreover, the braking capability of each vehicle plays a crucial role. Still we are able to use the same mathematical framework, conveniently packaged in the level set Matlab toolbox by Mitchell (2007).

The outline of this chapter is as follows. First the system model for the differential game formulation is presented in Section 5.1. In Section 5.2 we present the theoretical premise for computing safe sets and then apply it to platooning. Safe sets are derived for homogeneous and heterogeneous HDV platoons, which are verified through the simulation model presented in Section 3.2. The experimental setup for evaluating the safe sets is given in Section 5.3 together with experimental evaluations. The chapter concludes with a brief summary in Section 5.4.

[1]The extension to platoons with $N > 2$ vehicles is discussed in the chapter. The developed approach generalizes to this case, but the numerical computation are harder.

5.1 System Model

Let $i = 1, \ldots, N$ denote the vehicle order in the platoon. Applying Newton's second law of motion along with all the external forces inflicted upon a vehicle, a nonlinear vehicle model is derived as

$$\begin{aligned}
\dot{s}_1 &= v_1 \\
m_{\mathrm{t}_1}\dot{v}_1 &= F_1^{\mathrm{e}} - F_1^{\mathrm{b}} - F_1^{\mathrm{a}}(v_1) - F_1^{\mathrm{r}}(\alpha(s_1)) - F_1^{\mathrm{g}}(\alpha(s_1)) \\
&= k_1^{\mathrm{e}} T_1^{\mathrm{e}}(\omega_{\mathrm{e}_1}, \delta_1) - F_1^{\mathrm{b}} - k_1^{\mathrm{d}} v_1^2 - k_1^{\mathrm{r}} \cos\alpha(s_1) - k_1^{\mathrm{g}} \sin\alpha(s_1) \\
\dot{s}_i &= v_i \\
m_{\mathrm{t}_i}\dot{v}_i &= F_i^{\mathrm{e}} - F_i^{\mathrm{b}} - F_i^{\mathrm{a}}(v_i, d_{i-1,i}) - F_i^{\mathrm{r}}(\alpha(s_i)) - F_i^{\mathrm{g}}(\alpha(s_i)) \\
&= k_i^{\mathrm{e}} T_i^{\mathrm{e}}(\omega_{\mathrm{e}_i}, \delta_i) - F_i^{\mathrm{b}} - k_i^{\mathrm{d}} \Phi(d_{i-1,i}) v_i^2 - k_i^{\mathrm{r}} \cos\alpha(s_i) - k_i^{\mathrm{g}} \sin\alpha(s_i)
\end{aligned} \tag{5.1}$$

where

$$m_{\mathrm{t}_i} = \frac{J_{\mathrm{w}_i}}{{r_{\mathrm{w}_i}}^2} + m_i + \frac{{\gamma_{\mathrm{G}_i}}^2 {\gamma_{\mathrm{f}_i}}^2 \eta_{\mathrm{G}_i} \eta_{\mathrm{f}_i} J_{\mathrm{e}_i}}{{r_{\mathrm{w}_i}}^2} \tag{5.2}$$

is the total inertial mass, $i = 2, \ldots, N$, s_i is the absolute traveled distance for HDV i from a reference point common to all vehicles in the platoon, $d_{i-1,i} = s_{i-1} - s_i$ is introduced as the relative distance between ith vehicle its preceding vehicle for convenience, and F_i^{a}, F_i^{r}, F_i^{g} denote the external air drag, rolling resistance, and gravitational forces acting upon the vehicle, respectively. The force produced by the engine through fuel injection is denoted by $F_i^{\mathrm{e}} \geq 0$, $F_i^{\mathrm{b}} \geq 0$ denotes the braking force, and $\Phi(d_{i-1,i})$ denotes the nonlinear air drag function. The net engine torque is denoted by T_i^{e}, ω_{e_i} is the engine angular velocity, and k_i^z, $z \in \{\mathrm{e}, \mathrm{d}, \mathrm{r}, \mathrm{g}\}$, are characteristic coefficients. The control input $u_i = F_i^{\mathrm{e}} - F_i^{\mathrm{b}}$ is assumed to be a continuous function in time, which is always satisfied since the braking and the engine force are produced by a physical system. This provides a sufficient condition for the existence of a well defined solution to the above mentioned differential equations (Coddington and Levinson, 1984). The forces F_i^{e} and F_i^{b}, are assumed not to be applied simultaneously.

5.1.1 Two-Vehicle Platoon Model

The aim of this study is to guarantee the safety of HDVs in a platoon. For simplicity, the road is assumed to be flat. The two-vehicle platoon system, in Figure 5.1, can be reduced to

$$\dot{x} = f(x, u_1, u_2) = \begin{bmatrix} c_1^{\mathrm{u}} u_1 - c_1^{\mathrm{d}} v_1^2 - c_1^{\mathrm{r}} \\ -v_{21} \\ c_2^{\mathrm{u}} u_2 - c_1^{\mathrm{u}} u_1 - c_2^{\mathrm{d}}(d_{12})(v_1 + v_{21})^2 + c_1^{\mathrm{d}} v_1^2 - c_2^{\mathrm{r}} + c_1^{\mathrm{r}} \end{bmatrix} \tag{5.3}$$

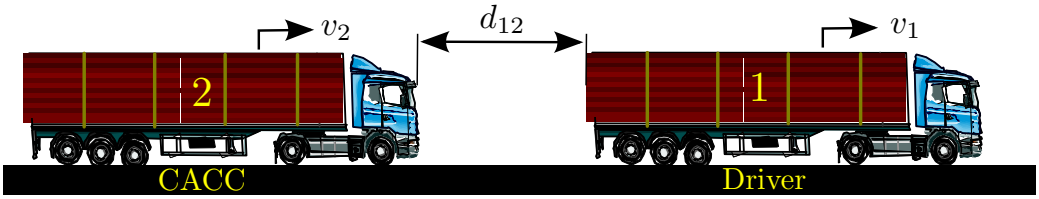

Figure 5.1: Two-vehicle platoon on a flat road where vehicle 1 is referred to as the lead vehicle and vehicle 2 is the follower vehicle.

where $x = [v_1 \ d_{12} \ v_{21}]^T$ and $c_i^z = k_i^z / m_{t_i}$. The state variable v_1 is the velocity of the lead vehicle, $d_{12} = s_1 - s_2$ denotes the relative distance between the vehicles, and $v_{21} = v_2 - v_1$ denotes their relative velocity. The model is limited to forward longitudinal direction. We focus on collision scenarios when vehicles are traveling with a given initial velocity and relative distance, at close inter-vehicle spacings.

5.2 Computing Safe Sets

In this section, we first briefly describe the safe sets computations based on pursuit-evasion games and reachability. Then safe sets are derived for the HDV scenarios of interest.

5.2.1 Safe Set Computation based on a Pursuit-Evasion Game

A pursuit-evasion game is a family of problems in which one group of members tries to capture another group in a given setting, where the system dynamics of the relative framework of the members are given by

$$\dot{x} = f(x, u_1, u_2), \quad x(0) = x_0, \tag{5.4}$$

see (Isaacs, 1965, Chapter 1.5), (Basar and Olsder, 1995, Chapter 8). Here $x(t) \in \mathbb{R}^n$, is the state of the system, $u_1(t) \in \mathbb{R}^{m_1}$ are the actions of one group of players, referred to as the *pursuers*, and $u_2(t) \in \mathbb{R}^{m_2}$ are the actions of the second group of players, referred to as the *evaders*. The problem can be described as a finite-time game where the pursuer and evader are trying to minimize respectively maximize a cost function depending only on the terminal state and time. By introducing the function $H(x, p, u) = p^T f(x, u_1, u_2)$, the game can be formulated as

$$\max_{u_2 \in \mathcal{E}} \min_{u_1 \in \mathcal{D}} H(x, p, u) = H(x, p, u^*) =: H^*(x, p) \tag{5.5}$$

where $p \in \mathbb{R}^n$ is referred to as the costates. The sets $\mathcal{D}$ and $\mathcal{E}$ are compact sets representing all possible actions of the pursuers and the evaders, respectively. The function H^* is the Hamiltonian. Necessary conditions for optimality can be derived based on these data, see (Basar and Olsder, 1995, Chapter 8).

Given actions $u_1 \in \mathcal{E}$ and $u_2 \in \mathcal{D}$, the ability to reach a defined unsafe set from a set of feasible initial states x_0 is of interest for establishing safety criteria. In Mitchell et al. (2005), it was shown that the unsafe set $\mathcal{U}(\tau)$ in which the pursuer in a two-person dynamic game can create a collision in the next τ time units despite the best effort from the evader, can be computed as $\mathcal{U}(\tau) = \{x \in \mathbb{R}^3 | \varphi(x, -\tau) \leq 0\}$, where $\varphi(\cdot\,, \cdot\,)$ is the viscosity solution of the (modified) Hamilton-Jacobi-Isaacs partial differential equation

$$\frac{\partial \varphi(x,t)}{\partial t} + \min(0, H(x, p, u^*)) = 0, \quad t \leq 0, \tag{5.6}$$

with suitable terminal conditions[2] $\varphi(x, 0) = \varphi_0(x)$. The equation is solved by starting at the boundary of the unsafe set $\partial\mathcal{U}(\tau)$. The set of states under consideration is

$$\chi(\tau) = \{x \in \partial\mathcal{U}(\tau) \mid p^T(0) f(x, u_1^*, u_2^*) < 0\}, \tag{5.7}$$

which denotes all states heading into the unsafe set. The reachable set is calculated by starting at $\partial\mathcal{U}(0)$ and simultaneously solving the equations corresponding to the optimality conditions. Hence, the trajectories are computed on the boundary of the set $\chi(\tau)$, from where it is possible to move away from the unsafe set. The procedure gives the surface sets that partitions the safe and unsafe regions.

5.2.2 Safe Set Computation for a Two-Vehicle Platoon

In the problem at hand, $f(x, u_1, u_2)$ in (5.4) corresponds to the platoon system in (5.3) and u_1^*, u_2^* are the optimal strategies for the lead vehicle and the follower vehicles, respectively. The unsafe set $\mathcal{U}(\tau)$ corresponds to a vehicle collision at time $\tau > 0$. Note that the game formulation leads to a conservative estimate of the unsafe set, since the lead vehicle's optimal control action is based on knowledge of how the follower vehicle will respond, but not vice versa, see Mitchell et al. (2005). Such a formulation is preferable to ensure safety in practice.

The Hamiltonian function for the two-vehicle platoon is

$$\begin{aligned} H^*(x,p) :=& \max_{u_2 \in \mathcal{E}} \min_{u_1 \in \mathcal{D}} p^T f(x, u_1, u_2) \\ =& \max_{u_2 \in \mathcal{E}} \min_{u_1 \in \mathcal{D}} \begin{bmatrix} p_1 & p_2 & p_3 \end{bmatrix} \begin{bmatrix} \dot{v}_1 \\ \dot{d}_{12} \\ \dot{v}_{21} \end{bmatrix} \\ =& - p_2 v_{21} - (p_3 - p_1) c_1^{\mathrm{u}} u_1^* + p_3 c_2^{\mathrm{u}} u_2^* + (p_3 - p_1) c_1^{\mathrm{d}} v_1^2 \\ & - p_3 c_2^{\mathrm{d}} (d_{12}) (v_1 + v_{21})^2 + (p_3 - p_1) c_1^{\mathrm{r}} + p_3 c_2^{\mathrm{r}}. \end{aligned} \tag{5.8}$$

With the formulation in (5.8), the lead vehicle determines its optimal control strategy based on the information regarding the follower vehicle's strategy. This is a

[2] In our case the terminal condition is when a collision has occurred, i.e. when $\varphi_0(x) = d_{12} = 0$.

reasonable assumption as we wish to find a set which guarantees that a collision can be avoided despite the worst possible behavior of the lead vehicle. The costates fulfill

$$\dot{p} = -\frac{\partial H^*}{\partial x} = \begin{bmatrix} 2p_3 c_2^{\mathrm{d}}(d_{12})(v_1 + v_{12}) - 2(p_3 - p_1)c_1^{\mathrm{d}} v_1 \\ p_3 \frac{1}{2} c_2^{\mathrm{w}} A_2 \rho k_{pw}(v_1 + v_{21})^2 \\ 2p_3 c_2^{\mathrm{d}}(d_{12})(v_1 + v_{21}) \end{bmatrix}. \tag{5.9}$$

The optimal strategy can easily be computed as

$$u_1^* = \frac{\hat{F}_1^{\mathrm{e}} - \hat{F}_1^{\mathrm{b}}}{2} + \mathrm{sgn}(p_3 - p_1)\frac{\hat{F}_1^{\mathrm{e}} + \hat{F}_1^{\mathrm{b}}}{2}, \quad u_2^* = \frac{\hat{F}_2^{\mathrm{e}} - \hat{F}_2^{\mathrm{b}}}{2} + \mathrm{sgn}(p_3)\frac{\hat{F}_2^{\mathrm{e}} + \hat{F}_2^{\mathrm{b}}}{2}, \tag{5.10}$$

where $\hat{F}_i^b > 0$ is the maximum brake force and $\hat{F}_i^e > 0$ is the maximum engine force of vehicle $i = 1, 2$.

5.2.3 Safe Set Computation for an N-Vehicle Platoon

The safe set computation approach for a two-vehicle derived in the previous section can be generalized to $N > 0$ vehicles. First we consider an $N = 3$ HDV platoon. Two states are added to (5.3) for the three-vehicle platoon system:

$$\dot{x} = f(x, u_1, u_2, u_3) = \begin{bmatrix} c_1^{\mathrm{u}} u_1 - c_1^{\mathrm{d}} v_1^2 - c_1^{\mathrm{r}} \\ -v_{21} \\ c_2^{\mathrm{u}} u_2 - c_1^{\mathrm{u}} u_1 - c_2^{\mathrm{d}}(d_{12}) v_2^2 + c_1^{\mathrm{d}}(v_1 + v_{21})^2 - c_2^{\mathrm{r}} + c_1^{\mathrm{r}} \\ -v_{32} \\ c_3^{\mathrm{u}} u_3 - c_2^{\mathrm{u}} u_2 - c_3^{\mathrm{d}}(d_{23})(v_1 + v_{21} + v_{32})^2 + c_2^{\mathrm{d}}(d_{12}) v_2^2 - c_3^{\mathrm{r}} + c_2^{\mathrm{r}} \end{bmatrix}, \tag{5.11}$$

where $x = [v_1 \ d_{12} \ v_{21} \ d_{23} \ v_{32}]^T$ and we have used $v_j = v_1 + \sum_{i=1}^{j-1} v_{i+1,i}$, for $j > 1$, in the expression for the third and last state. The costates satisfy $\dot{p} = -\frac{\partial H^*}{\partial x}$ with the Hamiltonian function

$$\begin{aligned} H^*(x, p) := & \max_{(u_2, u_3) \in \mathcal{E}} \min_{u_1 \in \mathcal{D}} p^T f(x, u_1, u_2, u_3) \\ = & -(p_3 - p_1)c_1^{\mathrm{u}} u_1^* + (p_3 - p_5)c_2^{\mathrm{u}} u_2^* + p_5 c_3^{\mathrm{u}} u_3^* - p_2 v_{\mathrm{r}_{12}} - p_4 v_{\mathrm{r}_{23}} \\ & - p_1(c_1^{\mathrm{w}} v_1^2 + c_1^{\mathrm{r}}) - p_3(c_2^{\mathrm{d}}(d) v_2^2 - c_1^{\mathrm{d}}(v_1 + v_{\mathrm{r}_{12}})^2 + c_2^{\mathrm{r}} - c_1^{\mathrm{r}}) \\ & - p_5(c_3^{\mathrm{d}}(d_{23})(v_1 + v_{\mathrm{r}_{12}} + v_{\mathrm{r}_{23}})^2 - c_2^{\mathrm{d}}(d_{12}) v_2^2 + c_3^{\mathrm{r}} - c_2^{\mathrm{r}}), \end{aligned} \tag{5.12}$$

where $\mathcal{E} = \mathcal{E}_2 \times \mathcal{E}_3$ is the compact set of controller actions for the two follower vehicles. The optimal strategies are given by

$$
\begin{aligned}
u_1^* =& \frac{\hat{F}_1^{\mathrm{e}} - \hat{F}_1^b}{2} + \operatorname{sgn}(p_3 - p_1)\frac{\hat{F}_1^{\mathrm{e}} + \hat{F}_1^b}{2}, \\
u_2^* =& \frac{\hat{F}_2^{\mathrm{e}} - \hat{F}_2^b}{2} + \operatorname{sgn}(p_3 - p_5)\frac{\hat{F}_2^{\mathrm{e}} + \hat{F}_2^b}{2}, \\
u_3^* =& \frac{\hat{F}_3^{\mathrm{e}} - \hat{F}_3^b}{2} + \operatorname{sgn}(p_5)\frac{\hat{F}_3^{\mathrm{e}} + \hat{F}_3^b}{2}.
\end{aligned} \tag{5.13}
$$

Thus, for a three-vehicle platoon the complexity of the pursuit-evasion solution increases. Note that the solution has a physical interpretation. For example, both p_3 and p_5 appear in the optimal controller for the second vehicle, as shown in (5.13). Hence, the middle vehicle must consider its safety strategy both with respect to its preceding and following vehicle to avoid a collision with either HDV.

In general, for an N-vehicle platoon the state is given by

$$x = [v_1 \quad d_{12} \quad v_{21} \quad d_{23} \quad \dots \quad v_{N,N-1}]^T$$

and its system dynamics corresponding to (5.12) is readily derived. Note that the controls u_1 and $(u_2, \dots, u_N)$ enter linearly. Hence, the optimal inputs to the Hamiltonian function, $H^*(x, p)$, can again be given analytically, as

$$
u_i^* = \begin{cases} \hat{F}_i^{\mathrm{e}} & \text{if} \quad p^T D_i > 0, \ i = 1, \dots, N \\ \hat{F}_i^{\mathrm{b}} & \text{otherwise,} \end{cases} \tag{5.14}
$$

where $D \in \mathbb{R}^{2N-1 \times N}$ is a matrix, with column vectors D_i in the ith column, containing 1 or -1 in the appropriate elements, e.g., $D_2 = [0 \ 0 \ 1 \ 0 \ -1]^T$ for the second vehicle in the three-vehicle platoon. The unsafe set $\mathcal{U}(\tau)$ is a $2N-1$ dimensional vector space. Even though analytical expressions for the N-vehicle optimal strategies can be found through the given framework, the computational cost for solving the partial differential equation to derive the safe sets grows exponentially with the state dimension. An added HDV to the platoon corresponds to the addition of two new states. Thus, it is extremely computationally expensive for online applications and in general hard to find accurate numerical solutions for the N-vehicle problem when N is large.

5.2.4 Numerical Evaluations

To compute the unsafe set from the solution of (5.6), the level sets methods toolbox of Mitchell (2007) is utilized. In this section, the scenarios are calculated; first we consider a simple setup with two identical platooning HDV's and then we study mass heterogeneity and uncertainties in braking capacity.

Identical HDVs

The collision avoidance scenario is first investigated for two identical HDVs. The vehicles have identical vehicle parameters in (5.1) and the gross mass of each HDV

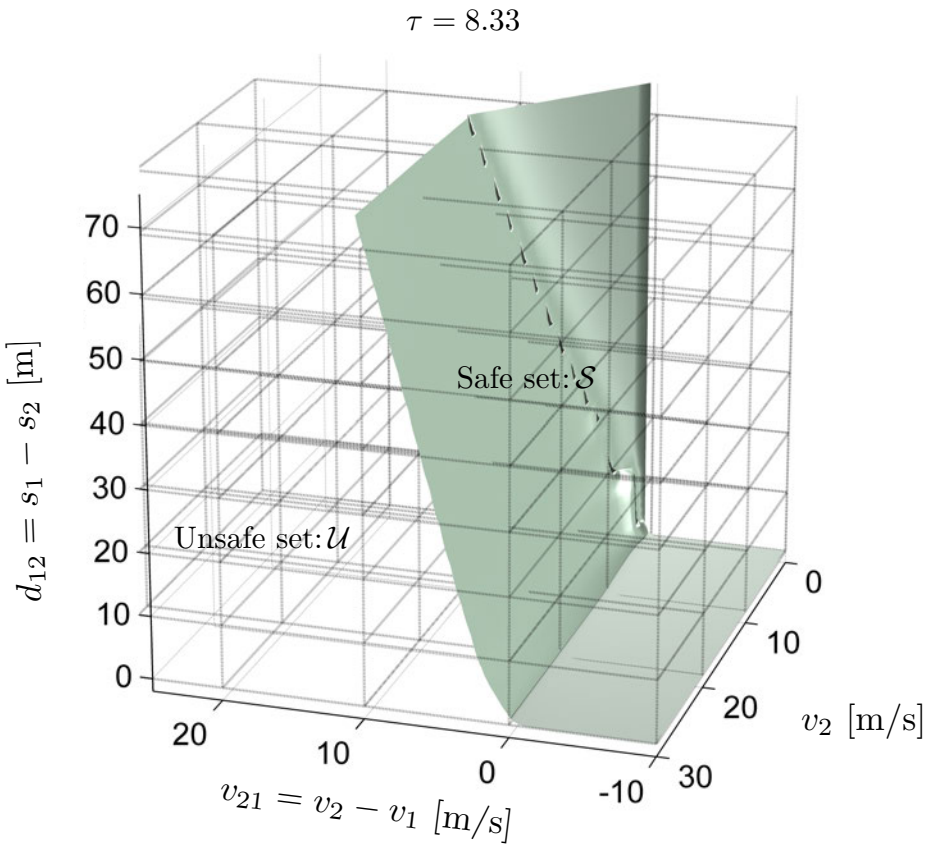

Figure 5.2: The backward reachable set obtained under the assumption that no delay is present in the system.

was chosen to be 40 t, which is the maximum allowed weight for long-haulage HDVs in most European countries. Their braking capacity is set to create a maximum deceleration of $-3\,\mathrm{m/s^2}$, which is considered to be a harsh braking. Commercial HDVs generally have a speed restriction of 90 km/h. The unsafe set is calculated backwards for $\tau \in [0, 8.33\,\mathrm{s}]$, where the upper bound is the time needed for the follower HDV to come to a full stop under the maximum deceleration constraint.

Figure 5.2 shows the boundary $\partial\mathcal{U}(\tau)$ of the unsafe set contained between the plotted level surface and $\mathcal{U}_0$. The safe set $\mathcal{S} = \mathbb{R}^3 \backslash \mathcal{U}$ is indicated as well. As $v_{21} = v_2 - v_1$ increases, the relative distance $d_{12} = s_1 - s_2$ must also increase. The fold in the boundary surface area is due to the physical constraint $v_1 \geq 0$. Any trajectory heading behind that surface area would imply that the lead vehicle has reversed to create a collision. If the follower vehicle is within the safe set, it will always be able to avoid a collision regardless of the best effort of the lead vehicle (pursuer) with respect to a compact set of controller actions. Thus, the least

restrictive controller could be implemented outside the unsafe set without increasing the risk of a collision. However, if the states are within the unsafe set a collision might occur given that the lead vehicle acts in the worst possible manner.

In platooning applications, the vehicles generally travel in what we here refer to as a *normal-mode*, where each vehicle is traveling at a constant velocity, $v_{21} = 0$, and a desired relative distance is set by the driver. Figure 5.2 reveals that a collision can be avoided for two identical HDVs if the lead vehicle is traveling at a higher velocity than the follower vehicle. However, if the vehicles are operating in normal-mode and has a relative distance $d_{12} \leq \psi$, where $\psi = \partial \mathcal{U}(\tau)|_{v,v_{21}=0}$, a collision could occur. The lead vehicle experiences a greater air drag and is therefore able to obtain a slightly higher braking force. Thus, if the vehicles are both traveling at a velocity $v \leq 2.5\,\mathrm{m/s}$, a collision could occur for $\psi = 0.2\,\mathrm{m}$. As both vehicles' velocities increase, the air drag and inherently the obtainable brake force becomes higher for the lead vehicle compared to the follower. Thus, a larger relative distance of $d_{12} > \psi = 1.1\,\mathrm{m}$ must be maintained at $v = 25\,\mathrm{m/s}$ to stay out of the unsafe region. Hence, the minimum relative distance that can be obtained for two identical vehicles depends on their initial velocity. Assuming that no delay is present in the system and the vehicles are traveling in normal-mode, the vehicles could maintain a relative distance of 1.2 m without compromising safety.

System Uncertainties and Vehicle Parameters

System uncertainties or varying vehicle parameters, such as mass, could cause a difference in braking capabilities between the vehicles. Having different braking capacity changes the shape of the safe sets. If the follower vehicle has a higher braking capacity, the level surface derived for neighboring vehicles with identical braking capacity will shift in the positive v_{21}-direction and the slope of the surface will decrease, as shown in Figure 5.3. This means that the follower vehicle will be able to lie closer without increasing the risk of a collision. The minimum safe relative distance is therefore shorter compared to the case of two identical vehicles.

However, if the lead vehicle has a greater braking capability a perturbation arises in the level surface at $v_{21} \approx 0$ and the slope becomes steeper. In this case a minimum distance of $d_{12} = 13\,\mathrm{m}$ must be maintained to remain outside the reachable set at normal-mode. Thus, the relative distance must be increased significantly if the lead vehicle has a stronger braking capability.

Delays for the platoon control system commonly occur due to detection, transmission, computation, and calculating the control command. A delay in the system implies that the lead vehicle will be able to act, change the relative velocity and distance, before the follower vehicle is able to react. A delay can be translated into a shift of the reachable set in Figure 5.2 by Δd_{12} units in the positive direction along the d_{12}-axis and by Δv_{21} units in the negative direction along the v_{21}-axis. However, no change occurs in the follower vehicle's velocity v_2, since it cannot react during the delay. Depending on the radar and the collision detection algorithm, a worst-case delay is approximately 500 ms for the considered vehicles. Hence, the

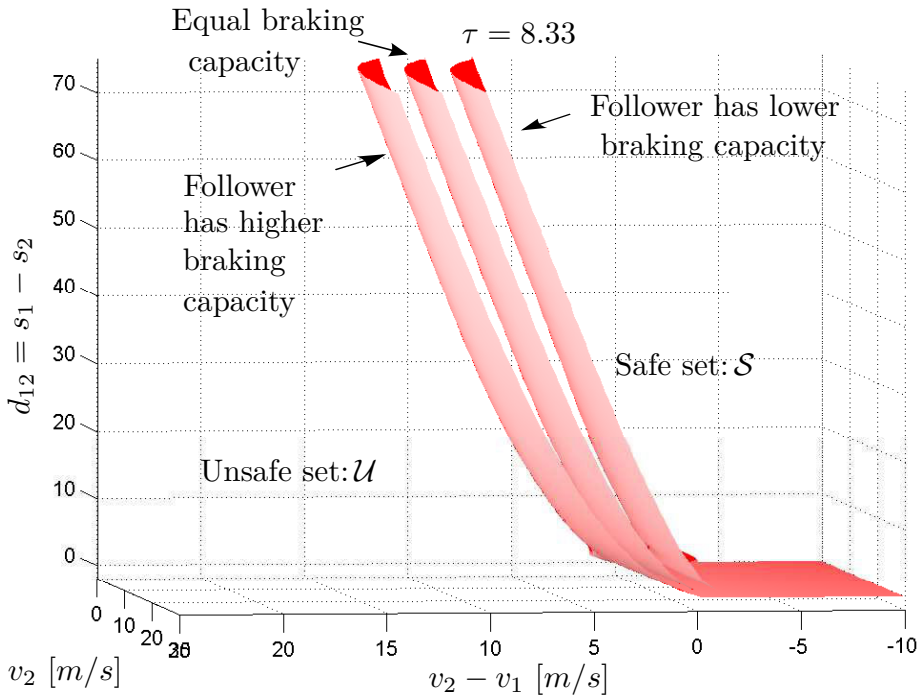

Figure 5.3: The case when both vehicles have are identical is given by the level surface in the center. If the braking capacity for the follower vehicle increased by 20 %, the nominal level surface shifts in the positive v_{21}-direction (to the left) and the slope of the surface has decreased. Similarly, if the follower vehicle has a 20 % higher braking capacity, the surface shifts in the negative v_{21}-direction (to the right) and the slope increases.

lead vehicle will be able to reduce the relative velocity by 3.25 m/s and the relative distance by 0.8 m if it is driving 25 m/s at normal-mode. Thus if the follower vehicle maintains $d_{12} \geq 2$ m, a collision can always be avoided for two identical vehicles according to the safe set in Figure 5.2.

Model Verification

To preliminary investigate the validity of the derived safety regions in Figure 5.2 as a precautionary measure, a simulation study is conducted in this section for a number of scenarios.

Two identical vehicles were simulated in the simulation model presented in Section 3.2, consisting of 3313 variables, 1058 equations, and 626 states for each vehicle. The model is verified to mimic real life behavior (Sandberg, 2001). Hence, two different simulation scenarios are presented in Figure 5.4. The velocity trajectory for the lead vehicle is displayed in the top plot and the velocity trajectory for the follower vehicle is displayed in the middle plot. The bottom plot shows the relative distance between the vehicles.

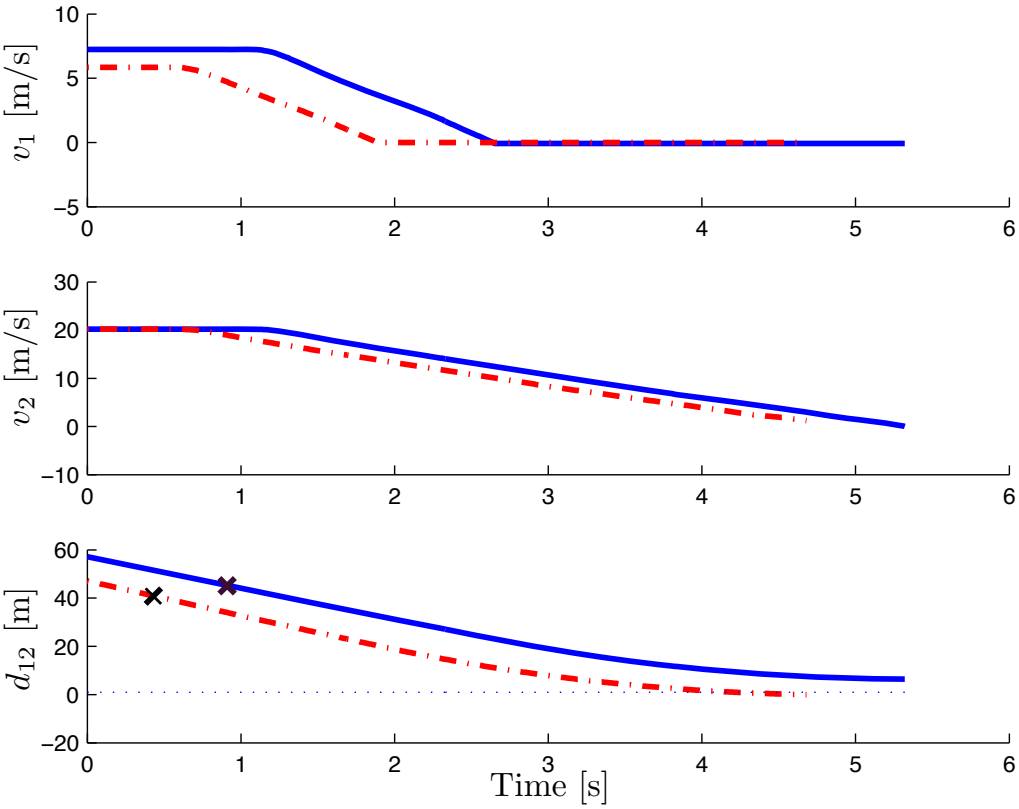

Figure 5.4: Simulated emergency brake scenario. Solid line illustrates the scenario with initial conditions selected on the level surface for two identical vehicles and the dashed line illustrates initial conditions behind the level surface. The ×:s in the bottom plot indicates the point where both vehicles initiates their optimal control inputs.

The first scenario was chosen as a point on the level surface in Figure 5.2. It can be described as an HDV traveling on a highway and another HDV appears in front, e.g. from a shoulder at a lower velocity. Upon entering, the vehicles suddenly brake due to an incident ahead on the road. The follower vehicle has a velocity of $v_2 = 20.23\,\mathrm{m/s}$ and approaches the lead vehicle entering with a $v_{21} = 13\,\mathrm{m/s}$ lower velocity. When a relative distance of $d_{12}(t_0) = 45.14\,\mathrm{m}$ is reached, both vehicles implement their optimal control input, derived in (5.10), at time $t_0 = 0.9\,\mathrm{s}$. We can see that a collision is avoided since both vehicles have come to rest at time $t_f = 5.3\,\mathrm{s}$ with a relative distance of $d_{12}(t_f) = 5.32\,\mathrm{m}$. Hence, collision could be avoided for a higher relative velocity or a lower relative distance, which is a point below the level surface. This is due to the problem formulation, which produces a preferred conservative level surface in safety applications.

In the second scenario a point below the level surface in Figure 5.2 was chosen by lowering the relative distance and increasing the relative velocity by 9.7 %. The follower vehicle has a velocity of $v_2 = 20.23\,\mathrm{m/s}$ and approaches the lead vehicle

Table 5.1: Table of several initial conditions for collision scenarios.

Simulation no.:	$v_{21}(t_0)$	$d_{12}(t_0)$	$v_2(t_0)$	$d_{12}(t_f)$
1)	18.3	71.9	25.1	10.9
2)	11.7	45.7	20.2	10.3
3)	3.6	13.7	10.4	6.7
4)	0.24	1.14	10.4	0.3
5)	0.2	1.14	15.3	0.5
6)	0.5	2.3	25.1	0.05

with a $v_{21} = 14.3\,\mathrm{m/s}$ higher velocity. Both vehicles intiate an emergency braking action, at time $t_0 = 0.5\,\mathrm{s}$, with a relative distance of $d_{12}(t_0) = 40.76\,\mathrm{m}$. The lead vehicle has come to a rest at time $t_f = 4\,\mathrm{s}$, while $v_2(t_f) > 0$ in Figure 5.4 and the relative distance is $d_{12}(t_f) = 0\,\mathrm{m}$. Hence, a collision has occurred.

Several scenarios were investigated for different points on the level surface in Figure 5.2 and within the reachable set. The results are summarized in Table 5.1, where the initial conditions for each collision scenario is given in the middle columns and the final relative distance is given in the fourth column.

As can be deduced from Table 5.1 and Figure 5.4, the safe set ensures that collision is avoided. The level surface is more accurate for simulations no.4-6, where the HDVs are operating close to normal-mode. Both the HDVs have come to a total halt at $d_{12} \leq 0.3\,\mathrm{m}$. For the scenarios when the relative velocities differ more, simulations no. 1-3, the vehicles come to rest at a larger relative distance. A collision occurs if the initial conditions for (d_{12}, v_{21}) are shifted 11 % below the level surface. Thus, a larger overapproximation is observed in these cases, which is due to the increased model uncertainty at lower velocities. Hence, even though (5.1) is a fairly simple model of an HDV, it seems to be a sufficient for this application.

5.3 Cooperative Braking Experiments

In this section, we first present the experimental setup for the two-vehicle platoon. To obtain reproducible results, the experiment procedure was automated. We present different braking scenarios that arise based on predefined reference speeds and relative distances. Several experiment results are presented subsequently to evaluate the derived safe sets.

5.3.1 Experimental Setup

Two standard Scania HDVs are utilized with additional control and communication hardware. Both HDVs have a 6×3 vehicle configuration and the masses were measured to be 25 t for the lead vehicle and 23.6 t for the follower vehicle. They

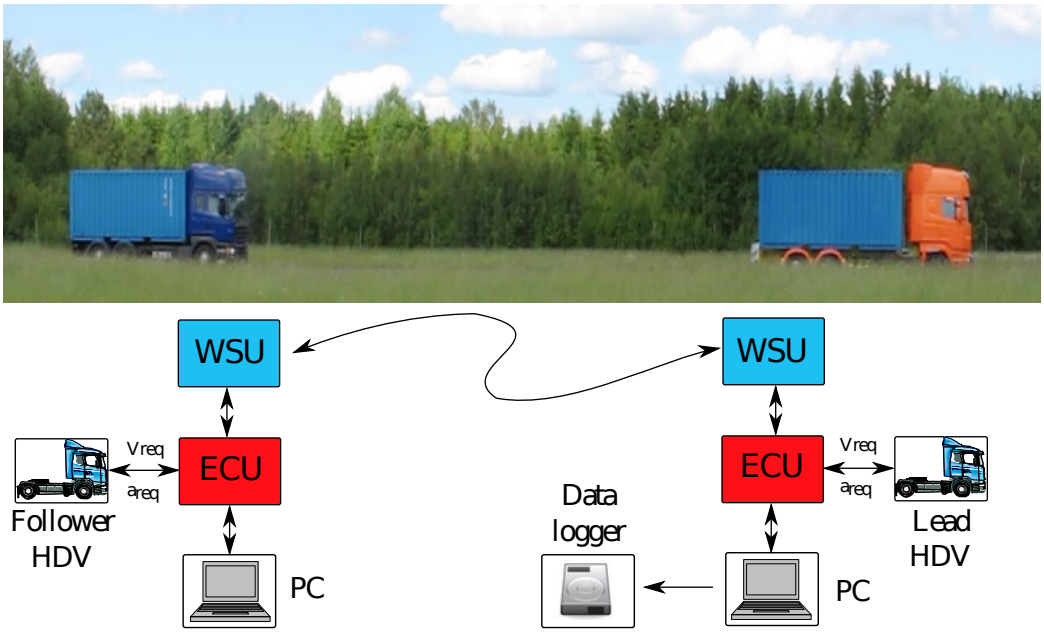

Figure 5.5: A schematic overlay of the experimental hardware setup. The top picture shows the HDVs utilized in this experiment. The HDV to the right is the lead and the left is the follower. The WSU, ECU, and PC communicate through CAN. As soon as new information is obtained through the ECU or the vehicle, it is broadcasted through the WSU.

are equipped with standard radars, which sends the relative distance with a 40 ms interval to the central coordinator electronic control unit (ECU) and is gated every 100 ms. An external supplier provides the radar with an internal filter of undisclosed characteristics. Both vehicles are equipped with a fully-automatic gearboxes. Standard ECUs, utilized in Scania HDVs, are modified to add the automated optimal control logic. As illustrated in Figure 5.5, a wireless sensor unit (WSU) carrying the standard wireless communication protocol IEEE 802.11p is mounted in each vehicle. The WSU is directly connected to the HDVs internal CAN system and messages are broadcast on demand. Thereby, the internal CAN signals, such as velocity, acceleration, and control inputs, are available to both vehicles. The data are logged in the lead vehicle.

To evaluate the safe sets the vehicles' cruise controller and internal brake request functionality are utilized. The safe set is divided into three regions, which results in three different scenarios to be evaluated. The first scenario is when the vehicles operate at normal-mode, with $v_{21} \approx 0$. The second experiment scenario evaluates the level surface for when the follower vehicle has a higher initial velocity, $v_{21} \geq 0$, and the control action is implemented. The final scenario encompasses the cases when a lead vehicle would increase its velocity until $v_{21} \leq 0$ and then suddenly initiate emergency braking. An automated procedure is used to guide the vehicles to

the desired initial conditions $(v_{21}(t_0), v_2(t_0), d_{12}(t_0))$ given by the level surface for each experiment. The experiments are conducted at several different initial velocities and data are logged for evaluation.

The control action, with a maximum reference deceleration of $-3\,\mathrm{m/s^2}$ is implemented at an relative distance of more than 30 m due to safety precautions. The brake system is calibrated as an attempt to eliminate any braking discrepancies in the vehicles. Finally, to reduce delays that can occur in the system, all control signals are first sent to the WSU. The WSU then transmits the signal while echoing the same information back through the internal CAN system. Thereby, both vehicles will be able to initiate their control actions nearly simultaneously.

5.3.2 Braking Scenarios

The results from a single run of experiments conducted for each of the three different scenarios are given in Figure 5.6. The top plots show the velocity trajectories v_1 and v_2 for the lead vehicle and for the follower vehicle, respectively. The inter-vehicle spacing d_{12}, during the experiments are shown in the middle plot and the acceleration for each vehicle is shown in the bottom two plots, where a_1 and a_2 denote the acceleration for the lead vehicle and for the follower vehicle, respectively. The solid lines show normal-mode scenario when the vehicles are traveling with the same velocity. The dashed lines show the results for the scenario when the follower vehicle has a lower initial velocity and the dotted lines show the results for the scenario when the follower vehicle has a higher initial velocity. In the normal-mode scenario, the vehicles accelerate to a given reference speed and then maintain the achieved velocity. The lead vehicle initially maintains a 5 km/h lower speed compared to the follower vehicle, as shown in the top plot. As the follower vehicle approaches and an relative distance of less than 50 m is reached, the lead vehicle changes its speed to match a relative distance of 30 m$\pm$0.1 m. When it is reached, both vehicles initiate their optimal control inputs with a maximum braking capacity of -3 $\mathrm{m/s^2}$. For this experiment the braking is observed at the 47 s time marker, when both the vehicles have reached 70 km/h. As given by the solid line in the middle plot of Figure 5.6, the relative distance remains nearly unchanged during the implementation of the braking strategies. Having almost identical vehicle configuration, the braking is initiated at an inter-vehicle spacing of 30 m and both vehicles come to rest at approximately 37 m. The bottom two plots show that the lead vehicle obtains a higher deceleration when the braking is initiated. However, follower vehicle obtains a slightly higher average deceleration during the remainder of the braking period and the inter-vehicle spacing is therefore increased. The relative distance changes more dramatically when the follower vehicle has a higher initial velocity. This is displayed by the dotted lines, which is the scenario when the follower vehicle approaches with a higher velocity of 60 km/h and the lead vehicle is traveling at 20 km/h. The collision test is in this case initiated at the 57 s time marker, where the initial relative distance is 65 m and both vehicles come to full stop at 23 m. If the lead vehicle starts to accelerate and reaches a higher relative speed when initiating an emergency brake, the inter-vehicle

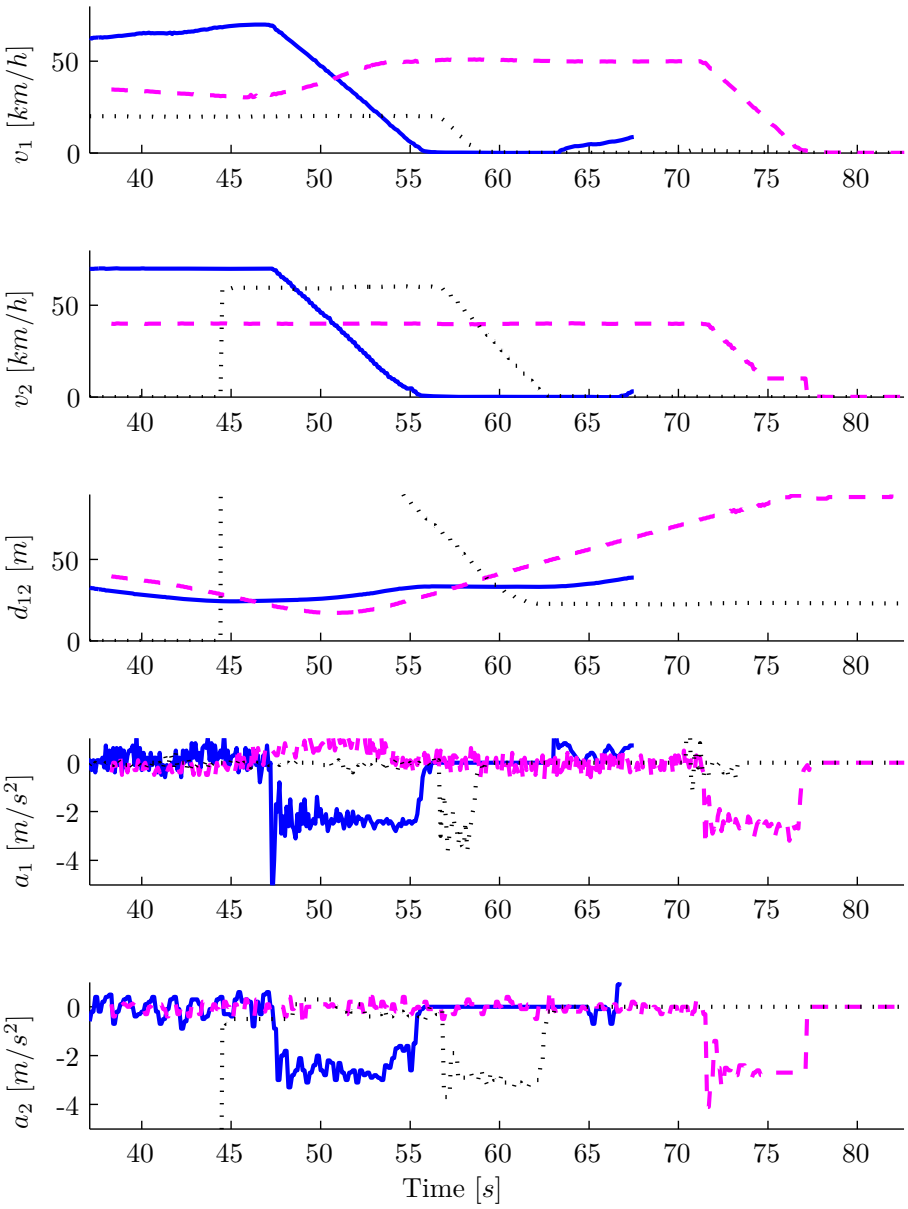

Figure 5.6: Experiment results for three different braking scenarios. The top plot shows the velocity trajectories, v_1, for the lead vehicle and the second to top plot shows the velocity trajectories, v_2, for the follower vehicle. The corresponding relative distance trajectories are shown in the middle plot. The bottom two plots show the acceleration a_1 and a_2 for the lead vehicle and for the follower vehicle, respectively. Solid line shows the results for an experiment conducted when the vehicles are traveling at the same initial velocity. Results for when the follower vehicle approaches the lead vehicle with a higher velocity are given by the dotted lines. Experimental results for when the lead vehicle initiates an acceleration and then emergency brakes are given by the dashed lines.

spacing with similar braking capacity seems to increase. This is given by the dashed trajectories in Figure 5.6. Here, the collision test is initiated around the 71 s time marker. The action is initiated when the vehicles has an inter-vehicle spacing of 76 m and come to a full stop at 87 m.

It should be noted that as the vehicles decelerate, their gearboxes automatically changes to lower gears. At lower speed, the difference in gearbox has a stronger effect. Hence, the dynamic behavior of the vehicles are different during deceleration at lower velocities. Furthermore, the bottom two plots in Figure 5.6 show a variation in the deceleration trajectories for the HDVs. Braking is carried out by executing a precomputed pressure to the brake disks in relation to the requested deceleration. The braking dynamics is nonlinear and changes with time.

Several collision experiments were conducted at various reference velocities to evaluate various points in the safe set, as illustrated by the trajectories in Figure 5.7. The $\times$ denotes the starting point for each trajectory and each trajectory ends when both vehicles have come to a full rest, with $v_2 = v_{21} = 0$. The control action in the experiments was implemented at an relative distance of more than 30 m due to safety precautions. However, the initial points of all the trajectories have been shifted to the minimum safe relative distance given by the safe set, based on the relative velocity and follower vehicle velocity at initial time of implementing the optimal control inputs. A delay of 200–300 ms has occasionally occurred and hence the minimum safety distance have been adjusted accordingly. Figure 5.7 shows the empirically obtained deceleration trajectories in comparison with the safe set for vehicles with identical braking power. None of the trajectories starting with $v_{21} \leq 0$ intersect the level surface for any initial v_2. However, some of the trajectories for starting points at $v_{21} \geq 0$ intersects the level surface and then comes back out again. This is due to the varying deceleration that occurs because of the nonlinearities in the braking system, which was seen in the bottom two plots of Figure 5.6. The trajectories would not intersect a safe set derived for a maximum braking capability of $\frac{\hat{F}^b}{m_t} = 4.8\,\mathrm{m/s^2}$, which is the deceleration that the lead vehicle initially obtained in the cases when the surface is breached. The braking capabilities were noted to vary significantly during some of the braking scenarios. This is not captured by the level set surface that divides the safe and unsafe sets. The vehicle control action momentarily exceeds the upper boundary of the assumed available control action. However, since the safe set is conservative, the vehicles come to full rest without causing a collision.

5.3.3 Safe Set Evaluation

Owing to the fact that the braking capability can change during an emergency braking, several experiments were conducted with varying braking capability for both vehicles. These experiments were focused on normal-mode platooning since it is the most common mode of operation. Figure 5.8 shows a two-dimensional projection of the deceleration trajectories, omitting the minor variation in relative velocity during the optimal control implementation. The top plot shows the collision

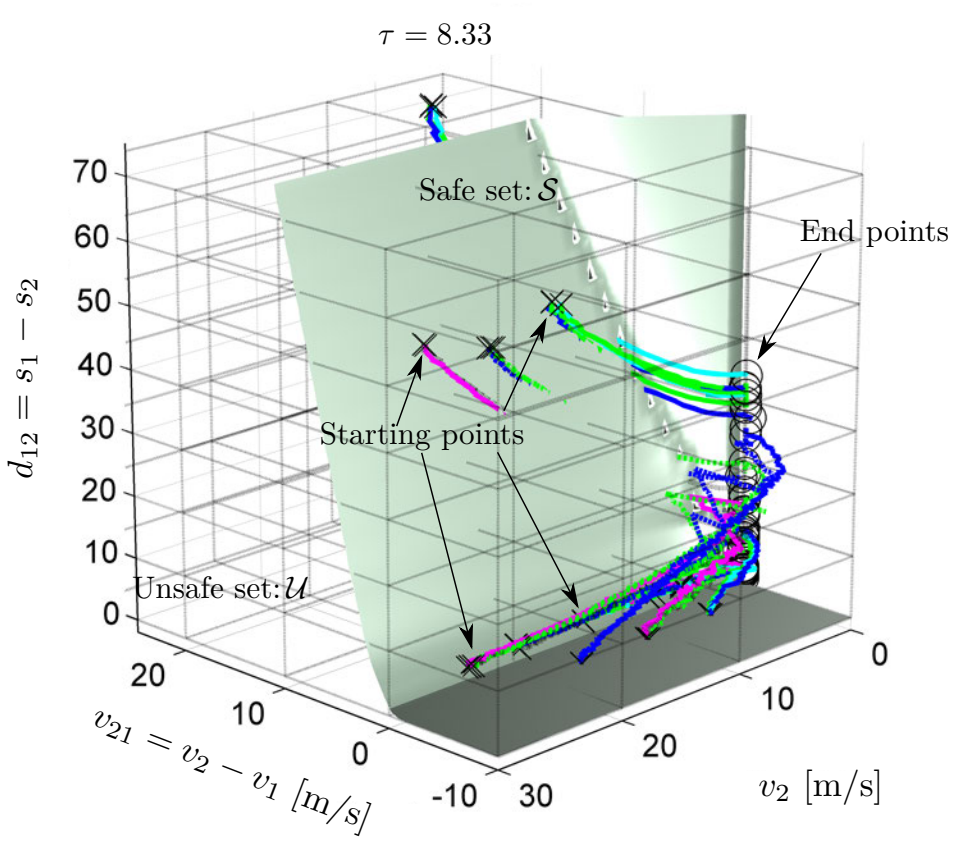

Figure 5.7: Three-dimensional plot of the empirical deceleration trajectories for varying initial velocities. The $\times$ denotes the starting point for each trajectory and $\circ$ the end points (at $v_1 = v_2 = 0$). Each color indicates an experiment obtained for a given initial vehicle velocity at time of emergency braking. The starting point of the trajectories is shifted to the minimum safe relative distance in the safe set based on the relative velocity and current follower vehicle velocity at the time of initiating the optimal control input.

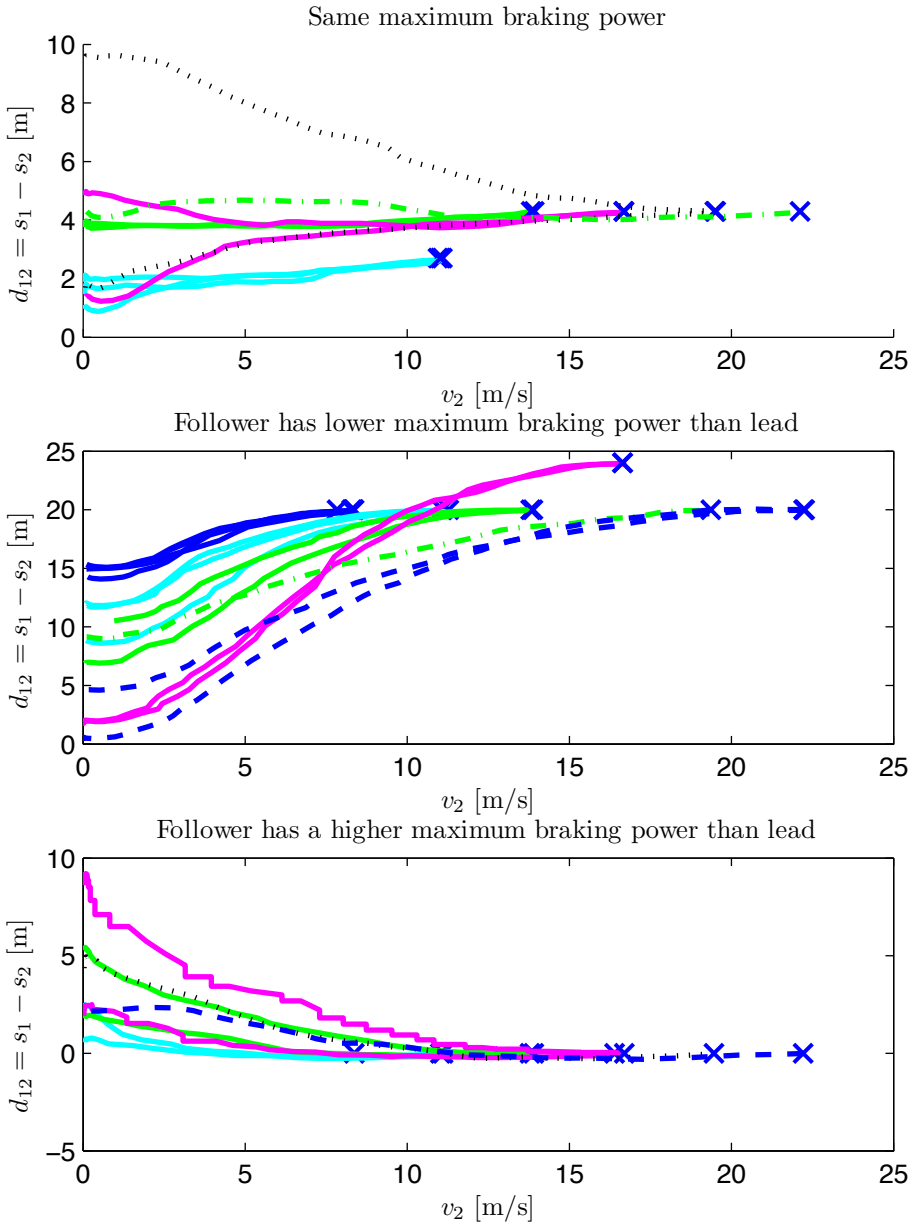

Figure 5.8: Two-dimensional plot of the empirical braking trajectories for varying initial velocities, where the $\times$ denotes the starting point for each trajectory. The trajectories are presented in the (d_{12}, v_2)-plane, omitting the slight variation in the relative velocity. Each color indicates a set of experiments obtained for a given initial follower vehicle velocity at time of emergency braking. The starting point of the trajectories is shifted to the minimum safe relative distance in the safe set with respect to initial relative velocity and current follower vehicle velocity.

tests for varying initial velocities and similar vehicle braking capacity. It can be seen that the relative distance remains fairly constant throughout the collision tests. However, below a velocity of 5 m/s the vehicles starts changing gears, which has a clear impact on the vehicle dynamics. The model for deriving the safe sets does not take gear change logic into consideration. Nevertheless, the safe sets are conservative and a collision is hence still avoided. The middle plot, in Figure 5.8, shows the deceleration trajectories for when the follower vehicle has a 30–40 % lower braking capacity. It can be seen that the relative distance is constantly decreasing. Most of the trajectories end with both vehicles at rest and still a few meters to spare. Finally, the bottom plot shows the deceleration trajectories for when the follower vehicle has a 20–30 % higher braking capacity. It can be seen that the relative distance remains the same or increases, which is congruent with the results obtained from the corresponding safe set. Hence, if the follower vehicle has a higher braking capacity, a relative distance within decimeters could have been maintained with the presented system and still no collision would have occurred.

5.4 Summary

It is fuel efficient to drive vehicles closely spaced to each other due to the inherent air drag reduction, as was shown in Chapter 4. A minimum distance for two HDVs can be deduced with respect to a compact set of controller actions without increasing the the risk of a collision despite the worst possible action by the vehicle ahead. Thus, if the minimum distance is determined for each vehicle pair, a collision can be avoided throughout the platoon. During normal-mode operation a minimum distance of 1.2 m should be maintained to ensure that a collision can be avoided for two identical vehicles when no delay is present in the system. Delays can be accounted for in the reachable set formulation through a simple translation. The derived minimum possible relative distance with a measured worst-case delay of 500 ms in this chapter for identical vehicles is 2 m, which is lower compared to what is utilized in commercial applications today.

A stronger overall braking capability in the follower vehicle creates the possibility of reducing the relative distance further. Thus, in platooning applications, the results suggest that HDVs with stronger braking capabilities should always be placed behind to enable the shortest possible relative distance without compromising safety. However, this might be contrary to fuel-efficient control criteria, where the follower HDV should have less stringent control actions.

Even though the model and the procedure utilized for deriving the safe sets do not encompass all nonlinear features of an HDV in motion, the sets serve as a reliable reference to ensure that a collision can be avoided. Both theoretical and empirical results show that it is suitable to order HDVs according to increasing braking capacity. Thereby, the inter-vehicle spacing can be reduced significantly without compromising safety. Naturally, it only holds under the assumption that the relative distance and velocity is available through reliable V2V communication

or that radar measurements are obtainable.

The experimental results presented in this chapter indicates that the derived safety sets are least conservative for platoons traveling under normal operational mode. The presented method forms a conservative safety set. Therefore, uncertainties from unmodeled dynamics do not cause a collision, as was seen in the experimental results. Hence, V2V communication enables HDVs to operate at very small inter-vehicle spacing.

Chapter 6

Decentralized Cooperative Control for Platooning

"*It is the weight, not numbers of experiments that is to be regarded.*"
Isaac Newton

The objective in heavy-duty vehicle (HDV) platooning is to maintain a predefined inter-vehicle spacing policy to the surrounding vehicles. With the aid of vehicle-to-vehicle (V2V) communication, vehicle characteristics and events, such as emergency braking, can be transmitted within radio range. Therefore, a minimum distance, far less than what is utilized in todays commercial systems, between two HDVs can be calculated with respect to a compact set of controller actions without increasing the risk of a collision despite the worst possible scenario displayed by the vehicle ahead. By traveling at a short relative distance to an HDV, the air drag is reduced substantially. Thus, a significant reduction in fuel consumption can be obtained. The effort needed to maintain the desired relative velocity varies with the relative distance. This creates a coupling of the dynamics between vehicles throughout the platoon. However, the control becomes increasingly stringent with shorter relative distance. Thereby, the fuel consumption increases due to the additional control effort, produced by the existing control systems, for maintaining the relative distance. Hence, it is of considerable interest for the industry to produce a new fuel-optimal control. The question of whether to implement a centralized, decentralized, or some combination of the control strategies then naturally arises.

The main motivation for considering a decentralized controller is the limited communication range that can be achieved in practice. It is difficult to realize a centralized controller under such constraints. Using a centralized controller is only possible if all the global states and system parameters are known to every vehicle in the platoon. In that case, a central unit, for example a vehicle in the platoon or a road side unit, determines the control actions for all the vehicles in the platoon. Therefore, a centralized control scheme requires an increase in communication with the number

of vehicles in the platoon. Furthermore, package drops or outages can occur in wireless transmission. A centralized system is more sensitive to communication delays and physical limitations on the radio range. It is often not realistic to assume that every vehicle in the platoon knows the state of every other vehicle instantaneously due to physical constraints in the information flow. It is, however, reasonable to assume that a vehicle is able to communicate with some vehicles within a given range. Hence, a decentralized strategy is suitable, where every vehicle determines its own control actions based on local information. Furthermore, a decentralized longitudinal control is practical to ensure scalability and robustness. However, other control applications, such as route assigning, coordinating, ordering and merging several platoons, are not time and information critical operations and thus suitable as centralized control strategies.

The main contribution of this chapter is to derive a decentralized controller for HDV platooning. We establish empirical performance results for the presented control design and present a qualitative verification of the transient dynamics in the simulation model that is presented in Section 3.2. We present a linear quadratic control framework for the design of a high-level cooperative platooning controller suitable for modern HDVs, which imposes a lower block-diagonal structure on the feedback gain matrix. We also consider realistic response delays for the low-level controller that governs the engine. The controller performance is evaluated through numerical and experimental studies. It is shown that the proposed controller allows for short time headways to achieve fuel efficiency, without compromising safety.

Several studies on vehicle platooning have been based on simplified theoretical models. However, as shown in this chapter, delays and nonlinear dynamics can significantly influence the closed-loop system. We present a method for designing suboptimal decentralized feedback controllers, with low computational complexity, that takes dynamic coupling and engine response delays into consideration. The controller performance is evaluated through implementation on commercial HDVs. The design method is scalable in the sense that an additional vehicle can be added at the tail of the platoon without mandating a change in the controllers of the already platooning vehicles. As modern HDVs in general have two separate low-level control systems for governing the longitudinal propulsion and deceleration of the vehicle, the engine management system (EMS) and the brake management system (BMS), we present a simple bumpless transfer scheme to switch between these systems. The proposed platooning controller can be easily implemented on modern HDVs without requiring any changes in the already existing vehicle architecture. We show that the controller behaves well even when performing outside the linear region of operation. We also show that the proposed controller attenuates the effect of disturbances downstream in the platoon, when studying scenarios that commonly occur on highways with dynamic operating conditions and physical constraints. Experimental results are given to qualitatively validate the proposed control system behavior. The experiments have been conducted on a test site south of Stockholm, using HDVs provided by Scania CV AB.

The outline of this chapter is as follows. We start by giving a short summary of

the system model in Section 6.1 and present a translation of the platoon performance criteria into quadratic costs. In Section 6.2 we develop a method for deriving the proposed decentralized controllers and then give a simple bumpless transfer scheme, based on performance and driver acceptance, for switching between the low-level EMS and BMS controllers. We also provide guidelines for how to set the weight parameters for the proposed controller. Simulation results are given in Section 6.3 to determine and evaluate the chosen weight parameters for the controller. The experimental setup based on three HDVs is presented in Section 6.4 together with the experimental results. The chapter is concluded with a brief summary in Section 6.5.

6.1 System Model

In this section, we present the models that serve as the basis for the controller design presented in Section 6.2. First a brief description of the longitudinal model of a vehicle traveling in a platoon is given. The longitudinal model is then extended to describe the dynamics of an HDV platoon. Then, we present a simple model for the vehicle engine system dynamics. Finally, we form the platoon model by combining and discretizing all the presented models. Recall that details of the vehicle model, the characteristic coefficients, and its derivation can be found in Chapter 3.

Let $i = 1, \dots, N$ denote the vehicle order in the platoon. Applying Newton's second law of motion along with all the external forces described above, a nonlinear vehicle model is derived as

$$\begin{aligned}
\dot{s}_1 &= v_1 \\
m_{\mathrm{t}_1}\dot{v}_1 &= F_1^{\mathrm{e}} - F_1^{\mathrm{b}} - F_1^{\mathrm{a}}(v_1) - F_1^{\mathrm{r}}(\alpha(s_1)) - F_1^{\mathrm{g}}(\alpha(s_1)) \\
&= k_1^{\mathrm{e}} T_1^{\mathrm{e}}(\omega_{\mathrm{e}_1}, \delta_1) - F_1^{\mathrm{b}} - k_1^{\mathrm{d}} v_1^2 - k_1^{\mathrm{r}} \cos\alpha(s_1) - k_1^{\mathrm{g}} \sin\alpha(s_1) \\
\dot{s}_i &= v_i \\
m_{\mathrm{t}_i}\dot{v}_i &= F_i^{\mathrm{e}} - F_i^{\mathrm{b}} - F_i^{\mathrm{a}}(v_i, d_{i-1,i}) - F_i^{\mathrm{r}}(\alpha(s_i)) - F_i^{\mathrm{g}}(\alpha(s_i)) \\
&= k_i^{\mathrm{e}} T_i^{\mathrm{e}}(\omega_i, \delta_i) - F_i^{\mathrm{b}} - k_i^{\mathrm{d}} \Phi(d_{i-1,i}) v_i^2 - k_i^{\mathrm{r}} \cos\alpha(s_i) - k_i^{\mathrm{g}} \sin\alpha(s_i)
\end{aligned} \tag{6.1}$$

where $i = 2, \dots, N$, s_i is the absolute traveled distance for HDV i from a reference point common to all vehicles in the platoon, $d_{i-1,i} = s_{i-1} - s_i$ is introduced as the relative distance between ith vehicle its preceding vehicle for convenience, v_i is the velocity, m_{t_i} is the total inertial mass, $F_i^{\mathrm{e}} \geq 0$ denotes the force produced by the engine through fuel injection, $F_i^{\mathrm{b}} \geq 0$ denotes the braking force, and k_i^l, $l \in \{\mathrm{e}, \mathrm{d}, \mathrm{r}, \mathrm{g}\}$, are characteristic coefficients. Moreover, F_i^{a}, F_i^{r}, and F_i^{g} denote the external air drag, rolling resistance, and gravitational forces acting upon the vehicle, respectively, and $\Phi(d_{i-1,i})$ denotes the empirically derived nonlinear air drag reduction due to a preceding vehicle. The control input T_i^{e} is the net engine torque, which is a function of the engine angular velocity ω_{e_i} and the injected fuel amount δ_i. It is determined by the EMS, which receives a velocity request as an input. Furthermore, the control input F_i^{b} is determined through the BMS, which

receives an acceleration demand as an input. The EMS determines the required fuel injection to produce the necessary propulsion torque for achieving the velocity input to the system. Similarly, the BMS determines the required force that needs to be generated to obtain the acceleration input to the system. To account for the additional system dynamics produced by the EMS, for simplicity, its computed control input is modeled as

$$T_{e_i} = K_i^{\mathrm{c}}(e_i + \frac{1}{T_i^{\mathrm{I}}}\int e_i dt), \tag{6.2}$$

where $e_i = v_i^{\mathrm{ref}} - v_i$ and K_i^{c}, T_i^{I} are design parameters that are set according to the engine type. By inserting the model for the EMS into (6.1), the nonlinear system model for a single HDV in a platoon is given as

$$\begin{aligned} m_{t_i}\dot{v}_i =& k_i^{\mathrm{e}}K_i^{\mathrm{c}}\big(e_i + \frac{1}{T_i^{\mathrm{I}}}\int e_i dt\big) - k_i^{\mathrm{d}}\varphi(d_{i-1,i})v_i^2 - k_i^{\mathrm{r}}\cos\alpha_i - k_i^{\mathrm{g}}\sin\alpha_i \\ =& k_i^{\mathrm{e}}K_i^{\mathrm{c}}v_i^{\mathrm{ref}} - k_i^{\mathrm{e}}K_i^{\mathrm{c}}v + z_i^{\mathrm{v}} - k_i^{\mathrm{d}}\varphi(d_{i-1,i})v^2 - k_i^{\mathrm{r}}\cos\alpha_i - k_i^{\mathrm{g}}\sin\alpha_i, \\ \dot{z}_i^{\mathrm{v}} =& \frac{k_i^{\mathrm{e}}K_i^{\mathrm{c}}}{T_i^{\mathrm{I}}}e_i \end{aligned} \tag{6.3}$$

where v_i^{ref} is the control input to the EMS and z_i^{v} is an integral state in the EMS model. The vehicle dynamics with the BMS is significantly faster, since a relatively large deceleration force can be produced by the brake system. Thus, it is assumed that the input to the BMS is obtained instantaneously, hence the nonlinear system model during braking is given as

$$m_{t_i}\dot{v}_i = ma_i^{\mathrm{ref}} - k_i^{\mathrm{d}}\Phi(d_{i-1,i})v_i^2 - k_i^{\mathrm{r}}\cos\alpha_i - k_i^{\mathrm{g}}\sin\alpha_i \tag{6.4}$$

where a_i^{ref} is the input signal to the BMS.

6.1.1 Platoon Model

Here, we develop a model to capture the platoon dynamics. We first introduce the discrete states

$$\begin{aligned} z_i^{\mathrm{v}}(k+1) &= z_i^{\mathrm{v}}(k) + T_s\zeta_i(v_i^{\mathrm{ref}}(k) - v_i(k)), \\ d_{i-1,i}(k+1) &= d_{i-1,i}(k) + T_s(v_{i-1}(k) - v_i(k)), \\ z_{i-1,i}^{\mathrm{d}}(k+1) &= z_{i-1,i}^{\mathrm{d}}(k) + T_s(d_{i-1,i}(k) - \tau v_i(k)), \end{aligned} \tag{6.5}$$

where $\zeta_i = k_{e_i}K_i^c/m_{t_i}T_i^I$, T_s is the sampling time, τ is the time headway constant, and $z_{i-1,i}^{\mathrm{d}}$ is the integral action for maintaining the time headway policy. Let the state vector be partioned as

$$x = [\underbrace{z_1^{\mathrm{v}}\ v_1}_{x_1}\ \underbrace{d_{12}\ z_{12}^{\mathrm{d}}\ z_2^{\mathrm{v}}\ v_2}_{x_2}\ \underbrace{d_{23}\ z_{23}^{\mathrm{d}}\ z_3^{\mathrm{v}}\ v_3}_{x_3}\ \dots\ \underbrace{d_{N-1,N}\ z_{N-1,N}^{\mathrm{d}}\ z_N^{\mathrm{v}} v_N}_{x_N}]^T. \tag{6.6}$$

The state $v_i(k+1)$ follows immediately from linearizing and discretizing (6.3) and (6.4), as described in Section 3.1.2. A discrete linearized state space representation of the system can then be given as

$$x(k+1) = \underbrace{\begin{bmatrix} A_{11} & 0 & 0 & \dots & 0 \\ A_{21} & A_{22} & 0 & \dots & 0 \\ 0 & A_{32} & A_{33} & \dots & 0 \\ \vdots & \vdots & \vdots & \ddots & \vdots \\ 0 & 0 & 0 & \dots & A_{NN} \end{bmatrix}}_{A} \underbrace{\begin{bmatrix} x_1(k) \\ x_2(k) \\ x_3(k) \\ \vdots \\ x_N(k) \end{bmatrix}}_{x(k)} + \underbrace{\begin{bmatrix} B_1 & 0 & 0 & \dots & 0 \\ 0 & B_2 & 0 & \dots & 0 \\ 0 & 0 & B_3 & \dots & 0 \\ \vdots & \vdots & \vdots & \ddots & \vdots \\ 0 & 0 & 0 & \dots & B_N \end{bmatrix}}_{B} \underbrace{\begin{bmatrix} u_1(k) \\ u_2(k) \\ u_3(k) \\ \vdots \\ u_N(k) \end{bmatrix}}_{u(k)}. \tag{6.7}$$

An Euler approximation is used to maintain the band diagonal system structure in the system matrices A and B. Considering the slow dynamics of the system (see Section 6.4), the Euler approximation is sufficiently accurate for the sampling times $T_s = 0.01\,\mathrm{s}$ used in this case. For simplicity we assume that the road grade, α_i, is constant due to lack of road topography preview information (Sahlholm and Johansson, 2010).

6.1.2 Performance Criteria

The performance criteria for the HDV platoon can be formulated into a quadratic cost, by imposing costs on deviating in relative velocity, spacing, and the control effort. Hence, we formulate the weight parameters for a quadratic cost function based upon performance and safety objectives. The overall objective of the vehicles traveling in a platoon is to reduce the fuel consumption, while maintaining a desired inter-vehicle spacing. Let $\mathcal{N}_i = [i-n_i, \dots, i-1]$ denote the set of n_i preceding vehicles that are within radio range of vehicle i and let $x_{\mathcal{N}_i}$ denote their corresponding states. Hence, the cost for each local subsystem in the HDV platoon can be set up as

$$\begin{aligned} J_i(u_i) &= \sum_{k=0}^{\infty} \Big(\sum_{\forall j \in \mathcal{N}_i} w_j^{\tau} (z_{ji}^{\mathrm{d}}(k))^2 + w_{ji}^{v} (v_j(k) - v_i(k))^2 + w_i^{u} (u_i(k))^2 \Big) \\ &= \sum_{k=0}^{\infty} \Big(\begin{bmatrix} x_{\mathcal{N}_i}(k) \\ x_i(k) \end{bmatrix}^T Q_i \begin{bmatrix} x_{\mathcal{N}_i}(k) \\ x_i(k) \end{bmatrix} + R_i (u_i(k))^2 \Big) \end{aligned} \tag{6.8}$$

where the dimension of Q_i varies with the number of vehicles within radio range and can be chosen differently for the vehicle controllers. $R_i = w_i^u$ is the control input weight, which is directly proportional to the vehicle propulsion or braking energy.

The weights give a direct interpretation of how to enforce the objectives for a vehicle traveling in a platoon. The value of w_{ji}^{v} sets a cost for deviating from the velocity of the preceding vehicles. The magnitude of w_i^{τ} determines the importance of not deviating from the desired time headway setting. Hence, a large w_i^{τ} puts emphasis on safety. If w_i^{τ} and w_{ji}^{v} are large, the control input creates an overshoot if the preceding vehicles deviates from the current velocity, since the controller mandates a quick compensation. Similarly, the controller is also sensitive to small disturbances in the preceding vehicles' behavior with large w_i^{τ} and w_{ji}^{v}. On the other hand, an overshoot also occurs if the weights are small, since a soft control allows for large initial deviation from the reference for inter-vehicle spacing, which must be compensated by catching up with a higher velocity. Hence, there is a trade-off in disturbance rejection and performance, when determining the weights. Finally, w_i^{u} punishes the control effort which is proportional to the fuel consumption. Since the performance criteria for the platoon can be formulated as the quadratic cost in (6.8), the infinite horizon linear quadratic regulator (LQR) is a suitable controller with low computational complexity and small memory usage.

6.2 Control Design

In this section, we present a method for deriving the stabilizing decentralized controller. The proposed controller is shown in detail in Figure 6.1. Finally a simple bumpless transfer scheme, based on performance and driver acceptance, is given for switching between the low-level EMS and BMS controllers.

6.2.1 Suboptimal Platooning Controller

The system state vector for deriving the control law when the vehicles are operated with the EMS is given by (6.6) and the control input is then given by $u^{\mathrm{e}} = [v_1^{\mathrm{ref}}\ v_2^{\mathrm{ref}}\ v_3^{\mathrm{ref}}\ \cdots\ v_N^{\mathrm{ref}}]^T$. However, the state vector for deriving the control law during braking is chosen as a subset of (6.6):

$$x^{\mathrm{b}} = [\underbrace{v_1}_{x_1^{\mathrm{b}}}\ \underbrace{d_{12}\ v_2}_{x_2^{\mathrm{b}}}\ \underbrace{d_{23}\ v_3}_{x_3^{\mathrm{b}}}\ \cdots\ \underbrace{d_{N-1,N}\ v_N}_{x_N^{\mathrm{b}}}]^T,$$

and the corresponding control input for the system is $u^{\mathrm{b}} = [a_1^{\mathrm{ref}}\ a_2^{\mathrm{ref}}\ a_3^{\mathrm{ref}}\ \cdots\ a_N^{\mathrm{ref}}]^T$. The integral state is omitted in the system model for the brake control law, mainly to remove the damping in the system that follows from having $z_{i-1,i}^{\mathrm{d}}$ in the feedback. By removing the state, the controller will try to maintain the larger equilibrium distance during a braking event, which is experienced as more safe and intuitive by the expert drivers that evaluated the system. The system matrices for when the vehicles are governed by the engine are denoted by A^{e} and B^{e}. The system matrices for when the vehicles are governed by the brakes are denoted by A^{b} and B^{b}, with rows and columns of (6.7) removed according to the definition of x^{b}. Note that A^{q}

and B^q, $q \in \{\mathrm{e}, \mathrm{b}\}$, are lower triangular band matrices. However, elements differ between the two modes of operation.

The particular structure of the system (6.7) can be divided into subsystems. Thereby, as presented in Algorithm 6.1, locally stabilizing controllers can be derived sequentially by starting from the lead vehicle and then transmitting the controller gain and subsystem parameters, along with the state information to all the follower vehicles. As a result of subsequently deriving controllers based on local model information and interconnections, a global suboptimal decentralized feedback control law, $u^q(k) = -L^q x^q(k)$, is produced with respect to (6.7), where L has a lower block diagonal form and is given as

$$L = \begin{bmatrix} L_{11}^q & 0 & 0 & \dots & 0 \\ L_{21}^q & L_{22}^q & 0 & \dots & 0 \\ L_{31}^q & L_{32}^q & L_{33}^q & \dots & 0 \\ \vdots & \vdots & \vdots & \ddots & \vdots \\ L_{N1}^q & L_{N2}^q & L_{N3}^q & \dots & L_{NN}^q \end{bmatrix}. \tag{6.9}$$

Note that the feedback gain matrix in (6.9) can have a lower band diagonal structure depending on the radio range. The decentralized optimization is performed for each subsystem, as described in Algorithm 6.1, where it is assumed that each subsystem is stabilizable and detectable. The controllers can then be derived as

Algorithm 6.1:

Step 0) Set the weight matrices Q_i^q, R_i^q, $i = 1, \dots, N$, positive definite and in accordance with the desired performance criteria. It is assumed that the pairs $(\bar{A}_{ii}^q, \bar{B}_i^q)$ and $(\bar{Q}_i^q, \bar{A}_{ii}^q)$, given in the algorithm, are stabilizable and detectable, respectively.

Step 1) Compute the optimal feedback controller, u_1^{q*}, for vehicle 1 (the lead vehicle) by solving

$$\begin{aligned} &\min_{u_1} \sum_{k=0}^{\infty} x_1^q(k)^T Q_1^q x_1^q(k) + u_1^q(k)^T R_1^q u_1^q(k) \\ &\text{s. t. } x_1^q(k+1) = A_{11}^q x_1^q(k) + B_1^q u_1^q(k). \end{aligned}$$

The optimal linear quadratic feedback controller is then given by

$$\begin{aligned} u_1^{q*}(k) &= -L_1^q x_1^q(k), \\ L_1^q &= (R_1^q + B_1^{qT} P_1^q B_1^q)^{-1} B_1^{qT} P_1^q A_1^q, \end{aligned}$$

where P_1^q is the unique positive definite solution of

$$P_1^q = A_{11}^{qT}(P_1^q - P_1^q B_1^q (R_1^q + B_1^{qT} P_1^q B_1^q)^{-1} B_1^{qT} P_1^q) A_1^q + Q_1^q.$$

Step 2) Compute the optimal feedback controllers, u_i^{q*}, for vehicles $i = 2, \ldots, N$,

$$\min_{u_i} \sum_{k=0}^{\infty} \begin{bmatrix} x_{\mathcal{N}_i}^q(k) \\ x_i^q(k) \end{bmatrix}^T Q_i^q \begin{bmatrix} x_{\mathcal{N}_i}^q(k) \\ x_i^q(k) \end{bmatrix} + u_i^q(k)^T R_i^q u_i^q(k)$$

s. t.

$$\begin{bmatrix} x_{\mathcal{N}_i}^q(k+1) \\ x_i^q(k+1) \end{bmatrix} = \underbrace{\begin{bmatrix} A_{\mathcal{N}_i\mathcal{N}_i}^q - B_{\mathcal{N}_i}^q L_{\mathcal{N}_i}^q & 0 \\ A_{\mathcal{N}_i i}^q & A_{ii}^q \end{bmatrix}}_{\bar{A}_{ii}^q} \begin{bmatrix} x_{\mathcal{N}_i}^q(k) \\ x_i^q(k) \end{bmatrix} + \underbrace{\begin{bmatrix} 0 \\ B_i^q \end{bmatrix}}_{\bar{B}_i^q} u_i^q(k).$$

Obtain optimal u_i^{q*} by solving

$$u_i^{q*}(k) = -L_i^q \begin{bmatrix} x_{\mathcal{N}_i}^q(k) \\ x_i^q(k) \end{bmatrix},$$
$$L_i^q = (R_i^q + \bar{B}_i^{qT} P_i^q \bar{B}_i^q)^{-1} \bar{B}_i^{qT} P_i^q \bar{A}_{ii}^q,$$

where P_i^q is the unique positive definite solution of

$$P_i^q = \bar{A}_{ii}^{qT}(P_i^q - P_i^q \bar{B}_i^q (R_i^q + \bar{B}_i^{qT} P_i^q \bar{B}_i^q)^{-1} \bar{B}_i^{qT} P_i^q)\bar{A}_{ii}^q + Q_i^q.$$

Theorem 6.2.1. *Consider a chain of N interconnected subsystems with dynamics given by* (6.7)*. Algorithm 6.1 provides a state-feedback controller $u = -Lx$ with L as in* (6.9) *that results in a globally asymptotically stable closed-loop system.*

Proof. Consider subsystems $(\bar{A}_{ii}^q, \bar{B}_i^q)$, $i = 1, \ldots, N$, as introduced in Algorithm 6.1. It is easy to see that with the specified state-feedback control law $u = -Lx$ the resulting closed-loop system has poles given as the solutions to

$$\prod_{i=1}^{N} \det\left[\lambda I - (A_{ii}^q - B_i L_i^q)\right] = 0.$$

Thus, Algorithm 6.1 produces a globally asymptotic stable system, since

$$\mathrm{Re}\left[\lambda_i \left(A_{ii}^q - B_i^q L_i^q\right)\right] < 1, \ \forall i.$$

The inequality for each subsystem's eigenvalues follows from the fact that the pairs $(\bar{A}_{ii}^q, \bar{B}_i^q)$ and $(\bar{Q}_i^q, \bar{A}_{ii}^q)$ are stabilizable and detectable, respectively. Hence, there exists a P_i^q such that the state-feedback gain matrix L_i^q produces an asymptotically stable closed-loop system (Anderson and Moore, 1989).

□

Remark 6.2.2. Algorithm 6.1 provides locally optimal state-feedback controllers, given that the linear quadratic controllers for all preceding vehicles are fixed. Thus, the ith vehicle optimizes its controller and obtains the minimum quadratic cost for the local system under consideration.

Note that even though the spacing states, $d_{i-1,i}$, between preceding vehicles are not controllable for an HDV downstream, an LQR solution can still be found since it is only required that each vehicle subsystem in Algorithm 6.1 is stabilizable and detectable. Another advantage of the proposed algorithm is that it is scalable. If a new vehicle would like to join the platoon at the tail, the decentralized platooning controllers do not need to be recomputed. Only the joining HDV needs to receive information regarding the parameters, control gains, and states from all the vehicles within communication range.

To choose the weights in (6.8), some engineering intuition is needed. One suggestion is to choose the weights such that the closed-loop system satisfy a condition on that disturbances should be attenuated between two neighboring vehicles. The l_2-condition, a common criterion for string stability (Swaroop, 1994), can be used as a reference for obtaining a desirable platooning behavior. The l_2-condition can viewed as a performance measure, which is given as

$$||G_i(z)||_\infty \leq 1, \tag{6.10}$$

where $G_i(z)$ is the transfer function between two neighboring vehicles, $Y_i(z) = G_i(z)Y_{i-1}(z)$, $||\cdot||_\infty$ denotes the maximum peak of the frequency response, and $Y_i(z) := \mathcal{Z}(y_i(k))$ is the $\mathcal{Z}$-transform of the discrete-time domain signal $y_i(k)$, which can either be chosen as the velocity $v_i(k)$ or the relative distance $d_{i-1,i}(k)$. The performance measure in (6.10) is similar to what was presented by Sheikholeslam and Desoer (1993) and Yamamura and Seto (2006). It states that the energy in the signal of a disturbance in velocity or relative distance from the preceding vehicle is attenuated by the follower vehicle if satisfied, which is a desirable property for vehicle platoons. It is a weaker condition than the l_∞-string stability condition (Swaroop and Hedrick, 1996), which implies that there exists a bounded set of initial conditions such that the peaks of the spacings errors remain uniformly bounded along the string of vehicles. If the performance measure in (6.10) is satisfied for all vehicles in the platoon, then it is a sufficient, but not necessary, condition for l_2-string stability.

The transfer function between two neighboring vehicles is given as

$$G_i(z) = e_i^T \left(zI - \begin{bmatrix} A^q_{i-1,i-1} - B^q_{i-1}L^q_{i-1} & 0 \\ A^q_{i-1,i} & A^q_{ii} \end{bmatrix} + \begin{bmatrix} 0 \\ B^q_i \end{bmatrix} L_i \right)^{-1} e_{i-1}, \tag{6.11}$$

where e_i is a column vector that extracts the velocity or relative distance of vehicle i, depending on the desired requirements. Hence, after calculating the controller

gains L_i in Algorithm 6.1, the condition (6.10) can be checked to ensure that the desired performance is obtained.

Proposition 6.2.3. *Consider the transfer function $G_i(z)$ in (6.11). Let $\{g_i(k)\}_{k\in\mathbb{N}}$ denote its impulse response. If $\{g_i(k)\}_{k\in\mathbb{N}}$ does not change sign, then $||G_i(z)||_\infty = ||G_i(z)||_1$.*

Proof. The $\mathcal{Z}$-transform of the impulse response $\{g_i(k)\}_{k\in\mathbb{N}}$ is given by $G_i(z) = \sum_{k=0}^{\infty} g_i(k)z^{-k}$. Considering that $G_i(z)$ is asymptotically stable[1], then $||G_i(z)||_\infty = \sup_{\omega\in[0,2\pi)} |G_i(e^{j\omega})|$. We have that

$$||G_i(z)||_\infty = \sup_{\omega} |G_i(e^{j\omega})| = \sup_{\omega} |\sum_{k=0}^{\infty} g_i(k)e^{-j\omega k}| \leq \sum_{k=0}^{\infty} |g_i(k)| = ||G_i(z)||_1, \quad (6.12)$$

where the last equality follows from the definition $||G_i||_1 = \sum_{k=0}^{\infty} |g_i(k)|$. Furthermore, we have that

$$\begin{aligned} ||G_i(z)||_\infty = \sup_{\omega} |G_i(e^{j\omega})| \geq & |G_i(e^{j0})| \\ = & |\sum_{k=0}^{\infty} g_i(k)| \quad (6.13) \\ = & \sum_{k=0}^{\infty} |g_i(k)| \quad (6.14) \\ = & ||G_i(z)||_1, \quad (6.15) \end{aligned}$$

where (6.13) and (6.14) follow from the definition of the $\mathcal{Z}$-transform and the fact that $\{g(k)\}_{k\in\mathbb{N}}$ does not change sign, respectively. Combining (6.12) and (6.15) concludes the proof.

□

Thus, as proved in Proposition 6.2.3, if the sign of the impulse response of the transfer function (6.11) does not change, the l_2- and the l_∞-string stability condition are equivalent, which means that both the maximum peak and the energy of a disturbance in the preceding vehicles' velocity or relative distance are attenuated. Hence, by satisfying (6.10) in the control design for a single vehicle in the platoon, the error magnitude can be locally attenuated. Note that if additional HDVs are added to the tail of the platoon, the transfer function (6.11) will not change and, inherently, the local string stability property is maintained with the proposed decentralized controller design regardless of the number of vehicles that are added.

[1] All poles are inside the unit circle for a discrete asymptotically stable discrete system

6.2.2 Bumpless Switching

The objective for introducing bumpless transfer, in addition, is to avoid overshoots, uncomfortable behavior, or even hardware damage, when switching between actuation with the EMS and BMS. A rather standard method is followed to do bumpless transfer as discussed next (Åström and Hägglund, 2006).

It is not fuel-efficient to brake, since the energy produced through diesel combustion is wasted through heat loss produced by the frictional forces in the brake discs. However, braking must be performed if the preceding vehicle decelerates by braking or the platooning HDVs are traversing a steep downhill segment without any preview information with respect to the upcoming topography (Alam et al., 2013*a*). Therefore, we propose a control system that switches between engine and brake control, as illustrated in Figure 6.1.

The decentralized high-level controller, in Figure 6.1, where L_i^{e} and L_i^{b} are established as given in Algorithm 6.1. A maximum velocity is enforced due to legislation on the speed demand to the EMS, which might saturate the control demand produced by the L_i^{e}. Hence, an anti-windup filter W, is implemented as

$$z_i^{\mathrm{v}}(k+1) = z_i^{\mathrm{v}}(k) + \zeta_i T_s (e_i(k) + \frac{1}{T_t} e_s(k)) \tag{6.16}$$

where $e_s = v_{\mathrm{ref}} - v_{\mathrm{LQR}}$ and T_t is a design parameter.

The switching guards, g_i in Figure 6.1, between the three modes of operation are defined as

$$g_1 : (d_{i-1,i} < \beta\tau v_i \text{ and } v_{i-1} < v_i) \text{ or } (b = 1 \text{ and } d_{i-1,i} < \tau v_i)$$

$$g_2 : d_{i-1,i} \geq \tau v_i \text{ and } v_{i-1} \geq v_i \text{ and } b = 0 \text{ and } d_s < d_{i-1,i}$$

$$g_3 : [v_i, d_{i-1,i}, v_r]^T \in \partial\mathcal{S}$$

$$g_4 : [v_i, d_{i-1,i}, v_r]^T \in \mathcal{S}$$

where $b \in \{0, 1\}$ is a binary signal that is transmitted if a preceding vehicle brakes, d_s is a minimum allowed spacing for safety, and $\beta \in [0, 1]$ is a design parameter that determines how much the relative distance is allowed to decrease from the reference for inter-vehicle spacing before the brakes should be applied. $\mathcal{S} = [0, v_i^{\max}] \times [d_{i-1,i}^{\min}, \infty] \times [v_r^{\min}, v_r^{\max}]$ denotes a safe set, derived through a game theoretical formulation for guaranteeing safety in HDV platooning (Alam et al., 2014*a*), where v_r is the relative velocity with respect to the preceding vehicle. A collision can always be avoided despite the worst-case behavior of the preceding vehicle if the vehicle states are inside the safe set, otherwise, a collision can occur. Hence, if a vehicle reaches the boundary of the safe set, denoted as $\partial\mathcal{S}$, an optimal collision avoidance brake request, a_{s}, is sent to the BMS to guarantee safety with the proposed controller. The collision avoidance is aborted and the less restrictive control is resumed once the vehicle reaches sufficiently inside the safe set. The controller

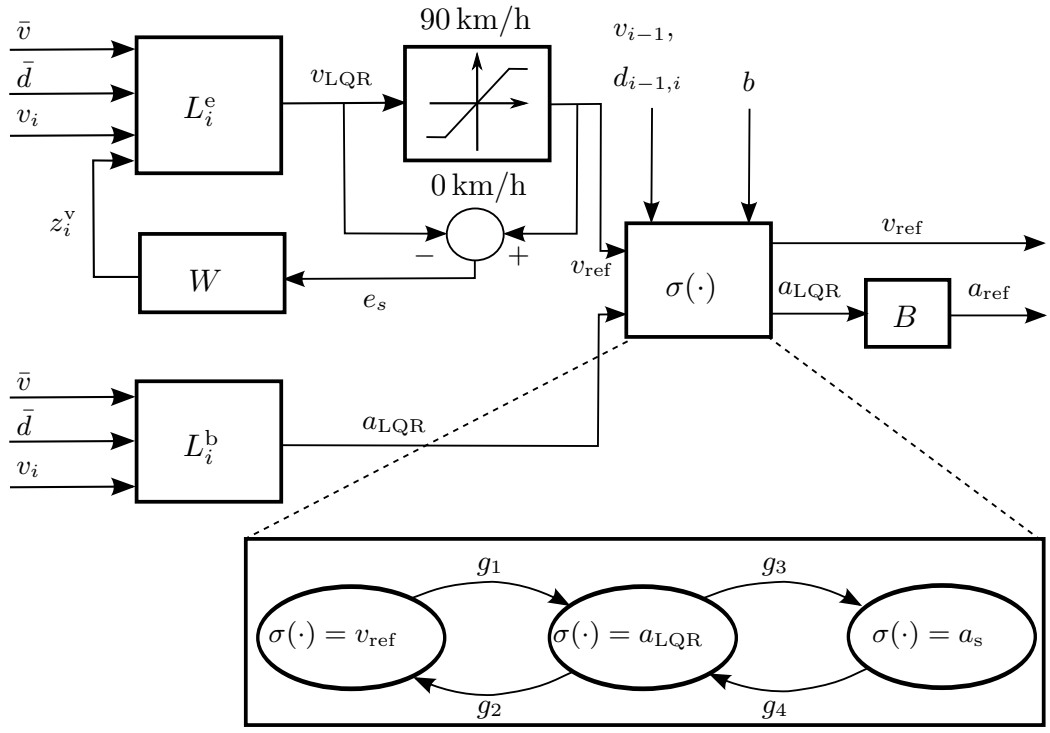

Figure 6.1: Overview of the proposed LQR with bumpless transfer. The velocity information from all the preceding vehicles is denoted by $\bar{v}$ and the inter-vechicle spacing information is denoted by $\bar{d}$. Velocity measured from the on-board sensors of the vehicle is denoted by v_{i}. The velocity as well as the distance measured from the preceding vehicle is denoted by $v_{\mathrm{i\text{-}1}}$ and $d_{\mathrm{i\text{-}1,i}}$, respectively. z_i^{v} denotes the integral state in the EMS model.

output, v_{ref}, is directly fed through if the vehicle operates within the allowed inter-vehicle spacing. If the spacing decreases below the allowed limit and the preceding vehicle has not started to increase its velocity, or if any of the preceding vehicles brake, the controller output, a_{LQR}, is fed through until the preceding vehicles cease braking and the desired inter-vehicle spacing is resumed.

If the inter-vehicle spacing decreases slightly, a reduced reference velocity is initially provided by the proposed controller to decelerate and the engine torque will drop to zero. A large jerk might occur when switching to braking, since the spacing is shorter than the reference. To facilitate a bumpless transfer when the controller switches to a_{ref}, a low pass filter, $B(z) = \frac{1-p}{z-p}$, is implemented after the switch, were $p \in [0, 1)$ is a design parameter for establishing the the rise-time of the filter. When switching back to governing the vehicle through the EMS, v_{ref} should be close to the current vehicle velocity and the integral state, z^{v}, must be initiated accordingly to avoid a switching transient. The minimum cost to go given in the infinite horizon LQR derivation is given by $x_k^T P x_k$ (Åström, 1970), at time k. Thus, the following optimization problem can be set up to facilitate a bumpless transfer

$$\min_{z_0^v} \begin{bmatrix} \bar{x}_0 \\ z_0^v \end{bmatrix}^T \bar{P} \begin{bmatrix} \bar{x}_0 \\ z_0^v \end{bmatrix}, \quad \text{s.t.} ||v_{\text{ref}} - v||_\infty \leq \varepsilon \tag{6.17}$$

where $\bar{x}_0$ are the known states and z_0^{v} is the initial integral state. The rearranged Riccati solution matrix is denoted as $\bar{P} = \begin{bmatrix} \bar{P}_{11} & \bar{P}_{12} \\ \bar{P}_{12}^T & \bar{P}_{22} \end{bmatrix}$, where the columns and rows in P corresponding to z_0^{v} is shifted to match the state vector in (6.17). Finally, $\varepsilon \geq 0$ is a design parameter that determines the level of smoothness in the transition. The solution to the optimization is given as

$$z_0^{\text{v}*} = \min\big(\max(\tilde{z}_0^{\text{v}}, \frac{-\varepsilon - L_x\bar{x}_0 - v}{L_z}), \frac{\varepsilon - L_x\bar{x}_0 - v}{L_z}\big), \tag{6.18}$$

where we have used the fact that $v_{\text{ref}} = -Lx_0 = -L_x\bar{x}_0 - L_z z_0^{\text{v}}$ and that $\tilde{z}_0^{\text{v}} = -2\bar{P}_{22}^{-1}\bar{P}_{12}^T\bar{x}_0$ is the solution to minimizing the quadratic cost in (6.17). Note that if $\varepsilon = 0$, the quadratic cost is neglected and a seamless transfer is obtained.

6.3 Numerical Evaluations

Numerical evaluations for a three-HDV platoon is presented in this section for typical highway scenarios. The scenarios are carried out by feeding an automated velocity or deceleration reference to the lead vehicle. The advanced simulation model in Section 3.2, is used to tune the weight parameters, Q_i^q and R_i^q, in the LQR cost formulation (6.8) and to evaluate the performance of the platooning vehicles. The simulation model consists of 3 313 variables, 1 058 equations, and 626 states for each vehicle, where each of the components in the powertrain is modeled carefully and verified to mimic real life behavior for a single HDV. The vehicle configuration and parameters in the given simulations are set with respect to the real vehicles that are used for a qualitative verification of the obtained results, as presented in Section 6.4. The time headway constant is set to $\tau = 1\,\text{s}$, which is typically the smallest adaptive cruise control setting in modern vehicles.

6.3.1 Acceleration Responses

Several step responses of varying step sizes were simulated to evaluate the proposed controller. In Figure 6.2, simulation results are given for a scenario when the lead vehicle initially drives at a low velocity of 50 km/h. After reaching steady state, the lead vehicle increases its velocity by 10 km/h, then maintains the new set velocity for 35 s and then performs an additional step of 10 km/h. The top plot in Figure 6.2 shows the velocity trajectories for the platooning vehicles, where the indices denote the vehicle position index in the platoon. The second from top plot shows the

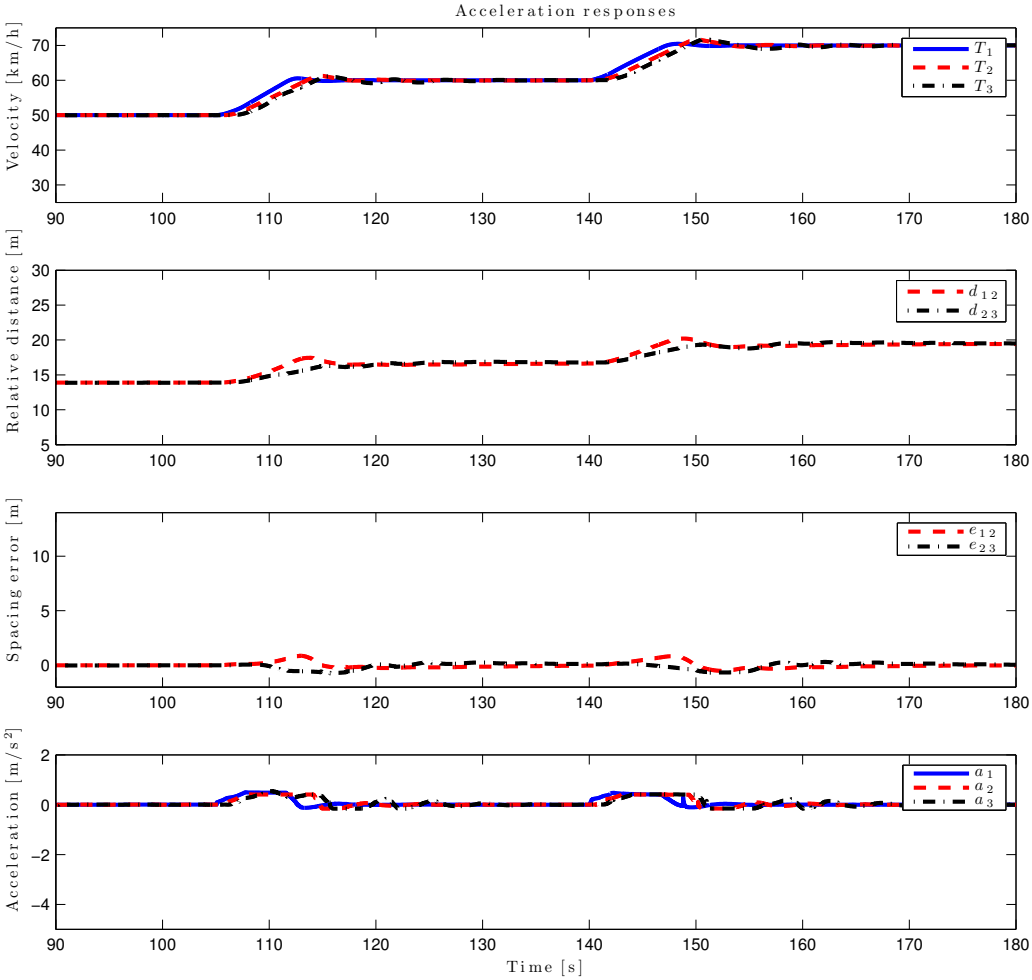

Figure 6.2: Simulated results for step responses when the first vehicle in the platoon increases its velocity by 10 km/h. The solid (blue) lines show the profiles for the lead vehicle, the (red) dashed lines show the profiles for the vehicle in the middle, and the (black) dashed-dotted lines show the profiles for the last vehicle in the platoon.

relative distances between the vehicles, the second from bottom plot shows the error in relative distance given as the deviation from the set time headway policy,

$$e_{i-1,i} = d_{i-1,i} - \tau v_i, \tag{6.19}$$

and the bottom plot shows the corresponding acceleration trajectories for all the vehicles. The results show that the overshoot in the velocity and relative distance is lower for the last vehicle compared to the vehicle in the middle of the platoon. The lead vehicle has an overshoot[2] in velocity of 6 % during the first step response

[2]The overshoot is given by the maximum deviation from the velocity increase divided by the velocity increase magnitude.

and an overshoot of 5 % during the second step response. The second vehicle has corresponding overshoots of 14 % and 17 %. The third vehicle has an overshoot of 12 % and 17 %, respectively. Hence, the overshoot is only dampened in the first step response. The attenuation is lost during the second step response because a gear change is made in the last vehicle during the step, which the two preceding vehicles deters until steady state is resumed. The deviation from the reference for inter-vehicle spacing is always smaller for the third vehicle during the steps. The sign of the deviation for the two follower vehicles is opposite because there is a slight lag in initiating the step for the second vehicle. However, the third vehicle experiences the same lag in response from the lead vehicle and considers the spacing error for all preceding vehicles. It can therefore handle the disturbance better. Furthermore, the propagated deviations from the reference for inter-vehicle spacing seem to stay bounded throughout the platoon.

6.3.2 Braking Responses

To evaluate the transient responses of the distributed controller during and after braking, several simulations were carried out with varying external deceleration magnitude given to the first vehicle's automated controller. Figure 6.3 displays the trajectories for when the first vehicle is given an external deceleration commandof $3\,\mathrm{m/s^2}$. After the vehicles reach a steady state velocity of 60 km/h, the braking is initiated until the lead vehicle has reduced its velocity by 10 km/h. The next braking is initiated after 18 s and the procedure is repeated until the lead vehicle has reached 30 km/h. It can be seen in the top plot of Figure 6.3 that both follower vehicles have a bigger undershoot in velocity, compared to the first vehicle, after each braking has ended. The first vehicle has an undershoot in velocity of 16 %, 25 %, 6 % during the first, second, and third step, respectively. The follower vehicles have corresponding undershoots in velocity of 19 %, 40 %, 19 %. Thus, the follower vehicles have larger undershoots in velocity, but the third vehicle never displays a bigger undershoot than its preceding vehicle. The spacing errors between the platooning vehicles, shown in the second from bottom plot, show that the controller in the third vehicle allows for a positive deviation from the reference for inter-vehicle spacing during deceleration. This is a consequence of the controller striving to compensate for the spacing error with respect to both preceding vehicles and not having the state $z^{\mathrm{d}}_{i-1,i}$ in the feedback control during braking. The desired time headway is later resumed after the braking is over. Because the braking event is transmitted through wireless communication, the second vehicle is also able to react very fast, only having a maximum deviation from the reference for inter-vehicle spacing of 0.6 m at most during the first braking. However, at the 130 s time marker, it can be seen that the second vehicle drops in velocity and requires some time to compensate for the increased deviation in spacing. This is due to a gear change at the moment the vehicle is about to resume the steady state velocity. Furthermore, the bottom plot in Figure 6.3 shows that the deceleration is lower for the last vehicle at the cost of having to brake over a longer time period. However, the required braking power

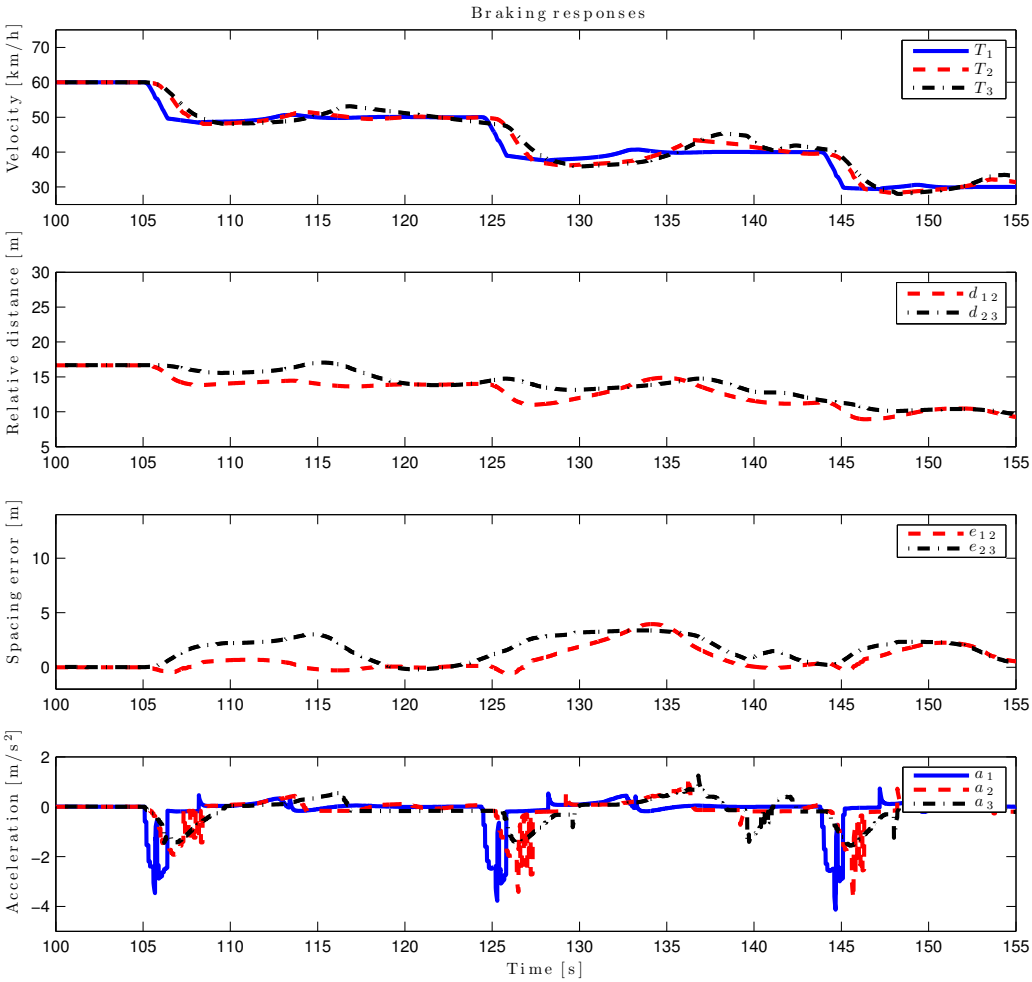

Figure 6.3: Simulation results when the first vehicle in the platoon decreases its velocity by 10 km/h through a deceleration of 3 m/s^2. The displayed profiles are denoted the same as previously, in Figure 6.2, to indicate the vehicle position in the platoon and the corresponding profiles.

to handle the disturbance is lowered along the platoon and it can be inferred that the controller operates smoothly and safely.

6.3.3 Alternating Acceleration Responses

The goal of this scenario is to excite unmodeled dynamics in all the platooning vehicles and evaluate the controller performance when the control input is saturated. To this end, the first vehicle, starting from steady state, then accelerates with a given acceleration until it reaches an upper velocity limit. It then decelerates with a given deceleration demand until a lower velocity limit is reached. The alternating harsh accelerations and decelerations could be considered as analogous to behavior

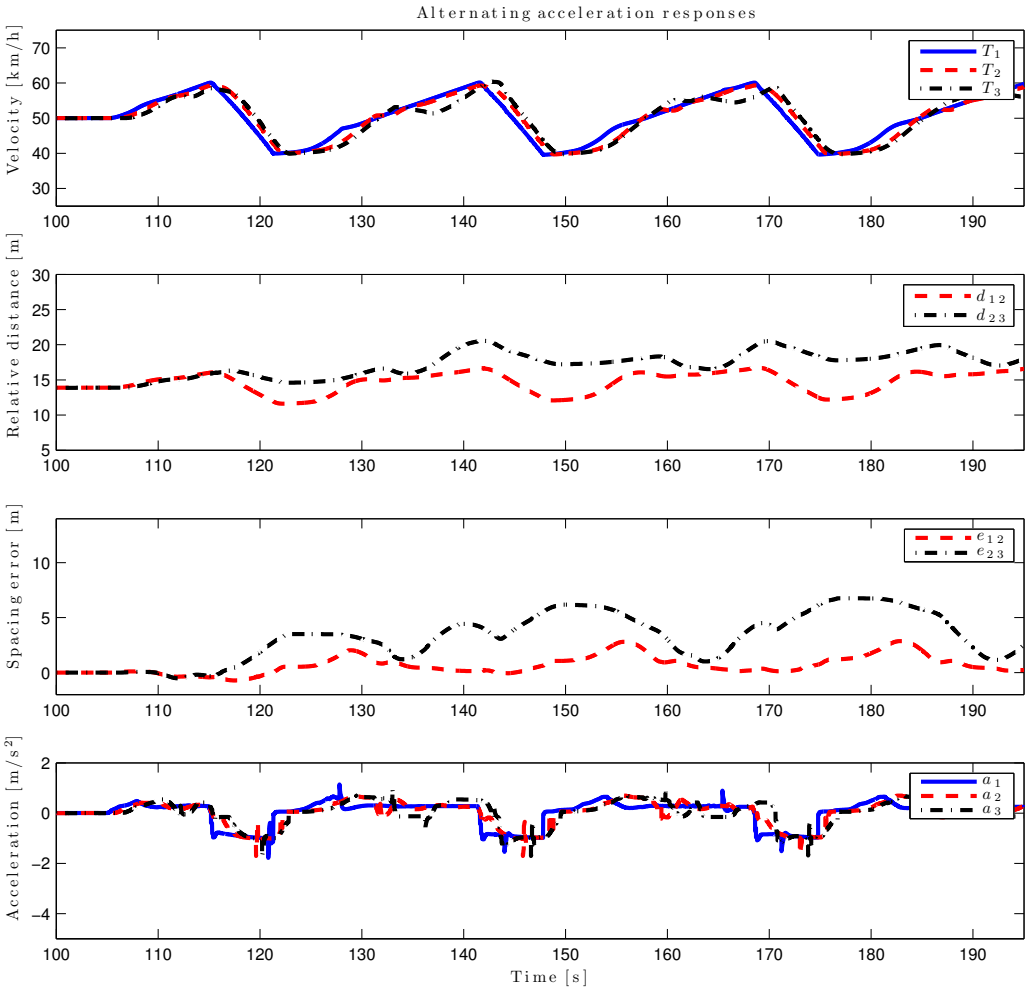

Figure 6.4: Simulation results to evaluate the controller performance when the lead vehicle varies its velocity. The displayed profiles are denoted the same as in Figure 6.2, to indicate the vehicle position in the platoon and the corresponding profiles.

observed in a traffic queue that can occur on highways. Figure 6.4 shows the trajectories of the three platooning HDVs in one such scenario, where the first vehicle initially maintains 50 km/h and then starts to accelerate with 0.5 m/s^2 until it reaches the upper limit of 60 km/h. When the upper limit is reached, it then decelerates with 1 m/s^2 until it reaches the lower limit of 40 km/h, for when it again resumes the acceleration to the upper set speed. It can clearly be seen in the top plot of Figure 6.4, between the 120–140 s time markers that the slope of the velocity changes during the acceleration. This occurs due to a gear change, during which an HDV can drop significantly in speed. The dynamics of the gear changes are not modeled and seems to occur at different times during the acceleration for all the vehicles depending on the current engine mode. The error in spacing, given

in the second from bottom plot, shows that the deviation from the reference for inter-vehicle spacing grows initially for the last vehicle with the proposed control law, but remains limited. The second vehicle in the platoon maintains the spacing with a largest observed deviation of 2.8 m. The third vehicle has a larger observed deviation of 6.8 m, due to the significant drops in speed during each gear change, and then compensates for the inter-vehicle spacing error during the acceleration. The top plot, with the velocity trajectories, and the bottom plot with the vehicle acceleration trajectories, show that the there is no overshoot in velocity or acceleration. However, a gear change causes an increase in spacing due to the velocity drop until the new gear is engaged and full engine torque is regained.

6.4 Experimental Evaluations

In this section, we first give the experimental setup for the three-vehicle platoon. We then present empirical results for the three scenarios, presented in Section 6.3, that were obtained on a 1.7 km flight runway, south of Stockholm. The same automated control strategy was used to govern the first vehicle in the experiment procedure, in order to obtain reproducible results. Several experimental results are presented to evaluate the performance of the proposed controller in practice.

6.4.1 Experimental Setup

Three standard Scania tractor-trailer HDVs are utilized with additional control and communication hardware. All tractors have a 4×2 vehicle configuration and the trailers have three axles. The masses are measured to be 37.47 t for the lead vehicle, 38.36 t for the second vehicle, and 39.44 t for the last vehicle in the platoon. They are equipped with a standard doppler radar, which sends the relative distance with a 40 ms interval to the central coordinator electronic control unit (ECU) and is gated every 100 ms. The final gear ratios are slightly different for each vehicle, with $i_f = 2.92$ for the lead vehicle, $i_f = 2.71$ for the second vehicle, and $i_f = 2.59$ for the third vehicle. All vehicles are equipped with slightly different, but fully-automatic gearboxes. Standard global positioning systems (GPSs) and ECUs, utilized in Scania HDVs, are used for positioning and to execute the proposed controller, respectively. As illustrated in Figure 6.5, a wireless sensor unit (WSU) carrying the standard wireless communication protocol IEEE 802.11p is mounted in each vehicle. The WSU is directly connected to the HDVs internal CAN system and messages are broadcast on demand. Thereby, the internal CAN signals such as velocity, acceleration, parameters, and control inputs are available to all the vehicles in range. The data are logged in all the vehicles.

6.4.2 Acceleration Responses

Due to the relatively short distance of the runway, it was difficult to achieve steady state and at the same time have enough distance to perform two desired step

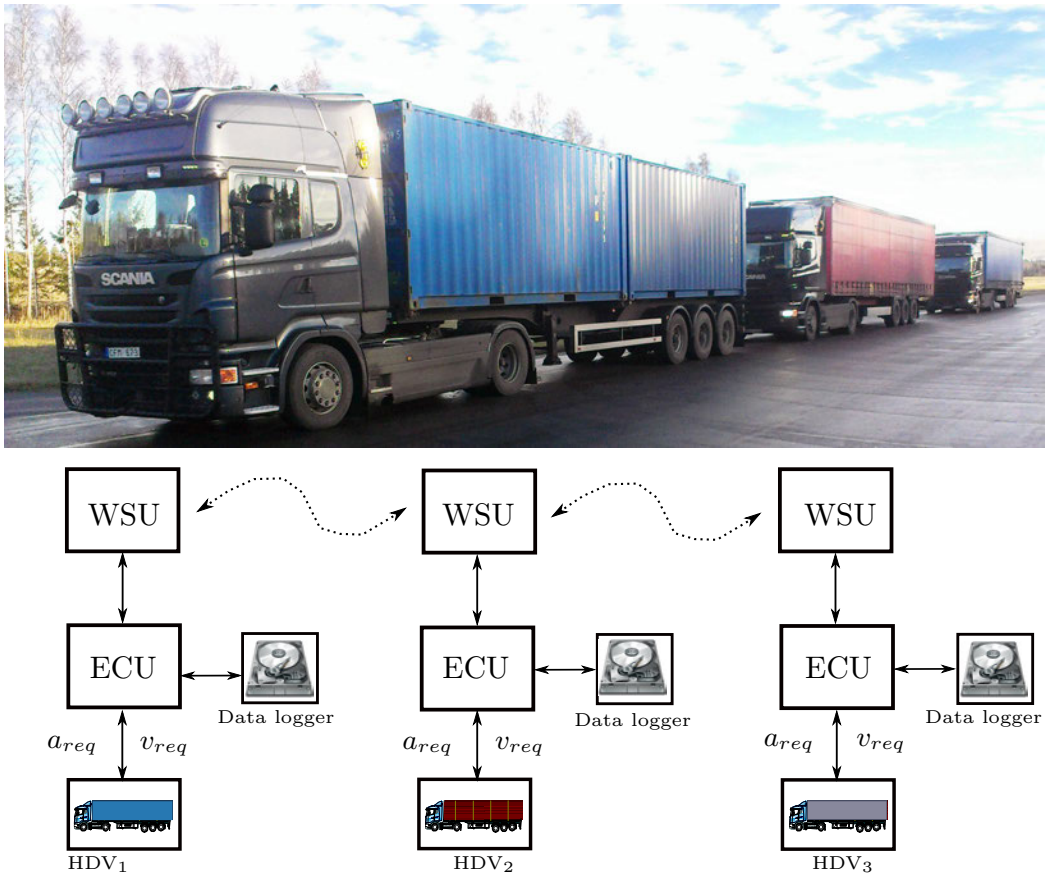

Figure 6.5: A schematic overlay of the experimental hardware setup. The top picture shows the HDVs utilized in these experiments. The left HDV is the lead. The WSU, ECU, and data logger communicate through CAN. As soon as new information is obtained through the ECU or the vehicle, it is broadcast through the WSU.

responses. The results for two step responses in the lead vehicle of 10 km/h are given in Figure 6.6, where the top plot shows the velocity trajectories for the three platooning HDVs. The second from top plot shows the inter-vehicle spacings and the second from bottom plot shows the deviation from the reference for inter-vehicle spacing, in which it can be seen that the vehicles had not yet been able to reach steady state at the beginning of the first step response. Finally, the bottom plot shows the vehicle acceleration trajectories. As shown in the second from bottom plot in Figure 6.6, there is a deviation from the reference for inter-vehicle spacing of 1.1 m for the middle vehicle and a deviation of 2.4 m for the third vehicle, when the step is initiated. The first vehicle has an overshoot in velocity of 14 % during the first step response and an overshoot of 8 % during the second step response. This is higher compared to the numerical results and is due to different cruise control (CC) logic in the first vehicle. However, the overshoots decrease in the second step, which is congruent with the simulation model. The second vehicle has

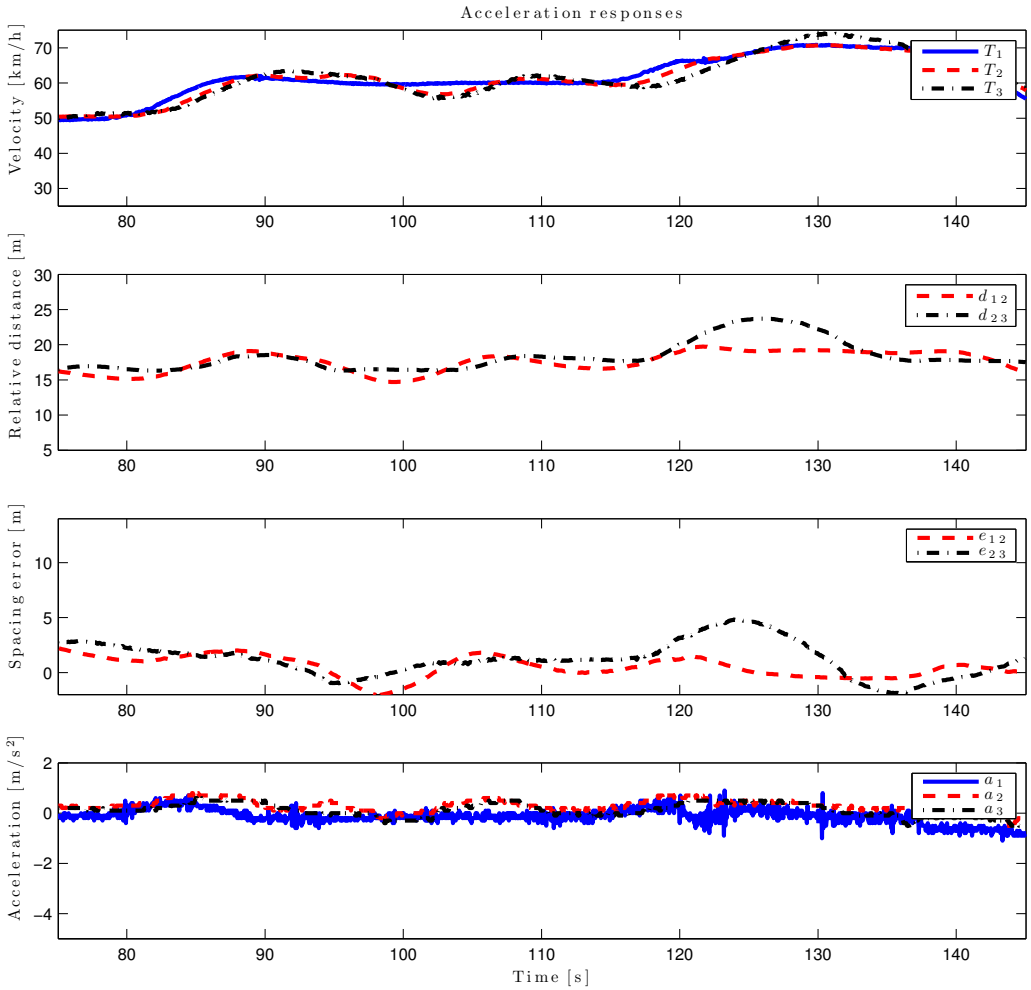

Figure 6.6: Experiment results for step responses when the first vehicle in the platoon increases its velocity by 10 km/h. The solid (blue) lines show the profiles for the lead vehicle, the (red) dashed lines show the profiles for the vehicle in the middle, and the (black) dashed-dotted lines show the profiles for the last vehicle in the platoon.

corresponding overshoots in velocity of 24 % and 8 %, respectively, and the third vehicle has overshoots in velocity of 33 % and 40 %. The variation for the error in relative distance is also initially smaller for the third vehicle. Then, at the 118 s time marker, a gear change is performed in the third vehicle just before the step response, which causes the vehicle to fall behind and thereby causing a large overshoot by catching up. A similar behavior is observed in the simulation model, with a less severe overshoot. The additional lag in handling the step response occurs because the last vehicle decelerates, i.e. coasts, just before the step is initiated. Hence, the turbo pressure is low, which limits the engine from outputting the desired torque until the turbo pressure is regained. Thus, the preceding vehicles manage to increase

their velocities before the third vehicle can do so, causing a large overshoot to compensate for the increased errors in spacing and velocity.

6.4.3 Braking Responses

The results obtained when the first vehicle, after reaching a steady state velocity of 60 km/h, brakes with $3\,\mathrm{m/s^2}$ until the velocity is reduced by 10 km/h and then repeats the procedure after 18 s, is given in Figure 6.7. As can be seen in the second plot from the bottom, the vehicles had nearly reached steady state when the first braking is initiated, with an error in relative distance close to zero. The acceleration trajectories for all the vehicles, given in the bottom plot, show that the first vehicle performs the strongest deceleration, whereas the third vehicle has an equal or smaller deceleration compared to the second vehicle. The first vehicle has undershoots in velocity of 41 % during the first two steps and 47 % in the last. The follower vehicles both have undershoots in velocity of 37 %, 45 %, and 48 %, respectively. Hence, the follower vehicles display a smaller undershoot during the first braking instance. In contrast to the simulation results, a severe overshoot in relative does not occur due to a gear change for the second vehicle. The third vehicle does not have a bigger undershoot than its preceding vehicle, which is congruent with the simulation model. The third vehicle maintains a larger relative distance, compared to the second vehicle, during the braking actions and then compensates for the error in relative distance after the braking is completed. A deviation from the reference for inter-vehicle spacing of -1.9 m occurs for the second vehicle, whereas the third vehicle always manages to maintain a positive deviation. After each braking event, when the proposed high-level controller switches back to the engine control, an unmodeled gear change occurs that results in an overshoot in desired inter-vehicle spacing. Nevertheless, the errors in relative distance stay limited. The controller performance is considered safe and the results are congruent with the simulation model.

6.4.4 Alternating Acceleration Responses

The results for the alternating accelerations and decelerations for the lead vehicle is given in Figure 6.8. It can be seen that the maximum deviation from the reference for inter-vehicle spacing is 7.2 m for the last vehicle, which is nearly the same in the simulation model. However, the maximum error is larger for the second vehicle in contrast to the simulation results. This is due to a difference in gear management logic between the real vehicles and the simulation model. A periodic behavior can be observed in the plot for the relative distances and in the plot for the error in relative distance. The top plot in Figure 6.8, for the velocity trajectories, reveals that a gear change occurs every other time an acceleration is performed, for the second vehicle, since there is a significant drop in velocity around the 105 s and 155 s time markers. The gear change results in a velocity decrease that creates an increase in relative distance. The second vehicle then manages to reduce the error in relative distance

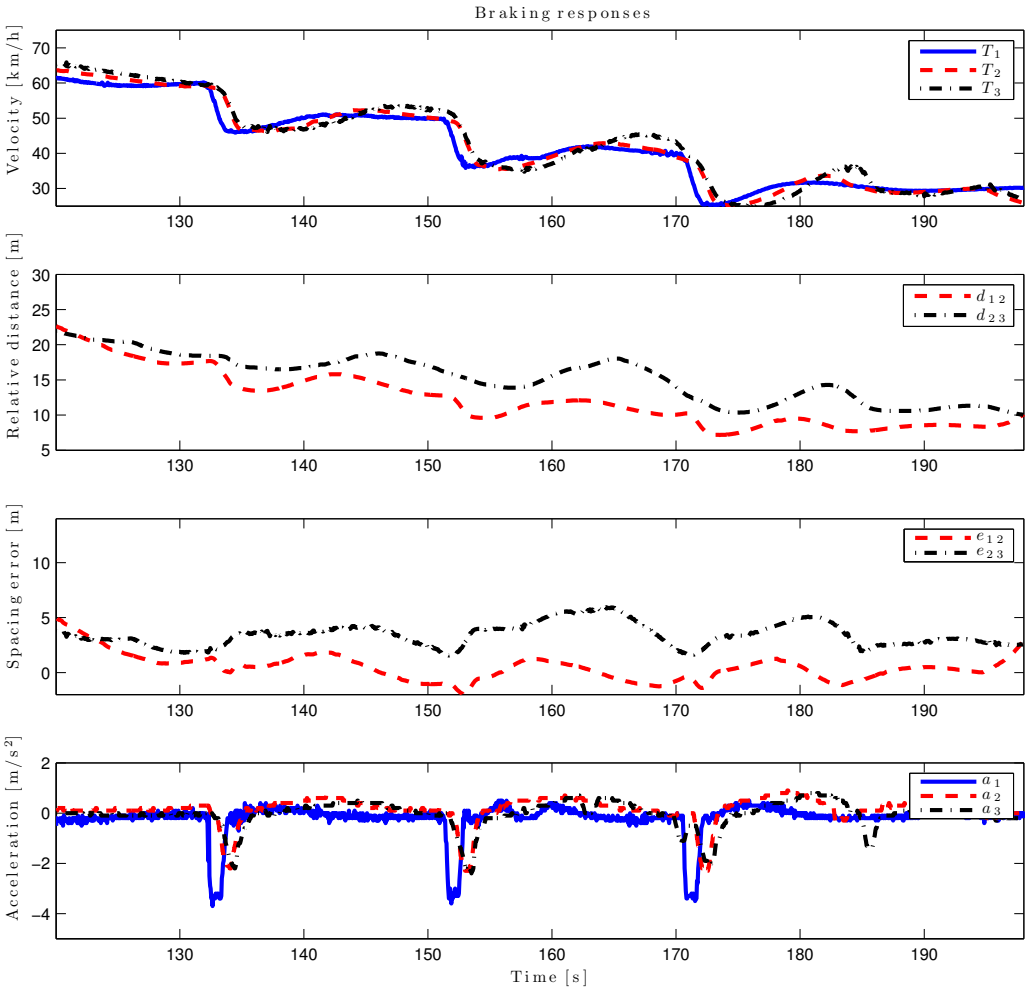

Figure 6.7: Experiment results obtained when the first vehicle in the platoon decreases its velocity by 10 km/h through a deceleration of 3 m/s^2. The displayed profiles are denoted the same as previously, in Figure 6.6, to indicate the vehicle position in the platoon and the corresponding obtained results.

during the next acceleration phase. When the desired time headway is recovered, the behavior is repeated. Nevertheless, it can be seen that the spacing errors are attenuated along the chain and they are bounded. The velocity trajectories in the top plot shows that there are no over- or under undershoots in velocity. Furthermore, the acceleration trajectories shown in the bottom plot reveals that a slightly harder braking is required for the third vehicle compared to the second vehicle, which is caused by maintaining a more accurate time headway.

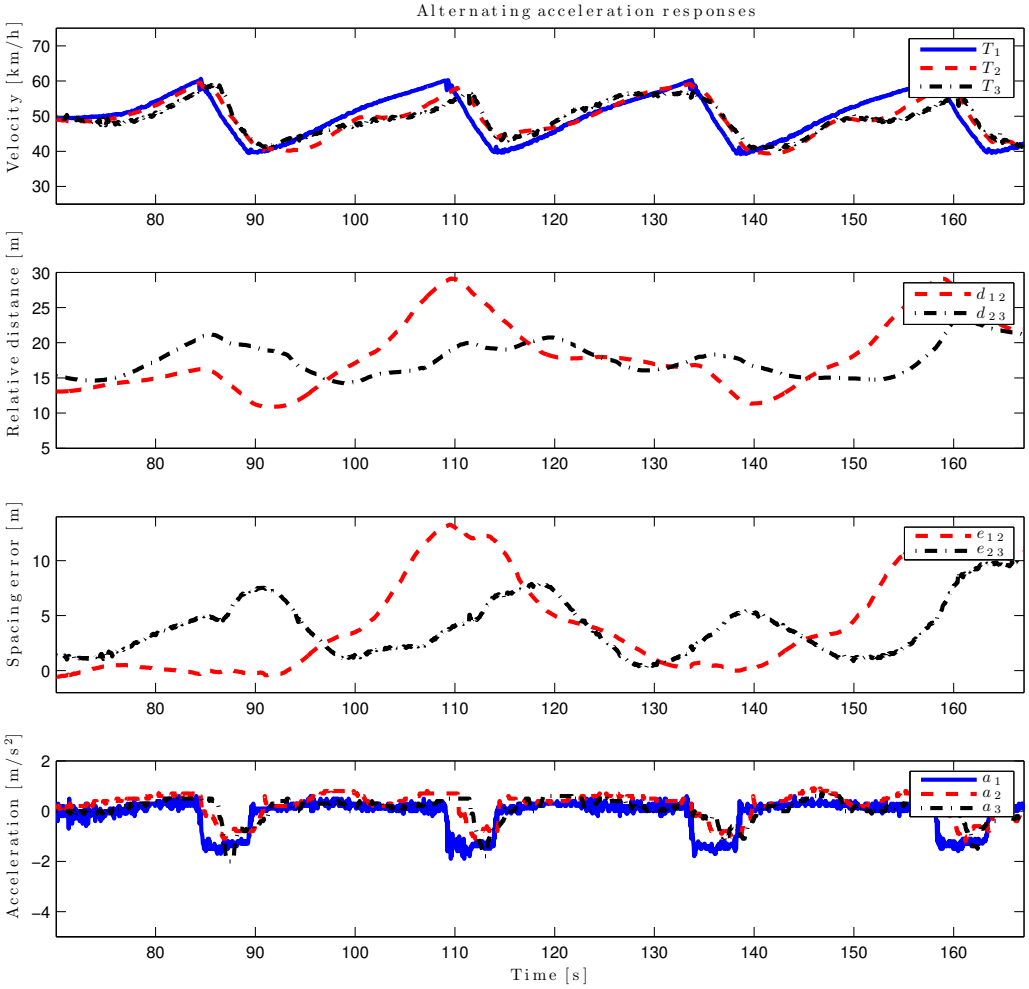

Figure 6.8: Experiment results to evaluate the controller performance when the lead vehicle varies its velocity. The displayed profiles are denoted the same as in Figure 6.6, to indicate the vehicle position in the platoon and the corresponding obtained results.

6.5 Summary

HDV platooning can be conducted with standardized sensors and control units that are already present on commercial HDVs today. A wireless sensor unit needs to be added, so that a wider range of information can be shared between the vehicles with low latency. By studying a three-HDV platoon in this chapter, we hope to have captured most of the dynamical behavior that occurs in a longer platoon consisting of a lead vehicle, follower vehicles, and a tail-end vehicle. A qualitative study has been presented between a simulation model and real life behavior of an HDV platoon. Even though the results differ to some extent, the simulation model mimics most of the dynamics that are observed in practice. It has been shown, both numerically

and through experiments, that the proposed decentralized high-level controller attenuates the disturbances produced by the lead vehicle and operates safely. The experimental results showed that the deviation from the reference for inter-vehicle spacing during the braking scenarios never decrease more than 1.9 m. Hence, it can be inferred that the vehicles could have operated at shorter time headways to achieve further air drag reduction, i.e., fuel-efficiency, without compromising safety. The controller performs well even though the vehicles operate to some extent outside the equilibrium points. However, there are still nonlinearities present in the system that causes unwanted behavior. In contrast to passenger vehicles, a gear change produced in an HDV has a significant impact on the velocity. We presented a simple model for the EMS and engine dynamics, which worked sufficiently well in most of the studied cases. However, there can still arise cases in the nonlinear engine dynamics that can cause unwanted response delays. These situations do not cause an issue with respect to safety, but degrade the tracking performance and increase the control input energy.

Chapter 7

Look-Ahead Control for Platooning

"*It is always wise to look ahead, but difficult to look further than you can see.*"

Winston Churchill

The focus within platooning in the current literature has mainly been on establishing optimal control policies based on linear models for maintaining a given spacing policy without considering the road topography. However, it is not realistic to assume that a vehicle platoon in practice consists of identical heavy-duty vehicles (HDVs) with equal cargo weight and thus the road grade might constrain an HDV in the platoon such that it cannot maintain the overall desired velocity for the platoon. Over steep uphill climb the inter-vehicle spacing is typically increased, when following a vehicle with a stronger engine or a lower mass. Over downhill segments the heaviest follower vehicle might have to brake to avoid coasting into the vehicle ahead. This has in particular been reported as an issue by professional HDV drivers in situations when no overtaking is possible, since constant braking can lead to brake failure due to overheating. Furthermore, braking is never fuel-efficient, since energy produced by the engine is lost through frictional heating of the brakes during braking.

Preview road grade information introduces a possibility to address the issues mentioned above and further improve the fuel-saving potential in HDV platooning. The idea of using preview road grade information for fuel-efficient control is not new and has been studied for HDVs that are traveling alone. Early work on utilizing road grade information, for a single vehicle, in vehicle speed control can be found in Schwarzkopf and Leipnik (1977), where a minimum-fuel problem for a nonlinear vehicle model is presented. More recent work on fuel-optimal control for a single HDV based on preview information of the road topography, referred to as look-ahead control (LAC), has been studied in Hellström (2010) and Fröberg (2008), where the presented controller is derived through dynamic programming. They showed that the fuel consumption can be reduced by adjusting the velocity prior to an uphill or a downhill segment based on the parameters and the nonlinear dynamics

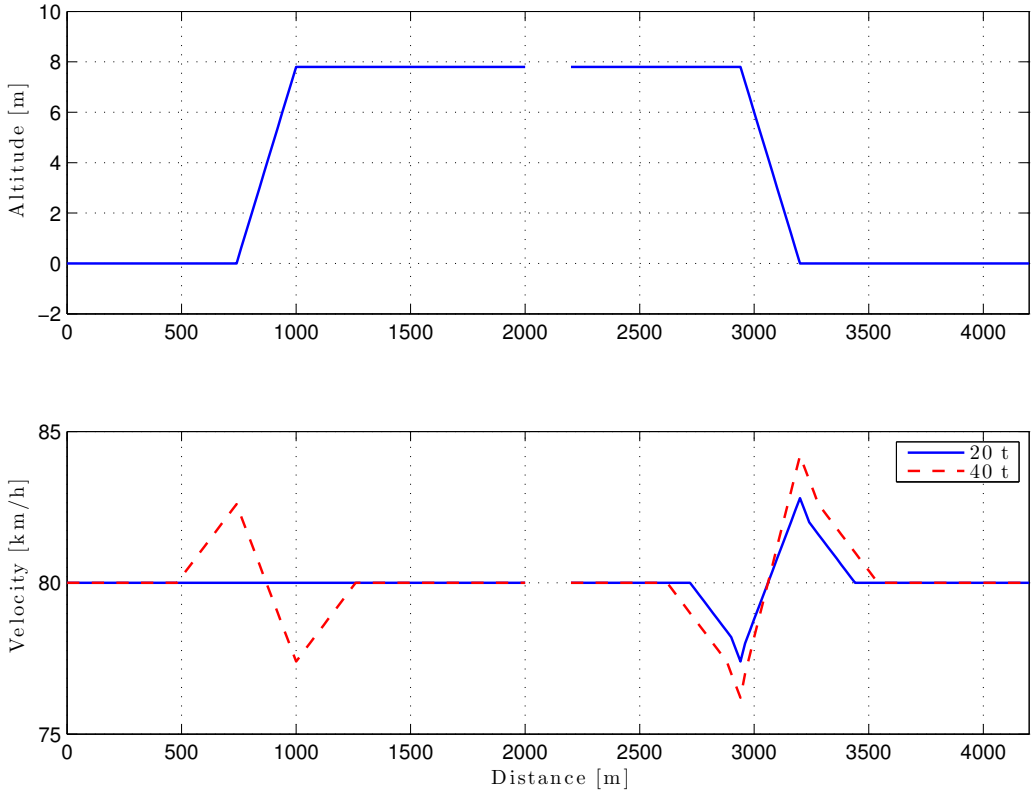

Figure 7.1: Fuel-optimal velocity profiles for a single HDV. The top plot shows the topography of the roads, where the uphill segment on the left side of the plot has a road gradient of 3 % and the downhill segment on the right side of the plot has a gradient of −3 %. The bottom plot shows the corresponding LAC velocity profiles for a light and a heavier HDV. The velocity profiles for the light vehicle is the solid (blue) line labeled as 20 t and for the heavier vehicle is the (red) dashed line labeled as 40 t.

of the HDV. The LAC[1] strategies for a single vehicle that is facing an uphill and downhill segment are shown in Figure 7.1. The top plot shows the road altitude profiles and the bottom plot shows the corresponding LAC velocity profiles for a light, 20 t, and a heavier, 40 t, HDV[2], with otherwise identical configuration. The vehicle is initially traveling at a road speed of 80 km/h and the difference in mass is chosen to illustrate how the LAC strategy varies for different vehicle characteristics. When facing an uphill segment the LAC strategy for the light vehicle is to maintain a constant velocity, since it is fuel-optimal to maintain a constant speed if possible, given that the traveling time is fixed (Chang and Morlok, 2005; Fröberg, 2008). However, for the heavier vehicle, which is not able to maintain the velocity over the uphill segment due to its extensive mass, the LAC strategy is to increase the

[1] A detailed description of the LAC is given in Section 7.2.
[2] 40 t is the maximum allowed weight for long-haulage HDVs in most European countries.

velocity before the hill to minimize the variation around the road speed. Similarly, when facing a downhill segment, the LAC strategy is to reduce the velocity before the downhill segment to avoid excessive braking, which becomes necessary if the vehicle exceeds an acceptable offset from the road speed limit when coasting along the decline.

It is not obvious how to extend LAC for a single vehicle to look-ahead control for HDV platooning. The individual optimal LAC strategies are not consistent with maintaing a constant inter-vehicle spacing for air drag reduction, which is the aim in HDV platooning. The instantaneous fuel consumption of a single HDV can increase by a factor of four, from 0.3 l/km to 1.2 l/km, over a steep uphill segment when the engine is operating at maximum torque. Hence, the air drag reduction has a lower effect on the total resistive forces that are exerted on an HDV in motion over steep hills. Furthermore, the individual LAC strategies might not be feasible when traveling in a platoon, since, for example, increasing the velocity prior to an uphill segment implies that the minimum safe distance constraint is transgressed if the preceding vehicle does not adjust its velocity. Hence, it is unclear whether or not it is feasible or fuel-efficient to utilize preview road gradient information in control for HDV platooning. A question arises of whether it is more fuel-efficient to maintain the platoon when traversing a hill or let the HDVs separate and then catch up, during or after the hill. Thus, it becomes interesting to investigate whether it is fuel-efficient to utilize a controller based on road preview information for HDV platooning, or if commercial controllers that aim to maintain the inter-vehicle spacing without considering the road characteristics are sufficient in this regard. Moreover, the computational cost for solving the dynamic programming in the LAC is exponential in the state dimension. Thus, a centralized solution is too computationally expensive for online applications and in general hard to solve for a large number of vehicles. Hence, the objective for the study in this chapter is to find a computationally feasible and fuel-efficient control strategy for HDV platoons when traversing steep uphill or downhill segments.

The main contribution of this chapter is to determine a fuel-efficient behavior for an HDV platoon when traversing a hill. We study commercially available controllers that could be utilized for platooning and propose two novel fuel-efficient controllers for HDV platooning based on road grade preview information. The proposed controllers are established with low computational complexity, since it is generally not possible to implement complex control algorithms due to the limited computational power in the on-board electronic control units. We study system uncertainties that commonly occur in practice, which might cause errors or loss of performance for the proposed controller. We also study the effect of a varying road topography and system uncertainties on the fuel consumption for HDV platooning. Hence, guidelines are determined for handling common system uncertainties that occur in practice, to maintain the fuel reduction potential. Furthermore, we investigate whether it is better to split up or maintain a platoon over steep hills and show that it is most fuel-efficient to maintain a platoon when traversing a hill as opposed to split the platoon and resume it during or after the hill. It is shown that the commercially

available adaptive cruise control (ACC) is not fuel-efficient for a varying topography and that the LAC for a single HDV is not practical in HDV platooning. Hence, we propose a cooperative look-ahead controller for platooning (CLAC), where the main idea is to initiate the control actions in a platoon based on a point in the road rather than simultaneously implementing each HDV's control action to maintain a fixed spacing.

The outline of this chapter is as follows. First we present the system model in Section 7.1, which serves as the basis for the model predictive controllers that are presented in Section 7.2. The behavior of the proposed controllers and commercially available controllers that can be used as an alternative, are evaluated in Section 7.3. Numerical results for the controllers are presented in Section 7.4. The effects that common system errors in practice have on the fuel reduction potential of the proposed controller is studied in Section 7.5. Finally, in Section 7.6 we present a brief summary of the results.

7.1 System Model

In this section, we present the vehicle dynamics and fuel consumption models that serve as a basis for the proposed controllers in Section 7.2. Recall, from Chapter 3, that the state equation of a single HDV in a platoon can be formulated as

$$\begin{aligned}
\frac{\mathrm{d}s_i}{\mathrm{dt}} &= v_i \\
\frac{\mathrm{d}d_{i-1,i}}{\mathrm{dt}} &= v_{i-1} - v_i \\
m_{t_i}(G)\frac{\mathrm{d}v_i}{\mathrm{dt}} &= F_i^{\mathrm{e}}(\delta_i, \omega_{\mathrm{e}_i}) - F_i^{\mathrm{b}} - F_i^{\mathrm{a}}(v_i, d_{i-1,i}) - F_i^{\mathrm{r}}(\alpha(s_i)) - F_i^{\mathrm{g}}(\alpha(s_i)) \\
&= k_i^{\mathrm{e}} T_i^{\mathrm{e}}(\delta_i, \omega_{\mathrm{e}_i}) - F_i^{\mathrm{b}} - k_i^d v_i^2 \Phi_i(d_{i-1,i}) - k_i^{\mathrm{r}} \cos\alpha(s_i) - k_i^{\mathrm{g}} \sin\alpha(s_i)
\end{aligned} \tag{7.1}$$

where F_i^{e}, F_i^{b}, F_i^{a}, F_i^{r}, F_i^{g} denote the engine, brake, air drag, rolling resistance, and gravitational forces acting upon the vehicle, respectively. The absolute traveled distance for the ith HDV from a reference point common to all vehicles in the platoon is denoted as s_i, $T_i^{\mathrm{e}}(\delta_i, \omega_{\mathrm{e}_i})$ denotes the net engine torque, δ_i is grams of fuel per engine cycle and cylinder, ω_{e_i} denotes the angular velocity of the engine, $m_{t_i}(G)$ denotes the accelerated mass for the current gear G, and $i = 1, \ldots, N$ denotes the vehicle position index in the platoon. The constants $k_i^{\mathrm{e}}, k_i^d, k_i^{\mathrm{r}}$, and k_i^{g} denote the characteristic vehicle and environment coefficients for the engine, air drag, road friction, and gravitation, respectively. The state variables v_i and $d_{i-1,i}$ denote the velocity for vehicle i and the inter-vehicle spacing with respect to the preceding vehicle, as shown in Figure 7.2. $\alpha(s_i)$ denotes the road gradient and the function $\Phi_i(d_{i-1,i})$ is a nonlinear mapping of the air drag reduction with respect to the position in the platoon.

The engine is modeled after a six cylinder 420 hp Scania engine, where the engine torque during fueling for a single HDV is given as

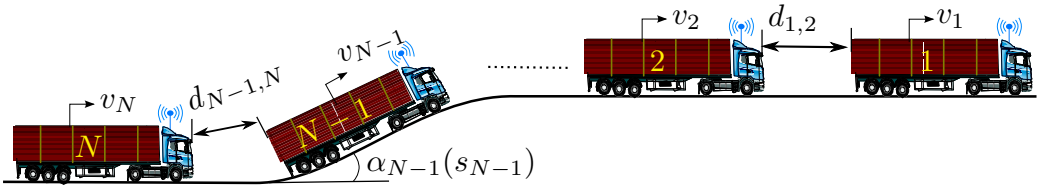

Figure 7.2: A platoon of N HDVs travelling on a road with gradient $\alpha_i(s_i)$ for vehicle i, inter-vehicle spacing $d_{i-1,i}$, and velocity v_i.

$$T_{\mathrm{e}}(\delta, \omega_{\mathrm{e}}) = a_{\mathrm{e}}\omega_{\mathrm{e}} + b_{\mathrm{e}}\delta(\omega_{\mathrm{e}}) + c_{\mathrm{e}}. \tag{7.2}$$

Here, $a_{\mathrm{e}}, b_{\mathrm{e}}, c_{\mathrm{e}}$ are characteristic coefficients, which are derived empirically from engine map data. When there is no fueling, $\delta = 0$, the vehicle is said to be coasting. The fueling is also derived empirically and given as

$$\delta(\omega_{\mathrm{e}}) = P\delta_{\max}(\omega_{\mathrm{e}}), \tag{7.3}$$

where $P \in [0, 1]$ is the normalized fueling quantity, $\delta_{\max}(\omega_e) = a_\delta\omega_{\mathrm{e}}^2 + b_\delta\omega_{\mathrm{e}} + c_\delta$ is the maximum fueling, and $a_\delta, b_\delta, c_\delta$ are constants. Hence, the fuel flow is given by

$$\dot{m}_\delta(\omega_{\mathrm{e}}, P) = \frac{n_{\mathrm{c}}}{2\pi n_{\mathrm{r}}}\omega_{\mathrm{e}}\delta(\omega_{\mathrm{e}}), \tag{7.4}$$

where n_{c} is the number of cylinders and n_{r} is the number of engine revolutions per cycle. The torque model (7.2) and fueling model (7.3) are quadratic approximations of measured data. However, since this chapter focuses on comparing different driving strategies with respect to relative fuel consumption it is deemed to be adequate and give realistic results (Sandberg, 2001).

7.2 Cooperative Look-Ahead Control

In this section, we first give a short description of the LAC for a single vehicle. A more detailed description can be found in Hellström (2010). We then present two novel controllers for platooning with road grade information.

7.2.1 Look-Ahead Control for a Single HDV

The LAC for a single vehicle is derived through model predictive control, where the road grade preview information is provided through map data. The objective is to minimize the fuel consumption with a given upper bound on the travel time, since increasing the traveling time indirectly reduces the fuel consumption due to a reduced air drag that occurs from a lower average velocity. The acceleration, brakes, and gear shifts can be controlled. Constraints, on for example control inputs, can also be included. The map data are available at given points on the road and the

optimization problem is solved numerically. Thus, we first transform the system models to the spatial domain by utilizing the chain rule, given as

$$\frac{\mathrm{d}h}{\mathrm{d}t} = \frac{\mathrm{d}h}{\mathrm{d}s}\frac{\mathrm{d}s}{\mathrm{d}t} = \frac{\mathrm{d}h}{\mathrm{d}s}v,$$

where $v > 0$ is the vehicle velocity, $h(s(t))$ denotes the considered continuous time functions in (7.1) and (7.4), and s is the distance travelled. Then the discretized process model is denoted as

$$x(k+1) = f(x(k), u(k)),$$

where $x(k) = [v(k), G(k)]^T$ and $u(k) = [P(k), \Delta G(k), F^{\mathrm{b}}(k)]^T$, at segment k on the road, are the discretized state and control vectors, respectively. The state $v(k)$ denotes the vehicle velocity and recall that $G(k) \in \mathbb{Z}^+$ is the current gear. The control inputs are the normalized fueling $P(k)$, gear change selector $\Delta G(k)$, and braking, $F^{\mathrm{b}}(k)$. Let $\mathcal{C} = \{[0,1] \times \{-1,0,1\} \times [0, F^{\mathrm{b}}_{\max}]\}$ denote the set of feasible control actions, where $F^{\mathrm{b}}_{\max}$ is the maximum braking force. Also, let the possible range of velocities be in the set $\mathcal{V} = \{v_{\min}, \ldots, v_{\max}\}$, where $v_{\min}$ is minimum accepted deviation from the road speed limit and $v_{\max}$ is the maximum allowed deviation from that speed. The corresponding finite set of gears is then denoted by $\mathcal{G}$. Finally, let the transition cost be defined as

$$V(x,u) = [1 \ c_1 \ c_2][\Delta m_\delta \ t \ |\Delta G|]^T,$$

where $t(k) = 2l/(v(k+1) + v(k))$ is the trip time over a road segment with length l, $\Delta m_\delta(k) = (m_\delta(k+1) - m_\delta(k))/l$ is the change in fuel consumption over the kth road segment, and $c_1,\ c_2$, are scalar penalty parameters. Note that the trip time $t(k)$, has been included in the cost function to relax the problem. A cost is also been put on changing the gear, since we assume in this model that a gear shift occurs instantaneously. Typically a gear shift increases the fuel consumption, since an unwanted small drop in velocity occurs, over the time it takes to disengage the active gear and engage a new gear, that must be recovered. Dividing the road grade horizon into M steps, the optimization problem can be set up as

$$\begin{aligned} J^* = \min_{u(0),\ldots,u(M-1)} & \sum_{k=0}^{M-1} V(x(k), u(k)) \\ \text{s.t. } & x(k+1) = f(x(k), u(k)), \\ & v(k) \in \mathcal{V},\ G(k) \in \mathcal{G},\ u(k) \in \mathcal{C},\ \forall k, \end{aligned} \tag{7.5}$$

The optimization problem is solved through dynamic programming (Bellman, 1957). The computational cost for solving the dynamic programming is exponential in the state dimension. However, with a given initial velocity, there is only a limited range of gears and velocities that are feasible in the search space defined by $\mathcal{V} \times \mathcal{G}$,

Algorithm 7.1 Dynamic programming for look-ahead control.

Input: Road grade $\alpha : \{0, \dots, M\} \to \mathbb{R}$, initial velocity and gear $(v_0, G_0) \in \mathcal{V} \times \mathcal{G}$
Output: $\{(v_k^*, G_k^*)\}_{k=0}^M$

$J_M(x^p) = 0, \forall\ x^p \in S_M$
for $k := M-1, \dots, 0$ **do**
  $(X_k(x^p), U_k(x^p)) \in \underset{(\hat{x}^q, \hat{u}^{(p,q)}) \in S_{k+1} \times \mathcal{C}^{(p,q)}}{\arg\min} \{V(x^p, \hat{u}^{(p,q)}) + J_{k+1}(\hat{x}^q)\},\ \forall x^p \in S_k$
  $J_k(x^p) = V(x^p, U_k(x^p)) + J_{k+1}(X_k(x^p)),\ \forall x^p \in S_k$
end for
$(v_0^*, G_0^*) = (v_0, G_0)$
for $k = 1, \dots, M$ **do**
  $(v_k^*, G_k^*) = X_k(v_{k-1}^*, G_{k-1}^*)$
end for

due to the physical properties of the system. Furthermore, braking is only considered when the upper bound in the velocity constraint is reached. Thereby, the number of control actions are reduced and the computational complexity is improved. Then, the possible states at road segment k are given by the set

$$S_k = \{x = [v, G]^T | v \in \mathcal{V}_k, G \in \mathcal{G}\}, \tag{7.6}$$

where $\mathcal{V}_k$ consists of the feasible range of velocities from the initial velocity. Let $\mathcal{C}^{(p,q)}$ be the set of all feasible control actions $u_k^{(p,q)}$ that drives the state of the system from $x^p \in S_k$ to the reachable state $x^q \in S_{k+1}$. The optimal solution is then given by Algorithm 7.1.

Recall that the fuel-optimal control for a single vehicle on a flat road is to maintain a constant velocity if possible, under the presumption that the travel time is fixed. Hence, any deviations in acceleration or deceleration result in an increased fuel consumption. Therefore, a change in reference speed is only required for steep hills, where the extensive mass of an HDV does not allow it to maintain the speed limit. We define small road gradients for an HDV, traveling in a platoon, using small angle approximation as

$$\alpha_l < \alpha < \alpha_u \tag{7.7}$$

where

$$\alpha_u(v_i, d_{i-1,i}) = \frac{k_i^e T_e(\delta_{max}, \omega_e) - k_i^d v_i^2 \Phi(d_{i-1,i}) - k_i^r}{k_i^g} > 0,$$
$$\alpha_l(v_i, d_{i-1,i}) = \frac{k_i^e T_e(\omega_e)|_{\delta=0} - k_i^d v_i^2 \Phi(d_{i-1,i}) - k_i^r}{k_i^g} < 0.$$

Here, $\alpha_u(v_i, d_{i-1,i})$ is the steepest road gradient for which the velocity can be maintained in an uphill climb with maximum net engine torque and $\alpha_l(v_i, d_{i-1,i})$ is

the steepest road gradient for which an HDV can maintain a constant velocity by coasting and not having to brake. Steep hills are thereby defined as road segments with gradients outside the range in (7.7).

7.2.2 Look-Ahead Control for HDV Platoons

By utilizing wireless communication, a cooperative control strategy can be established, where a vehicle in the platoon can receive information regarding the intended velocity profiles of its neighboring vehicles within radio range. We present two decentralized control strategies based on preview information for HDV platooning as follows, since a centralized solution is computationally too expensive for online applications and in general hard to solve for an arbitrary number of vehicles.

Adaptive Look-Ahead Control

A novel decentralized adaptive LAC (ALAC) can be derived by receiving the intended velocity profile of the preceding vehicle through wireless communication and then adaptively optimizing the velocity profile with the added constraint of avoiding a collision. We assume that the initial speed and spacing are to be resumed at the end of the spatial horizon. Because the preceding vehicle has already determined its optimal velocity strategy, it is straightforward to calculate how the spacing will change with respect to the subject vehicle at each segment in the horizon. Hence, increasing the number of states in the dynamic programming solution by adding an additional state for the inter-vehicle spacing can be avoided. Constraints on minimum spacing can be set in the optimization problem and the system dynamics, consisting of fuel consumption and vehicle motion, is now calculated as a function of spacing as well. The optimization problem (7.5) can hence be reformulated for the i:th vehicle as

$$\begin{aligned} J_i^* = & \min_{u_i(0),\ldots,u_i(M-1)} \sum_{k=0}^{M-1} V(x_i(k), u_i(k)) \\ \text{s.t. } & x_i(k+1) = f_i(x_i(k), d_{i-1,i}(k), u_i(k)), \\ & v_i(k) \in \mathcal{V}_k,\ G_i(k) \in \mathcal{G}_k,\ u_i(k) \in \mathcal{C}_k,\ \forall k, \\ & d_{i-1,i}^{\min} \leq d_{i-1,i}(k). \end{aligned} \tag{7.8}$$

For each candidate velocity trajectory obtained in the optimization problem, the inter-vehicle spacing is directly mapped over each road segment as $d_{i-1,i} = \int_0^l \frac{v_{i-1}^* - v_i}{v_i} ds$, where v_{i-1}^* is the precomputed optimal velocity trajectory for the preceding vehicle. Hence, the sought after fuel-optimal control set can be derived in the same manner as for the LAC, given an initial and final velocity and inter-vehicle spacing. The proposed ALAC is derived based on the assumption that the preceding vehicle in the platoon is not willing to change its optimal velocity strategy.

Cooperative Look-Ahead Control

Considering the case when the platooning vehicles are willing to change their velocity strategy to serve a common purpose, a new cooperative control strategy based on road grade preview information can be established. Assuming that each vehicle transmits their individual LAC strategies, the CLAC can be derived as

$$\begin{aligned} i^* &= \arg\max_i \Delta(v_i^*),\ \forall i \\ v^*(s) &= v_{i^*}(s) \end{aligned} \tag{7.9}$$

for all vehicles, where $\Delta(v_i^*) = \max_s(v_i^*(s)) - \min_s(v_i^*(s))$ is a function that computes the maximum variation in magnitude of a given LAC velocity profile. Hence, the proposed CLAC in (7.9) considers all the LAC strategies in the platoon and the velocity profile that requires the largest adjustment in velocity to address the constraint imposed by the upcoming steep hill segment is set to be the common velocity profile for all vehicles. If not all the HDVs in the platoon are within radio range, the CLAC can still be achieved through a suitable consensus algorithm (Xiao and Boyd, 2003). As opposed to following a velocity profile simultaneously, the velocity profile is tracked from the same point on the road. Hence, the follower vehicles defers their control action until they reach the point where the lead vehicle started to change its speed and cooperatively allow for small changes in inter-vehicle spacing. Illustrative examples to obtain a better intuition behind the behavior of the ALAC and CLAC strategies are provided in the next section.

7.3 Evaluation of Platoon Controls Responses

In this section, the ACC, LAC, ALAC, and CLAC behaviors are given for steep uphill and downhill segments, for which the corresponding fuel consumption results are evaluated in Section 7.4. For clarity and relevance, two neighboring HDVs of different masses, 20 t and 40 t are considered throughout this section. HDVs of equal mass would be able to maintain the same velocity with respect to any topography. Hence, the CLAC strategy in (7.9) is obtained per definition in such cases by using the LAC strategies for the individual vehicles.

7.3.1 Control Strategies for Steep Uphill Segments

For steep uphill segments, the follower vehicle is constrained to the preceding vehicle's velocity profile if the preceding vehicle is heavier. The fuel-saving potential with a road grade preview controller is negligible in this case, since it is obtained mainly by maintaing the spacing over uphill segments, as shown in Section 7.4. Therefore, only the case when a lighter vehicle precedes a heavier vehicle is considered. We introduce three commercially available control strategies as an alternative for the two proposed novel controllers. The commercially available controllers are also

used to enable comparison of the potential benefits from the proposed controllers. The vehicles are initially in steady state with a set velocity of 80 km/h and inter-vehicle spacing of 5 m before traversing the hill in each considered scenario, unless otherwise stated. Velocity and spacing between the vehicles might vary during the hill, but are resumed afterward. The velocity is not allowed to drop below $d_{i-1,i}^{\min} = 4\,\mathrm{m}$, due to safety constraints, and the allowed velocity range is constrained to $\{v_{\min}, \ldots, v_{\max}\} = \{75, \ldots, 85\}\,\mathrm{km/h}$, which is set based on legislation and driver acceptance constraints.

Figure 7.3 shows the trajectories produced by the different controllers.[3] Five velocity trajectories are shown in the middle plot for two neighboring vehicles in a platoon, where the preceding HDV, with subindex i, has a mass of 20 t and the follower vehicle, with subindex $i+1$, has a mass of 40 t. Two of the trajectories correspond to the original LAC strategy and the other velocity trajectories correspond to the ACC, the proposed ALAC, and the CLAC strategy. The top plot shows the experienced road topography for each velocity profile and the bottom plot shows the corresponding inter-vehicle spacing. As can be seen in Figure 7.3, the lead vehicle does not experience the uphill climb as steep due to its smaller mass and therefore maintains a constant speed. Hence, the LAC behaves like a CC in this case.

LAC: The individual LAC strategies for a steep uphill segment could be implemented for a vehicle in a platoon if it travelled at a larger inter-vehicle spacing, such that the safety constraint for minimum allowed relative distance is not violated. The velocity trajectories in this case are given by the solid (blue, LAC) line, denoted by v_i^{LAC}, for the preceding vehicle and the solid (magenta, LAC), denoted by v_{i+1}^{LAC}, line for the follower vehicle. The corresponding inter-vehicle spacing is given by the solid (magenta, LAC) line, denoted as $d_{i,i+1}^{\mathrm{LAC}}$ in the bottom plot of Figure 7.3. To allow for an initial inter-vehicle spacing of 5 m shortly before the uphill climb, three control strategies are given.

LAC/ACC: The dashed (red, ACC) curves display the velocity and inter-vehicle spacing profile for the first control strategy, when the follower vehicle's controller is trying to maintain the inter-vehicle spacing. This corresponds to a control strategy that is based on local state information such as the ACC. When entering the steep uphill segment the follower vehicle starts to drop in velocity even though maximum net engine torque is applied, whereas the preceding vehicle can maintain its velocity. Therefore, the inter-vehicle spacing increases initially and the controller for the follower vehicle strives to correct the error in desired inter-vehicle spacing by increasing the velocity after the hill to catch up in a fast and fuel-efficient manner. When the distance is reduced to a certain extent, the follower vehicle starts to coast, cutting off the fuel injection, and resumes platooning with lowered air drag at the point of matching the set spacing.

ALAC: The dashed-dotted (black, ALAC) velocity trajectory that is lowered

[3]Note that each controller produces a different average velocity before arriving at the hill. Thus, the hill is entered at different times, as seen in the slightly varying time position of the uphill segment plots. Furthermore, in contrast to most commercial ACCs for HDVs that are designed with respect to driver comfort, we consider a fuel-efficient ACC.

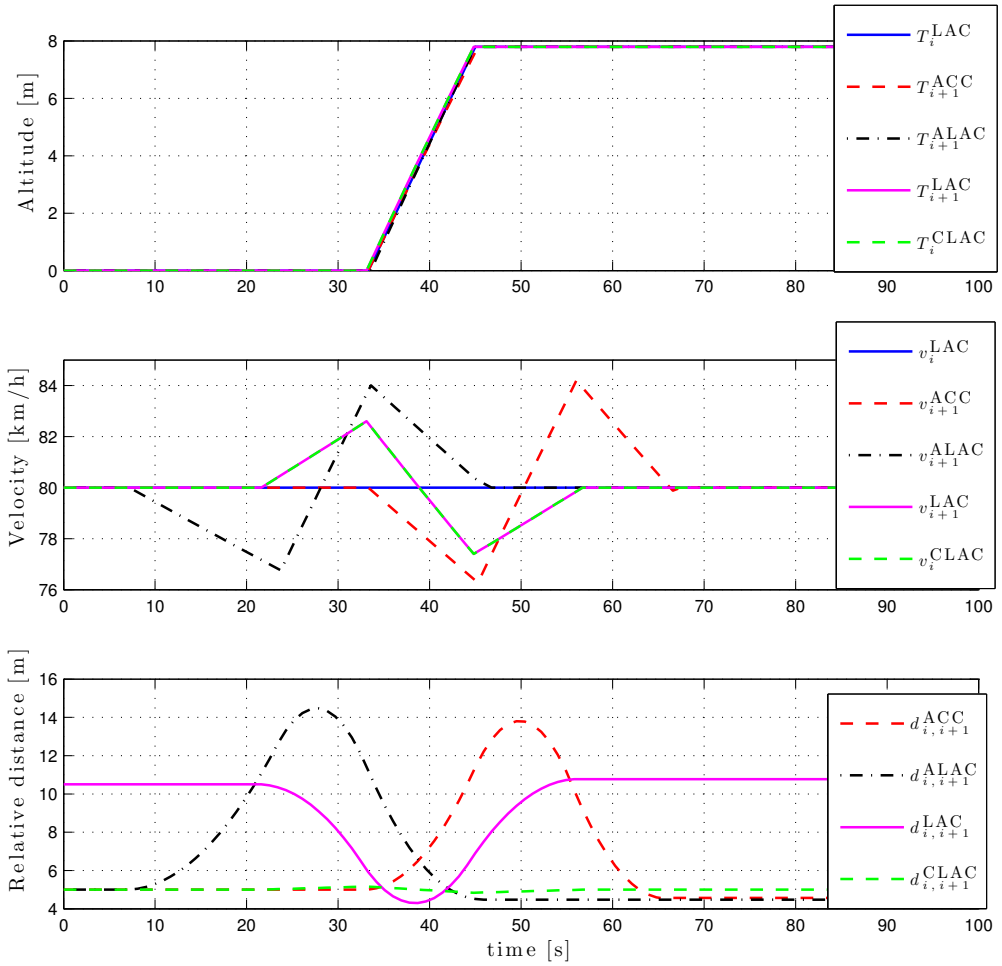

Figure 7.3: Results for different control strategies that governs neighboring HDVs in a platoon over a 240 m long uphill segment, with road grade 3 %. The total road length is 2 km. The top plot shows the experienced road topography with respect to each control strategy. The experienced topography for the preceding vehicle is denoted by T_i^z and the experienced topography for the follower vehicle is denoted by T_{i+1}^z, where $z \in \{\mathrm{LAC}, \mathrm{ACC}, \mathrm{ALAC}, \mathrm{CLAC}\}$ denotes the corresponding control strategy. The velocity trajectories for the preceding vehicle is denoted by v_i^z and v_{i+1}^z for the follower vehicle. The bottom plot shows the corresponding inter-vehicle spacing, denoted by $d_{i,i+1}^z$.

prior to the uphill climb in Figure 7.3 shows the second strategy, where the follower vehicle uses the adaptive control strategy (7.8) to avoid a collision. The controller reduces the speed by coasting and thereby increases the inter-vehicle spacing before the uphill segment. Hence, the follower is eventually able to increase its speed and follow a similar LAC profile for a single vehicle over the uphill segment. Thereby, the vehicles are able to maintain a small inter-vehicle spacing before the hill, without transgressing the safety constraint. However, the deviation from the initial

velocity varies similarly compared to the LAC/ACC combination. This could induce disturbances that are difficult to handle further downstream in the platoon.

CLAC: The dashed (green, CLAC) trajectories show the velocity profile and slight variation in spacing that occurs with the CLAC. Here, the preceding vehicle cooperatively adjusts its velocity profile to match the constrained LAC profile for the follower vehicle. Thereby, the deviation in inter-vehicle spacing is reduced compared to the previous controllers and inherently a lower air drag is achieved throughout the hill. Furthermore, if the follower vehicles downstream in the platoon follow the velocity trajectory, from the same point in the road, the heterogenous platoon will act as a homogenous platoon and reduce the variation in velocity between the vehicles in the platoon.

7.3.2 Control Strategies for Steep Downhill Segments

For steep downhill segments, the additional constraint of avoiding braking must be taken into consideration and hence, as opposed to control for steep uphills, both cases of having a lighter or heavier preceding vehicle compared to the follower vehicle is addressed. The trajectories for facing a downhill segment when the heavier HDV is preceding the lighter HDV are shown in Figure 7.4. They are subindexed by i for the preceding vehicle and by $i+1$ for the follower vehicle. The top plot shows the experienced road topography, the middle plot shows the velocity trajectories based on the corresponding control strategy, and the bottom plot shows the inter-vehicle spacing with respect to each velocity profile. Four different control strategies are illustrated in Figure 7.4.

LAC: The trajectories with superindex LAC shows the case when the LAC strategy is utilized by both vehicles and the inter-vehicle spacing is 8.7 m, so that the lower boundary of 4 m is not breached.

CC/ACC: The dashed (red, CC) lines display the trajectories for when the preceding vehicle is governed by the commercial CC and the follower vehicle is governed by the ACC. The corresponding relative distance, which is kept constant with the ACC, is given in the bottom plot. The CC has no information regarding the oncoming topography. Thus, the velocity increases when entering the downhill segment and it is forced to brake when it exceeds the allowed velocity limit. The follower vehicle tracks the velocity with its ACC and is able to maintain the inter-vehicle spacing throughout the hill to obtain the benefits from a low air drag. However, it is forced to brake eventually and thus reduces the fuel-saving potential.

ALAC: The dashed-dotted (black, ALAC) trajectories display the ALAC strategy for when the follower vehicle receives information through wireless communication regarding the preceding HDV's LAC velocity profile. Thereby, it can adapt and avoid a collision by initially reducing its speed to increase the inter-vehicle spacing and then compensate by maintaining the gained speed over the downhill segment a while afterward. When the spacing is increased, the follower vehicle finally reduces its velocity by coasting to match the desired spacing and speed of the preceding vehicle. Hence, for this case, the ALAC finds a strategy such that the initial inter-vehicle

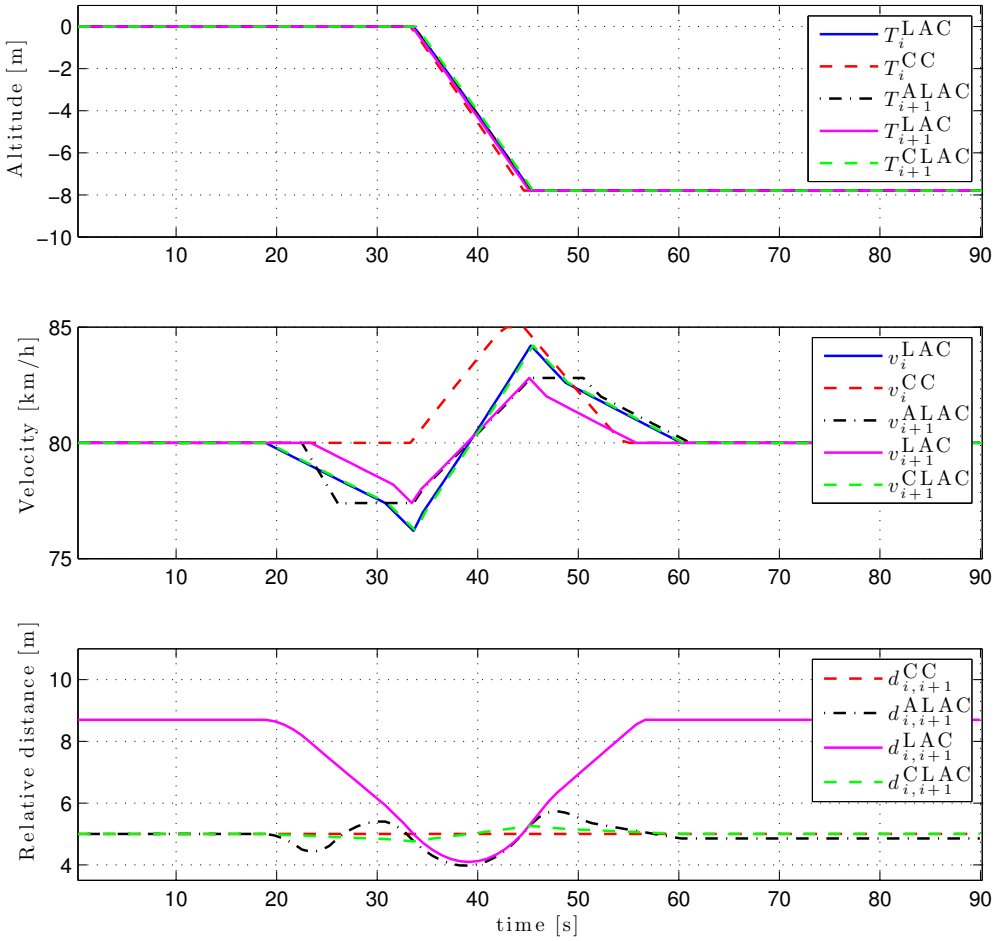

Figure 7.4: Results for different control strategies governing neighboring HDVs in a platoon during a 240 m long downhill segment with road grade -3 %. The heavier HDV is preceding the lighter HDV. The total road length is 2 km. The displayed profiles are denoted the same as previously, in Figure 7.3, to indicate the corresponding control strategy and platoon position.

spacing of 5 m can be maintained without large deviations in the desired inter-vehicle spacing and without having to brake over the downhill segment.

CLAC: The final control strategy, CLAC, is displayed by the dashed (green, CLAC) trajectories. The controller operates cooperatively by comparing the intended LAC velocity profiles for both vehicles. The heavier preceding vehicle needs to deviate its velocity the most from the nominal road speed, hence both vehicles agree to follow that profile. Consequently, the vehicles behave like a homogenous platoon and obtain the smallest deviation in inter-vehicle spacing in comparison with the other mentioned control strategies. Hence, the air drag is reduced furthest with this controller and braking over the downhill segment can be avoided.

The trajectories for the reverse order, when the preceding HDV weighs 20 t and the follower HDV weighs 40 t, are given in Figure 7.5.

LAC: For this ordering, both vehicles can use their LAC and maintain the small inter-vehicle spacing of 5 m before the downhill segment, since the follower will initiate its speed reduction before the preceding lighter HDV. Hence, there is no need for an ALAC in this case. The trajectories produced by this controller is displayed by the solid (blue, LAC) trajectory for the preceding vehicle and the solid (magenta, LAC) trajectory for the follower vehicle. The corresponding increase in relative distance is given in the bottom plot by the solid (magenta, LAC) curve.

CC/ACC: The dashed (red, CC) trajectories display the scenario when the preceding vehicle is governed by the CC and the follower vehicle is governed by the ACC. The preceding HDV does not reach the maximum speed constraint and can resume its set speed by cutting off the fuel injection throughout the downhill segment and afterward. However, the follower vehicle must brake all the way during that stretch to maintain a constant spacing due to its heavier mass.

LAC/ACC: The dashed-dotted (black, ACC) trajectories display the scenario when the preceding vehicle is governed by the LAC and the follower vehicle is governed by the ACC. In this case, the ACC must brake over the entire stretch that the preceding vehicle is adapting its speed through the LAC to address the constraints imposed by the hill.

CLAC: The trajectories for the cooperative look-ahead controller is given by the dashed (green, CLAC) curves. In this case the preceding vehicle agrees to track the trajectory of the follower vehicle, since it requires the largest velocity changes when facing the downhill segment. Thereby, the follower vehicle is able to avoid braking. The preceding vehicle vehicle has to inject a small amount of fuel to follow the agreed velocity profile. However, the small increase in fuel consumption is less than the fuel saved for the subject vehicle and the follower vehicle by allowing for a maintained small inter-vehicle spacing over the entire road stretch.

7.4 Evaluation of Fuel-Saving Possibilities

In this section, we evaluate the fuel-efficiency of the proposed controller strategies, which are based on preview information of the topography. The hill characteristics change with the grade or the length of the hill. We study the total fuel consumption for two neighboring HDVs that travel over a 2 km long road with a 240 m or 320 m steep hill. The length of the hill is chosen such that it is a significant part of the total road stretch and the road grade for the considered uphills and downhills is 3 % and -3%, respectively. The most fuel-efficient controller is determined for the considered hills. Finally, we apply the proposed CLAC on an $N = 9$ HDV platoon of masses ranging between 20 t to 40 t and evaluate the performance for two hills.

The relative fuel consumption for two HDVs of masses 20 t and 40 t traveling as a platoon facing an uphill segment are given in Table 7.1. Table 7.2 lists the relative fuel consumption when facing a downhill segment with the preceding HDV being

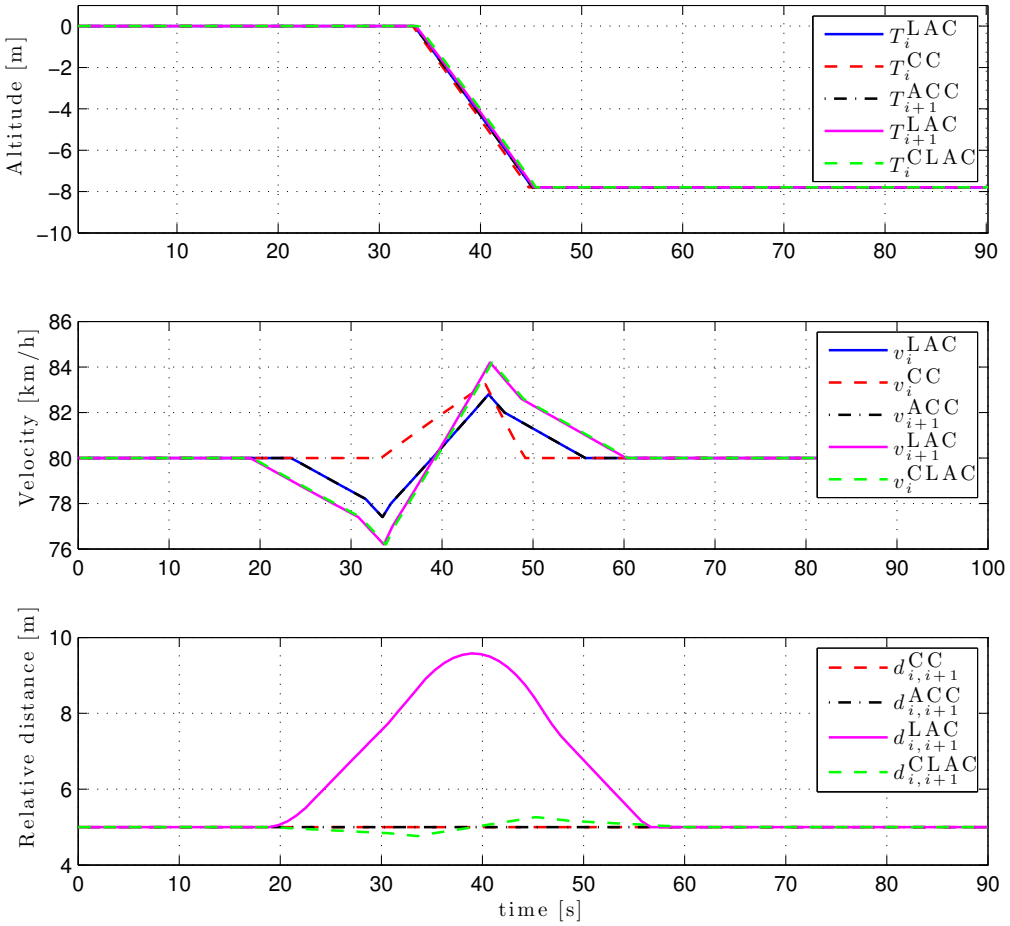

Figure 7.5: Trajectories for different control strategies governing neighboring HDVs in a platoon during a 240 m long downhill segment with road grade -3 %. The lighter HDV is preceding the heavier HDV. The total road length is 2 km. The displayed profiles are denoted the same as in Figure 7.3, to indicate the corresponding control strategy and platoon position.

heavier and Table 7.3 lists the results when facing a downhill segment with the preceding HDV being lighter. The relative fuel consumption is given in comparison with the total fuel consumption of two HDVs traversing the hills alone with their individual LAC, which is denoted as Nominal in the tables. The Hypothetical controller gives the scenario when both HDVs are governed by the optimal LAC for a single HDV and hypothetically obtain the air drag reduction for having a constant relative distance of 5 m to the neighboring vehicle. It is not practically feasible, but gives the theoretically highest obtainable fuel reduction. The first column lists the controllers that are considered in the order {preceding, follower}, the second column gives the relative fuel consumption obtained for a 240 m long hill, and the third column gives the relative fuel consumption obtained for a 80 m longer hill. The

average velocity for all the control strategies, except for the {CC, ACC} combination when traveling downhill, is 80 km/h. The vehicles travel at an initial inter-vehicle spacing of 5 m, unless otherwise stated. A 5 m inter-vehicle spacing corresponds to a 42 % air drag reduction for the follower vehicle and a 8 % air drag reduction for the preceding vehicle (Wolf-Heinrich and Ahmed, 1998).

7.4.1 Fuel Savings over Steep Uphill Segments

The results in Table 7.1 show that there is a vast fuel-saving potential in platooning when traversing an uphill segment compared to the nominal case. Increasing the inter-vehicle spacing to 10.5 m so that both vehicles can maintain their individual LAC strategies without violating the minimum spacing constraint is more fuel-efficient compared to governing the preceding HDV with the LAC and the follower vehicle with the ACC at the same spacing setting. It is more fuel-efficient to govern the preceding vehicle with the LAC and the follower vehicle with the ACC at a smaller spacing setting of 5 m. The ALAC strategy that aims to increase the spacing before the uphill climb is not as fuel-efficient in comparison for this case. The maximum fuel reduction of 7.8 % is obtained with the cooperative CLAC strategy, when the lighter vehicle refrains from its own LAC and complies with the constrained follower vehicle profile. Note that if the order of the HDVs were reversed the fuel reduction would be the same for the CLAC, since the air drag is not mass dependent. The third column of Table 7.1 shows that an improved fuel reduction of 0.7 % can be obtained with the CLAC compared to the commercially available {LAC, ACC} combination, where the LAC for the lighter preceding HDV, shown in Figure 7.3, behaves like a CC in this case. It can also be seen that the fuel-saving potential is decreased for a longer uphill segment. Increasing the length of the uphill segment forces the HDVs who cannot maintain their velocity to reduce their speed in the uphill more in comparison with the shorter uphill segment. This is equivalent to the behavior for a steeper uphill segment. For very steep uphill segments, where the HDV reaches its speed boundary, no additional fuel saving can be obtained with a road grade preview controller.

7.4.2 Fuel Savings over Steep Downhill Segments

Table 7.2 shows that it is more fuel-efficient to govern the preceding vehicle with the CC and the follower vehicle with the ACC for an inter-vehicle spacing of 5 m compared to the nominal case of traveling alone with the LAC. The fuel consumption is reduced further by increasing the inter-vehicle spacing so that both HDVs can be governed by their individual LAC without violating the minimum spacing constraint. The fuel-efficiency is further improved by governing the follower vehicle with the ACC at the same initial spacing. Using the ALAC further reduces the fuel consumption. However, governing the lead vehicle with the LAC and the follower vehicle with the ACC at a spacing of 5 m is more fuel-efficient. The maximum fuel reduction is obtained with the CLAC strategy. For a downhill segment this controller has a

Table 7.1: Table of relative fuel consumption for different uphill control strategies with a lighter preceding HDV. The uphill segment has a grade of 3 %.

Controllers: $\{HDV_i, HDV_{i+1}\}$	Fuel Consumption [%] (240 m uphill)	Fuel Consumption [%] (320 m uphill)
Nominal	100	100
{LAC, ACC}∗	93.50	95.34
{LAC, LAC}∗	93.00	94.29
{LAC, ACC}	92.50	93.45
{LAC, ALAC}	92.54	93.20
{CLAC, CLAC}	92.24	92.81
Hypothetical	92.23	92.76

* Results obtained for initial inter-vehicle spacing of 10.5 m for the 240 m segment and 15.5 m for the 320 m segment.

Table 7.2: Table of relative fuel consumption for different downhill control strategies with a heavier preceding HDV. The downhill segment has a grade of -3 %.

Controllers: $\{HDV_i, HDV_{i+1}\}$	Fuel Consumption [%] (240 m downhill)	Fuel Consumption [%] (320 m downhill)
Nominal	100	100
{CC, ACC}	91.97	96.07
{LAC, LAC}∗	88.12	87.80
{LAC, ACC}∗	88.10	88.47
{LAC, ALAC}	87.88	87.04
{LAC, ACC}	87.17	86.04
{CLAC, CLAC}	87.15	86.03
Hypothetical	87.65	86.76

* Results obtained for initial inter-vehicle spacing of 8.7 m for the 240 m segment and 12 m for the 320 m segment.

higher fuel reduction than the hypothetic case. As opposed to traveling in an uphill, when traveling in a downhill the air drag has a larger effect on the required engine torque input to handle the imposed constraints. Therefore, the LAC is no longer optimal in a downhill due to the lowered air drag. Hence a slightly higher fuel saving is obtained for the CLAC strategy.

Table 7.3 shows it is still more fuel-efficient to platoon by governing the preceding 20 t vehicle with the CC and the follower 40 t vehicle with the ACC in the 240 m long downhill segment, compared to the nominal case. However, for the 320 m

Table 7.3: Table of relative fuel consumption for different downhill control strategies with a lighter preceding HDV. The downhill segment has a grade of -3 %.

Controllers: $\{\text{HDV}_i, \text{HDV}_{i+1}\}$	Fuel Consumption [%] (240 m downhill)	Fuel Consumption [%] (320 m downhill)
Nominal	100	100
{CC, ACC}	97.80	100.77
{LAC, ACC}	91.15	91.91
{LAC, LAC}	87.83	87.52
{CLAC, CLAC}	87.50	86.65
Hypothetical	87.65	86.76

long downhill segment it would have been more fuel-efficient for the vehicles to travel alone with their individual LAC. During the longer downhill segment a larger amount of energy is wasted, since the follower HDV is forced to brake when they are governed by the CC and ACC respectively. The same conclusion can be drawn for the {CC, ACC} combination in Table 7.2, with the reverse ordering of the HDVs. Governing the preceding vehicle with the LAC and the follower vehicle with the ACC improves the fuel-efficiency, but the same issue of braking arises for a longer downhill segment. Both individual LAC can be used for the given vehicle order without compromising safety, which further reduces the fuel consumption. The highest fuel reduction is obtained for the CLAC strategy. An improved fuel reduction of 14 % can be obtained in this case with the CLAC compared to the {CC, ACC} combination. A longer downhill segment enables an increased fuel saving irrespective of vehicle order with the CLAC. Note that the fuel reduction is slightly different for the CLAC in Table 7.2 and Table 7.3. This is due to a varying engine efficiency at different engine speeds in the engine model (7.2). The air drag reduction experienced by each HDV will be different based on the vehicle order. Hence, the required engine torque to facilitate the decelerations will differ, which results in the differences in fuel reduction. However, the energy required at the wheels to propel the HDVs forward is the same irrespective of vehicle order.

7.4.3 Fuel Savings for an N-HDV Platoon over Steep Hills

When facing both the uphill or a downhill segments the results show that the CLAC is the most fuel-efficient control strategy. However, the results in Tables 7.1–7.2 show that there is only a slight difference in fuel saving obtained from the CLAC compared to letting the preceding HDV be governed by the LAC and the follower vehicle by the ACC. The main fuel saving is obtained from the air drag reduction by maintaining the small inter-vehicle spacing. Using the ACC implies that the HDVs simultaneously change their velocity. The lead HDV accelerates to resume the road

speed after exiting the uphill segment. The follower vehicles in a platoon would then have to accelerate in the uphill climb, which is not always feasible. Similarly, the lead HDV decelerates after exiting a downhill segment. The follower vehicles, still traveling along the downhill segment, would then have to brake with the ACC, which is fuel-inefficient. Hence, even though the commercially available controllers might be fuel-efficient for two vehicles, disturbances in the sense of large variations in velocity and inter-vehicle spacing will grow for a longer platoon, which requires excessive control actions in handling. Thus, it is both fuel-efficient and desirable in practice to implement the CLAC strategy, which initiates the change in velocity at a specific point in the road for all HDVs, as opposed to simultaneously changing the velocity to maintain the spacing.

Fig 7.6 shows the trajectories for an $N = 9$ heterogeneous HDV platoon traversing an uphill and a downhill segment with the CLAC strategy. It can be observed from the offset in the velocity trajectories given in the middle plot, that each vehicle defers its control action to track the agreed velocity profile until it reaches the same point. The top plot shows that the uphill segment is entered when each HDV in the platoon reaches the maximum velocity and equivalently for the downhill segment. The bottom plot shows that there is an equal change in the inter-vehicle spacing between all HDVs. A fuel-saving of 12.1 % over the 2 km long road with the uphill segment and a fuel-saving of 18.7 % over the road of same length with a downhill segment is achieved for the whole platoon in total compared to if each HDV would have traveled the same road profile alone with their individual LAC. Hence, the fuel savings are significant for a long HDV platoon. The proposed CLAC produces a homogeneous platooning behavior, which allows for a maintained small inter-vehicle spacing. Thereby, accelerations over uphill climbs and unnecessary braking are avoided. It also produces a robust behavior in the sense that largely varying behavior between the platooning vehicles for addressing topography constraints can be avoided.

7.5 Influence of System Uncertainties

The proposed CLAC is based on the most restrictive LAC velocity profile in the platoon. However, the vehicle parameters might change over time due to ageing or damage. The vehicle mass is generally estimated and hence not known perfectly. Furthermore, the global positioning system (GPS) accuracy can vary and the map data might contain measurement errors. In this section, we give a qualitative analysis based on simulation results for how such system uncertainties affects the fuel-saving potential.

We study two different types of system uncertainties: vehicle parameter errors and road parameter errors. The main focus is directed toward the vehicle that determines the CLAC strategy. Vehicle parameter errors have a direct influence on the obtainable acceleration of the vehicle over the hill segment during coasting or when maximum torque is applied. Uncertainties are typically known to exist

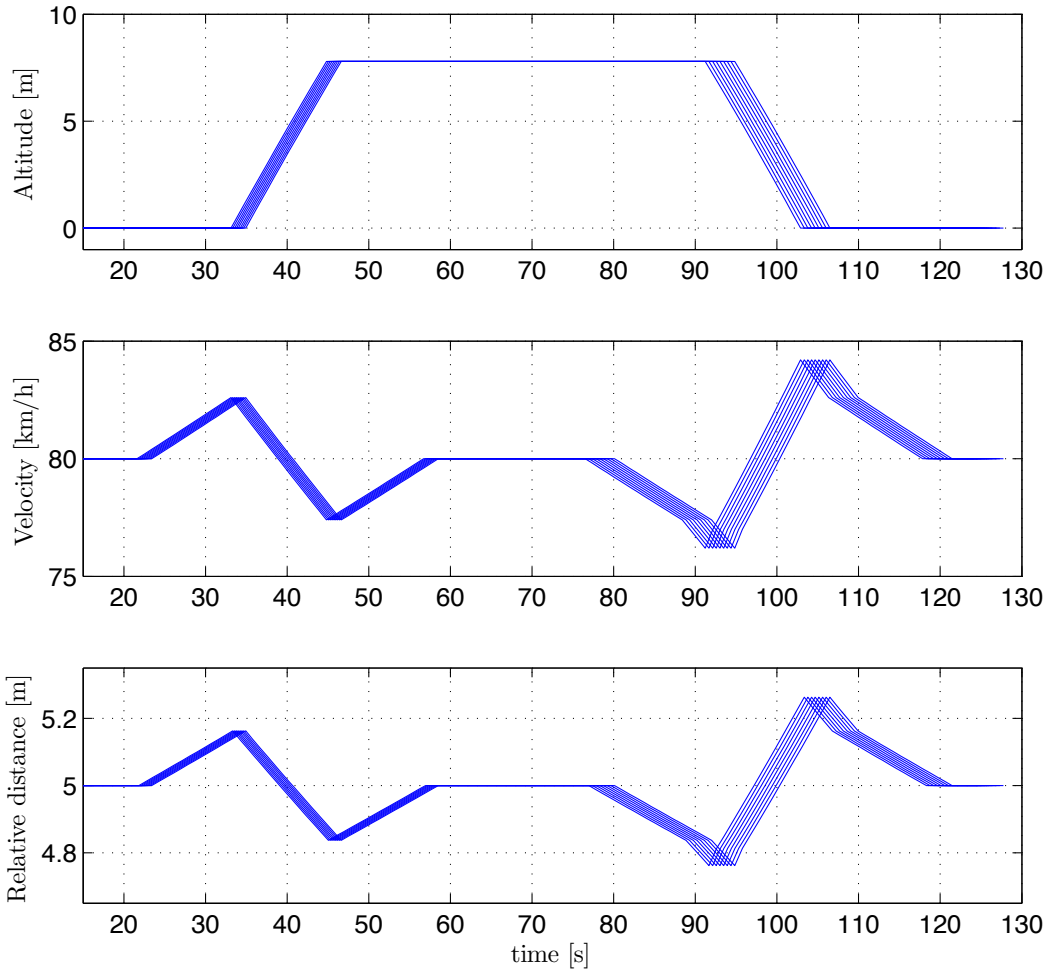

Figure 7.6: Trajectories produced by the CLAC strategy for an $N = 9$ HDV platoon traveling over a 4 km long road with uphill and downhill segments of 240 m. The lead HDV's trajectories are the ones that change earliest. The mass configuration of the platoon is $[m_1, \ldots, m_9] = [20, 25, 30, 35, 40, 35, 30, 25, 20]$ tons, which are common for long-haulage HDVs in Europe. The top plot shows the experienced topography for each HDV. The middle plot shows their velocity trajectory and the bottom plot shows the corresponding inter-vehicle spacing between neighboring vehicles.

in the wheel radius, conversion efficiencies in the powertrain, maximum available engine torque, the roll resistance coefficient, and vehicle mass. The vehicle mass contains the largest uncertainty and has the most significant effect on the HDV dynamics. The variation of the CLAC velocity profile increases with the mass. If the mass is overestimated when traveling over a downhill segment, the expected acceleration will not be obtained. In this case, the platooning HDVs can simply inject a small amount of fuel to obtain a higher acceleration and follow the common CLAC velocity trajectory. However, if the mass is underestimated, the vehicle will

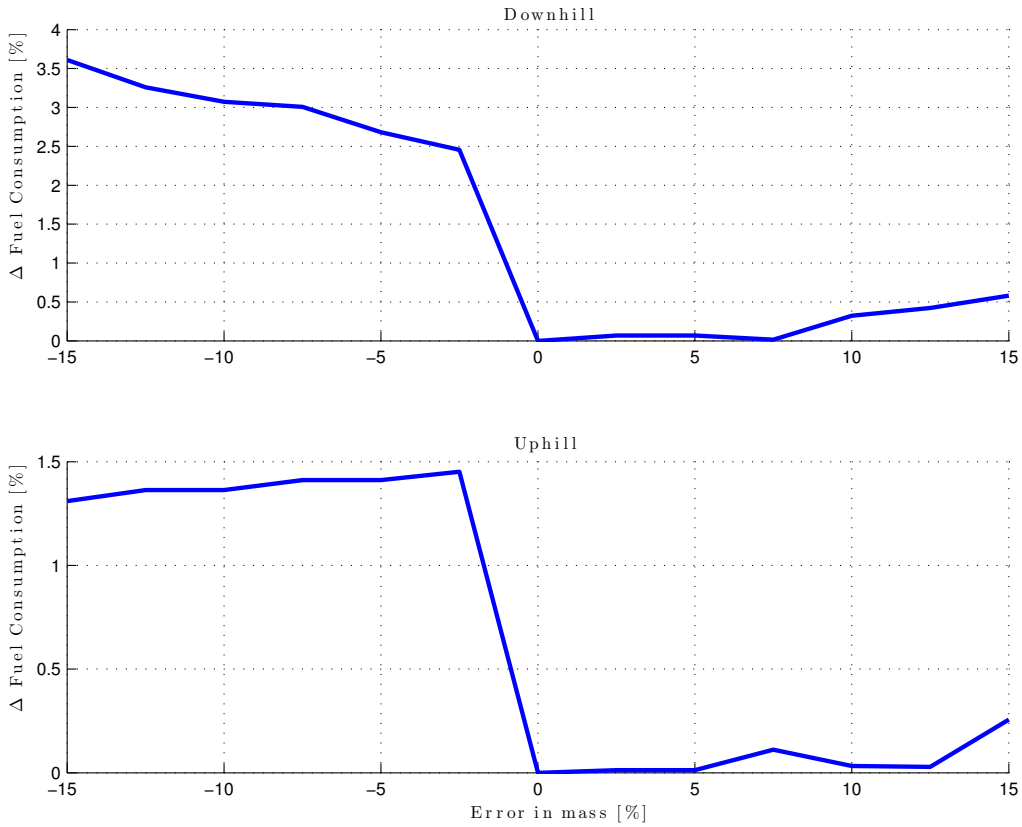

Figure 7.7: Change in fuel consumption due to an error in mass with the CLAC strategy for an $N = 5$ HDV platoon. The mass configuration of the platoon is $[m_1, \ldots, m_5] = [20, 30, 40, 30, 20]$ tons. The results in the top plot are based on the fuel consumption for the entire platoon, when travelling over a 2 km long road with a downhill segment of 240 m and a $-3.8\,\%$ road grade. The bottom plot results are derived for an equally long uphill with $3\,\%$ slope.

have no choice but to apply the brakes to maintain a lower acceleration. The top plot in Figure 7.7 shows how a percentage error in mass, of the HDV that determines the CLAC strategy, affects the fuel consumption for a heterogeneous platoon of five HDVs that are traversing a downhill. It can be inferred from the results that having a negative estimation error, i.e. deriving the CLAC strategy from a model with an underestimated mass and hence causing the vehicles to brake throughout the hill, can reduce the fuel reduction potential significantly. On the other hand, overestimating the mass in the CLAC strategy only has a slight increase in the fuel consumption over a downhill compared to knowing the mass perfectly.

The bottom plot in Figure 7.7 shows the change in fuel consumption due to an error in mass, when traveling over a road with a steep uphill segment. Over a steep uphill segment, the vehicle with the largest required velocity drop, will determine the CLAC strategy for all the vehicles. If the agreed velocity profile cannot be maintained

over the uphill segment with the planned gear, a gear shift is made to obtain the necessary engine torque. A lower gear typically results in a 10–20 % increase of the net engine torque output, depending on the gear ratio configuration. However, shifting down to a lower gear will dramatically increase the fuel consumption, as can be deduced from the jump in fuel consumption when underestimating the mass that is observed in the bottom plot of Figure 7.7. The results show that deriving an CLAC strategy for the whole platoon with an underestimated mass, believing that the heaviest HDV is lighter than what it is, gives a significant increase in fuel consumption for the platoon. The small and negligible reduction in change of fuel consumption when having larger underestimated mass occurs since a lower mass will result in a CLAC strategy with less velocity variation and the gear change is then over a shorter period. However, in practice a gear change will result in a velocity drop due to a lag that occurs before being able to engage the new gear, which is not considered in our simple CLAC strategy. Hence, the improvement is unlikely to be observed in practice. All the vehicles will be able to maintain the velocity over the uphill segment if the mass is overestimated. The resulting effect on the whole platoon is that it drives a velocity profile with a higher variance than needed, which produces a slightly increased fuel consumption. Hence, it is favorable to overestimate the HDV mass given that the speed limit constraint is not violated, when determining the CLAC strategy in the presence of vehicle uncertainties.

Road parameter errors can occur due to uncertainties in GPS positioning, in map road grade information, or in map hill-length information. We do not consider the latter two errors, since iterative map updates can be performed to increase the precision in map data (Sahlholm and Johansson, 2010). Furthermore, the length and slope of a road section tend not to change significantly over time, while GPS positioning can be afflicted by larger errors. A consequence of errors in GPS positioning is that the hill will be entered earlier or later than expected. When facing an uphill segment, the HDVs will not reach the desired maximum velocity before the hill or the vehicles will reach it earlier than planned. In the latter case, the vehicles can simply maintain the maximum planned velocity and then follow the rest of the CLAC strategy when entering the hill. However, for the first case when the lead vehicle has not managed to increase its velocity sufficiently before arriving at the hill, it will have to commence deceleration immediately at that point so that the follower vehicles will be able to maintain the inter-vehicle spacing. A higher velocity is required after the hill to maintain the average velocity. In either case the increase in fuel consumption is negligible, since a LAC only increases the average velocity over uphill segments and does not reduce the fuel consumption significantly compared to the conventional CC (Hellström, 2010). Another possibility is to split up the platoon and resume platooning after the hill. However, this also does not change the fuel consumption notably.

When facing a steep downhill segment, the HDVs will initially decelerate to the desired speed and then accelerate over the decline. If the platoon believes that the downhill will occur earlier, due to a negative GPS offset along the road, all platooning vehicles are able to decelerate to the planned minimum velocity. Since

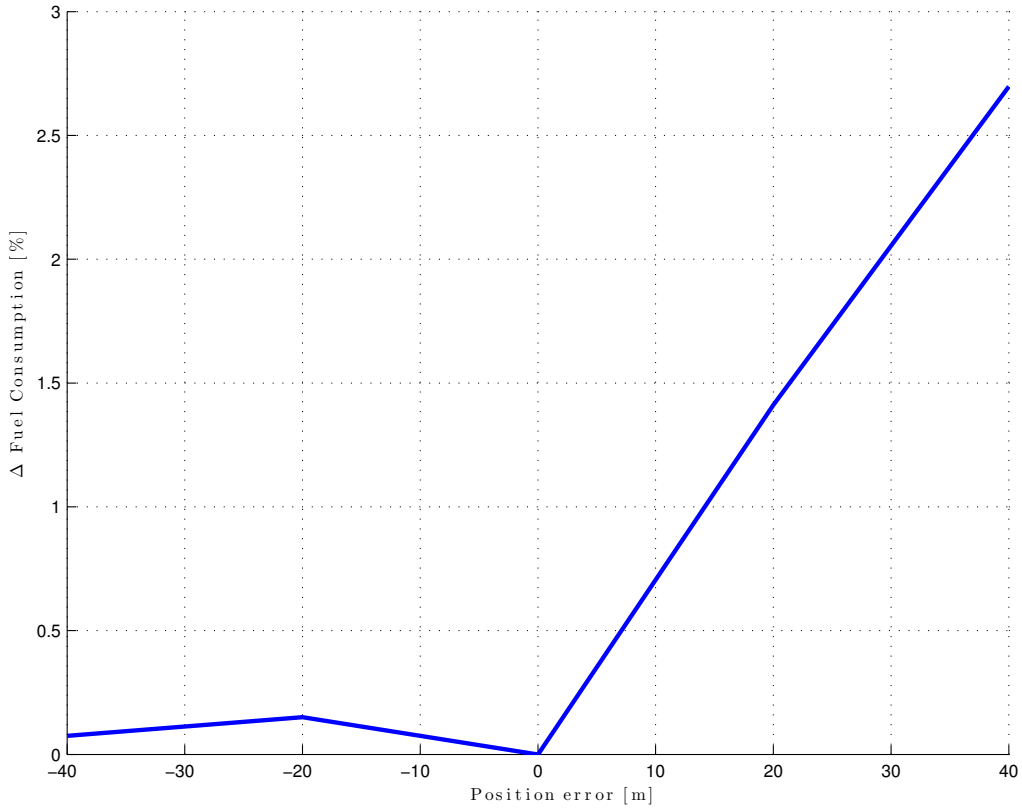

Figure 7.8: Change in fuel consumption due to an error in GPS position along the road with the CLAC strategy for an $N = 5$ HDV platoon. The mass configuration of the platoon is $[m_1, \ldots, m_5] = [20, 30, 40, 30, 20]$ tons. The results are based on the fuel consumption for the entire platoon, when travelling over a 2 km long road with a downhill segment of 240 m and a $-3.8\,\%$ road grade.

the expected acceleration does not occur, the speed can be maintained until the downhill segment is reached and the CLAC strategy can be resumed. However, if there is a positive GPS offset along the road, the vehicles will reach the downhill segment before the minimum velocity drop is obtained. The vehicles then start accelerating by coasting from a higher initial velocity than expected in the downhill. Hence, they will have to brake before exiting the hill in order not to violate the upper speed bound. The results for change in fuel consumption with respect to errors in GPS position along the road is given in Figure 7.8. It can be seen that a negative bias does not change the fuel consumption notably. However, a positive bias, which forces the vehicles to brake in the downhill, has a significant increase in the fuel consumption. Thus, it is fuel-efficient to initiate the deceleration at a sufficient distance before the hill such that the minimum velocity given by the CLAC can always be reached. Note that the increase in fuel consumption only occurs because there is an upper bound on the allowed velocity range, forcing the vehicles to brake.

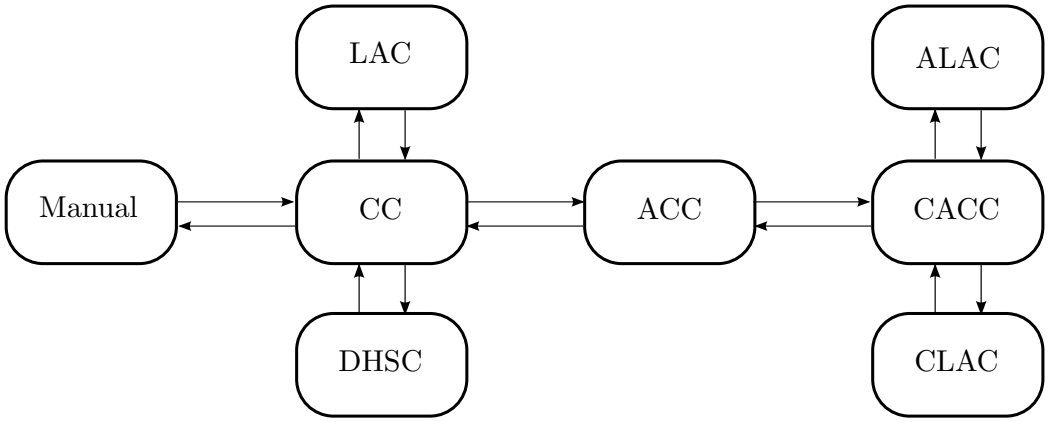

Figure 7.9: Illustration of a finite state machine for the commercially available speed control systems, given in Figure 2.4, in combination with the proposed look-ahead controller for HDV platooning. If road grade preview information is available and the vehicles in the platoon are not willing to cooperate, the ALAC is active. The CLAC is active if the vehicles are willing to cooperatively form a common look-ahead control strategy for all platooning vehicles with respect to the most restricted vehicle in the platoon. If road grade preview information is not available, the cooperative adaptive cruise control (CACC) is active. Finally, if V2V communication is lost, the ACC becomes active in the vehicle platoon and the relative distance is adjusted for safety.

7.6 Summary

It is fuel-efficient to consider the road grade preview information in HDV platooning. A simple cooperative controller for HDV platooning, based on road grade preview information and wireless communication, has been proposed that is close to the theoretically highest obtainable fuel reduction. The controller enables a homogeneous behavior for a heterogeneous platoon under topography constraints, such that the inter-vehicle spacing can be maintained for fuel-efficiency. It also produces a robust behavior in the sense that largely varying behavior between the platooning vehicles for addressing topography constraints can be avoided and inter-vehicle spacing can be maintained throughout a hill. For fuel-efficiency the platoon should be maintained when traversing a hill, as opposed to letting the HDVs separate due to imposed constraints and then resume platooning by catching up after the hill. Thus, it is favorable to have a cooperative LAC strategy, which initiates the change in velocity at a specific point in the road for all HDVs, in contrast with simultaneously changing the velocity to maintain the spacing. The presented controllers, based on road grade preview information and wireless communication, fit nicely into the already existing software control architecture in commercial HDVs, as illustrated in Figure 7.9.

The CLAC can reduce the fuel consumption for two neighboring HDVs up to 14 % over a road with a downhill segment compared to the commercially available CC and ACC that could currently be utilized for platooning in practice. For an uphill

climb, it can be observed that a more subtle benefit of 0.7 % improvement can be obtained with the proposed controller. However, the fuel-saving potential increases with the number of vehicles in the platoon. Furthermore, the CLAC is also favorable because it does not mandate any accelerations over uphill segments or braking over downhill segments, which commonly occurs for synchronous control strategies. The CLAC is also feasible in practice, since each HDV's intended velocity profile given by the commercially available LAC system can be transmitted. It is then simple to compare the profiles such that the profile with the most restrictive LAC velocity profile can be agreed upon. In the presence of vehicle parameter uncertainties, it is favorable to overestimate the vehicle mass when forming CLAC strategies to maintain the fuel reduction potential. For GPS positioning uncertainties along the road, it is fuel-efficient to assume that the hill starts earlier in the road rather than later.

Chapter 8

Experimental Evaluation of Platooning

"*The value of an idea lies in the using of it.*"

Thomas A. Edison

Cooperative control for heavy-duty vehicle (HDV) platooning can already be implemented with today's technology. Wireless communication in addition to radar information enables the possibility of forming cooperative decisions based on actions and information from the neighboring vehicles. Most studies on control for vehicle platoons have been based on simplified theoretical models, see, e.g, the survey (Tsugawa, 1999; Kavathekar and Chen, 2011). It is still unclear how the unmodeled nonlinearities, such as gear changes, brake dynamics, engine dynamics, and a varying road topography affect the control performance in practice. In particular for HDVs, the road grade has a significant effect on the vehicle dynamics: An HDV can generally not maintain its velocity when traversing steep uphill segments and it typically accelerates when coasting over a steep downhill segment. The acceleration when coasting[1] varies with vehicle mass. Hence, unwanted behavior for heterogenous platoons, such as braking to avoid coasting into the vehicle ahead, might arise over road segments with a varying topography for cooperative adaptive cruise controllers (CACCs) that are based on linear models. Even under normal operating conditions, when the platoon is traveling at constant speed, additional control actions for maintaining the desired relative distance are required, since external forces exert unmodeled disturbances on the system dynamics. Thus, it is important to understand the limitations when implementing a CACC based on simplified models. It is interesting to study the performance and evaluate the fuel-saving potential of these controllers in practice.

In this chapter we evaluate the performance of the decentralized CACC presented in Chapter 6 for a three-HDV platoon. The objective is to evaluate the performance of this simple controller and identify possible issues that might arise in a practical

[1] A vehicle is said to be coasting when it is moving forward even though no fuel is injected and no braking is applied.

setup. We present a framework for conducting experiments with repeatable results, despite varying weather conditions and other external disturbances. The direction of the wind might vary, which can have a significant effect on the air drag force. Furthermore, the air density changes with variation in temperature or humidity, the road friction changes if it rains, and traffic might also impose unplanned control actions. All these factors affect the fuel consumption. The presented results are based on data recorded over 2700 km per vehicle. Empirical results are presented for the proposed CACC through experiments conducted over a Swedish highway with varying topography. We show that a significant fuel saving can be obtained for a three-vehicle platoon with the proposed controller on roads with small road grades. However, a large varying gravitational force can excite nonlinear vehicle dynamics in practice, which has a significant influence on the performance of the closed-loop system. Consequently, the fuel savings can drastically reduce. The experiments were conducted using HDVs provided by Scania CV AB.

The outline of this chapter is as follows. First, the experiment setup and procedure for obtaining accurate and reproducible results are presented in Section 8.1. The controller performance and the fuel savings for each vehicle in the platoon are evaluated based on the experiment in Section 8.2. Finally, in Section 8.3, we discuss issues that reduce the fuel-saving potential and propose possible solutions. The chapter concludes with a brief summary in Section 8.4.

8.1 Experiment Setup

In this section, we first present the platform for implementing the CACC and the configuration parameters for the three-vehicle platoon. We then give a detailed description of how the experiments were conducted.

Three standard Scania tractor-trailer HDVs, denoted HDV_1, HDV_2, and HDV_3, are utilized with additional control and communication hardware, as illustrated in Figure 8.1. All tractors have a 4×2 vehicle configuration and the trailers have three axles. The total length of each vehicle configuration is 18 m. The third vehicle is not as tall as the other vehicles and therefore has a larger wind deflector. Nevertheless, the total frontal area, in combination with the attached trailer, is $10.2\,\mathrm{m}^2$ for all three vehicles. The masses are measured to be 37.47 t for HDV_1, 38.36 t for HDV_2, and 39.44 t for HDV_3. All vehicles are equipped with slightly different, but automatic gearboxes and they are operated with a 480 hp engine. The vehicles have a standard doppler radar, which sends the relative distance with a 40 ms interval to the central coordinating electronic control unit (ECU). The final gear ratios are slightly different for each vehicle, with $i_f = 2.92$ for HDV_1, $i_f = 2.71$ for HDV_2, and $i_f = 2.59$ for HDV_3. A small final drive implies that the vehicle will run faster for a fixed RPM of the engine and a large final drive implies that the vehicle can output a larger propulsion torque. Standard global positioning systems (GPSs) and ECUs, as utilized in Scania HDVs, are used for positioning and to execute the proposed control. A wireless sensor unit (WSU) with the standard wireless communication

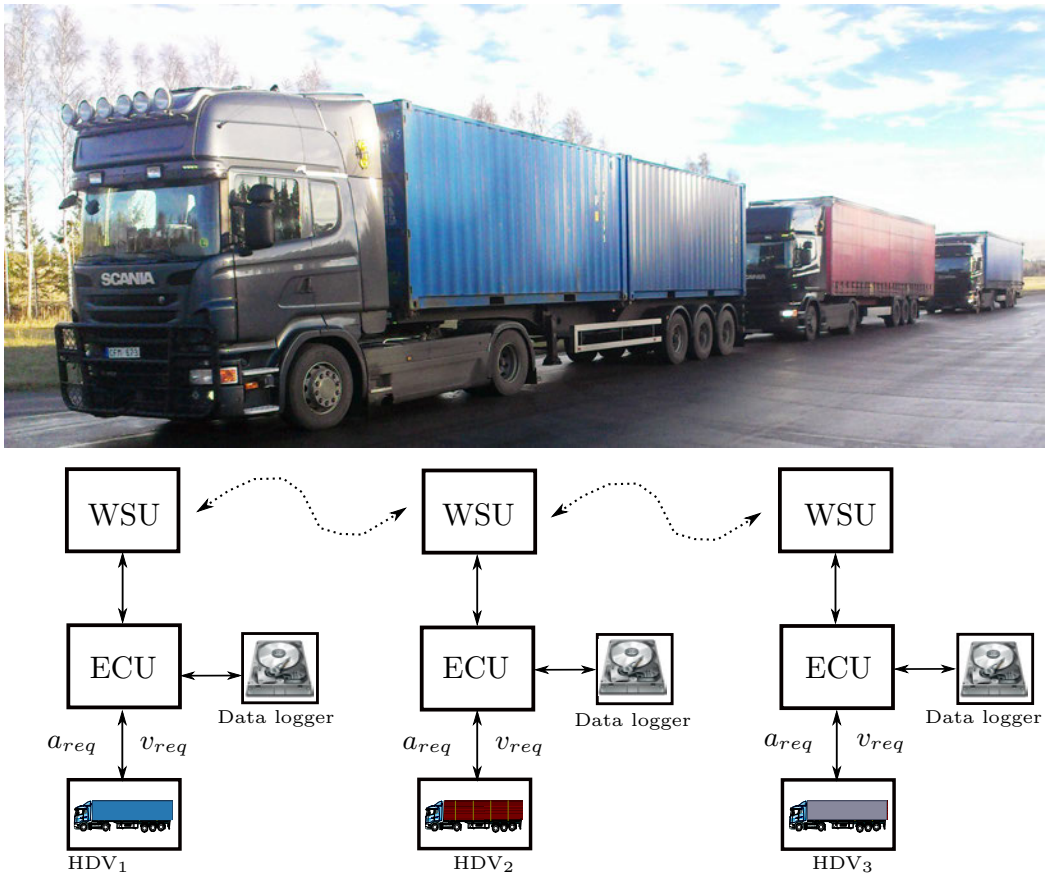

Figure 8.1: A schematic overlay of the experimental hardware setup. The top picture shows the HDVs utilized in these experiments. The left HDV is the lead. The WSU, ECU, and data logger communicate through CAN. As soon as new information is obtained through the ECU or the vehicle, it is broadcast through the WSU.

protocol IEEE 802.11p is mounted in each vehicle. The WSU is directly connected to the HDVs internal controller area network (CAN) and messages are broadcast on demand. Thereby, the internal CAN signals such as velocity, acceleration, system model parameters, and control inputs are available to all vehicles within range.

The experiments are conducted on a highway between the Swedish cities Mariefred and Eskilstuna, west of Stockholm, as shown in the map of Figure 8.2. The top plot shows the altitude profile and the bottom plot shows the corresponding road grade profile. Data are collected when the vehicles start at the cross ($\times$, red) and head westbound until they reach the circle ($\circ$, red). The vehicles then turn and data are recorded starting from the circle, heading eastbound, and finishing at the cross. We refer to one such west- plus eastbound drive as a test-run. The total road length between the markers is 45 km and, therefore, one test-run amounts to 90 km. As shown by the road grade profile, in the middle plot of Figure 8.2, the road under consideration is fairly hilly with road grade segments of $\pm 3\,\%$. To obtain

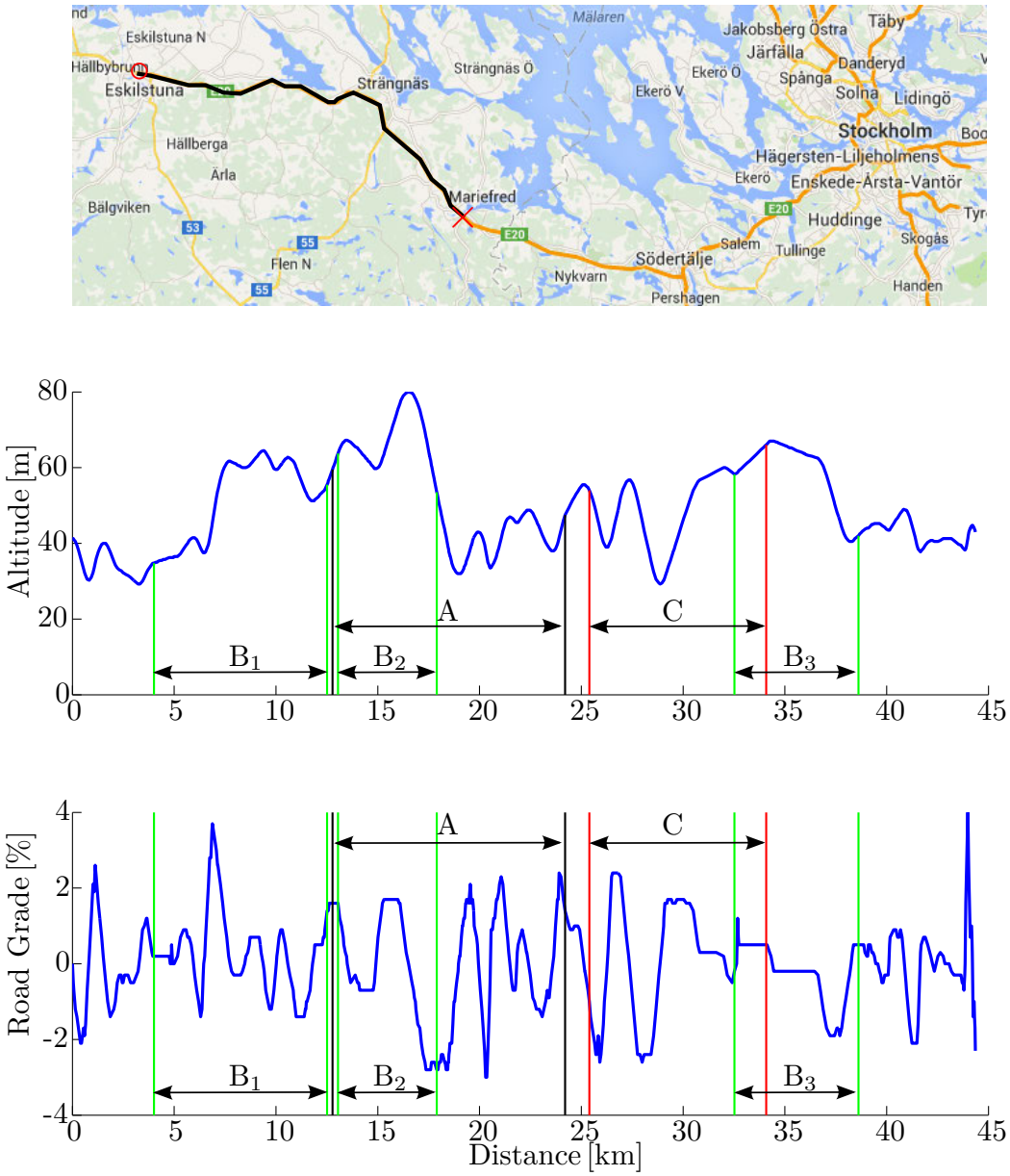

Figure 8.2: Road data for the Swedish highway between Mariefred and Eskilstuna that was utilized during the experiments. The altitude and road grade profile corresponds to the westbound part, where the vehicles start at the (red) × and finish at the (red) ∘ of the map. The road segments denoted by A, B_1, B_2, B_3, and C are discussed in Section 8.2.

normal vehicle operating temperature, the vehicles are driven 35 km before starting the test-runs, as a large amount of energy from the fueling is initially spent on heating up the various components, such as the oil for lubrication and the cabin. Six test-runs are conducted every day, over five days. Consequently, the experiments are conducted and data are collected over a total of 2700 km per vehicle. The aim is to determine the fuel-saving potential of HDV platooning and evaluate the controller performance. Two test-runs are conducted each day when the vehicles operate alone to determine the average fuel consumption over the road stretch without any air drag reduction from platooning. An additional two test-runs are conducted each day when the vehicles are operated as a platoon to investigate the change in fuel consumption over the same stretch and in similar weather conditions. In the final two test-runs of the day, the positions of the two follower vehicles are interchanged to determine if the position in the platoon has an effect on the fuel-saving potential. HDV_1 is always kept in the first platoon position to maintain the overall platoon behavior. HDV_2 and HDV_3 are follower vehicles. The vehicle speed sensor in commercial vehicles can have a slight offset. Therefore, the vehicle speed for each vehicle is calibrated with respect to the common GPS speed information before the experiment trials. The maximum allowed road speed in Sweden for HDVs with the configuration at hand is 80 km/h. However, the nominal operating speed for all vehicles was set to 75 km/h, with a downhill speed control (DHSC) offset of 10 km/h, to reduce the traffic interference as much as possible. By operating the vehicles at a lower than allowed speed, it is expected that surrounding vehicles pass the platoon and do not change the operating conditions of a test-run by cutting in-between. The CACCs of the follower vehicles are set to maintain a time headway gap of $\tau = 1\,\mathrm{s}$. Operating at closer spacings is currently not allowed in Sweden due to legislation[2].

8.2 Experiment Results

In this section, we first investigate the controller performance based on experimental results. Then, we evaluate the fuel-saving. The weather conditions change over time, which affects the instantaneous fuel consumption for an HDV and can create a variation in fuel consumption from day to day. Hence, in this section, we try to perform the experiments in a way to achieve reproducible and reliable results.

8.2.1 Controller Performance

Several test-runs are conducted. The results for one test-run over the westbound part is shown in Figure 8.3. Starting from the top, the first plot shows the altitude profile with respect to the third vehicle in the platoon. The second plot shows the velocity profiles for the three-vehicle platoon. The third plot shows the relative distance between the vehicles, where d_{12} denotes the distance between the first

[2]The Swedish law does not directly state that operating at closer spacing is illegal. It falls under the category of reckless behavior and is therefore subject to penalties.

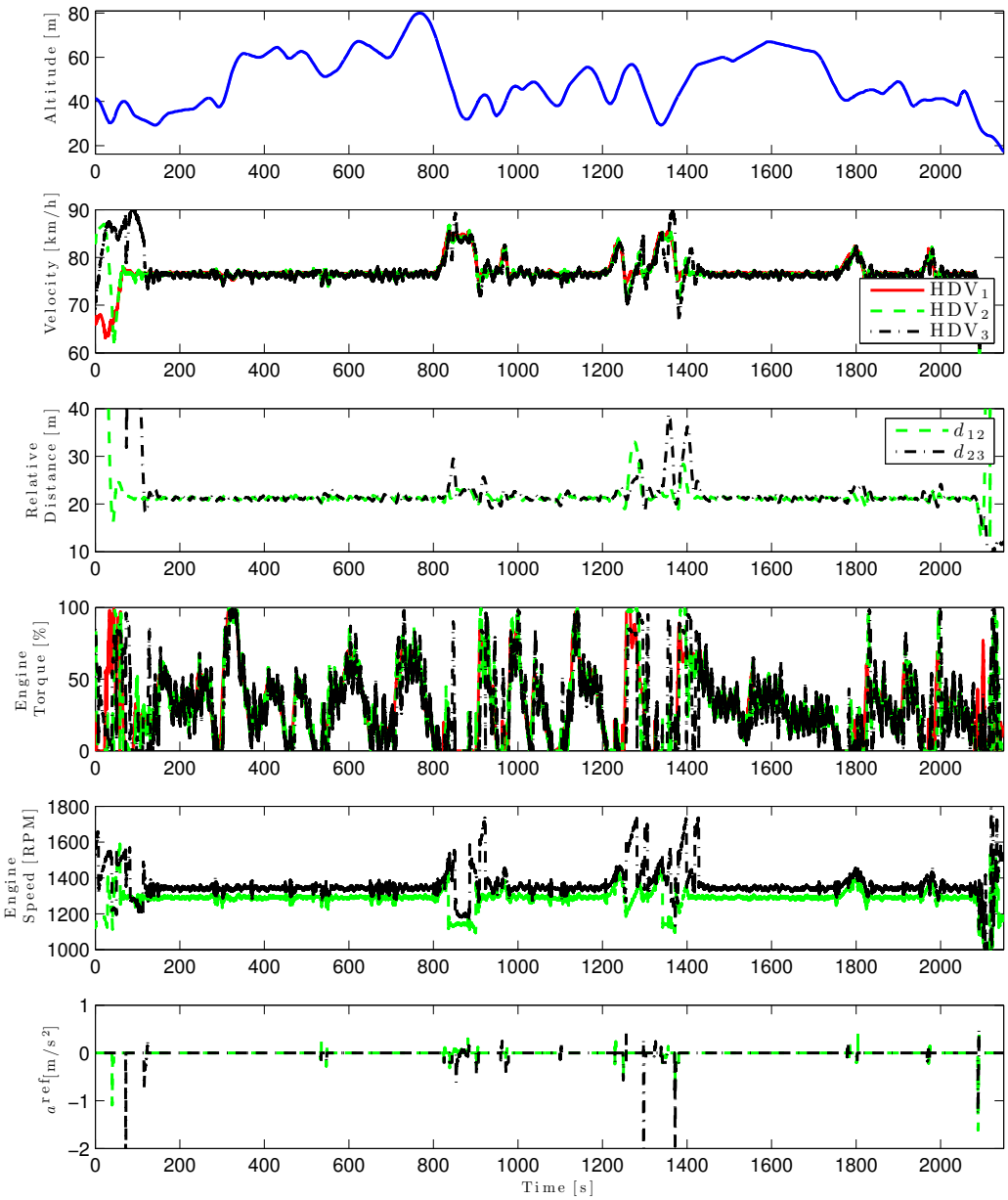

Figure 8.3: Experiment results obtained for the three-vehicle platoon traveling over the westbound part. The vehicle order for these results are HDV_1 as lead vehicle, HDV_2 as the second vehicle in the platoon, and HDV_3 is the tail-end vehicle. In all plots, except the top, the solid (red) lines are the profiles for the first vehicle in the platoon, the dashed (green) lines are the profiles for the second vehicle, and the dashed-dotted (black) lines are the profiles for the third vehicle.

and the second vehicle and d_{23} denotes the distance between the second and the third vehicle. The fourth plot shows the normalized engine torque for all vehicles. The fifth plot shows the engine speed for the second and third vehicle, where the sudden jumps in RPM, for example between the 800–900 s time markers, signify gear changes. Finally, the sixth (bottom) plot shows the corresponding brake requests. Note that a small braking force might be needed to maintain the relative distance to a lighter preceding vehicle when coasting over a downhill segment. Therefore, a positive braking request, which can be seen in the bottom plot, implies that the brakes are active to facilitate the desired acceleration.

It can be observed that the CACC works well and is able to maintain the inter-vehicle spacing over most parts of the road. The test-runs are initialized by letting the vehicles travel at a large inter-vehicle spacing followed by a merging action, as illustrated between the 0–200 s time markers in Figure 8.3. The lead vehicle is governed by a cruise control (CC) that is set at the nominal operating speed of 75 km/h. The follower vehicles are governed by the CACC, which acts as a CC if no preceding vehicle is detected. To catch up with the lead vehicle the set speed for the follower is higher than the nominal operating speed. When a wireless connection is established and relevant information is obtained, the CACC reduces the speed reference to merge with the vehicle ahead.

The velocity and relative distance between the vehicles do not vary significantly over segments with small road grade. For example, the unbiased sample standard deviations[3], over the segment denoted by B_3 in Figure 8.3 for the velocity are $\sigma_1^{\mathrm{v}} = 0.3\,\mathrm{km/h}$, $\sigma_2^{\mathrm{v}} = 0.4\,\mathrm{km/h}$, and $\sigma_3^{\mathrm{v}} = 0.4\,\mathrm{km/h}$ for the first, second, and third vehicle, respectively. Small disturbances produced by the varying road grade create a variation in velocity for the follower vehicles. This is also confirmed by the sample standard deviation for the inter-vehicle spacing, given by $\sigma_{12}^{\mathrm{d}} = 0.3\,\mathrm{m}$ and $\sigma_{23}^{\mathrm{d}} = 0.3\,\mathrm{m}$. Thus, it can be inferred that the CACC performs well when the deviations from steady-state operations are small. Moreover, as indicated by the brake requests, the follower vehicles seem to brake over steep downhill segments. Braking is required in these cases, since the follower vehicles are heavier than the lead vehicle. Thus, they coast with a higher acceleration over the downhill segments and inherently would slide in to the preceding vehicle if braking is not performed. The trajectories for the engine speed show that a braking is often followed by a gear change. Hence, a jump occurs in the engine speed as can be seen between the 800–1000 s time markers in the fifth plot.

The results in Figure 8.4, corresponding to segment A in Figure 8.2, show that unwanted braking actions can occur over steep downhill segments with the CACC due to lack of road grade information. Figure 8.4 zooms in to the interval 600–1150 s of Figure 8.3. Note that a high variation in relative velocity arise over the downhill segment between 750–950 s. Here, the first vehicle starts to coast when entering the

[3]We define the unbiased sample standard deviation as $\sigma_i = \sqrt{\frac{1}{n-1}\sum_{k=1}^{n}(y_i(k) - \bar{y}_i)^2}$, where $i = 1, 2, 3$ denotes the vehicle position index in the platoon, n is the number of samples, $y_i(k)$ is the value for the kth sample in platoon position i, and $\bar{y}_i = \frac{1}{n}\sum_{k=1}^{n} y_i(k)$

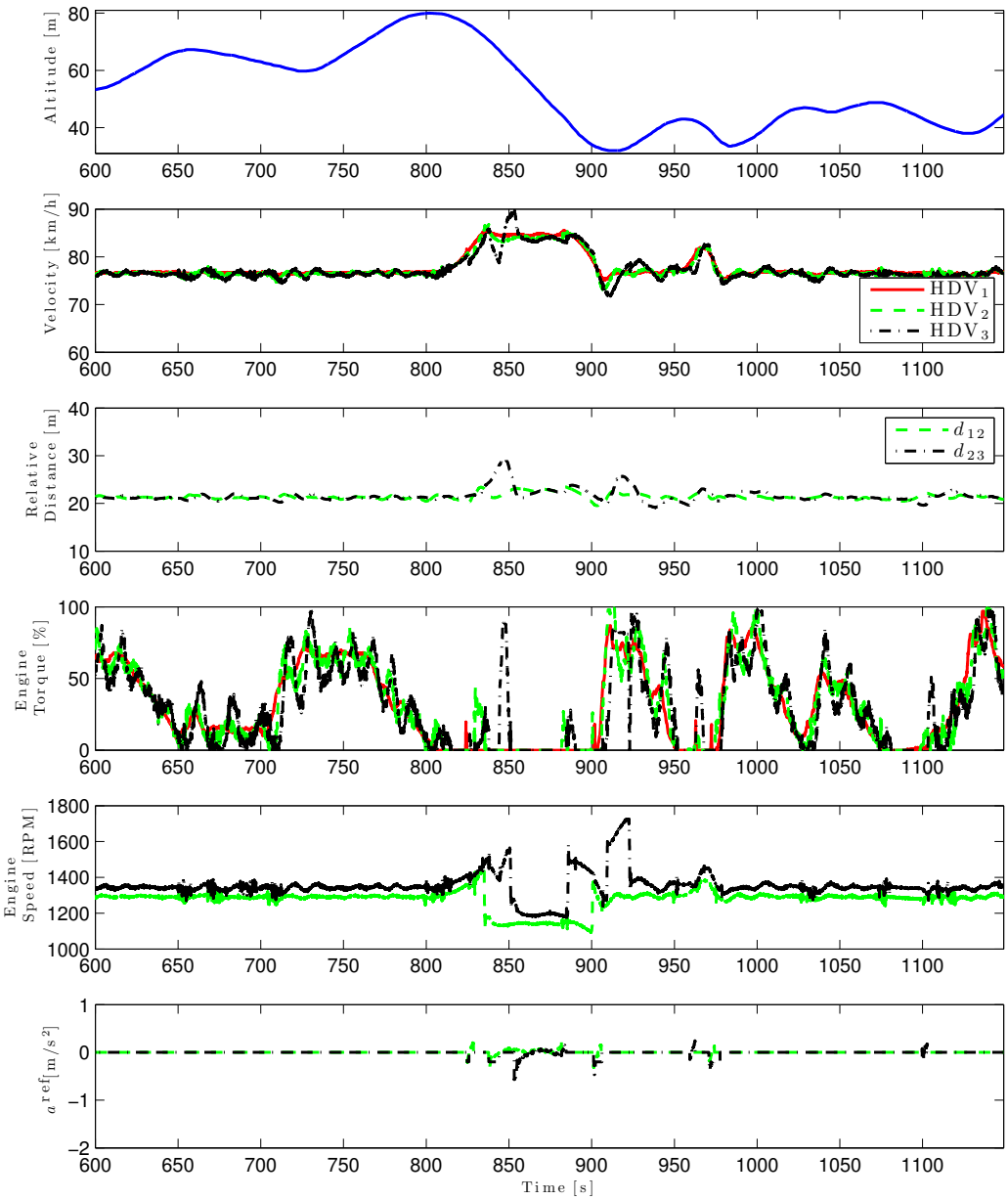

Figure 8.4: Experiment results obtained for the three-vehicle platoon when traveling over road segment A in Figure 8.2, which correspond to the road segment between the 600–1150 s time markers in Figure 8.3.

downhill segment by cutting off the fuel injection and thereby reducing the engine torque to zero, as shown in the fourth plot. However, due to its extensive vehicle mass, the first vehicle continues to accelerate until the DHSC constraint is reached at 830 s. The second vehicle initially increases the torque to maintain the relative distance and then reduces it to zero when entering the downhill segment. The second vehicle, being heavier, then obtains a higher velocity over the downhill segment and is forced to apply the brakes in order not to slide in to the preceding vehicle. The same behavior can be observed for the third vehicle, which is heaviest. However, in this case an excessive unmodeled braking action increases the spacing more than desired and inherently increases the variation in velocity. Hence, additional fueling is necessary to close the gap, as shown by the increase in engine torque for the third vehicle around the 850 s time marker. Thus, unmodeled dynamics in the braking system can induce a behavior that increases the fuel consumption. The fuel consumption under these circumstances are discussed in Section 8.2.2. Furthermore, the varying topography seems to induce large changes in engine torque. The third plot from the bottom shows that the engine torque for the second vehicle varies more in comparison with the first vehicle. This is due to the additional transient control actions that are necessary for maintaining the spacing when disturbances are imposed on the system. The variation in engine torque is marginally higher for the third vehicle, since it has a higher mass and lower final gear ratio compared to the second vehicle.

8.2.2 Fuel Savings

In order to obtain reliable results for evaluating the fuel reduction potential of HDV platooning, only the relative fuel consumption is considered each vehicle. Errors can arise in comparing fuel consumption data from different sensors in different vehicles. Furthermore, the same gear is utilized when driving over small road grades to obtain comparable results for the fuel consumption. A higher gear over the same road stretch implies a lower fueling. Gear changes were only allowed over steep hill segments. Note that the engine Fuel–Torque–RPM mapping is nonlinear. Therefore, the fuel consumption might vary considerably if, for example, the RPM would be slightly different between test-runs. Hence, it is interesting to study the propulsion energy[4] to remove the dependance on the specific engine properties. The total fuel consumption over each test-run is obtained by integrating the instantaneous fuel consumption, which is recorded over the CAN.

Small Road Grade Segments

The normalized fuel and energy consumptions for test-runs over small road grade segments corresponding to the segments B_1, B_2, B_3 in Figure 8.2, are given in Figure 8.5. By small road grade segments, we mean segments where the vehicles

[4]We define the propulsion energy as $E = \int T_e \omega_e dt$, where T_e is the net engine torque and ω_e the angular velocity.

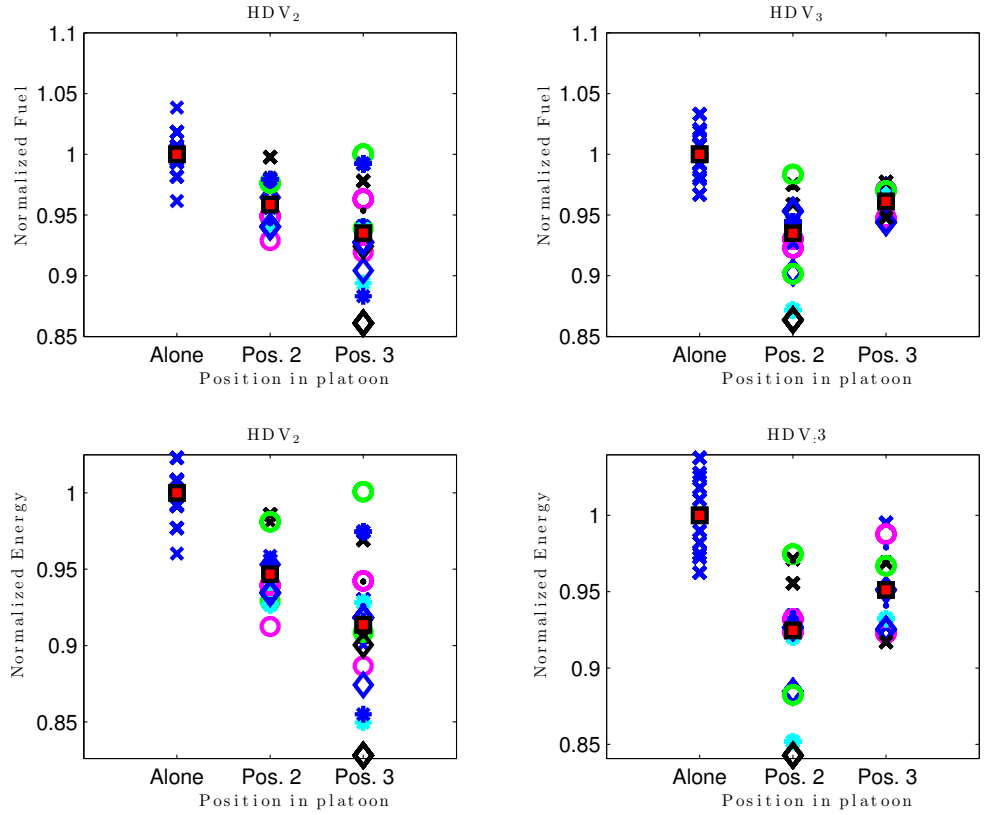

Figure 8.5: Normalized fuel- and energy consumption results for the numerous experiments between Mariefred-Eskilstuna over the road segments B_i, $i = 1, 2, 3$, in Figure 8.2. The plots on the left show the results for HDV_2 and plots on the left show the results for HDV_3. The top two plots show the normalized fuel consumption and the bottom plots show the corresponding normalized energy consumption for each vehicle.

do not have to brake when coasting over a downhill segment or change the gear for maintaining the speed in uphill climbs. A little less than half of the considered road stretch falls under this classification. The two plots to the left in Figure 8.5 show the results for HDV_2 and the two plots to the right show the results for HDV_3. The top two plots show the normalized fuel consumption and the bottom plots show the corresponding normalized energy consumption for each vehicle. The fuel consumption and energy consumption over a single test-run are normalized with respect to the average fuel- and energy consumption, respectively, when driving alone on the same day. Data are given for the follower vehicles when they travel alone, in second position, and in third position. The markers $\times, \diamond, \circ, \cdot$, and $*$ denote the measured normalized fuel consumption over a single test-run. The (red) squares with (black) borders denote the average fuel consumption over all the test-runs in

Table 8.1: Average velocity sample standard deviations σ_i^{v} over all test-runs for HDV_i.

	Alone	Pos. 2	Pos. 3
HDV_2	0.11	0.51	0.48
HDV_3	0.11	0.26	0.63

the corresponding platoon position. The correlation between the fuel consumption for the follower vehicles are illustrated by the marker type and color. For example, a black $\diamond$ can be seen in Figure 8.5 for HDV_3, when it is traveling in the second platoon position. HDV_2 is then traveling in the third platoon position. Hence, the corresponding fuel consumption and energy consumption for HDV_2 is also given by a black $\diamond$.

The results show that a significant fuel saving can be obtained when traveling in a platoon. The fuel consumption is reduced on average by 4.1 % for HDV_2, when traveling in the second platoon position. It is reduced further when traveling in the third position, where the fuel consumption is reduced on average by 6.5 %. The corresponding energy reduction is 5.3 % or 8.6 % when traveling in second and third position, respectively. The saving in propulsion energy from the engine is higher compared to the fuel savings, since the internal engine losses varies for different operating points. HDV_3 achieves an average fuel reduction of 6.5 % or 3.9 % and an average energy reduction of 7.5 % or 4.9 %, when traveling in the second or third platoon position, respectively. As opposed to HDV_2, the fuel saving is less when operating in the third position. The average fuel consumption is increased in this case since the control effort is increased, which can be inferred by studying the variation in vehicle velocity for all the vehicles. The results for the sample standard deviation in velocity for the two follower vehicles, given in Table 8.1, indicate that a larger overall control effort is required for HDV_3, when HDV_2 is the preceding vehicle and has a larger variance in velocity. The CACC in HDV_2 produces a higher variation in velocity compared to HDV_3, when traveling as the second vehicle in the platoon. Hence, HDV_2 experiences a lower variance in velocity from both preceding vehicles and inherently produces a lower control effort when it is traveling in third position, compared to HDV_3. It can be concluded that the behavior of the preceding vehicle has a notable effect on the fuel savings of the follower vehicle. Note that some markers in Figure 8.5 for one HDV do not have a corresponding marker for the other vehicle. The reason for this can be that the surrounding traffic could occasionally interrupt a test-run by cutting in-between the platooning vehicles. In those cases, the vehicles automatically opened up the gap when the unknown vehicle was detected by the radar. Hence, the fuel consumption increased due to additional control actions for handling the traffic disturbance and the air drag reduction was lost during that period. Thus, the data for those instances were discarded.

In Figure 8.2 we normalized the fuel consumption across the different driving scenarios. This is because numerous factors influence fuel consumption. For example,

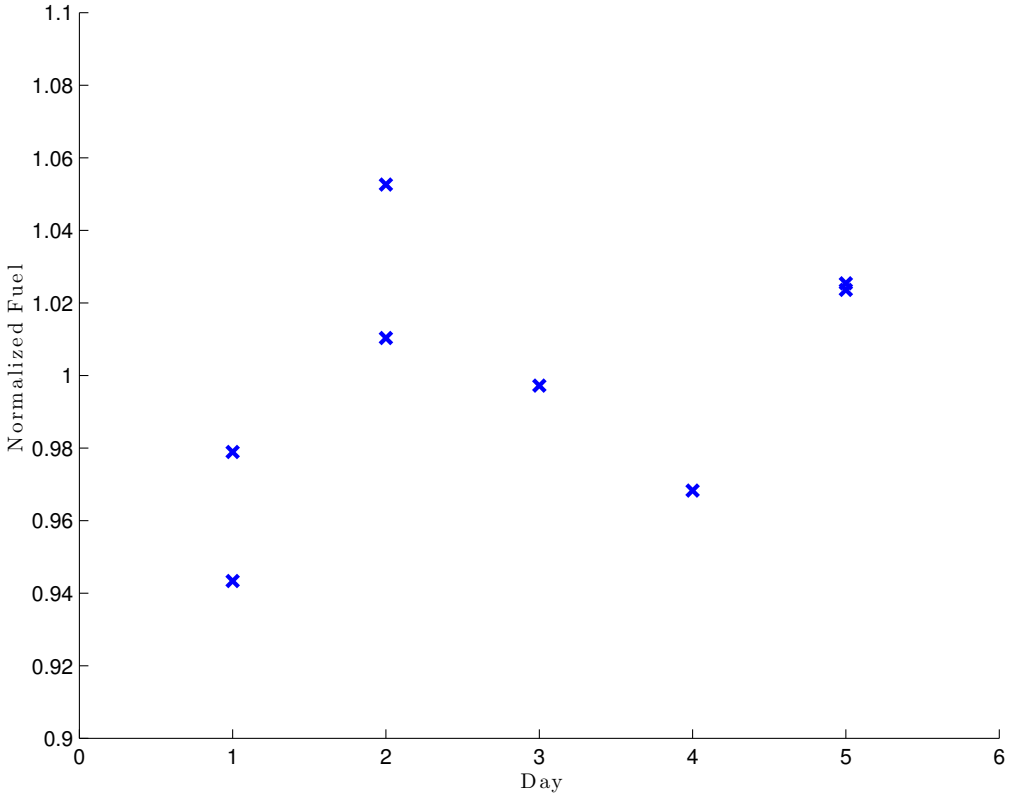

Figure 8.6: Normalized fuel consumption for HDV_3 when driving alone for each day. The fuel consumption results are normalized with respect to the average fuel consumption for all the days. The data for one of the test-runs on day 3 and day 4 are discarded, since those runs were interrupted by surrounding traffic.

the wind speed adds to the vehicle velocity and has a quadratic influence on the air drag force. Moreover, the temperature and the precipitation influence fuel consumption. In fact, during the days for the test-runs, the temperature fluctuated between -1 and 8 °C over the five day period and the road was wet due to rain on some days. Thus, as illustrated in Figure 8.6, the fuel consumption when traveling alone varied ±6 % between days. The markers represent the normalized fuel consumption over a single test-run when traveling alone, where the results are normalized with respect to the average fuel consumption for all the days.

Steep Road Grade Segments

As shown in the previous section, the linear controller can obtain a significant fuel saving over road segments with small road gradients. However, steep road gradients create undesirable behavior due to unmodeled system dynamics. Such a case is

illustrated in Figure 8.7, corresponding to road segment C in Figure 8.2. All vehicles initially travel at the same velocity and with a constant inter-vehicle spacing. When entering the first downhill segment, at the 70 s time marker, the vehicles start to coast by cutting off the fuel injection and thereby reducing the engine torque to zero. As the velocity increases, the inter-vehicle spacing remains constant. For a time headway spacing policy, however, the desired relative distance increases with the velocity. Thus, the follower vehicles eventually have to apply their brakes, as can be seen right after the 100 s time marker in the bottom plot in Figure 8.7. Hence, the spacing is increased and the engine turbo pressure remains low for both follower vehicles. The lead vehicle drops slightly in velocity when it enters the followed uphill segment, but increases the engine torque as soon as possible to maintain the set velocity. The follower vehicles observe that the lead vehicle is initially slowing down and the CACC thus defers the increase in velocity until the desired relative distance is resumed. In addition, a delay arises in building up the turbo pressure and, inherently, the engine torque, when entering the uphill segment. Furthermore, the acceleration is constrained due to extensive vehicle masses and engine torque saturations. Thus, the relative velocity to the preceding vehicle increases and the relative distance grows over the uphill segment. Moreover, HDV_2 changes gear in the middle of the uphill segment, as indicated by the sudden short drop in velocity, which further increases the relative distance. To regain the desired relative distance after the uphill climb, fuel is injected to increase the velocity. However, since a downhill segment follows, the velocity is increased too much and the follower vehicles must brake in the downhill to maintain the desired relative distance. Finally, additional fuel is injected in the downhill because a higher deceleration than desired was initially produced by the unmodeled dynamics in the braking system. Performing a similar analysis to what was presented in Figure 8.5, we find that the fuel consumption is actually increased on average by 4 % for HDV_2 compared to driving alone, but is unchanged for HDV_3, when traveling in the second platoon position over the the entire road segment shown in Figure 8.7. The unaffected fuel consumption for HDV_3 in the second platoon position can be explained by the results given in Figure 8.8. It illustrates the behavior over the same road stretch when the order of the follower vehicles is changed, such that HDV_3 is in the second platoon position and HDV_2 is in the third position. A similar behavior can be observed for this vehicle ordering, where the inter-vehicle spacing increases over the uphill segment starting at the 120 s time marker. However, a gear change does not occur for HDV_3 in this case, which produces a smoother behavior when catching up with the lead vehicle. The braking over the following downhill segment is also reduced. HDV_2, on the other hand, performs a gear change over the uphill climb, which even for this case causes it to brake over the following downhill segment when it is catching up. A smoother overall behavior and significantly less braking is achieved over the entire road stretch with HDV_3 in the second platoon position, in comparison with HDV_2. Thus, the fuel consumption is unchanged for HDV_3 in this case.

Recall that HDV_3 is the heaviest vehicle in the platoon. Hence, it has difficulties in maintaining the inter-vehicle spacing over uphill segments and has to brake

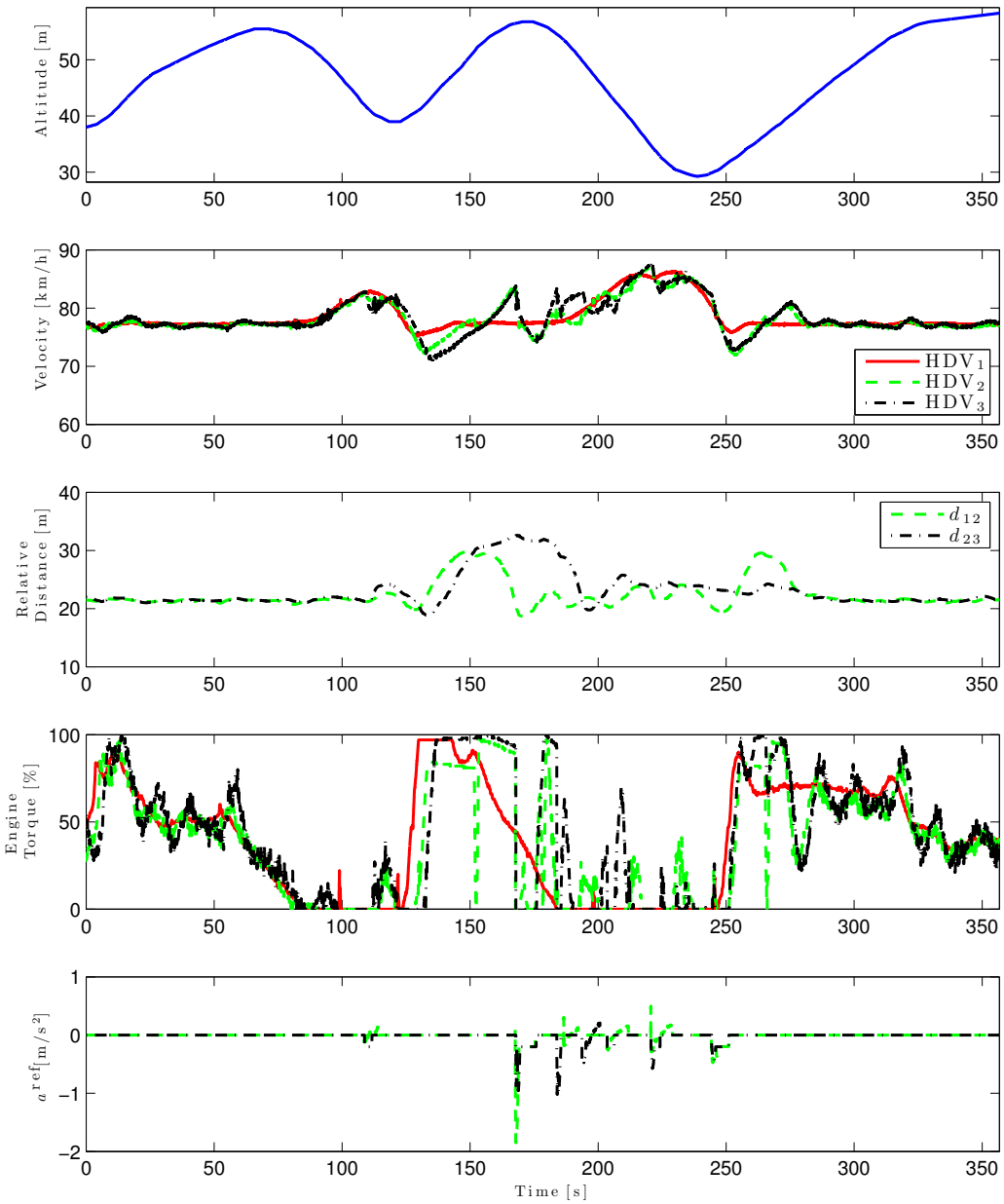

Figure 8.7: Experiment results obtained for the three-vehicle platoon when traversing road segment C in Figure 8.2. The vehicle order for these results are HDV_1 as lead vehicle, HDV_2 as the second vehicle, and HDV_3 is the tail-end vehicle.

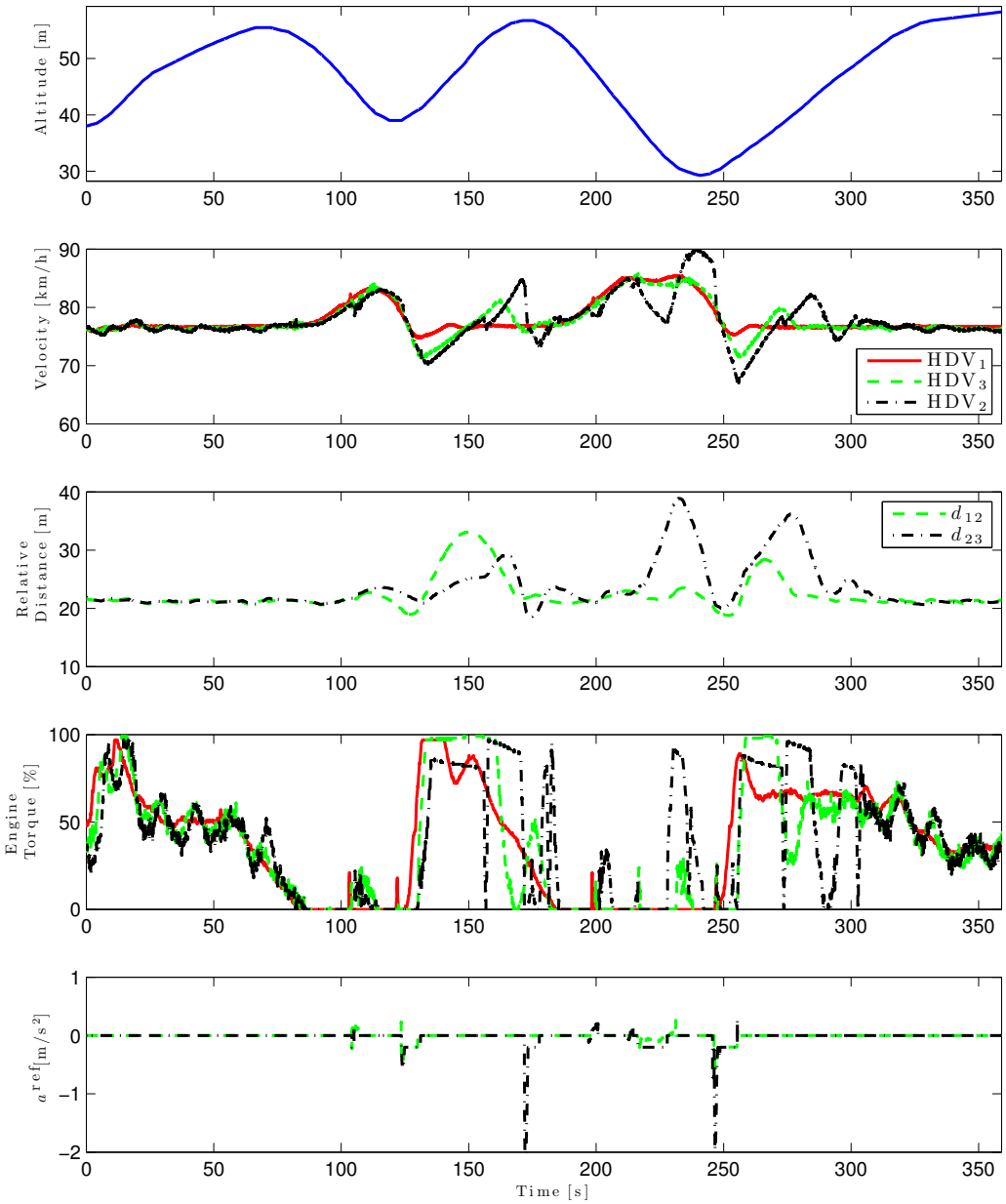

Figure 8.8: Experiment results obtained for the three-vehicle platoon when traversing road segment C in Figure 8.2. Different from Figure 8.7, is that the vehicle position for HDV_2 and HDV_3 is interchanged. The vehicle order is now HDV_1 as lead vehicle, HDV_3 as the second vehicle, and HDV_2 is the tail-end vehicle. The profiles are labeled accordingly.

slightly over the downhill segments to avoid coasting into the lead vehicle, when traveling in the second platoon position. The unfavorable gear change performed by HDV_2 in Figure 8.8 over the uphill segment increase the inter-vehicle spacing and creates additional braking. The fuel consumption is increased by 12 % and by 9 % in the third platoon position for HDV_2 and HDV_3, respectively. Thus, due to unmodeled road topography and engine dynamics, the fuel-saving potential due to air drag reduction in platooning can be lost over hilly road segments such as the ones presented in Figure 8.7. The solution to this problem is to use predictive information in the CACC, as further discussed in the next section.

8.3 Discussion

The CACC is designed to obtain a quick response when deviations in the set velocity and relative distance occurs, as presented in Chapter 6. However, it then becomes sensitive to small variations in the preceding vehicles behavior. On the other hand, if the controller response is made slower, i.e., less sensitive to small variations in the preceding vehicles behavior, large overshoots arise when compensating for larger variations in velocity. Hence, there is a trade-off between sensitivity to slow varying disturbances and maintaining the desired relative distance. Furthermore, the CACC is based on a time headway policy, which induces excessive braking when coasting over downhill segments. A time headway spacing policy, as opposed to a constant spacing policy, typically produces a more fuel-efficient control behavior (Omae et al., 2014). The results show that a time headway spacing policy is not desirable when coasting over downhill segments.

The proposed linear CACC is not fuel-efficient over varying steep road segments. The main losses in fuel saving occur, in particular, when traveling over an uphill segment that is followed by a downhill segment. The relative distance is increased over the uphill, which in turn is followed by excessive braking for the considered heterogenous HDV platoon over the downhill segment. This behavior is caused by delays in engine dynamics and since the lead vehicle unavoidably drops slightly in velocity when entering a steep uphill segment. Hence, difficulties arise when predictive road grade information is not available. To counteract the performance deterioration, first the inter-vehicle spacing should be maintained if possible when entering a steep uphill segment. If it is not possible, e.g., due to a limited engine power, then the follower vehicles should regain the desired inter-vehicle spacing by avoiding braking. Using feedforward in the controller can compensate for this unwanted behavior. Information that the lead vehicle has entered a steep uphill segment can be forwarded to the follower vehicles. Thereby, the turbo pressure can be increased in time such that sufficient engine torque is obtained and the relative distance is maintained in the uphill. Furthermore, the reference signal for the velocity, in addition to the state of the preceding vehicles, should be used in the feedback control. The follower vehicles will then know that the reference velocity of the lead vehicle is not reduced when entering the uphill segment. Similarly, if the

Table 8.2: Average fuel and energy savings over all small road grade segments.

	Fuel savings:		Energy savings:	
	Pos. 2	Pos. 3	Pos. 2	Pos. 3
HDV_2	4.1 %	6.5 %	5.3 %	8.6 %
HDV_3	6.5 %	3.9 %	7.5 %	4.9 %

follower vehicles are not able to maintain the inter-vehicle spacing over the uphill climb, the lead vehicle can send information that it has entered a downhill segment. Thereby, the follower vehicles can adapt their strategy for catching up.

If map data are available, a fuel and time optimal model predictive controller based on road grade preview information, as presented in Chapter 7, can be used. By forming a cooperative strategy based on the upcoming road topography characteristics, a suitable velocity and gear shifting strategy can be established. It is, for example, more fuel-efficient to avoid braking for all vehicles in the platoon by letting the lighter vehicles accelerate slightly with added engine torque over the downhill segments. Thereby, energy obtained from fuel combustion is not lost through heat produced by the frictional forces in the braking system. The vehicles should strive to follow the same velocity trajectory over the same points on the road. Thereby, a significant increase in fuel saving is obtained over steep hills by allowing for small deviations in relative distance, instead of a time headway spacing policy.

8.4 Summary

Linear controllers can obtain a significant fuel saving over road segments with small road gradients. However, steep road gradients create undesirable behavior due to unmodeled system dynamics. In this chapter we have investigated how the proposed controller performs and identified some of the main issues that arise for fuel-efficient control of HDV platoons in practice. The CACC works well and is able to maintain the inter-vehicle spacing over most parts of the roads. Small disturbances in the vehicle velocity produced by the varying road topography are not amplified for the follower vehicle. However, unwanted behaviors arise when platooning over steep road grade segments. Disturbances from unmodeled gear changes and the time headway policy create excessive braking, in particular over steep downhill segments. Furthermore, the unmodeled nonlinearities in the braking system induce a behavior that increases the overall fuel consumption.

We have also investigated the fuel reduction potential for a three-HDV platoon, which is governed by a CACC that is based on linear models for engine and brake control. The average fuel and energy savings for the three-vehicle platoon over all test-runs are summarized in Table 8.2. It is evident that the proposed simple decentralized controller can achieve a significant fuel reduction for road segments

with small road grade. Thus, substantial fuel-savings can be obtained from HDV platooning in practice. However, the fuel savings vary with respect to the behavior of the preceding vehicles. HDV_2 achieves a fuel reduction in both considered platoon positions, whereas HDV_3 only saves fuel in the second platoon position due to the controller responses to the unfavorable behavior of HDV_2. The results presented in this chapter also show that the fuel-saving potential obtained from the air drag reduction in platooning can be lost over steep road segments, due to constraints set by the road topography and the limited engine power.

Chapter 9

Conclusions and Future Outlook

"*If we knew what it was we were doing, it would not be called research, would it?*"

Albert Einstein

Heavy-duty vehicle (HDV) platooning is a promising means to reduce fuel consumption, improve safety, reduce congestion, decrease emission of harmful exhaust gasses, and aid the driver in complex driving situations. In this thesis, a system for dividing the complex problem into manageable subsystems for fuel-efficient optimal control has been presented. Nonlinear and linear HDV platooning models have been derived. We have investigated the current fuel reduction potential of HDV platooning for vehicles governed by a commercial adaptive cruise control. It has been shown through analytical and experimental results that it is both fuel-efficient and possible to operate the vehicles at a much shorter inter-vehicle spacing than what is currently done by commercially available systems, without compromising safety. We have also argued why a decentralized control strategy is favorable and presented an algorithm that produces a simple and energy-efficient decentralized controller with good tracking performance, stability, and scalability. It has been shown through empirical findings that, even though the proposed controller is fuel-efficient over roads with small road gradient, the fuel savings can be lost over certain steep hill segments in practice. We have presented two model predictive control policies and shown that it is fuel-efficient to consider the road grade preview information. This chapter concludes the thesis by detailing the inferrences that can be drawn from the obtained results and outlines directions for possible future work in this area.

9.1 Conclusions

Vehicle platooning is becoming increasingly important. Even though platooning offers many benefits in traffic networks, it mostly offers functionality to improve

driver comfort for passenger vehicles. The ground transportation industry on the other hand has a strong incentive to utilize platooning applications due to the fuel-price sensitive market and long freight transport assignments. Hence, platooning will most likely find an initial market entry in the transportation industry due to the high demand and strong business case.

The simulation results in Chapter 4, derived from a validated simulation model, showed that a fuel reduction of 4.7–7.7 % in HDV platooning for identical vehicles can be obtained depending on the time headway setting in the adaptive cruise controller. If the lead vehicle is 10 t lighter a corresponding 3.8–7.4 % fuel reduction can be obtained. Similarly, if the lead vehicle is 10 t heavier a 4.3–6.9 % fuel reduction can be obtained. Hence, HDV heterogeneity and order have a significant impact on the fuel reduction possibilities. Furthermore, reducing the inter-vehicle spacing for HDVs traveling in a platoon yields the highest fuel reduction potential. Thus, it seems most beneficial to reduce the inter-vehicle spacing for HDVs traveling in a platoon.

The results presented in Chapter 5 showed that the relative distance can be reduced significantly compared to what is utilized in current commercial systems. During normal operation a minimum distance of 1–2 m can be maintained without increasing the risk of a collision despite the worst possible behavior displayed by the preceding vehicle. The safe relative distance varies with braking capability and communication and computation delays within the system. A stronger overall braking capability in the follower vehicle creates the possibility of reducing the relative distance further. Thus, in platooning applications the results suggested that vehicles with stronger braking capabilities should always be placed last to enable the shortest possible relative distance without increasing the risk of a collision. This could easily be achieved with wireless communication if the braking capabilities and mass are transmitted between each vehicle in the platoon. However, rearranging the HDVs on a highway is not always feasible. Hence, another approach to ensure safety and obtain a minimum relative distance is to set maximum braking constraints through wireless communication within the platoon. Producing the maximum brake torque through the internal brake system after a request could take up to 0.4 s depending on the vehicle configuration, which will be propagated downstream through the platoon. However, if the first vehicle transmits that it is initiating an emergency brake to all the following vehicles within the platoon, they will be able to commence their control actions almost simultaneously and thereby prevent a propagation of actuation delay. This in turn would enable a shorter inter-vehicle spacing between all the follower vehicles.

In Chapter 6, we presented a method for designing suboptimal decentralized feedback controllers for HDV platooning that takes dynamic coupling and engine response delays into consideration. The aim was to propose a simple and implementable fuel-efficient cooperative controller that could be utilized for practical evaluation of the fuel-saving potential of HDV platooning. An interesting observation can be made with respect to the system behavior due to the time-varying nature of the desired relative distance: As a disturbance is introduced by changing the

velocity of the lead vehicle, the relative distance will initially change between the first two vehicles in the platoon. However, as the velocity increases or decreases for the lead vehicle, so will the desired relative reference distance. Hence, if for example the lead vehicle accelerates, the follower vehicles will defer their control actions accordingly until the relative distance is increased and produce a smoother control input to change their own speed. Thus, a lower control effort will be mandated from the follower vehicle. The proposed controller is designed to obtain a quick response when a change in the legislated road speed occurs, but without becoming too sensitive to small variations in the preceding vehicles behavior. If the controller response is made too slow, i.e., less sensitive to small variations in the preceding vehicles behavior, large overshoots arise when compensating for larger variations in velocity. Hence, there is a trade-off between sensitivity to slow varying disturbances and maintaining the desired relative distance. The experimental results showed that the deviation from the reference for inter-vehicle spacing during the braking scenarios never decrease more than 1.9 m. Thus, the vehicles could have operated at a much closer inter-vehicle spacing without increasing the risk of a collision and thus obtained a higher fuel reduction.

In Chapter 7, we presented a method for deriving two fuel-optimal controllers based on road grade preview information for HDV platooning. A surprising result was that the fuel-savings obtained for the proposed cooperative look-ahead controller is very close to a hypothetically optimal fuel reduction, defined as when each vehicle uses its individual fuel-optimal velocity strategy while hypothetically obtaining the air drag reduction from maintaining a constant relative distance to neighboring vehicles (even if it cannot be constant in practice). Hence, the results suggested that deriving the globally optimal velocity profile for a centralized solution might only create marginal improvements in fuel savings. Furthermore, the presented results show that it is important to consider the road grade preview information in HDV platooning. It is fuel-efficient to maintain the platoon when traversing a hill, as opposed to letting the platoon separate due to imposed constraints and then resume platooning by catching up after the hill. In particular, the results showed that it is fuel-efficient and desirable for heterogenous vehicle platoons, where the vehicles are constrained by different limitations in maximum engine power, to initiate the control actions based on a point in the road rather than simultaneously implementing each HDV's control action to maintain a fixed spacing. The overall fuel-saving potential is improved by maintaining the short relative distance to the preceding vehicle over an uphill climb and hence slow down if the follower vehicle is not able to maintain the nominal road speed. Over a downhill segment, it is fuel-efficient for a preceding vehicle to inject additional fuel and thereby increase its acceleration if it causes the follower vehicle to refrain from braking. A fuel reduction of 12 % or 19 % can be achieved with a cooperative control policy, when traversing steep uphill or downhill segments, respectively. Furthermore, it was shown that the fuel-saving potential for the proposed controller is not overly sensitive to errors in vehicle mass or positioning, since the main fuel reduction is obtained from the air drag reduction. Thus, significant losses in the fuel-saving potential can be avoided, e.g., due to errors

in the look-ahead control trajectory, as long as the inter-vehicle spacing can be maintained.

The experimental results in Chapter 8 showed that a fuel reduction of 3.9–6.5 % can be obtained for a heterogenous platoon of HDVs on a Swedish highway. The savings depend on the vehicle position in the platoon and the behavior of the preceding vehicles. The proposed decentralized controller, which is based on simple linear models and no road topography information, is fuel-efficient over roads with relatively small road gradients. Steep hills saturate the low-level engine control input over uphill climbs and create accelerations when coasting over downhill segments. Thus, if the relative distance cannot be maintained over an uphill segment that is followed by a downhill segment, an excessive braking occurs when catching up to regain the relative distance. A consequence of the braking is waste of fuel. Another interesting observation can be made when studying the implications for a time headway spacing policy over a steep downhill segment. As the HDVs enter the downhill segment, each vehicle starts to coast by cutting off the fuel injection. Hence, the velocities of the vehicles increase and the inter-vehicle spacing remains constant or changes very slowly. A time headway policy implies that the desired relative distance increases with the vehicle velocity. Therefore, the control strategy executes a braking request when coasting over the downhill segment to increase the spacing, which is not necessary in this case. Moreover, an unexpected gear change over an uphill segment can give the follower vehicles the impression that it is intentionally slowing down for a short period. Therefore, the follower vehicles will cut off their fuel injection to match the speed, which also lowers the engine turbo pressure. Consequently, the inter-vehicle spacing will increase in this case, since it takes time to increase the turbo pressure when striving to regain the nominal speed. Such behavior is unwanted and fuel-inefficient. Thus, the intention of a gear change should be communicated to all follower vehicles in order to prevent an increased fuel consumption over the hill segment.

With the results obtained in this thesis, it is clear that a substantial fuel reduction potential exists for HDV platooning. The results indicate that a maximum fuel reduction can be achieved at a short relative distance due to the air drag reduction and that a relatively small inter-vehicle spacing can be obtained without compromising safety. The results also show that a cooperative control strategy, where the HDVs interact and consider the dynamics of their neighbors, produces a lowered energy consumption downstream. However, safety is an issue as inter-vehicle communication cannot be guaranteed at all time. If communication is available, the inter-vehicle spacing can be relatively small without compromising safety. When communication is lost, the spacing should be increased. Thus, the available information structure dictates the inter-vehicle spacing indirectly, creating a need for a graceful degradation scheme in the architecture presented in Chapter 3.

9.2 Future Outlook

> "*Nothing in life is to be feared, it is only to be understood. Now is the time to understand more, so that we may fear less.*"
>
> Marie Curie

The simulation and experimental results in this thesis have mainly been based on 2–3 HDVs traveling at the shortest allowed time headway setting on Swedish highways. Studies on the air drag reductions suggest that the wind reduction is additionally lowered for vehicles traveling further down the platoon and at shorter inter-vehicle spacings. Thus, further experiments conducted with respect to the fuel reduction for several HDVs in a platoon and at smaller inter-vehicle spacing is crucial to get a better understanding of the real-life fuel reduction potential of HDV platooning.

The safety analysis presented in this thesis has been performed based on certain simplifications. In realistic scenarios the vehicles commonly travel along a varying road topography. Due to the extensive mass of an HDV, the gravitational force has a significant impact on the overall braking power. Hence, studying the impact of a varying road incline serves as a natural direction to establish minimum safe relative distances for HDV platooning. Additional factors may also shape the safety boundary, which was not considered in the presented work. One of the vehicles might be traveling on a wet patch or the tires might be in bad condition, reducing the braking capabilities. Also, unmodeled nonlinearities might arise in the applied brake force due to temperature variation. Although the experimental results confirm the numerical evaluations, the results reveal that the influence of the unmodeled nonlinear braking system and gear changes are important. Furthermore, extending the experimentally evaluated and validated model to both longitudinal and lateral motion is of high relevance. Finally, we believe that finding a novel computational method for computing safe sets for more than two HDVs is interesting, since establishing what minimum distance can be maintained between HDVs in a heterogeneous platoon is not evident. Investigating these factors requires a more advanced vehicle model and computation method. It is therefore a possible avenue for continued work in this area.

The results in Chapter 6 showed that the controller performance is improved with increasing position index in the platoon. However, the effects of unmodeled nonlinearities, such as gear changes, brake blending, and engine dynamics, can cause undesirable behavior in some cases. To handle these effects the intention of a necessary gear change could be broadcasted so that the rest of the platooning vehicles will be able to make informed decisions regarding whether to change gear simultaneously or to deter the action. Thus, a high-level control law for the gear management system might be necessary to further improve the control performance. The main drawback of the proposed controller is that it does not directly account for the physical constraints present in the systems. Currently the linear quadratic weights are adjusted in an ad hoc manner until the constraints criteria are met

and the performance criteria are satisfied. A systematic optimal control procedure is preferable, which can directly consider the system constraints when deriving the fuel-optimal controller. A more sophisticated engine model might possibly be required to capture the behavior that affects the tracking performance. One solution might be to not only transmit the actual velocity of the vehicles in the platoon over the communication network, but also the reference velocity. Thereby, each vehicle would be able to determine when the control action to the engine is resumed and increase the turbo pressure to reduce the response delay. Investigating these possibilities require further experiments.

The proposed controller based on road grade preview information in this thesis does not require knowledge of the specific vehicle parameters such as mass or maximum available engine torque, or any information regarding the dynamics of the surrounding vehicles. We have provided a simple open-loop approach for how to handle system uncertainties, such that the fuel saving with the proposed cooperative look-ahead cruise control (CLAC) is maintained. However, disturbances in the form of an unexpected gear change, by for example a preceding vehicle, or nonlinearities in the engine dynamics might cause an HDV to deviate from the CLAC velocity trajectory. A feedback solution for how to handle such deviations, where for example a new locally corrected velocity profile is established, is necessary. Further investigation into this is a natural next step in utilizing road grade preview information for HDV platooning control.

Finally, we also believe that a relevant future research direction for HDV platooning is work in the top layer of the architecture presented in Chapter 3. In particular coordination and routing to create vehicle platoons is an important research area for establishing vehicle platoons. Several control policies currently exist for control of vehicle platoons and research projects have recently emerged worldwide to evaluate various performance criteria for HDV platoons in practice. However, as goods have different origins, destinations, and time restrictions, it is not evident how the HDVs can fully utilize the platooning benefits during individual transport missions. Thus, there is a need to systematically coordinate scattered vehicles on the road network to form platoons in order to maximize the benefits of platooning.

Nomenclature

Acronyms and Abbreviations

ABS	Anti-Lock Braking System
ACC	Adaptive Cruise Control
ADAS	Advanced Driver Assistance Systems
ALAC	Adaptive Look-Ahead Cruise Control
BMS	Brake Management System
CAN	Controller Area Network
CACC	Cooperative Adaptive Cruise Control
CAM	Cooperative Awareness Message
CC	Cruise Control
CFD	Computational Fluid Dynamics
CLAC	Cooperative Look-Ahead Cruise Control
CORDIS	Community Research and Development Information Service
DENM	Decentralized Environmental Notification Message
DHSC	Down Hill Speed Control
ECC	Economical Cruise Control
EMS	Engine Management System
ERTICO	European Road Transport Telematics Implementation Co-ordination Organization
ESP	Electronic Stability Program
GPS	Global Positioning System
HDV	Heavy-Duty Vehicle
ICT	Information and Communication Technology
ITF	The International Transport Forum
ITS	Intelligent Transportation Systems
LAC	Look-Ahead Cruise Control
LAN	Local Area Network

LQR	Linear Quadratic Regulator
MAC	Medium Access Control
MPC	Model Predictive Control
OECD	Organization for Economic Co-operation and Development
PATH	Partners for Advanced Transportation Technology
SARTRE	Safe Road Trains for the Environment: EU project
UMTS	Universal Mobile Telecommunications System
VANET	Vehicular Ad hoc Network
V2I	Vehicle-to-Infrastructure
V2V	Vehicle-to-Vehicle
V2X	Vehicle-to-Vehicle and/or Infrastructure
WSU	Wireless Sensor Unit

Bibliography

802.11p. *Status of project IEEE 802.11, Task Group p, Wireless Access in Vehicular Environments (WAVE)* (2014). URL `http://www.ieee802.org/11/Reports/tgp_update.htm`. Accessed: April 9, 2014.

ACEA. European Motor Vehicle PARC 2010, European Automobile Manufacturers' Association (2012). URL `http://www.acea.be/uploads/statistic_documents/ANFAC_Report_2010_(2012).pdf`. ANFAC Report.

M. Adolfson. Cooperative dynamic formation of platoons for safe and energy-optimized goods transportation. In *93rd Annual Meeting of the Transportation Research Board*. Washington D.C., USA (2014). (Oral presentation).

AEA Technology. Reduction and testing of greenhouse gas (ghg) emissions from heavy duty vehicles - lot 1: Strategy. Technical report, Ricardo (2011).

A. Alam. *Optimally Fuel Efficient Speed Adaptation*. Master's thesis, Royal Institute of Technology, Automatic Control (2008).

A. Alam. *Fuel-Efficient Distributed Control for Heavy Duty Vehicle Platooning*. Licentiate thesis, Royal Institute of Technology, SE-100 44 Stockholm, Sweden (2011).

A. Alam, J. Andersson, H. Gustafsson, H. Pettersson, P. Sahlholm, and H. Schauman. *Method and system for speed verification.* European patent application number: 11193590.4 (filed 2011*a*).

A. Alam, J. Andersson, H. Gustafsson, H. Pettersson, P. Sahlholm, and H. Schauman. *Metod i samband med trafikövervakning, och ett trafikövervakningssystem [Method in connection with traffic monitoring and a traffic monitoring system].* Swedish patent application number: 1150073-3 (filed 2011*b*).

A. Alam, J. Andersson, and P. Sahlholm. *A Vehicle Speed Control Method*. International patent application number: PCT/SE09/050030 (filed 2009*a*).

A. Alam, J. Andersson, and P. Sahlholm. *Determination of acceleration behavior*. International patent application number: PCT/SE09/051299 (filed 2009*b*).

A. Alam, A. Gattami, and K. H. Johansson. An experimental study on the fuel reduction potential of heavy duty vehicle platooning. In *13th International IEEE Conference on Intelligent Transportation Systems*. Madeira, Portugal (2010).

A. Alam, A. Gattami, and K. H. Johansson. Suboptimal decentralized controller design for chain structures: Applications to vehicle formations. In *50th IEEE Conference on Decision and Control and European Control Conference*. Orlando, FL, USA (2011*a*).

A. Alam, A. Gattami, K. H. Johansson, and C. J. Tomlin. Establishing safety for heavy duty vehicle platooning: A game theoretical approach. In *18th IFAC World Congress*. Milan, Italy (2011*b*).

A. Alam, A. Gattami, K. H. Johansson, and C. J. Tomlin. Guaranteeing safety for heavy duty vehicle platooning: Safe set computations and experimental evaluations. *Control Engineering Practice*, 24: 33 – 41 (2014*a*).

A. Alam, A. Johansson, R. Lyberger, and H. Pettersson. *Method and system for spacing adjustment in a moving vehicle train.* International patent application number: PCT/SE13/050317 (filed 2012*a*).

A. Alam, K.-Y. Liang, and A. Gattami. *Metod i samband med fordonståg, och ett fordon som använder metoden [A method in connection to vehicle trains and a vehicle that uses that method].* Swedish patent application number: 1150579-9 (filed 2011*c*).

A. Alam, J. Mårtensson, and K. H. Johansson. Look-ahead cruise control for heavy duty vehicle platooning. In *16th International IEEE Conference on Intelligent Transportation Systems*, 928–935. Hague, The Netherlands (2013*a*).

A. Alam, J. Mårtensson, and K. H. Johansson. Cooperative control with preview topography information under system uncertainties for heavy-duty vehicle platooning (2014*b*). Submitted for journal publication.

A. Alam, J. Mårtensson, and K. H. Johansson. Experimental evaluation of decentralized cooperative cruise control for heavy-duty vehicle platooning (2014*c*). Submitted for journal publication.

A. Alam, S. Nilsson, J. Kemppainen, H. Pettersson, and H. Pettersson. *System and method for assisting a vehicle when overtaking a vehicle train.* International patent application number: PCT/SE13/050674 (filed 2012*b*).

A. Alam, S. Nilsson, J. Kemppainen, H. Pettersson, and H. Pettersson. *System and method for regulating of vehicle pertaining to a vehicle train.* International patent application number: PCT/SE13/050673 (filed 2012*c*).

A. Alam, S. Nilsson, J. Kemppainen, H. Pettersson, and H. Pettersson. *System and method for regulation of vehicles in vehicle trains.* International patent application number: PCT/SE13/050672 (filed 2012*d*).

A. Alam, S. Nilsson, J. Kemppainen, H. Pettersson, and H. Pettersson. *System and method pertaining to vehicle trains.* International patent application number: PCT/SE13/050687 (filed 2012*e*).

A. Alam, S. Nilsson, J. Kemppainen, H. Pettersson, and H. Pettersson. *System och metod för att assistera ett fordon vid omkörning av fordonståg [System and method for assisting a vehicle when overtaking a vehicle train].* Swedish patent number: 1250627-5 (Granted 2014*a*).

A. Alam, S. Nilsson, J. Kemppainen, H. Pettersson, and H. Pettersson. *System och metod för reglering av fordon i ett fordonståg [System and method for regulating of vehicle pertaining to a vehicle train].* Swedish patent number: 1250628-3 (Granted 2014*b*).

A. Alam, H. Pettersson, T. Sandberg, and J. Dellrud. *Method and management unit pertaining to vehicle trains.* International patent application number: PCT/SE12/050066 (filed 2011*d*).

N. Alam, A. T. Balaei, and A. Dempster. Relative positioning enhancement in vanets: A tight integration approach. *IEEE Transactions on Intelligent Transportation Systems*, 14(1): 47–55 (2013*b*).

M. Ali. *Decision Making and Control for Automotive Safety.* Ph.D. thesis, Department of Signals and Systems, Chalmers University of Technology, Göteborg, Sweden (2012).

M. Althoff and J. M. Dolan. Reachability computation of low-order models for the safety verification of high-order road vehicle models. In *American Control Conference*. Montreal, Canada (2012).

L. Alvarez and R. Horowitz. Safe platooning in automated highway systems. Technical report, Safe Platooning in Automated Highway Systems (1997). Research Report UCB-ITS-PRR-97-46.

B. D. O. Anderson and J. B. Moore. *Optimal Control: Linear Quadratic Methods.* Prentice-Hall International, Inc. (1989). ISBN: 0-13-638651-2.

K. J. Åström. *Introduction to Stochastic Control Theory.* Academic Press, New York and London (1970).

K. J. Åström and T. Hägglund. *Advanced PID Control.* ISA - Instrumentation, Systems, and Automation Society, New York (2006). ISBN: 1-55617-942-1.

G. J. Babu. *Look-Ahead Platooning through Guided Dynamic Programming.* Master's thesis, Royal Institute of Technology, Automatic Control (2013).

H. S. Bae, J. Ryu, and J. C. Gerdes. Road grade and vehicle parameter estimation for longitudinal control using gps. In *IEEE Conference on Intelligent Transportation Systems*, 166–171. Oakland, CA, USA (2001).

B. Bamieh and M. R. Jovanović. On the ill-posedness of certain vehicular platoon control problem. *IEEE Transactions on Automatic Control*, 50(9) (2005).

B. Bamieh, M. R. Jovanović, P. Mitra, and S. Patterson. Effect of topological dimension on rigidity of vehicle formations: Fundamental limitations of local feedback. In *47th IEEE Conference on Decision and Control*, 369–374. Cancun, Mexico (2008).

B. Bamieh, F. Paganini, and M. A. Dahleh. Distributed control of spatially invariant systems. *IEEE Transactions on Automatic Control*, 47(7) (2002).

P. Barooah and J. P. Hespanha. Error amplification and disturbance propagation in vehicle strings with decentralized linear control. In *44th IEEE Conference on Decision and Control and the European Control Conference*, 1350–1354. Seville, Spain (2005).

P. Barooah, P. G. Mehta, and J. P. Hespanha. Mistuning-based control design to improve closed-loop stability margin of vehicular platoons. *IEEE Transactions on Automatic Control*, 54(9): 2100–2113 (2009).

M. Barradi, A. Hafid, and J. Gallardo. Establishing strict priorities in ieee 802.11p wave vehicular networks. In *IEEE Global Telecommunications Conference*, 1–6. Miami, FL, USA (2010).

T. Basar and G. J. Olsder. *Dynamic Noncooperative Game Theory.* Academic Press, New York, 2nd edition (1995). ISBN: 978-0-89871-429-6.

A. M. Bayen, S. Shanthanam, I. Mitchell, and C. J. Tomlin. A differential game formulation of alert levels in ETMS data for high altitude traffic. In *GNC Conference*, volume AIAA, 2003-5341. Austin, Texas (2003).

R. Bellman. *Dynamic Programming.* Princeton University Press, Princeton, NJ, USA, 1 edition (1957).

K. Bilstrup, E. Uhlemann, and E. Strom. Scalability issues of the mac methods stdma and csma of ieee 802.11p when used in vanets. In *IEEE International Conference on Communications Workshops (ICC), 2010*, 1–5. Capetown, South Africa (2010).

V. D. Blondel and J. N. Tsitsiklis. A survey of computational complexity results in systems and control. *Automatica*, 36(9): 1249–1274 (2000).

C. Bonnet and H. Fritz. Fuel consumption reduction in a platoon: Experimental results with two electronically coupled trucks at close spacing. In *Future Transportation Technology Conference & Exposition*. Costa Mesa, CA, USA (2000). SAE paper 2000 - 01 - 3056.

F. Browand. Reducing aerodynamic drag and fuel consumption. In *Global Climate and Energy Project, Workshop on Advanced Transportation*. Stanford University, USA (2005). (Oral presentation).

F. Bu, H.-S. Tan, and J. Huang. Design and field testing of a cooperative adaptive cruise control system. In *American Control Conference*, 4616–4621 (2010). Developed under the California PATH research project.

L. Bühler. *Fuel-Efficient Platooning of Heavy Duty Vehicles through Road Topography Preview Information*. Master's thesis, Royal Institute of Technology, Automatic Control (2013).

C2C. *CAR 2 CAR Communication Consortium* (2002). URL `http://www.car-to-car.org/index.php?id=22`. Accessed: April 2, 2014.

R. Chandler, R. Herman, and E. Montroll. Traffic dynamics: Studies in car following. *Operations Research*, 6: 165–184 (1958).

D. Chang and E. Morlok. Vehicle speed profiles to minimize work and fuel consumption. *Journal of transportation engineering*, 131: 173–185 (2005).

K.-C. Chu. Decentralized control of high-speed vehicular strings. *Transportation Science*, 8(4): 361–384 (1974).

E. A. Coddington and N. Levinson. *Theory of Ordinary Differential Equations*. Krieger Pub Co, 1st edition (1984). ISBN: 978-0898747553.

D. Corona and B. De Schutter. Adaptive cruise control for a smart car: A comparison benchmark for mpc-pwa control methods. *IEEE Transactions on Control Systems Technology*, 16(2): 365–372 (2008).

R. D'Andrea. A linear matrix inequality approach to decentralized control of distributed parameter systems. In *Proceedings of the American Control Conference*, volume 3, 1350–1354. Philadelphia, PA, USA (1998).

A. Davila, E. Aramburu, and A. Freixas. Making the best out of aerodynamics: Platoons. In *SAE International*. USA (2013). SAE Technical Paper 2013-01-0767.

B. De Schutter, T. Bellemans, S. Logghe, J. Stada, B. De Moor, and B. Immers. Advanced traffic control on highways. *Journal A*, 40(4): 42–51 (1999).

S. Deutschle, G. C. Kessler, C. Lank, G. Hoffmann, M. Hakenberg, and M. Brummer. Use of electronically linked konvoi truck platoons on motorways. *ATZ autotechnology Edition: 2010-04* (2010).

U. Dietz. Cellular vehicle communications: Preliminary results from the cocar project. In *1st ETSI TC ITS Workshop*. Sophia Antipolis, France (2009).

C. V. Driel, M. Hoedemaeker, and B. V. Arem. Impacts of a congestion assistant on driving behaviour and acceptance using a driving simulator. *Transportation Research Part F Traffic Psychology and Behaviour*, 10(2): 139–152 (2007).

W. B. Dunbar and R. M. Murray. Receding horizon control of multi-vehicle formations: a distributed implementation. *Automatica*, 42: 549–558 (2006).

Dynasim. *User Manual Dymola 6 Additions*. Dynasim AB, Research Park Ideon, SE-223 70 Lund, Sweden (2007).

S. Eichler, C. Schroth, and J. Eberspächer. Car-to-car communication. In *VDE-Kongress 2006*. VDE VERLAG GmbH (2006).

ERTICO. *ITS can help improve our daily lives* (2014). URL `http://www.ertico.com/about-ertico-its/index.html`. Accessed: April 2, 2014.

ETSI. *Intelligent Transportation Systems* (2014). URL `http://www.etsi.org/website/Technologies/IntelligentTransportSystems.aspx`. Accessed: March 31, 2014 - ©European Telecommunications Standards Institute 2008. Further use, modification, redistribution is strictly prohibited. ETSI standards are available form http://pda.etsi.org/pda/.

ETSI EN 302 571. *ETSI EN 302 571 V1.2.0* (2014). URL `http://www.etsi.org/deliver/etsi_en/302500_302599/302571/01.02.00_20/en_302571v010200a.pdf`. Accessed: April 10, 2014.

ETSI EN 302 637-2. *Intelligent Transport Systems (ITS); Vehicular Communications; Basic Set of Applications; Part 2: Specification of Cooperative Awareness Basic Service (V1.3.0)* (2014). URL `http://www.etsi.org/deliver/etsi_en/302600_302699/30263702/01.03.00_20/en_30263702v010300a.pdf`. Accessed: April 10, 2014.

ETSI EN 302 637-3. *Intelligent Transport Systems (ITS); Vehicular Communications; Basic Set of Applications; Part 3: Specification of Decentralized Environmental Notification Basic Service (V1.2.0)* (2014). URL `http://www.etsi.org/deliver/etsi_en/302600_302699/30263703/01.02.00_20/en_30263703v010200a.pdf`. Accessed: April 10, 2014.

European Commission. *Innovation policy: ICT for Competitiveness and Innovation* (2009). URL `http://ec.europa.eu/enterprise/sectors/ict/files/standardisation_mandate_en.pdf`. Mandate M/453 on Cooperative ITS.

European Commission. *White paper on transport - Roadmap to a Single European Transport Area - Towards a competitive and resource efficient transport system* (2011). URL `http://eur-lex.europa.eu/LexUriServ/LexUriServ.do?`

uri=CELEX:52011DC0144:EN:NOT. European Strategies, Publications Office of the European Union, Luxembourg.

European Commission. *EU transport in figures - Statistical pocketbook*. Publication Office of the European Union, Luxembourg, Belgium, (2013).

European Commission. *Climate Action* (2014). URL http://ec.europa.eu/clima/policies/transport/index_en.htm. Accessed: February 18, 2014.

Eurostat. *Energy, transport and environment indicators*. European Union, 1st edition (2011). ISBN: 978-92-79-21384-7.

S. Ezell. *Intelligent Transportation Systems*. The Information Technology & Innovation Foundation (2010). URL http://www.itif.org/files/2010-1-27-ITS_Leadership.pdf.

P. S. Fancher, J. O'Day, H. Bunch, M. Sayers, and C. B. Winkler. Retarders for heavy vehicles: Evaluation of performance characteristics and in-service costs. Technical report, Highway Safety Research Institute, The University of Michigan, Ann Arbor, Michigan (1981).

F. Farokhi and K. H. Johansson. A game-theoretic framework for studying truck platooning incentives. In *16th International IEEE Conference on Intelligent Transportation Systems*, 1253–1260. Hague, The Netherlands (2013).

H. Fathy, D. Kang, and J. Stein. Online vehicle mass estimation using recursive least squares and supervisory data extraction. In *American Control Conference*, 1842–1848 (2008).

N. Ferreira, J. Fonseca, and J. Gomes. On the adequacy of 802.11p mac protocols to support safety services in its. In *IEEE International Conference on Emerging Technologies and Factory Automation, ETFA*, 1189–1192 (2008).

H. Feyzmahdavian, A. Alam, and A. Gattami. Optimal distributed controller design with communication delays: Application to vehicle formations. In *IEEE 51st Annual Conference on Decision and Control*, 2232–2237. Maui, HI, USA (2012).

Freescale. *MPC5674F Microcontroller Data Sheet*. Freescale Semiconductor, Inc. (2014). URL {http://cache.freescale.com/files/32bit/doc/data_sheet/MPC5674F.pdf}.

A. Fröberg. *Efficient Simulation and Optimal Control for Vehicle Propulsion*. Ph.D. thesis, Linköpings universitet (2008).

A. Fröberg, E. Hellström, and L. Nielsen. Explicit fuel optimal speed profiles for heavy trucks on a set of topographic road profiles. In *SAE World Congress*, 2006-01-1071 in SAE Technical Paper Series. Detroit, MI, USA (2006).

A. Geiger, M. Lauer, F. Moosmann, B. Ranft, H. Rapp, C. Stiller, and J. Ziegler. Team annieway's entry to the 2011 grand cooperative driving challenge. *IEEE Transactions on Intelligent Transportation Systems*, 13(3): 1008–1017 (2012).

General Motors. *To New Horizons* (1939). URL `http://www.etsi.org/deliver/etsi_en/302600_302699/30263703/01.02.00_20/en_30263703v010200a.pdf`. Accessed: April 10, 2014.

A. Girard. Reachability of uncertain linear systems using zonotopes. In *Proceedings of the 8th international conference on Hybrid Systems: computation and control*, HSCC'05, 291–305 (2005).

P. Gupta and P. Kumar. The capacity of wireless networks. *IEEE Transactions on Information Theory*, 46(2): 388–404 (2000).

V. Gupta, B. Hassibi, and R. Murray. On the synthesis of control laws for a network of autonomous agents. In *Proceedings of the American Control Conference*, volume 6, 4927–4932. Boston, MA, USA (2004).

F. Gustafsson. Automotive safety systems. *IEEE Signal Processing Magazine*, 26(4): 32–47 (2009).

L. Guzzella and A. Sciarretta. *Vehicle Propulsion Systems*. Springer Berlin Heidelberg New York, 2nd edition (2007). ISBN: 978-3-540-74691-1.

G. Hammar and V. Ovtchinnikov. *Structural Intelligent Platooning by a Systematic LQR Algorithm*. Master's thesis, Royal Institute of Technology, Automatic Control (2010).

B. J. Harker. Promote-chauffeur ii & 5.8 ghz vehicle to vehicle communications system. In *International Conference on Advanced Driver Assistance Systems*, 81–85 (2001). (IEE Conf. Publ. No. 483).

J. K. Hedrick, D. McMahon, V. Narendran, and D. Swaroop. Longitudinal vehicle controller design for ivhs systems. In *Proceedings of American Control Conference*, 3107–3112 (1991).

E. Hellström. *Look-ahead Control of Heavy Vehicles*. Ph.D. thesis, Linköping University (2010).

E. Hellström, J. Åslund, and L. Nielsen. Design of a well-behaved algorithm for on-board look-ahead control. In *IFAC World Congress*. Seoul, Korea (2008).

E. Hellström, A. Fröberg, and L. Nielsen. A real-time fuel-optimal cruise controller for heavy trucks using road topography information. In *SAE 2006 World Congress*. Detroit, MI, USA (2006). SAE paper 2006-01-0008.

Y. Ho and K. Chu. Team decision theory and information structures in optimal control problems-part I. *IEEE Transactions on Automatic Control*, 17(1): 15–22 (1972).

R. Horowitz and P. Varaiya. Control design of an automated highway system. volume 88, 913–925 (2000).

P. Ioannou and C. Chien. Autonomous intelligent cruise control. *IEEE Transactions on Vehicular Technology*, 42(4): 657–672 (1993).

R. Isaacs. *Differential Games*. Dover Publications, Inc. (John Wiley) (1965). Reprinted 1999.

ITF. *Combating road deaths moves up on global policy agenda* (2011). URL `http://www.internationaltransportforum.org/Press/PDFs/2011-05-26Safety.pdf`. Press release.

ITSA. *Intelligent Transportation Society of America* (2014). URL `http://www.itsa.org`. Accessed: April 2, 2014.

ITSJP. *ITS Japan* (2014). URL `http://www.its-jp.org/english/`. Accessed: April 2, 2014.

M. Ivarsson, J. Åslund, and L. Nielsen. Look ahead control - consequences of a nonlinear fuel map on truck fuel consumption. In *Institution of Mechanical Engineers, Part D, Journal of Automobile Engineering*. Washington, DC, USA (2011).

D. Jiang and L. Delgrossi. Ieee 802.11p: Towards an international standard for wireless access in vehicular environments. In *IEEE Vehicular Technology Conference, VTC 2008*, 2036–2040 (2008).

K. H. Johansson, M. Törngren, and L. Nielsen. Vehicle applications of controller area network. In *Handbook of networked and embedded control systems*, 741–765. Springer (2005).

M. R. Jovanović and B. Bamieh. On the ill-posedness of certain vehicular platoon control problems. In *43rd IEEE Conference on Decision and Control*. Atlantis, Paradise Island, Bahamas (2004).

E. D. Kaplan and C. J. Hegarthy. *Understanding GPS - Principles and Applications*. Artech House, Inc., 685 Canton Street, Norwood, MA 02062, 2nd edition (2006). ISBN: 1-58053-894-0.

P. Kavathekar and Y. Chen. Vehicle platooning: A brief survey and categorization. In *ASME/IEEE International Conference on Mechatronic and Embedded Systems and Applications, Parts A and B*. Washington, DC, USA (2011).

J. Kemppainen. *Model Predictive Control for Heavy Duty Vehicle Platooning*. Master's thesis, Linköping University, Automatic Control (2012).

O. Khorsand, A. Alam, and A. Gattami. Optimal distributed controller synthesis for chain structures: Applications to vehicle formations. In *9th International Conference on Informatics in Control, Automation and Robotics*. Rome, Italy (2012).

R. Kianfar, P. Falcone, and J. Fredriksson. A distributed model predictive control (mpc) approach to active steering control of string stable cooperative vehicle platoon. In *7th IFAC Symposium on Advances in Automotive Control*. Tokyo, Japan (2013).

R. Kianfar, P. Falcone, and J. Fredriksson. A control matching-based predictive approach to string stable vehicle platooning. In *19th World Congress of the International Federation of Automatic Control*. Cape Town, South Africa (2014).

U. Kiencke and L. Nielsen. *Automotive Control Systems*. Springer Verlag, Berlin (2003).

S. Knorn and R. H. Middleton. String stability analysis of a vehicle platoon with communication range 2 using the two-dimensional induced operator norm. In *European Control Conference*, 3354–3359. ZÃ‚Ÿrich, Switzerland (2013).

A. Lagerberg and B. Egart. Backlash estimation with application to automotive powertrains. *IEEE Transactions on Control Systems Technology*, 15(3): 483–493 (2007).

J. Larson, C. Kammer, K.-Y. Liang, and K. H. Johansson. Coordinated route optimization for heavy-duty vehicle platoons. In *16th International IEEE Conference on Intelligent Transportation Systems*, 1196–1202. Hague, The Netherlands (2013).

M. Larsson, J. Lindberg, J. Lycke, K. Hansson, E. R. A. Khakulov, F. Svensson, I. Tjernberg, A. Alam, J. Araujo, F. Farokhi, E. Ghadimi, A. Teixeira, D. V. Dimarogonas, and K. H. Johansson. Towards an indoor testbed for mobile networked control systems. In *Proceedings of the 1st Workshop on Research, Development, and Education on Unmanned Aerial Systems*, 51–60 (2011).

H. L. Lee, V. Padmanabhan, and S. Whang. Information distortion in a supply chain: The bullwhip effect. *Management Science*, 50(12): 1875–1886 (2004).

W. Levine and M. Athans. On the optimal error regulation of a string of moving vehicles. *IEEE Transactions on Automatic Control*, 11(3): 355–361 (1966).

K.-Y. Liang. *Linear Quadratic Control for Heavy Duty Vehicle Platooning*. Master's thesis, Royal Institue of Technology, Osquldas väg 10, 100 44 Stockholm, Sweden (2011).

K.-Y. Liang. *Coordination and Routing for Fuel-Efficient Heavy-Duty Vehicle Platoon Formation*. Licentiate thesis, Royal Institute of Technology, SE-100 44 Stockholm, Sweden (2014).

K.-Y. Liang, A. Alam, and A. Gattami. The impact of heterogeneity and order in heavy duty vehicle platooning networks. In *3rd IEEE Vehicular Networking Conference*. Amsterdam, Netherlands (2011).

K.-Y. Liang, J. Mårtensson, and K. H. Johansson. When is it fuel efficient for a heavy duty vehicle to catch up with a platoon? In *7th IFAC Symposium on Advances in Automotive Control*. Tokyo, Japan (2013).

K. Lidström, K. Sjöberg, U. Holmberg, J. Andersson, F. Bergh, M. Bjäde, and S. Mak. A modular CACC system integration and design. *IEEE Transactions on Intelligent Transportation Systems*, 13(3): 1050–1061 (2012).

P. Lingman. *Integrated Brake Control: Downhill Driving Strategies*. Ph.D. thesis, Chalmers University of Technology, Göteborg, Sweden (2005).

I. B. Makhlouf and H. D. S. Kowalewski. Safety verification of a controlled cooperative platoon under loss of communication using zonotopes. In *4th IFAC Conference on Analysis and Design of Hybrid Systems*. TU Eindhoven, Netherlands (2012).

J. Marshak. Elements for a theory of teams. *Management Science*, 127–137 (1955).

J. Mårtensson, A. Alam, S. Behere, M. Khan, J. Kjellberg, K.-Y. Liang, H. Pettersson, and D. Sundman. The development of a cooperative heavy-duty vehicle for the GCDC 2011: Team Scoop. *IEEE Transactions on Intelligent Transportation Systems*, 13(3): 1033–1049 (2012).

D. Q. Mayne. Sequential design of linear multivariable systems. *Proceedings of the Institution of Electrical Engineers*, 126(6): 568–572 (1979).

P. Meisen, T. Seidl, and K. Henning. A data-mining technique for the planning and organization of truck platoons. In *International Conference on Heavy Vehicles*. Paris, France (2008).

S. Melzer and B. Kuo. A closed-form solution for the optimal error regulation of a string of moving vehicles. *IEEE Transactions on Automatic Control*, 16(1): 50–52 (1971*a*).

S. M. Melzer and B. C. Kuo. Optimal regulation of systems described by a countably infinite number of objects. *Automatica*, 7: 359–366 (1971*b*).

R. Middleton and J. Braslavsky. String instability in classes of linear time invariant formation control with limited communication range. *IEEE Transactions on Automatic Control*, 55(7): 1519–1530 (2010).

V. Milanes, S. Shladover, J. Spring, C. Nowakowski, H. Kawazoe, and M. Nakamura. Cooperative adaptive cruise control in real traffic situations. *IEEE Transactions on Intelligent Transportation Systems*, 15(1): 296–305 (2014).

I. Mitchell. A toolbox of level set methods (version 1.1). Vancouver, BC, Canada (2007). Tech. Rep. TR-2007-11, [Online]. Available: http://www.cs.ubc.ca/~mitchell/ToolboxLS/toolboxLS-1.1.pdf.

I. Mitchell, A. Bayen, and C. Tomlin. A time-dependent Hamilton-Jacobi formulation of reachable sets for continuous dynamic games. *IEEE Transactions on Automatic Control*, 50(7): 947–957 (2005).

S. Moon, I. Moon, and K. Yi. Design, tuning, and evaluation of a full-range adaptive cruise control system with collision avoidance. *Control Engineering Practice*, 17(4): 442–455 (2009).

G. Naus, R. Vugts, J. Ploeg, R. van de Molengraft, and M. Steinbuch. Towards on-the-road implementation of cooperative adaptive cruise control. In *16th World Congress on Intelligent Transport Systems and Services, Stockholm, Sweden* (2009).

G. J. L. Naus. *Model-based control for automotive applications*. Ph.D. thesis, Eindhoven University of Technology, Eindhoven, Netherlands (2010).

S. Nilsson. *Sensor Fusion for Heavy Duty Vehicle Platooning*. Master's thesis, Linköping University, Automatic Control (2012).

D. Norrby. *A CFD study of the aerodynamic effects of platooning trucks*. Master's thesis, Royal Institute of Technology (2014).

OECD/ITF. *International transport outlook 2013: Funding transport* (2013). URL `http://www.keepeek.com/Digital-Asset-Management/oecd/transport/itf-transport-outlook-2013_9789282103937-en\#page7`. OECD Publishing/ITF.

M. Omae, R. Fukuda, T. Ogitsu, and W.-P. Chiang. Spacing control of cooperative adaptive cruise control for heavy-duty vehicles. In *7th IFAC Symposium on Advances in Automotive Control*. Tokyo, Japan (2014).

C. H. Papadimitriou and J. N. Tsitsiklis. Intractable problems in control theory. *SIAM Journal on Control and Optimization*, 24(1): 639–654 (1986).

L. Peppard. String stability of relative-motion pid vehicle control systems. *IEEE Transactions on Automatic Control*, 19(5): 579–581 (1974).

H. Pettersson. *Estimation and Pre-Processing of Sensor Data in Heavy Duty Vehicle Platooning*. Master's thesis, Linköping University, Automatic Control (2012).

L. Pipes. An operational analysis of traffic dynamics. *Journal of Applied Physics*, 24: 274–281 (1953).

J. Ploeg, B. Scheepers, E. van Nunen, N. V. de Wouw, and H. Nijmeijer. Design and experimental evaluation of cooperative adaptive cruise control. In *14th International IEEE Conference on Intelligent Transportation Systems*, 260–265. Washington DC, USA (2011).

J. Ploeg, N. van de Wouw, and H. Nijmeijer. l_p string stability of cascaded systems: Application to vehicle platooning. *IEEE Transactions on Control Systems Technology*, 22(2): 786–793 (2014).

R. Rajamani and C. Zhu. Semi-autonomous adaptive cruise control systems. In *Proceedings of the American Control Conference*, volume 2, 1491–1495. San Diego, CA, USA (1999).

R. Rajamani and C. Zhu. Semi-autonomous adaptive cruise control systems. *IEEE Transactions on Vehicular Technology*, 51(5): 1186–1192 (2002).

T. Robinson, E. Chan, and E. Coelingh. Operating platoons on public motorways: An introduction to the sartre platooning programme. In *17th World Congress on Intelligent Transport Systems*. Busan, Korea (2010).

G. Rödönyi, P. Gáspár, and J. Bokor. Unfalsified uncertainty modeling for computing tight bounds on peak spacing errors in vehicle platoons. In *American Control Conference*, 3057–3062. Washington, DC, USA (2013).

G. Rödönyi, P. Gáspár, J. Bokor, and L. Palkovics. Experimental verification of robustness in a semi-autonomous heavy vehicle platoon. *Control Engineering Practice*, 28: 13–25 (2014).

J. Rogge and D. Aeyels. Decentralized control of vehicle platoons with interconnection possessing ring topology. *44th IEEE Conference on Decision and Control and the European Control Conference*, 1491–1496 (2005).

R. Rothery, R. Silver, R. Herman, and C. Torner. Analysis of experiments on single-lane bus flow. *Journal of the Institute for Operations and the Management Sciences*, 12(6): 913–933 (1964).

A. Ryan, M. Zennaro, A. Howell, R. Sengupta, and J. K. Hedrick. An overview of emerging results in cooperative UAV control. In *43rd IEEE Conference on Decision and Control*, volume 1, 602–607 (2004).

P. Sahlholm. *Distributed Road Grade Estimation for Heavy Duty Vehicles*. Ph.D. thesis, Royal Institute of Technology (KTH) (2011).

P. Sahlholm and K. H. Johansson. Road grade estimation for look-ahead vehicle control using multiple measurement runs. *Control Engineering Practice*, 18(11): 1328–1341 (2010).

T. Sandberg. *Heavy Truck Modeling for Fuel Consumption, Simulations, and Measurements*. Licentiate thesis LiU-TEK-LIC-2001:61, Linköpings universitet, S-581 83 Linköping, Sweden (2001).

N. R. Sandell and M. Athans. Solution of some nonclassical lqg stochastic decision problems. *IEEE Transactions on Automatic Control*, 19(2): 108–116 (1974).

Scania CV AB. *Annual Report*. Scania CV AB (2010).

M. Schittler. State-of-the-art and emerging truck engine technologies for optimized performance, emissions and life cycle costs. In *9th Diesel Emissions Reduction Conference*. Rhode Island, USA (2003).

A. Schwarzkopf and R. Leipnik. Control of highway vehicles for minimum fuel consumption over varying terrain. *Transportation Research*, 11(4): 279–286 (1977).

P. Seiler, A. Pant, and J. K. Hedrick. Disturbance propagation in vehicle strings. *IEEE Transactions on Automatic Control*, 49(10): 1835–1842 (2004).

P. Seiler, B. Song, and J. K. Hedrick. Development of a collision avoidance system. In *SAE 1998 World Congress*. Detroit, MI, USA (1998). SAE paper 980853.

A. Shaout and M. A. Jarrah. Cruise control technology review. *Computers & Electrical Engineering*, 23(4): 259–271 (1997).

E. Shaw and J. K. Hedrick. String stability analysis for heterogeneous vehicle strings. In *American Control Conference*, 3118–3125. New York, USA (2007).

S. Sheikholeslam and C. A. Desoer. Longitudinal control of a platoon of vehicles with no communication of lead vehicle information: A system level study. *IEEE Transactions on Vehicular Technology*, 42(4) (1993).

R. Siegwart and I. R. Nourbakhsh. *Introduction to Autonomous Mobile Robots*. MIT Press (2004).

SPITS. *SPITS: the Strategic Platform for Intelligent Traffic Systems* (2014). URL `http://www.cvisproject.org/en/news/spits_the_strategic_platform_for_intelligent_traffic_systems.htm`. Accessed: April 3, 2014.

S. S. Stanković, M. J. Stanojević, and D. D. Šiljak. Decentralized overlapping control of a platoon of vehicles. *IEEE Transactions on Control Systems Technology In Control Systems Technology*, 8(5): 816–832 (2000).

S. Sudin and P. A. Cook. Two-vehicle look-ahead convoy control systems. In *59th IEEE Vehicular Technology Conference, VTC*. Milan, Italy (2004).

D. Swaroop. *String stability of interconnected system: An application to platooning in automated highway systems*. Ph.D. thesis, University of California at Berkeley (1994).

D. Swaroop and J. K. Hedrick. String stability of interconnected systems. *IEEE Transactions on Automatic Control*, 41(3): 349–357 (1996).

D. Swaroop, J.K., C. C. Chien, and P. Ioannou. A comparision of spacing and headway control laws for automatically controlled vehicles. *Vehicle System Dynamics*, 23(1) (1994).

H. J. Tehrani. *Study of Disturbance Models for Heavy-duty Vehicle Platooning*. Master's thesis, Royal Institute of Technology (KTH) (2010).

S. Tsugawa. An overview on control algorithms for automated highway systems. In *IEEE/IEEJ/JSAI International Conference on Intelligent Transportation Systems*, 234–239. Tokyo, Japan (1999).

S. Tsugawa. An overview on an automated truck platoon within the energy its project. In *7th IFAC Symposium on Advances in Automotive Control*. Tokyo, Japan (2013).

A. Vahidi and A. Eskandarian. Research advances in intelligent collision avoidance and adaptive cruise control. *IEEE Transactions on Intelligent Transportation Systems*, 4(3): 143–153 (2003).

A. Vahidi, A. Stefanopoulou, and H. Peng. Recursive least squares with forgetting for online estimation of vehicle mass and road grade: Theory and experiments. *Vehicle System Dynamics*, 43: 31–57 (2005).

E. van Nunen, R. Kwakkernaat, J. Ploeg, and B. D. Netten. Cooperative competition for future mobility. *IEEE Transactions on Intelligent Transportation Systems*, 13(3): 1018–1025 (2012).

P. Varaiya. Smart cars on smart roads: Problem of control. *IEEE Transactions on Automatic Control*, 38(2) (1993).

M. Walden and A. Garrod. A european low cost mmic based millimetre-wave radar module for automotive applications. In *33rd European Microwave Conference*, 1195–1198 (2003).

J. Wang and R. Rajamani. The impact of adaptive cruise control systems on highway safety and traffic flow. *Proceedings of the Institution of Mechanical Engineers Part D: Journal of Automobile Engineering*, 218, no. 2: 111–130 (2004*a*).

J. Wang and R. Rajamani. Should adaptive cruise-control systems be designed to maintain a constant time gap between vehicles? *IEEE Transactions on Vehicular Technology*, 53(5): 1480–1490 (2004*b*).

H. S. Witsenhausen. A counterexample in stochastic optimum control. *SIAM Journal on Control and Optimization*, 6(1): 131–147 (1968).

H. S. Witsenhausen. Separation of estimation and control for discrete time systems. *Proceedings of the IEEE*, 59(11): 1557–1566 (1971).

H. Wolf-Heinrich and S. R. Ahmed. *Aerodynamics of Road Vehicles*. Society of Automotive Engineers, Inc, Warrendale (1998).

L. Xiao and S. Boyd. Fast linear iterations for distributed averaging. *Systems and Control Letters*, 53: 65–78 (2003).

Y. Yamamura and Y. Seto. A study of string-stable acc using vehicle-to-vehicle communication. In *SAE 2006 World Congress*. Detroit, Michigan, USA (2006). SAE paper 2006-01-0348.

H. Yamazaki, K. Okamoto, K. Aoki, and Y. Ito. Fuel saving effect of single file platooning trucks on expressway. In *JSAE Annual Congress (Fall)* (2009). In Japanese.

D. Yanakiev and I. Kanellakopoulos. Nonlinear spacing policies for automated heavy-duty vehicles. *IEEE Transactions on vehicular technology*, 47(4) (2008).

M. Zabat, S. Farascaroli, F. Browand, M. Nestlerode, and J. Baez. Drag measurements on a platoon of vehicles. Technical report, California Partners for Advanced Transit and Highways (PATH), UC Berkeley, USA (1994).

"*A scientific truth does not triumph by convincing its opponents and making them see the light, but rather because its opponents eventually die and a new generation grows up that is familiar with it.*"

Max Planck

TRITA-EE 2014:027
ISBN 978-91-7595-194-2
ISSN 1653-5146

www.kth.se